Earth 362

Data analysis for Earth and Planetary Sciences

“Whenever I hear ‘everybody knows’ I wonder: how do they know it, and is true?”
Seismologist David Jackson

Serpens South Star Cluster

(NASA/JPL-Caltech/L. Allen (Harvard-Smithsonian CfA) & Gould's Belt Legacy Team

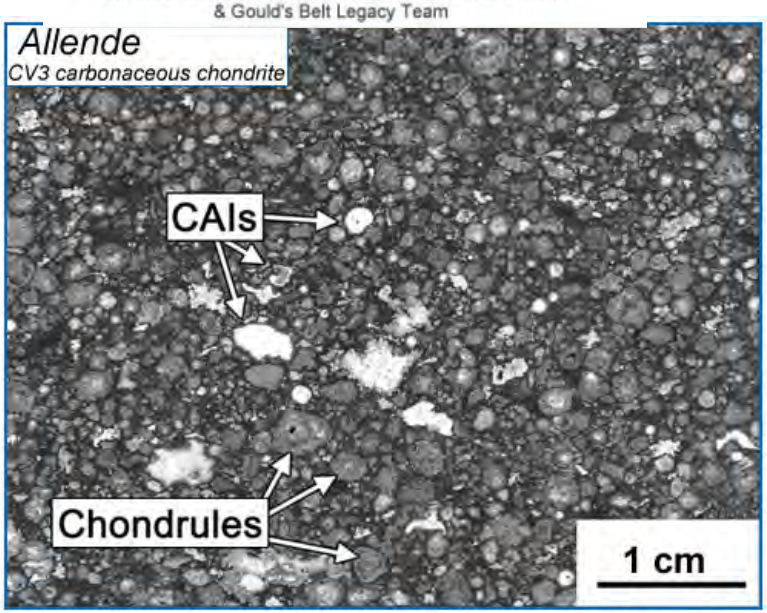

(From MacPherson, G. J. and Boss, A. (2011) Cosmochemical evidence for astrophysical processes during the formation of our solar system, *PNAS*, v. 108(48), p. 19152-19158, doi: 10.1073/pnas.1110051108.)

Time Scales of Solid Formation & Disk Evolution

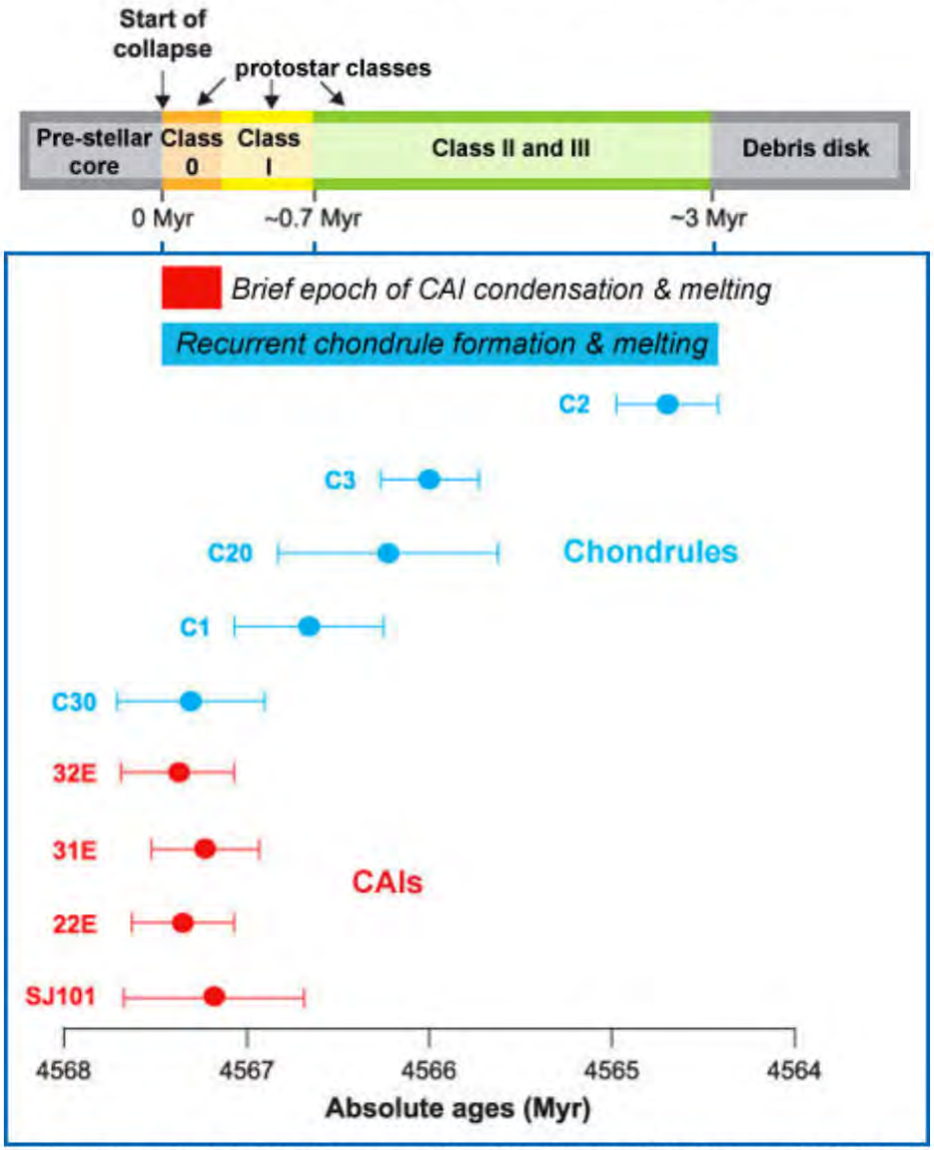

(From Connelly *et al.*, 2012, *Science*, v. 338, p.651-655, doi: 10.1126/science.1226919.)

Can mine leave no trace in BWCA?

By Dave Orrick
dorrick@pioneerpress.com

POSTED: 12/20/2014 02:02:16 PM CST | UPDATED: 12 DAYS AGO

Twin Metals mine

Twin Metals is envisioning an underground mine in the Superior National Forest to extract copper, nickel and platinum-related metals.

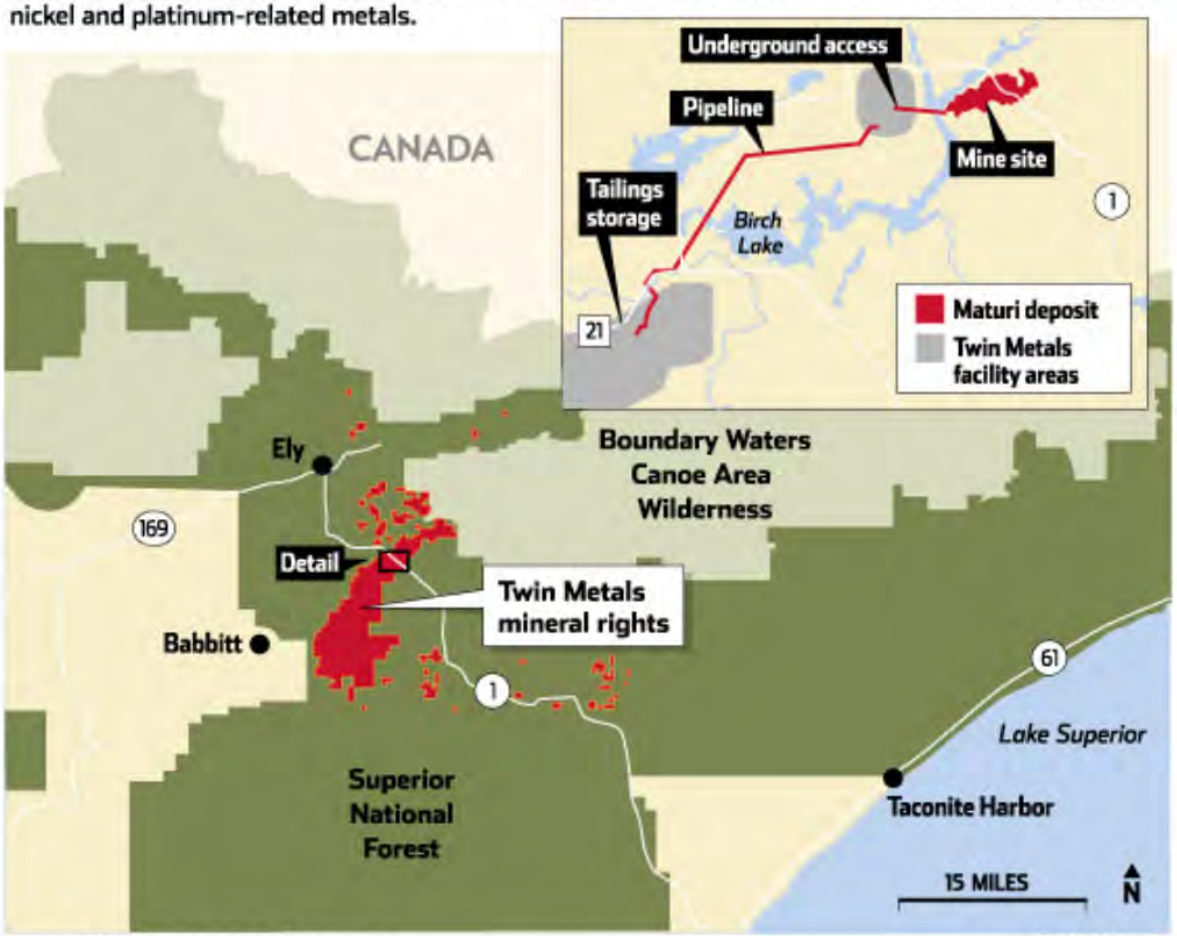

Sources: Twin Metals, public documents

PIONEER PRESS

How safe is shale gas extraction?

A spokesman for the Royal Academy of Engineering, which produced an influential 2012 report on shale gas with the Royal Society that concluded it could be safe if it was properly regulated, said the risks from fracking were very low.

"Our conclusion was that if carried out to highest standards of best practice, the risks are very low for any environmental contamination. The most serious risks come in the drilling and casing and surface operations rather than the fracturing itself."

"You can't eliminate the risk of something going wrong, but you can monitor very closely and be very open and transparent about what's going on."

On the chief scientific adviser's report, he said: "I think he's making a very broad and general point."

Greenpeace UK's energy campaigner, Louise Hutchins, said: "This is a naked-emperor moment for the government's dash to frack. Ministers are being warned by their own chief scientist that we don't know anywhere near enough about the potential side effects of shale drilling to trust this industry. The report is right to raise concerns about not just the potential environmental and health impact but also the economic costs of betting huge resources on an unproven industry. Ministers should listen to this appeal to reason and subject their shale push to a sobering reality check."

Guardian
11/28/14

Global warming predictions

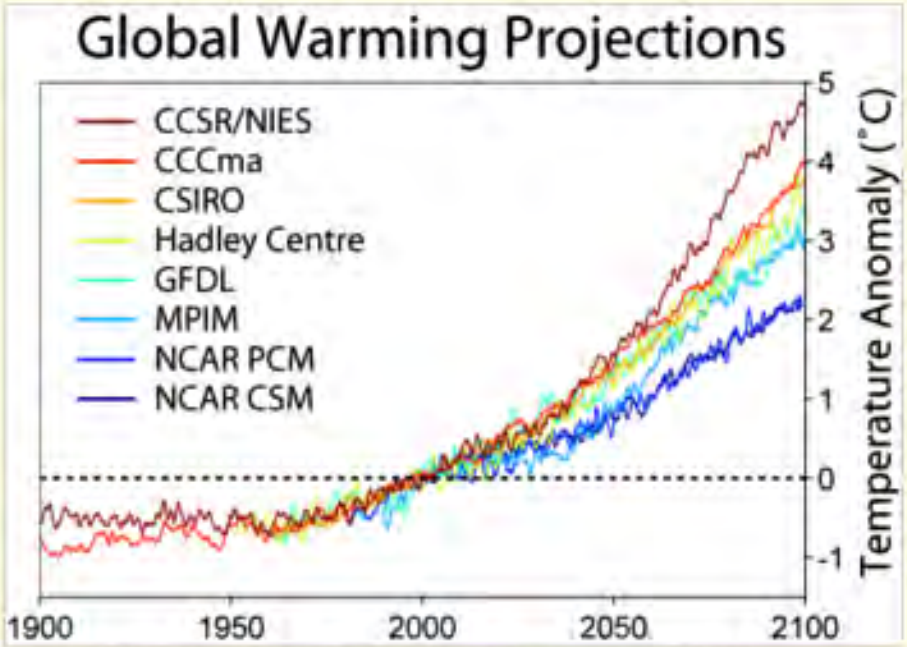

The different predictions of global mean temperature change obtained from 8 different climate models under the SRES A2 emissions scenario (one which assumes no significant action to combat greenhouse gas emissions).

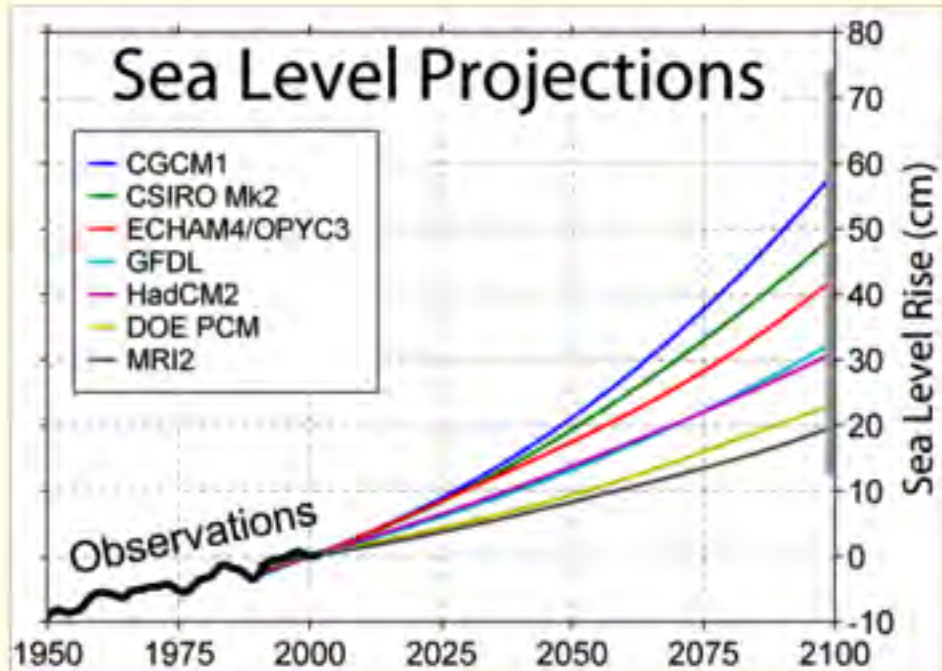

The predicted change in global mean sea level in a range of climate models following a business as usual emissions scenario (IS92a). The grey bar at 2100 indicates the full uncertainty range.


AN
RT

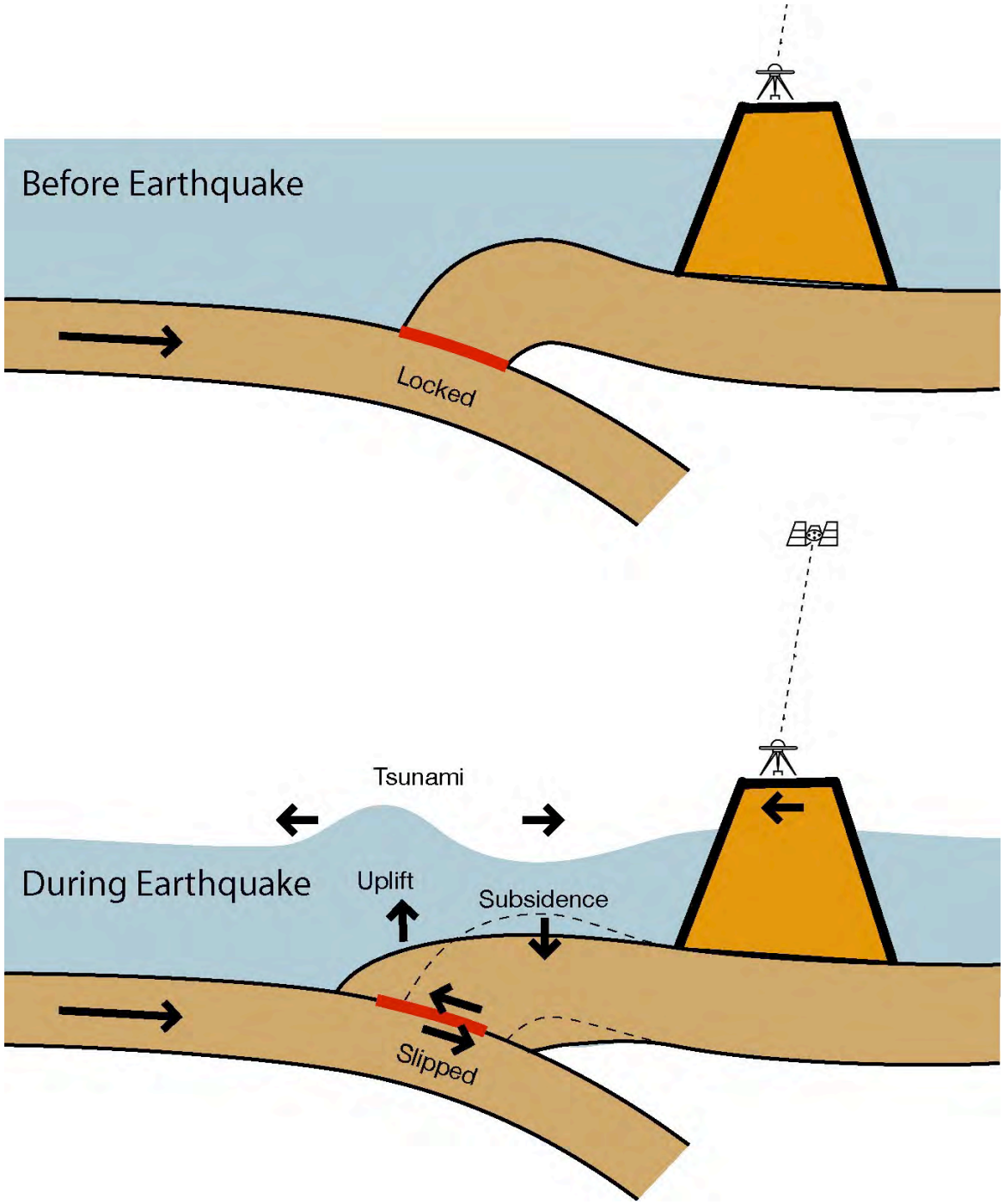
Before Earthquake
Locked
Tsunami
During Earthquake
Uplift
Subsidence
Slipped

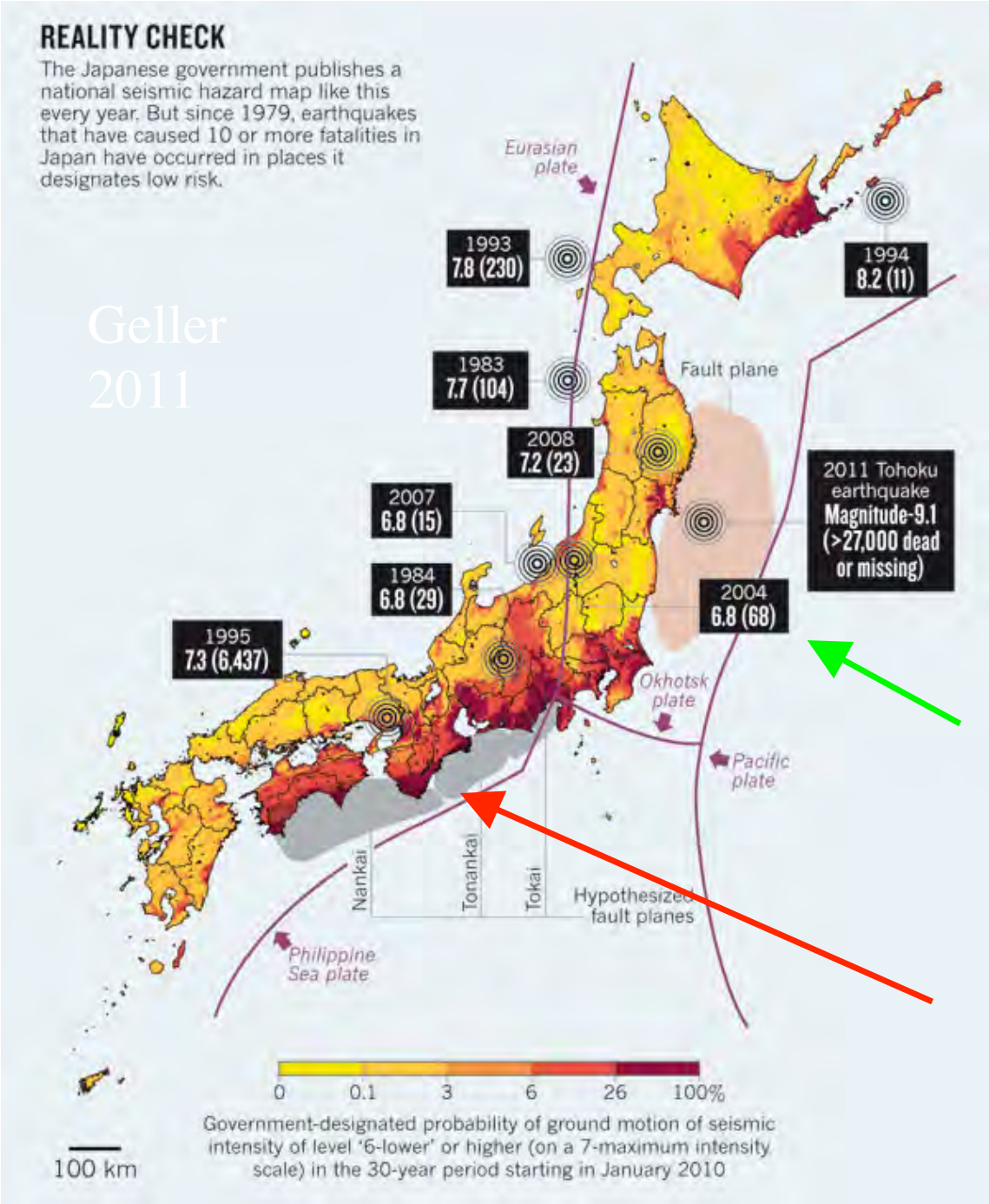

Japan's earthquake hazard map

2011 M 9.1 Tohoku, 1995 Kobe M 7.3 & others in areas mapped as low hazard

In contrast: map assumed high hazard in Tokai "gap"

Planning assumed maximum magnitude 8
Seawalls 5-10 m high

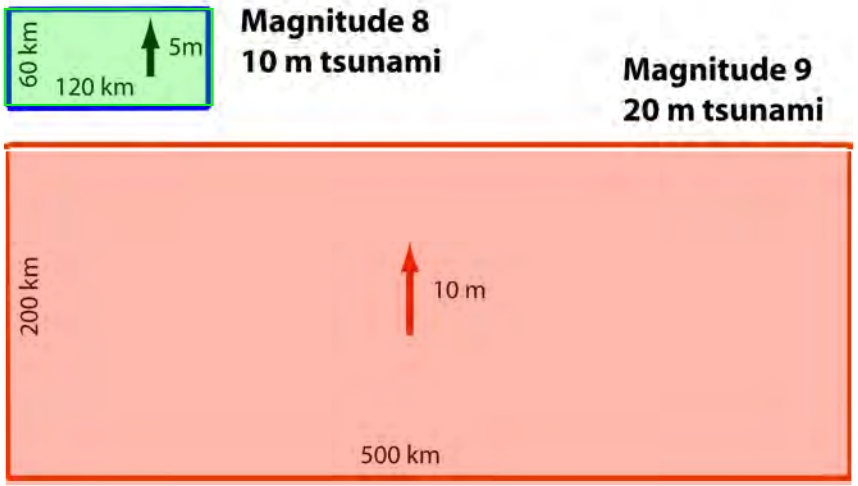

Stein & Okal, 2011

NYT

CNN

Tsunami runup approximately twice fault slip (Plafker, Okal & Synolakis 2004)

M9 generates much larger tsunami

Tsunami radiates energy perpendicular to fault
Thus largest landward of highest slip patches

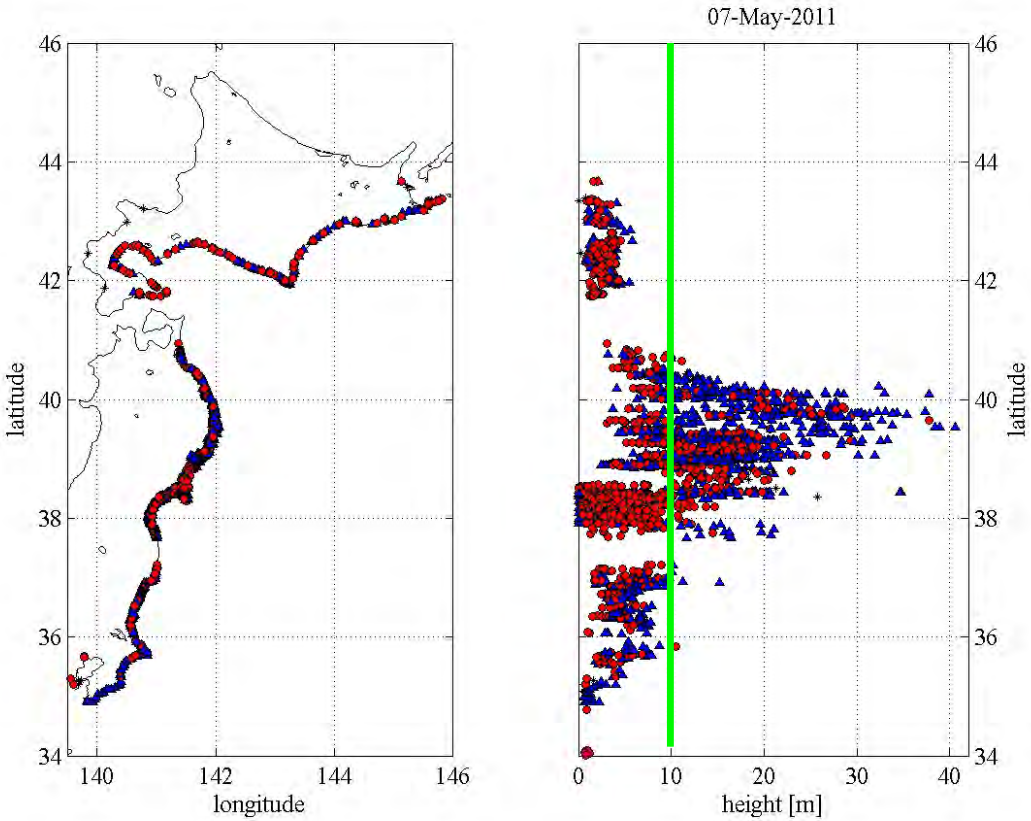

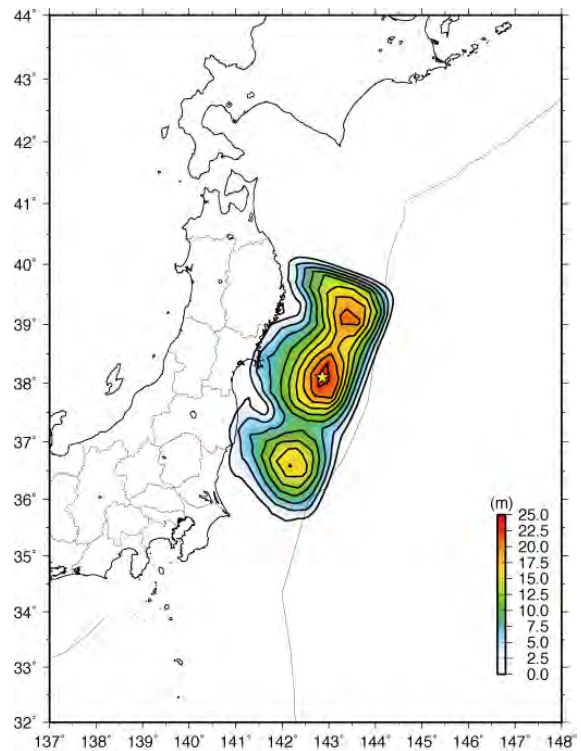

http://www.coastal.jp/tsunami2011/index.php?FrontPage

http://www.geol.tsukuba.ac.jp/~yagi-y/EQ/Tohoku/

Didn't consider historical record of large tsunamis

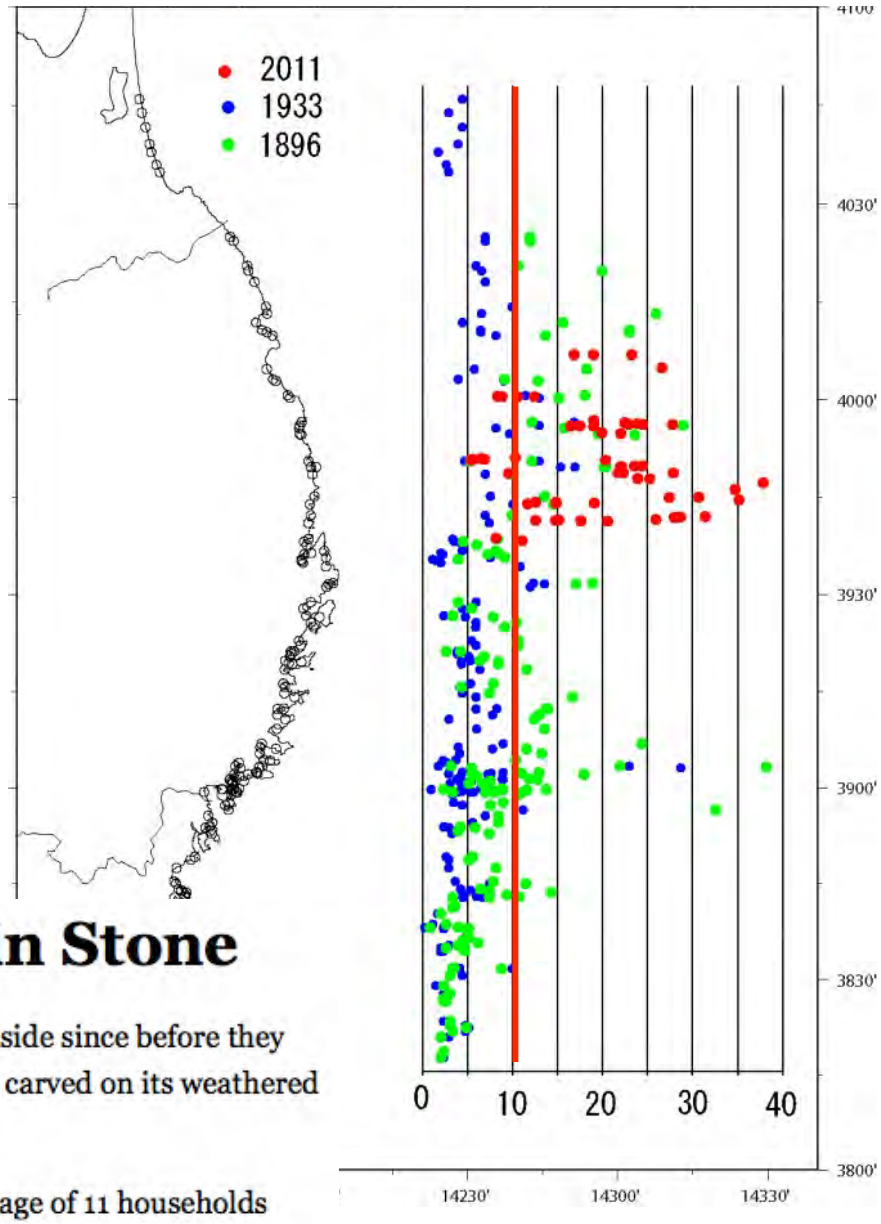

Tsunami Warnings, Written in Stone

By MARTIN FACKLER

ANEYOSHI, Japan — The stone tablet has stood on this forested hillside since before they were born, but the villagers have faithfully obeyed the stark warning carved on its weathered face: "Do not build your homes below this point!"

Residents say this injunction from their ancestors kept their tiny village of 11 households safely out of reach of the deadly tsunami last month that wiped out hundreds of miles of Japanese coast and rose to record heights near here. The waves stopped just 300 feet below the stone.

NYT 4/20/11

New Madrid shown as hazardous as California

Buildings should be built to same standards (FEMA)

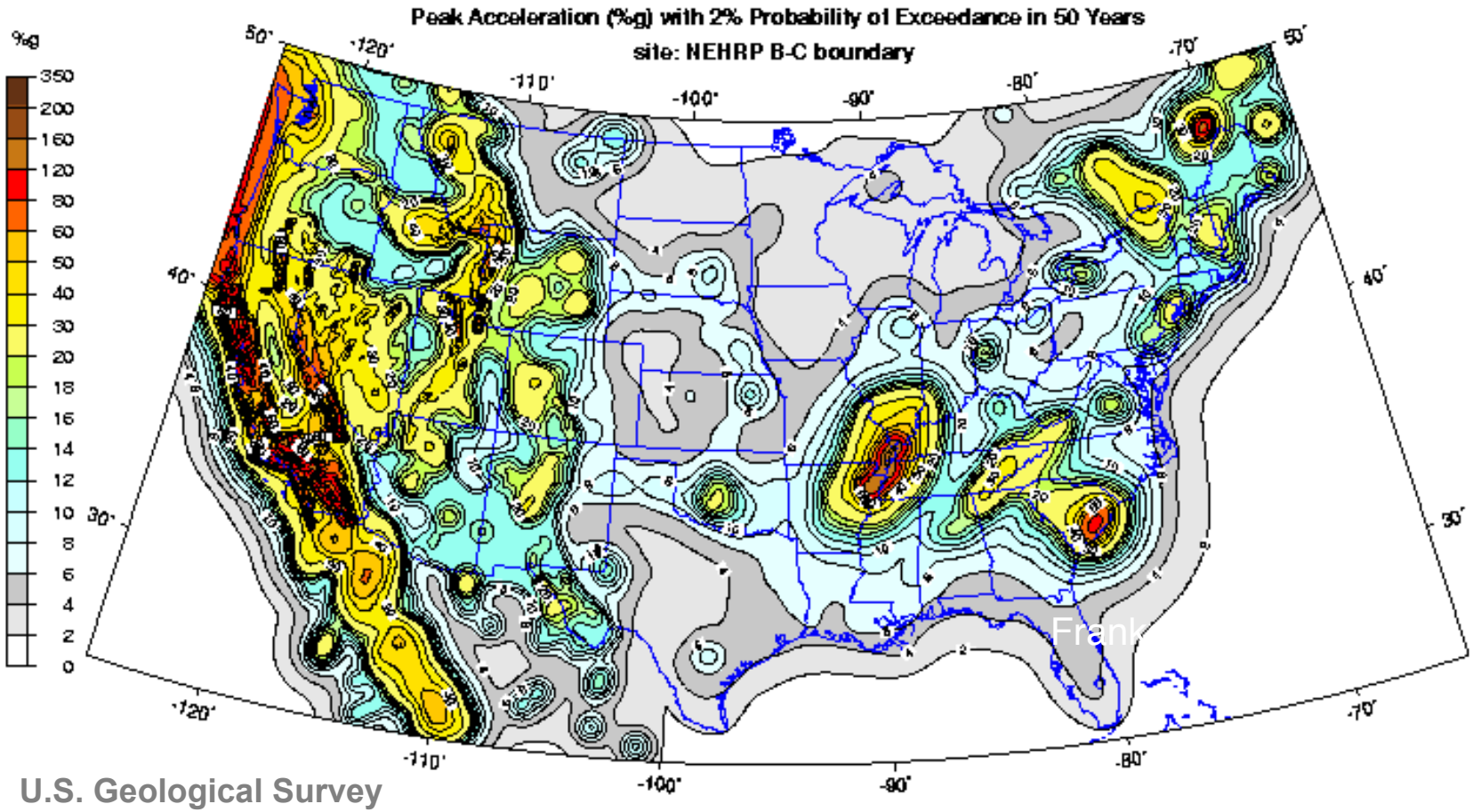

U.S. Geological Survey

Does this make sense?

Hurricane Ike "hits" Miami

Hurricane Ike Projected Path:Hurricane Ike Track

By Dylan on Sep 5, 2008 in US News | | ShareThis |

Hurricane Ike Projected Path:Hurricane Ike Track **- Hurricane Ike is currently a Category 3 hurricane with winds of 125 mph as of 5 a.m. EDT Friday. The national hurricane center revealed that Hurricane Ike will keep on weakening but is still a dangerous hurricane.Hurricane Ike is located about 460 miles north of the Leeward Islands and will hit the Turks and Caicos Islands and the Bahamas on Sunday.**
Hurricane Ike Projected Path:Hurricane Ike Track

Ike's actual track

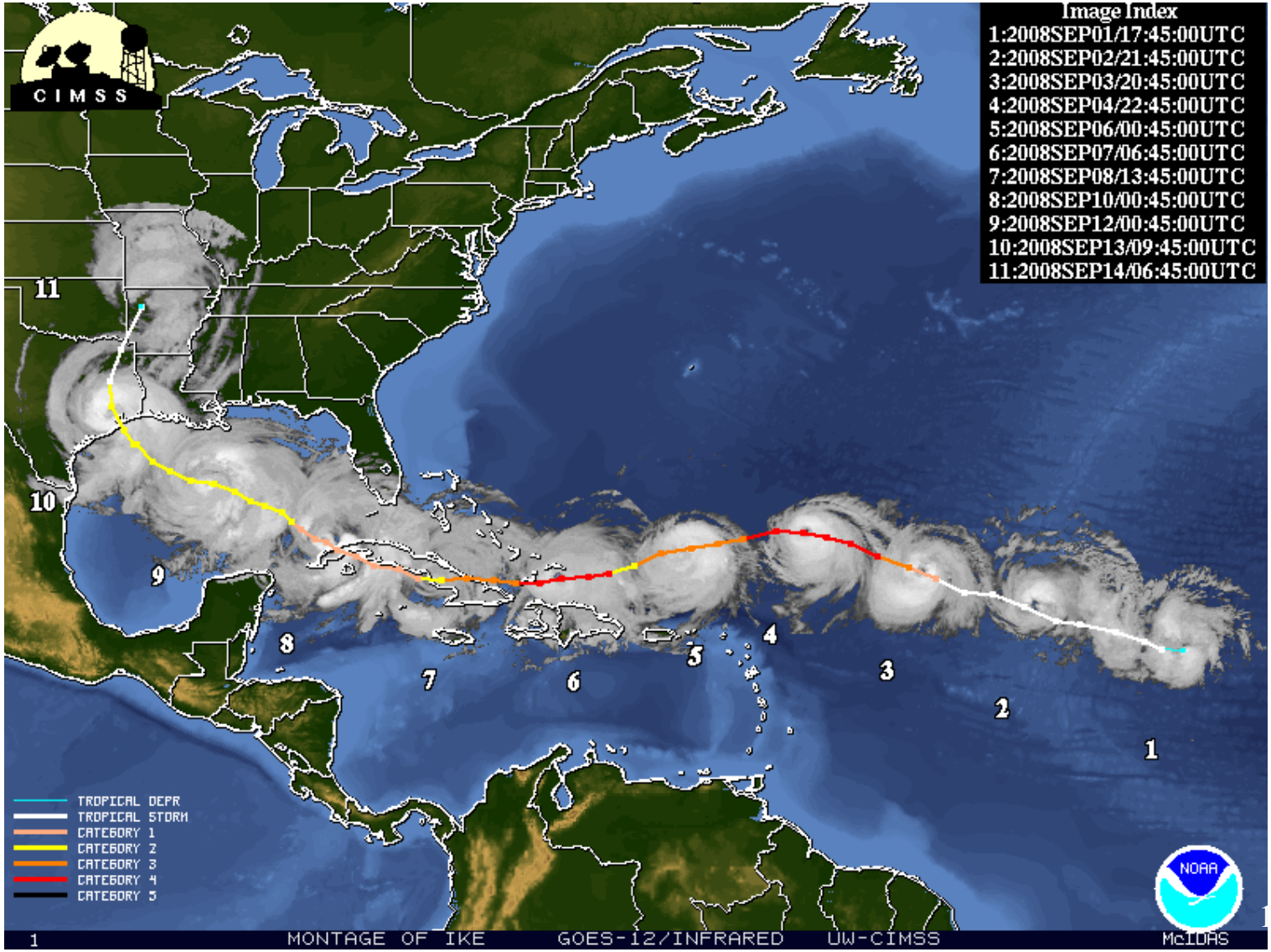

Hurricane Ike's 9-Foot Floods to Bring "Certain Death"

Ike brings certain death

Willie Drye
for National Geographic News
September 12, 2008

Hurricane Ike's expected massive storm surge and flooding have prompted National Weather Service officials to issue a rare and chilling "certain death" warning as the storm barrels toward the Texas coast tonight.

(See Hurricane Ike photos.)

Enlarge Photo

Printer Friendly
Email to a Friend

SHARE What's This?
Digg
StumbleUpon
Reddit

"We rarely issue this warning unless there is a severe, impending catastrophe," said Chris Sisco, a meteorologist at the National Hurricane Center in Miami. "It's very serious."

The warning reads: "Neighborhoods that are affected by the storm surge ... and possibly entire coastal communities ... will be inundated during the period of peak storm tide.

"Persons not heeding evacuation orders in single-family, one- or two-story homes may face certain death. ... Widespread and devastating personal property damage is likely elsewhere."

Sisco said Ike's storm surge—a mound of water created by a hurricane's winds—could reach 20 feet (6.1 meters) around the center of the storm.

Actual deaths: ~50 of 40,000

Error 800 x

Why Hurricane Ike's "Certain Death" Warning Failed

Willie Drye
for National Geographic News
September 26, 2008

As residents of Galveston, Texas, were allowed to return to the devastated island this week, experts puzzled over why tens of thousands of others had remained during Hurricane Ike—despite the National Weather Service's "certain death" warning.

Among the possible explanations: memories of a chaotic 2005 evacuation, an anti-government attitude, and a false sense of security fueled by TV news and the abundance of hurricane data on the Web.

Enlarge Photo

Printer Friendly

Email to a Friend

SHARE What's This?

Digg

(See full Hurricane Ike coverage: photos, stories, and videos.)

Avoiding Chaos

Gene Hafele, director of the Houston-Galveston National Weather Service office, said about 500,000 people in and around Galveston were in a mandatory evacuation zone, and only about 300,000 left.

Bill Read, director of the National Hurricane Center in Miami, estimated there were about 140,000 people in the smaller, "certain death" zone. About 70 percent of those residents evacuated. That left nearly 40,000 people to contend with the worst of the storm surge.

Hurricane Irene evacuation defended by New York mayor Michael Bloomberg

Politicians issued dramatic warnings but their fears were unfounded and some say they went too far

Chris McGreal in Washington
guardian.co.uk, Sunday 28 August 2011 15.44 EDT

A larger | smaller

Hurricane Irene dumped vast amounts of water on the eastern US at the weekend, cut electricity to millions of people and prompted warnings of extensive flash flooding further inland.

But ultimately the storm failed to deliver the catastrophic blow politicians had feared when they ordered the evacuation of more than 2 million people, shut down public transport in New York and other cities, and put the military on alert.

Why are hurricane forecasts still so rough?

For example, we do not know for sure whether Irene will make landfall in the Carolinas, on Long Island, or in New England, or stay far enough offshore to deliver little more than a windy, rainy day to East Coast residents.

Nor do we have better than a passing ability to forecast how strong Irene will get. In spite of decades of research and greatly improved observations and computer models, our skill in forecasting hurricane strength is little better than it was decades ago. Why is this so, and how should we go about making decisions in the context of uncertain forecasts?

K. Emanuel CNN 8/26/11

Challenges in Predicting the Intensity of Storms

By HENRY FOUNTAIN

Irene may be the first hurricane to hit the East Coast in several years, but in one respect it is like all the others that have come and gone before it: forecasters have had difficulty predicting its strength.

"We've had a wonderful history of improving tracking forecasts," said Clifford Mass, an atmospheric scientist at the University of Washington who works on numerical modeling of storms. A hurricane, he said, is essentially like a top, and it is relatively easy to gauge the steering winds and other forces that will move it.

"But we have not gotten good in intensity forecasts," Dr. Mass said. "To get the intensity right, we have to get the innards of the storm right."

NYT 8/28/11

Scientists defend warning after tsunami nonevent

The warning was ominous, its predictions dire: Oceanographers issued a bulletin telling Hawaii and other Pacific islands that a killer wave was heading their way with terrifying force and that "urgent action should be taken to protect lives and property."

But the devastating tidal surge predicted after Chile's magnitude 8.8-earthquake for areas far from the epicenter never materialized. And by Sunday, authorities had lifted the warning after waves half the predicted size tickled the shores of Hawaii and tourists once again jammed beaches and restaurants.

Was Hawaii's tsunami warning overblown?

01:45 PM

Share 4 Yahoo! Buzz Share E-mail Save P

63 Comments

7 Recom

City spends $330,000 responding to potential threat

Perils of prediction: are scientists prepared to warn the public about geologic hazards?

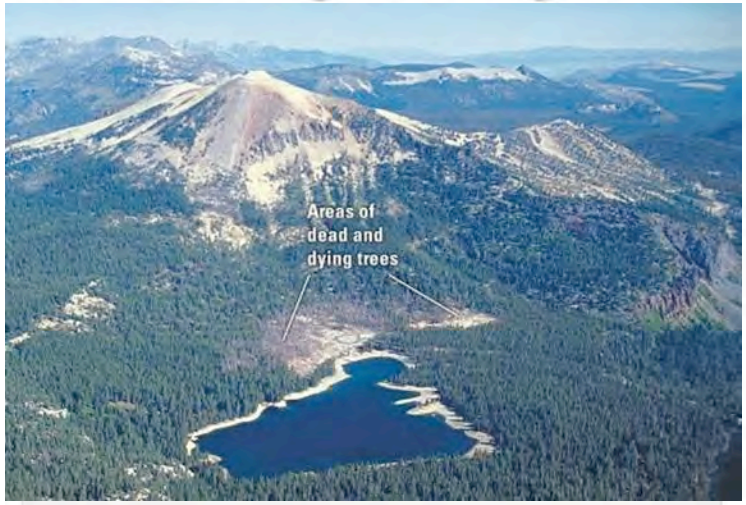

Science News

6/15/91

The town of Mammoth Lakes doesn't look kindly on federal geologists. In this quiet ski-center community nestled at the foot of California's Sierra Nevada range, residents have even coined their own name for the U.S. Geological Survey.

They call it the U.S. Guessing Society.

The town's antipathy toward the USGS has stewed for almost a decade, ignited in 1982 by a series of federal announcements and media reports about a potential volcanic eruption, which residents blame for a subsequent nose dive in the local economy. Only recently has the local real estate market climbed back up to its pre-1982 level, they say.

The local economy collapsed, said Glenn Thompson, Mammoth Lakes' town manager. Housing prices fell 40 percent overnight. In the next few years, dozens of businesses closed, new shopping centers stood empty and townspeople left to seek jobs elsewhere. (NYT 9/11/90)

Predicted disaster probabilities are often very inaccurate

Apocalytic claims do not have a good track record. And arguments that statistics support such claims - particularly arguments that simple, easily understood numbers are proof that the future holds complex, civilization-threatening changes - deserve the most careful inspection .”

J. Best: *More Damned Lies and Statistics: How Numbers Confuse Public Issues*

Sinking of the ocean liner *Andrea Doria* in 1956

Experts thought that large ships couldn't run into each other, because radar let them see in night and fog. Moreover, modern ships were unsinkable because they were divided into watertight compartments and designed to float even if two compartments filled with water.

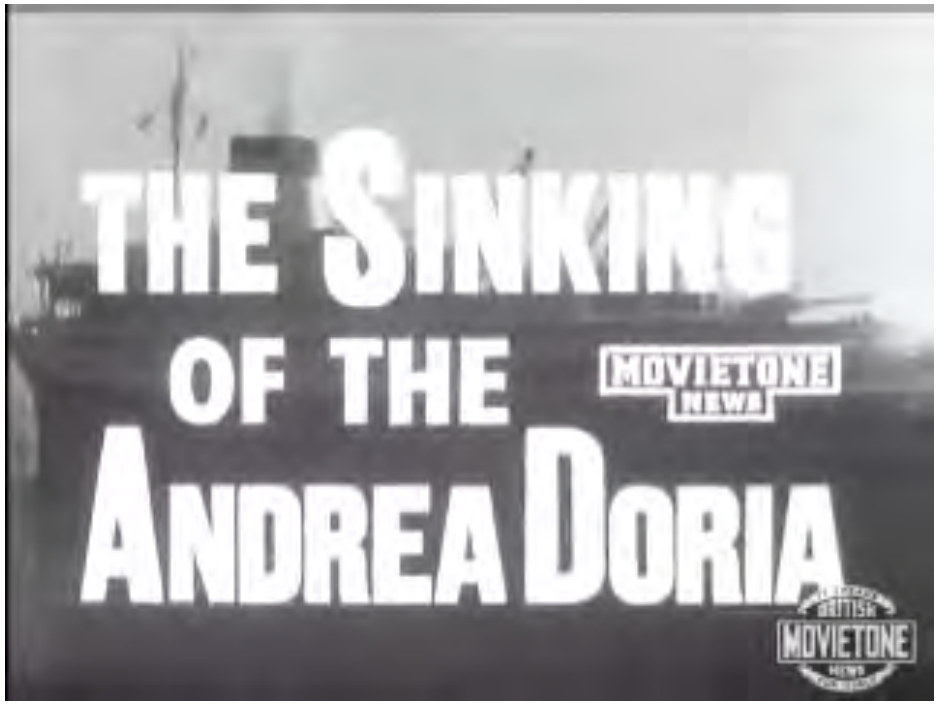

Collapse of Long Term Capital Management

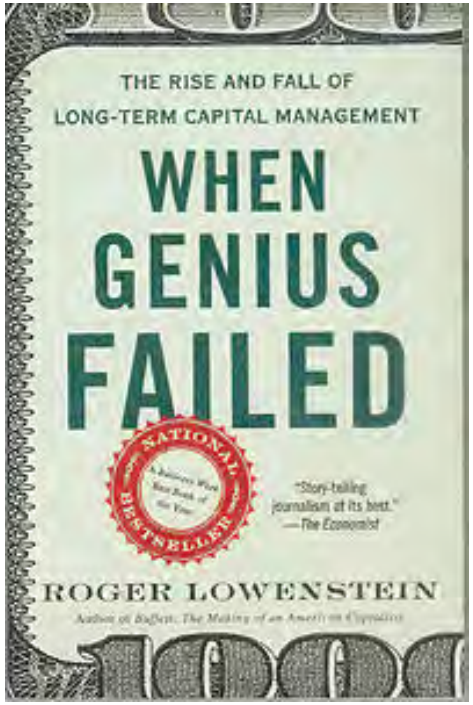

ESSAY

Long-Term Capital: It's a Short-Term Memory

By ROGER LOWENSTEIN

A FINANCIAL firm borrows billions of dollars to make big bets on esoteric securities. Markets turn and the bets go sour. Overnight, the firm loses most of its money, and Wall Street suddenly shuns it. Fearing that its collapse could set off a full-scale market meltdown, the government intervenes and encourages private interests to bail it out.

The firm isn't Bear Stearns — it was Long-Term Capital Management, the hedge fund based in Greenwich, Conn., and the rescue occurred 10 years ago this month.

The Long-Term Capital fiasco momentarily shocked Wall Street out of its complacent trust in financial models, and was replete with lessons, for Washington as well as for Wall Street. But the lessons were ignored, and in this decade, the mistakes were repeated with far more harmful consequences. Instead of learning from the past, Wall Street has re-enacted it in larger form, in the mortgage debacle cum credit crisis.

Why the experts missed the crash

Which forecasters should you trust on the direction of the economy and the markets? Ask Philip Tetlock, who knows the kind of expert worth listening to - and what to listen for.

By Eric Schurenberg, Money Magazine EMAIL
Last Updated: February 18, 2009: 4:10 PM ET

(Money Magazine) -- You've probably never wanted expert insight more than today - and never trusted it less. After all, the intelligent, articulate, well-paid authorities voicing these opinions are the ones who created the crisis or failed to predict it or lost 30% of your 401(k) in it.

Americans were shocked at how wrong the experts were. You weren't. Why not?

My research certainly prepared me for widespread forecasting failures. We found that our experts' predictions barely beat random guesses - the statistical equivalent of a dart-throwing chimp - and proved no better than predictions of reasonably well-read nonexperts. Ironically, the more famous the expert, the less accurate his or her predictions tended to be.

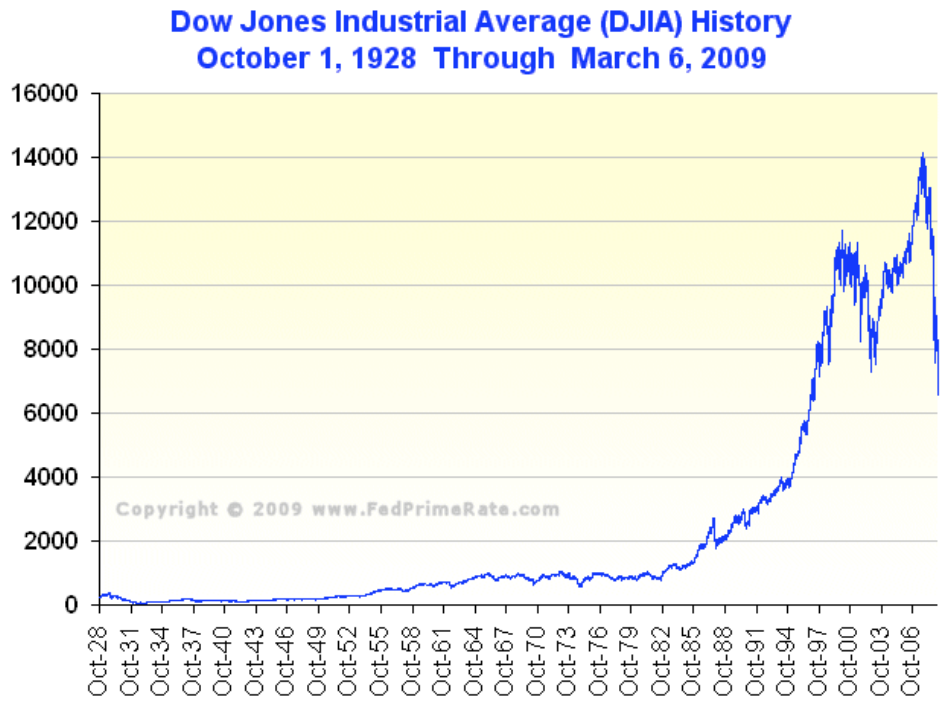

http://money.cnn.com/2009/02/17/pf/experts_Tetlock.moneymag/index.htm?postversion=2009021816

Annual GDP growth: predicted vs actual

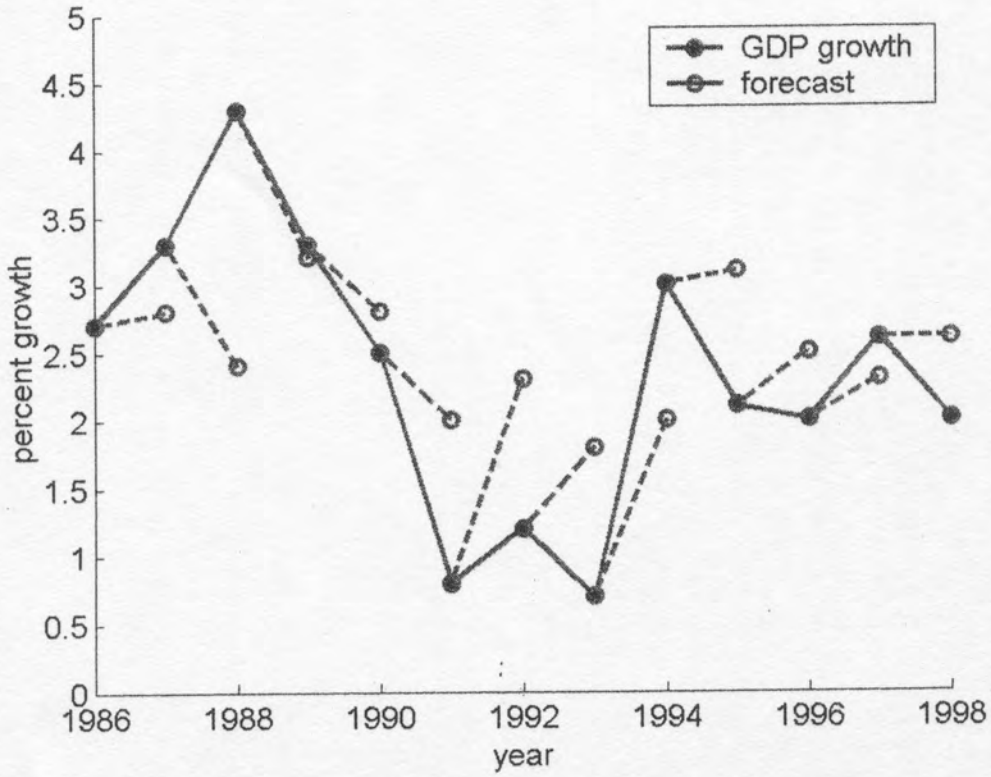

FIGURE 6.2. GDP growth for the G7 countries, plotted against the OECD one-year predictions, for the period 1986 to 1998. Standard deviation

"All models are wrong. Some models are useful."

George Box, statistics pioneer

"There are known knowns. These are things we know that we know. There are known unknowns. That is to say, there are things that we know we don't know. But there are also unknown unknowns. There are things we don't know we don't know."

Secretary of Defense Donald Rumsfeld

"As individuals, most of us intuitively understand uncertainty in minor matters. We do not expect weather forecasts to be perfect, and we know that friends are often late. But, ironically, we may fail to extend our intuitive skepticism to truly important matters. As a society, we seem to have an increasing expectation of accurate predictions about major social and environmental issues, like global warming or the time and place of the next major hurricane. But the bigger the prediction, the more ambitious it is in time, space, or the complexity of the system involved, the more opportunities there are for it to be wrong. *If there is a general claim to be made here, it may be this: the more important the prediction, the more likely it is to be wrong."*

Oreskes (2000)

Y2K

Much ado made that on January 1, 2000 computer systems would fail, because dates used only two digits

U.S. government established major programs headed by FEMA

Estimated $300 billion spent on preparations

Few major problems occurred, even among businesses and foreign countries who made little or no preparation

1976 SWINE FLU
“APORKALPSE”

CDC reported "strong possibility" of epidemic. HEW thought "chances seem to be 1 in 2” and “virus will kill one million Americans in 1976."

President Ford launched program to vaccinate entire population despite critics’ reservations

40 million vaccinated at cost of millions of dollars before program suspended due to reactions to vaccine

About 500 people had serious reactions and 25 died, compared to one person who died from swine

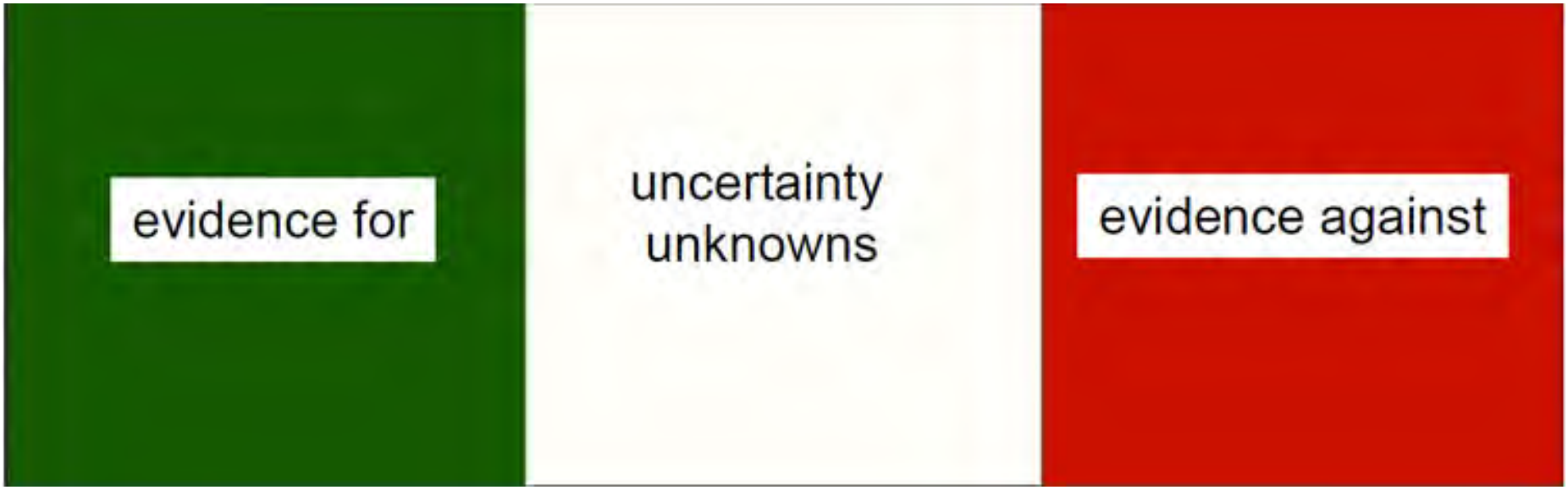

Green evidence for	White uncertainty	Red evidence against
50%	30%	20%

Precision vs accuracy

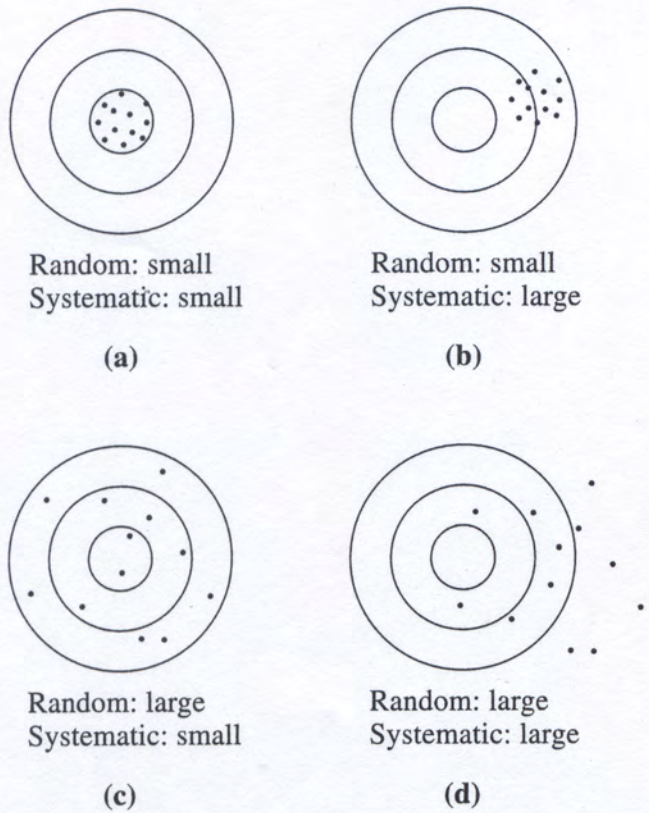

Figure 4.1. Random and systematic errors in target practice. **(a)** Because all shots arrived close to one another, we can tell the random errors are small. Because the distribution of shots is centered on the center of the target, the systematic errors are also small. **(b)** The random errors are still small, but the systematic ones are much larger—the shots are "systematically" off-center toward the right. **(c)** Here, the random errors are large, but the systematic ones are small—the shots are widely scattered but not systematically off-center. **(d)** Here, both random and systematic errors are large.

Taylor

Precision vs accuracy

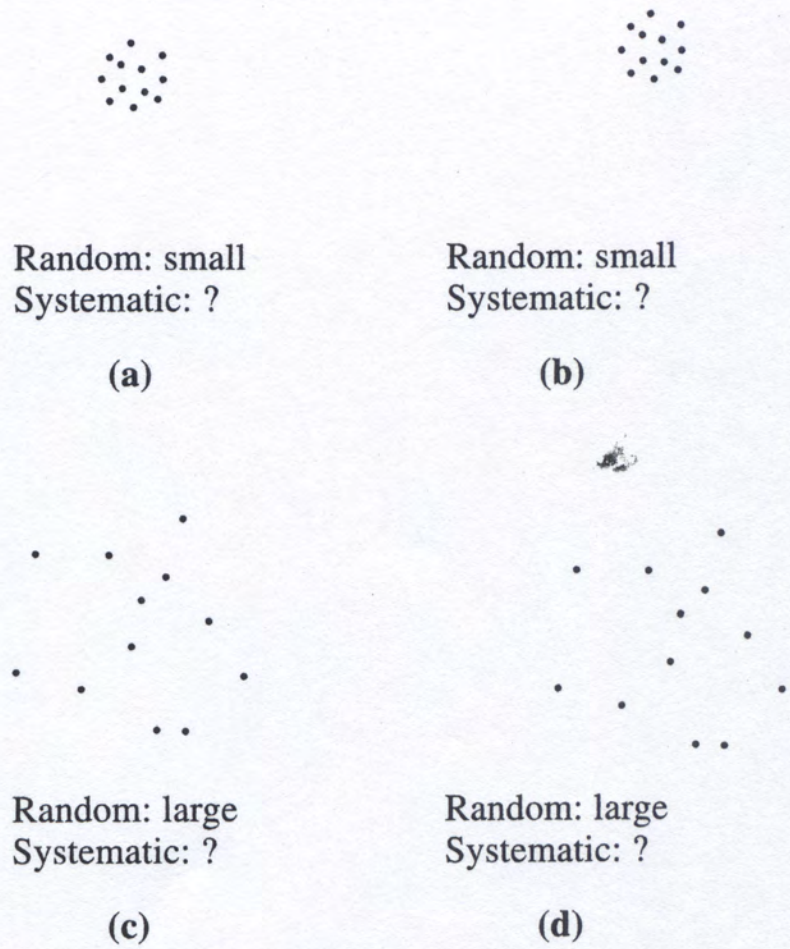

Figure 4.2. The same experiment as in Figure 4.1 redrawn without showing the position of the target. This situation corresponds closely to the one in most real experiments, in which we do not know the true value of the quantity being measured. Here, we can still assess the random errors easily but cannot tell anything about the systematic ones.

Taylor, 1997

Taylor

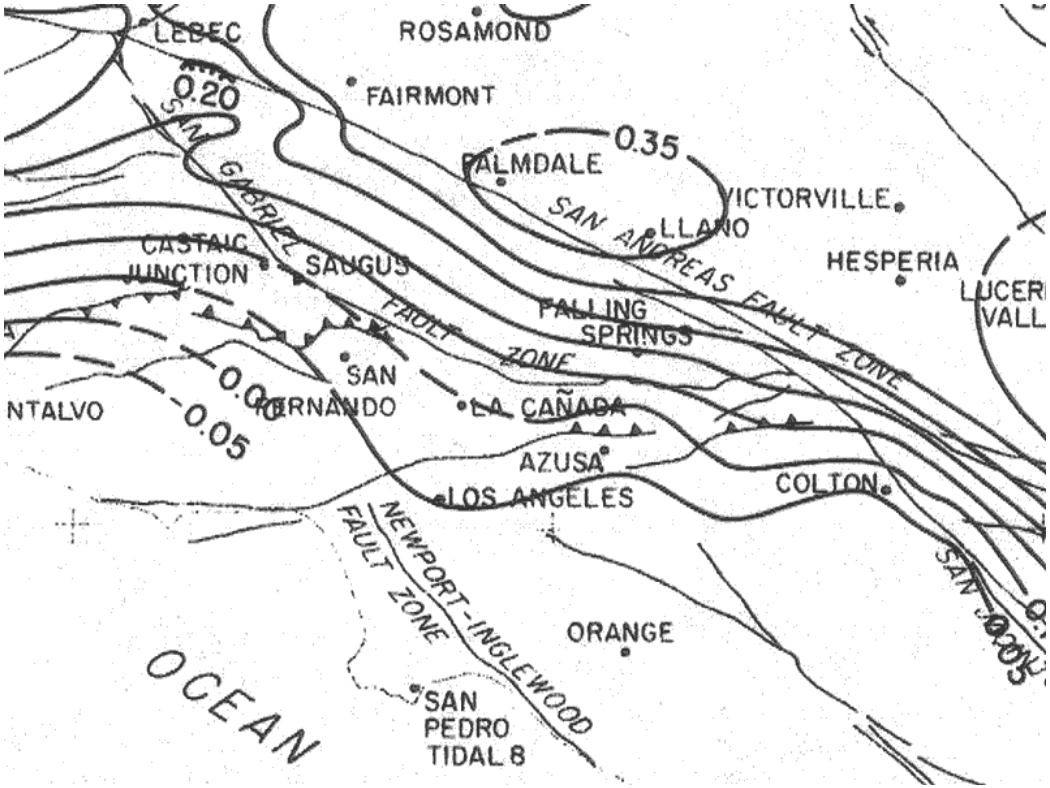

Palmdale Bulge

Efforts have been made to identify ground deformation preceding earthquakes. The most famous was the report in 1975 of 30-45 cm of uplift along the San Andreas Fault near Palmdale, California. This highly publicized "Palmdale Bulge" was interpreted as evidence for an impending large earthquake and was a factor in the U.S. government's decision to launch the National Earthquake Hazards Reduction Program aimed at studying and predicting earthquakes.

USGS director McKelvey expressed his view that a great earthquake would occur in the area possibly within the next decade that might cause up to 12,000 deaths, 48,000 serious injuries, 40,000 damaged buildings, and up to $25 billion in damage.

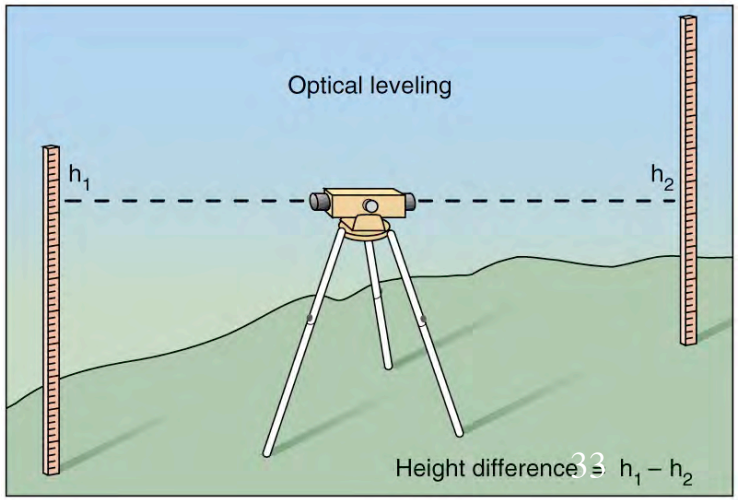

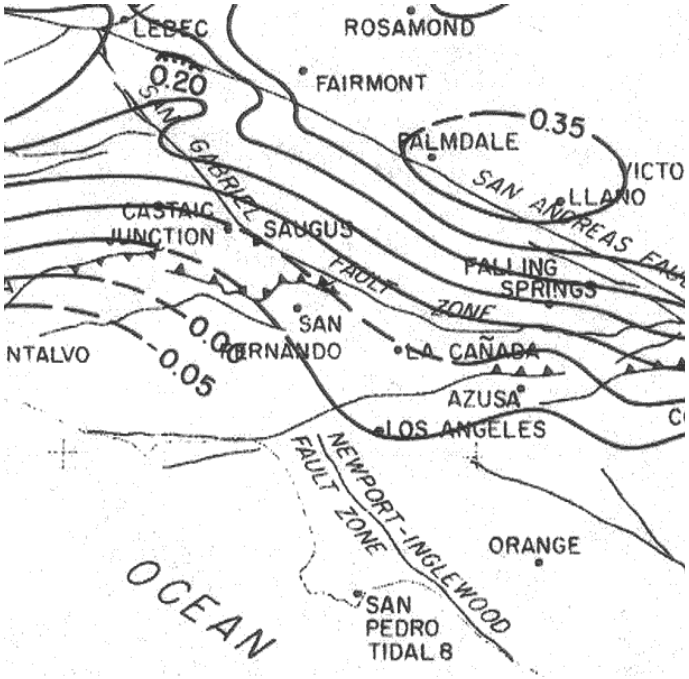

'Palmdale bulge': new study turns geological 'mountain' into molehill

By Robert C. Cowen, Natural scienc editor of The Christian Science Monitor
OCTOBER 29, 1980

Save for later

They called it the "Palmdale bulge" -- a major and rapid uplift of an extensive area of southern California between 1959 and 1974. Fears that it presaged an earthquake abounded.

Now it appears that the bulge is a mirage, an artifact of systematic errors in the relevant geodetic data.

"The inference of widespread aseismic [not caused directly by earthquake] uplift in southern California is not justified," say David D. Jackson, Wook B. Lee, and Chi-Ching Liu of the University of California at Los Angeles (UCLA). "Corrected data show no significant vertical motion except at the time of the [1971] San Fernando earthquake," they add.

In other words, crustal movement associated with a known earthquake in the area stands out. But the aseismic uplift -- that intriguing inexplicable bulge -- is no more. It only seemed to be there because of errors in reading the measuring rods used to detect changes in elevation over the nearly two-decade period.

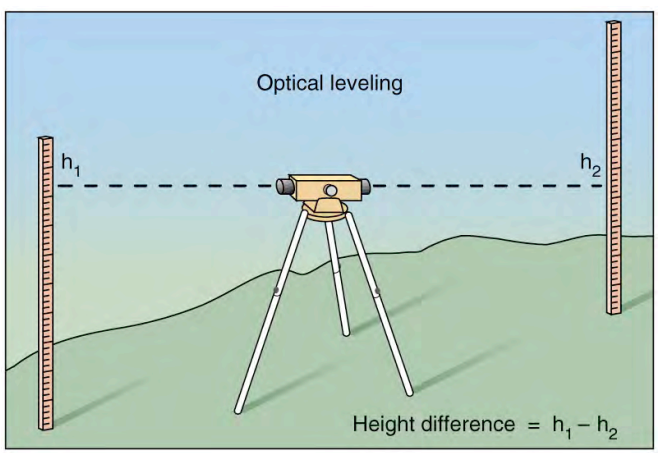

Some of the (generally small) discrepancies between plate motion rates found from space geodesy & from magnetic anomalies result from errors in the paleomagnetic timescale

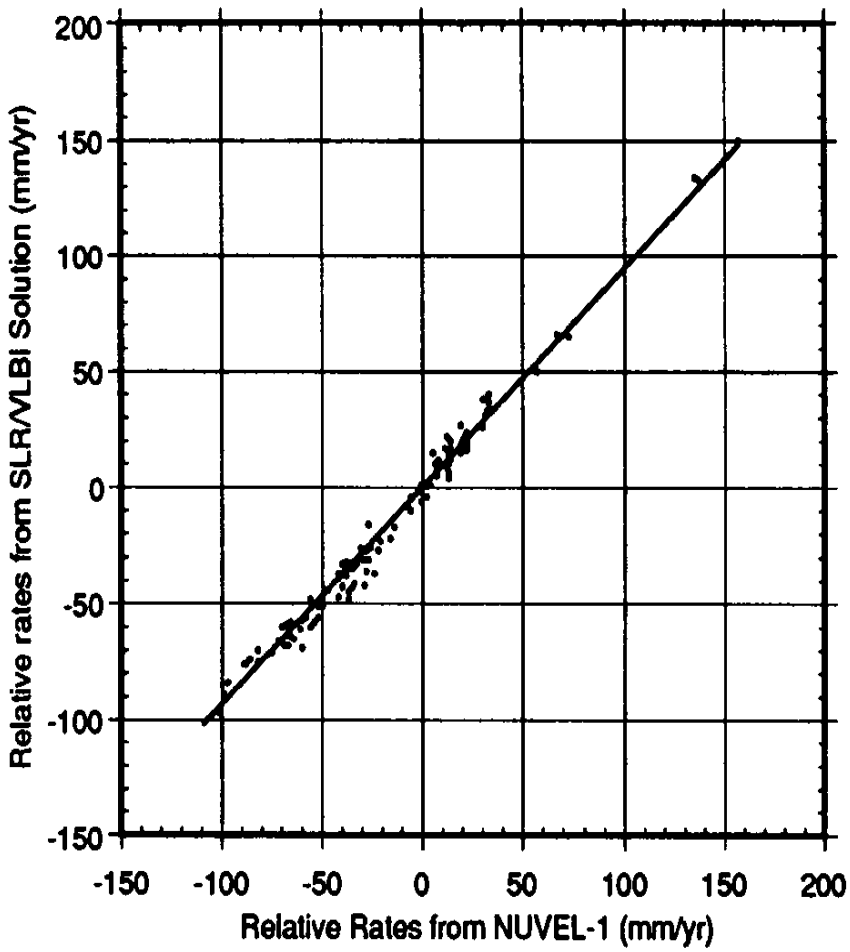

USING KNOWN HISTORY OF EARTH'S MAGNETIC FIELD, ANOMALIES CAN BE COMPUTED AND COMPARED TO THOSE OBSERVED TO DETERMINE SPREADING RATES

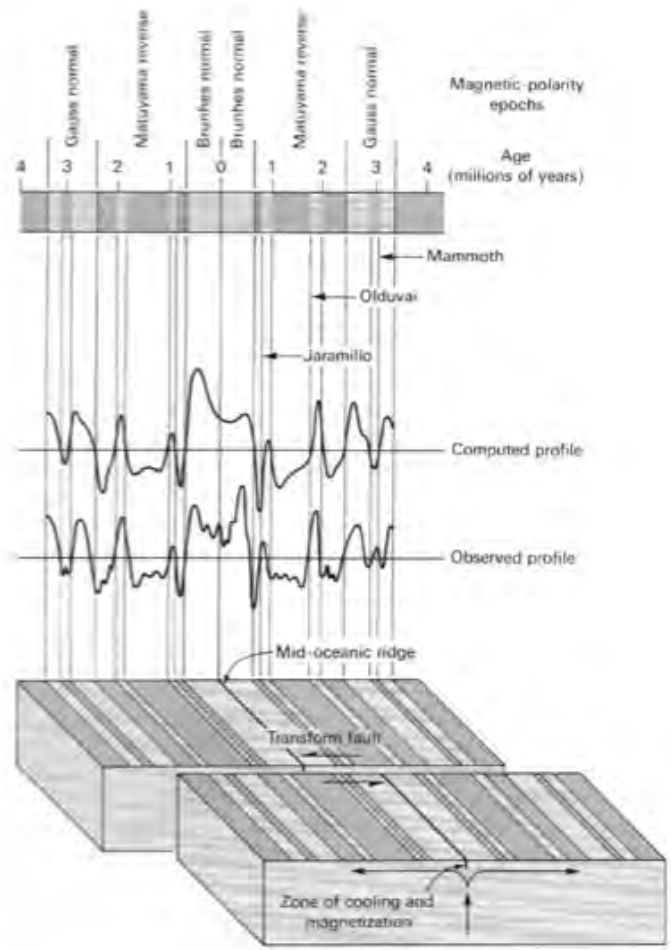

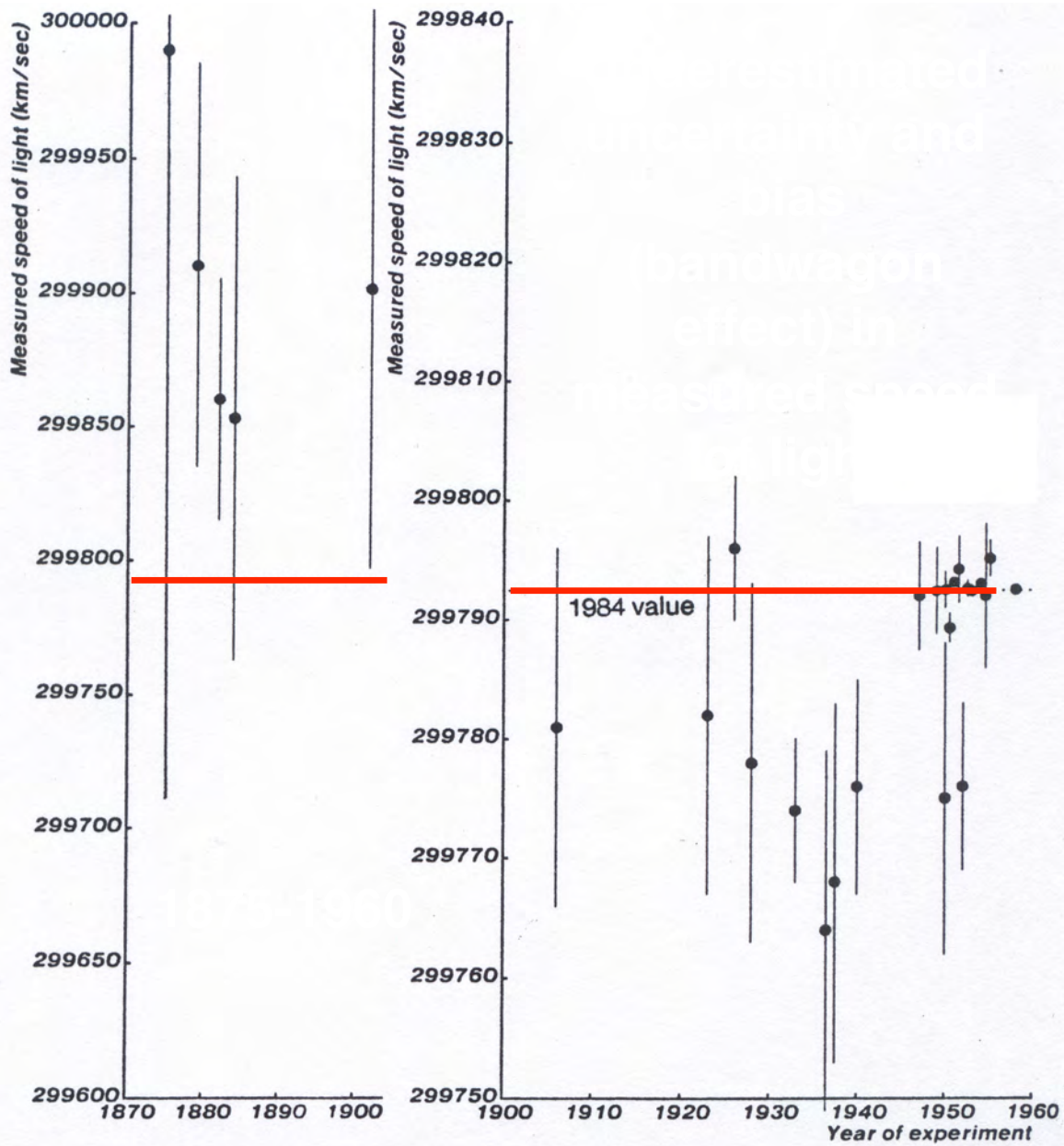

Figure 4.1. Experimental measurements of the speed of light between 1875 and 1960. Vertical bars show reported uncertainty as standard error. Horizontal dashed line represents currently accepted value. Less than 50% of the error bars enclose the accepted value, instead of the expected 70%. From Henrion and Fischoff, 1986.

Uncertainties are hard to assess and generally underestimated

Systematic errors often exceed measurement errors

Millikan's measurement of electron charge

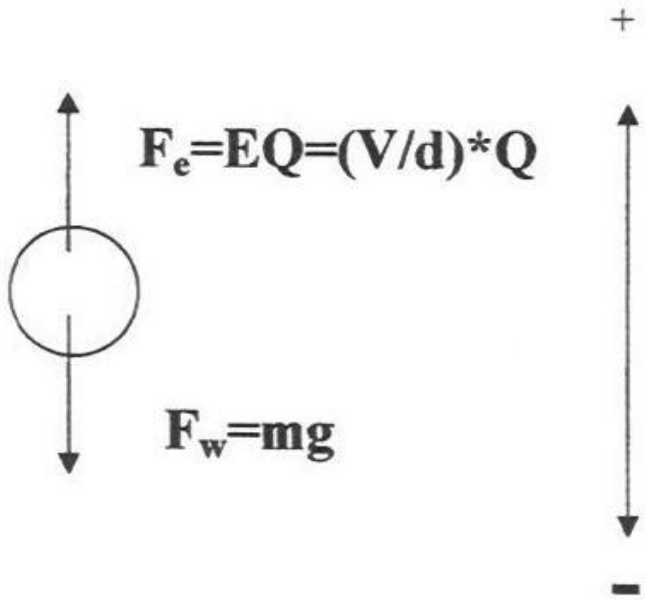

Although R. Millikan reported using all the observations in his Nobel prize-winning (1910) study of the charge of the electron, his notebooks show that he discarded 49 of 107 oil drops that appeared discordant, increasing the apparent precision of the result. Millikan's exclusions enabled him to quote that he had calculated the charge of to better than one half of one percent; in fact, if Millikan had included all of the data he threw out, it would have been within 2%. While this would still have resulted in Millikan having measured the charge better than anyone else at the time, the slightly larger uncertainty might have allowed more disagreement with his results within the physics community, which Millikan likely tried to avoid.

Number of human chromosome pairs

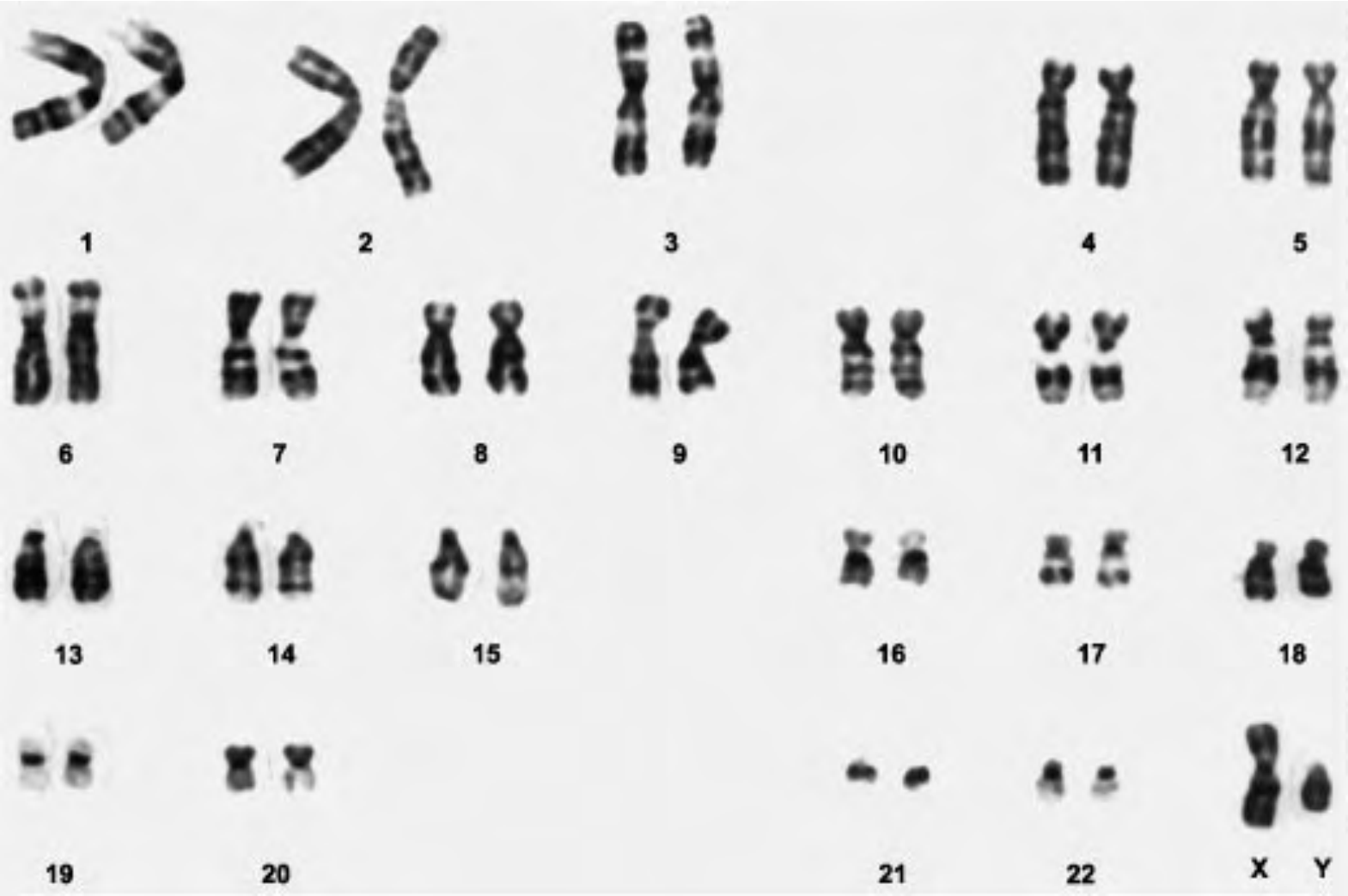

1921-1955 24; now 23

Robbins et al., 1993

Spatial sampling of stream gauges

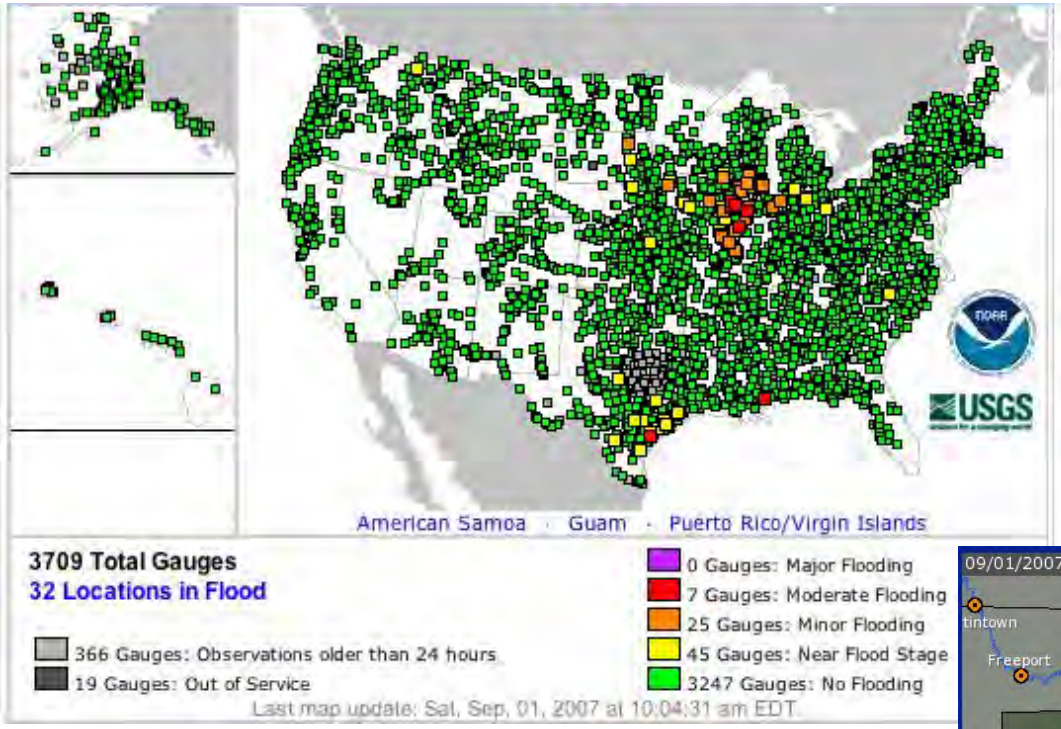

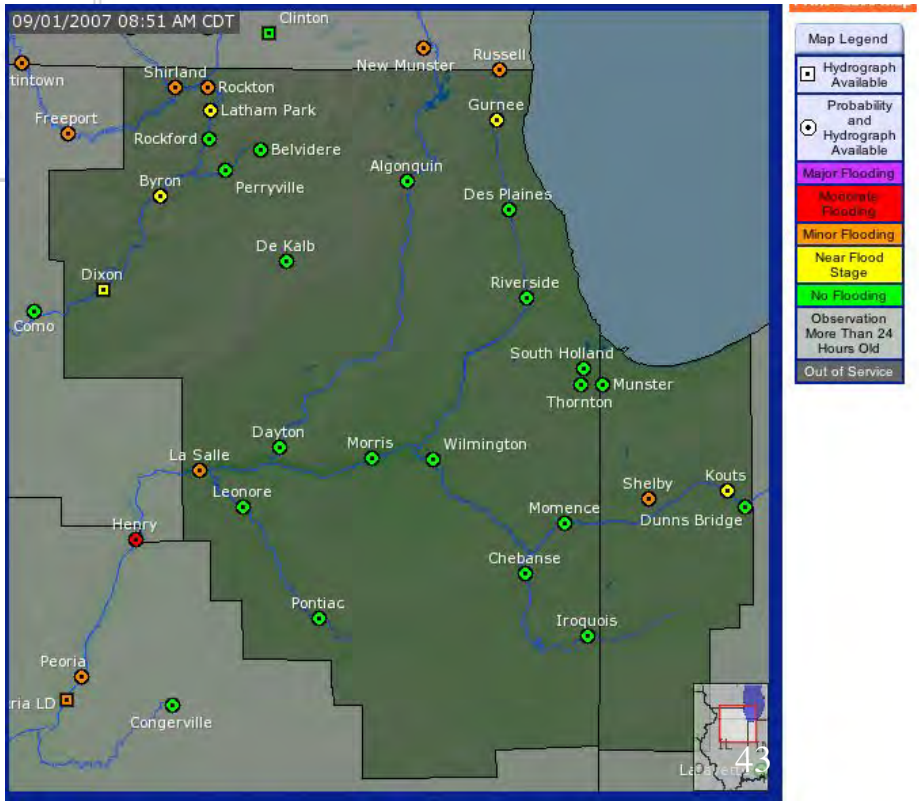

Limitations of global data coverage

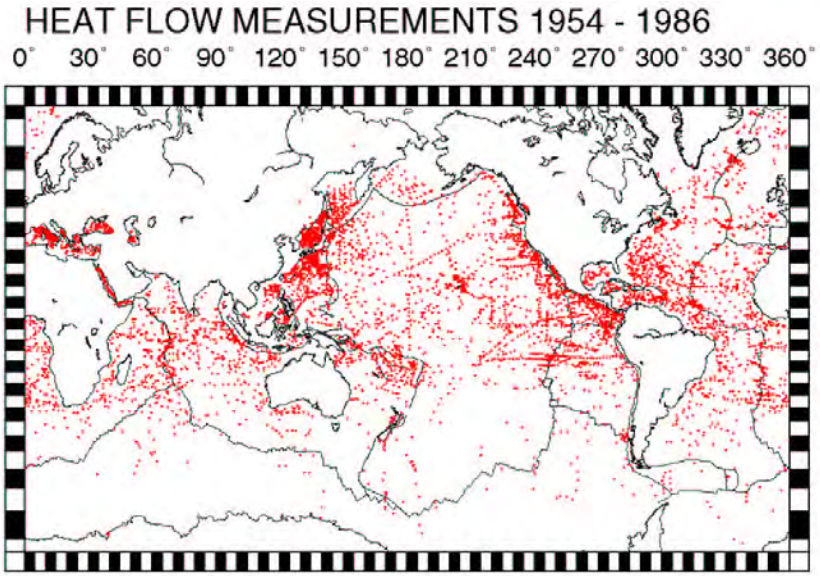

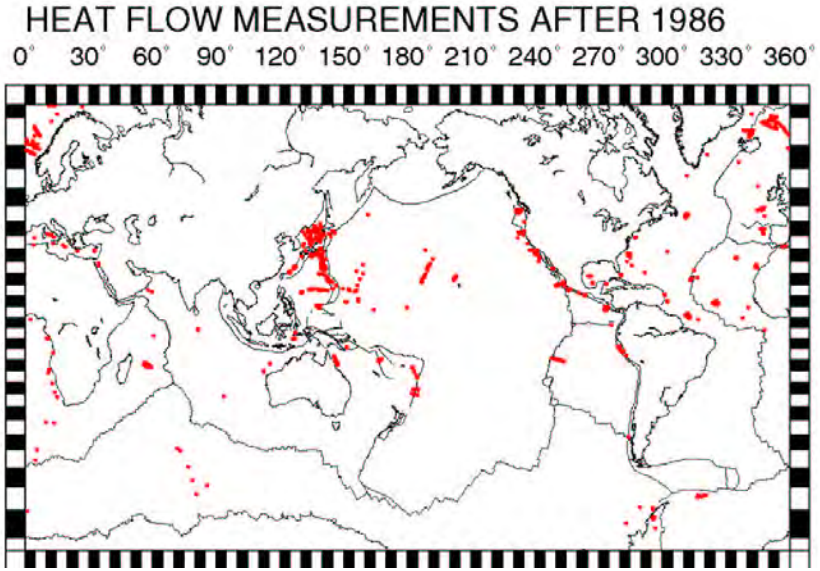

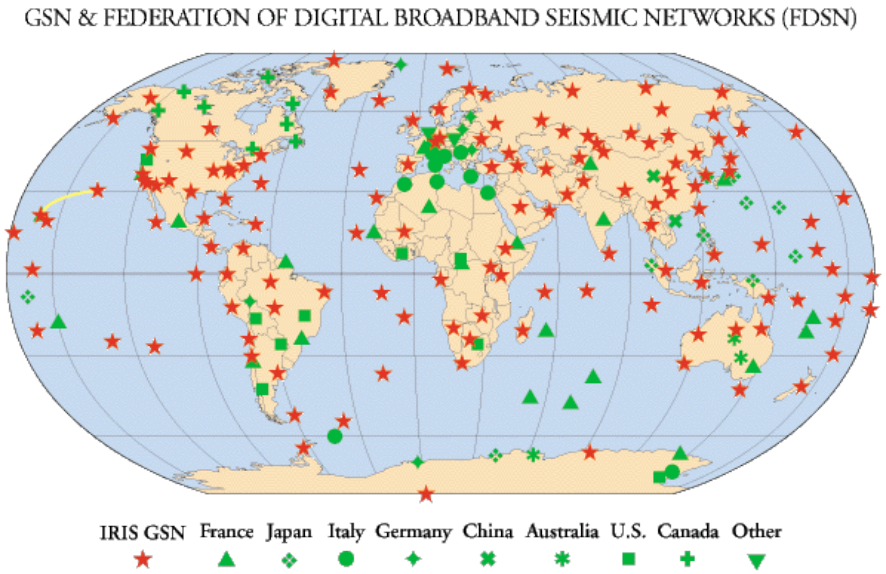

Define area of hurricane

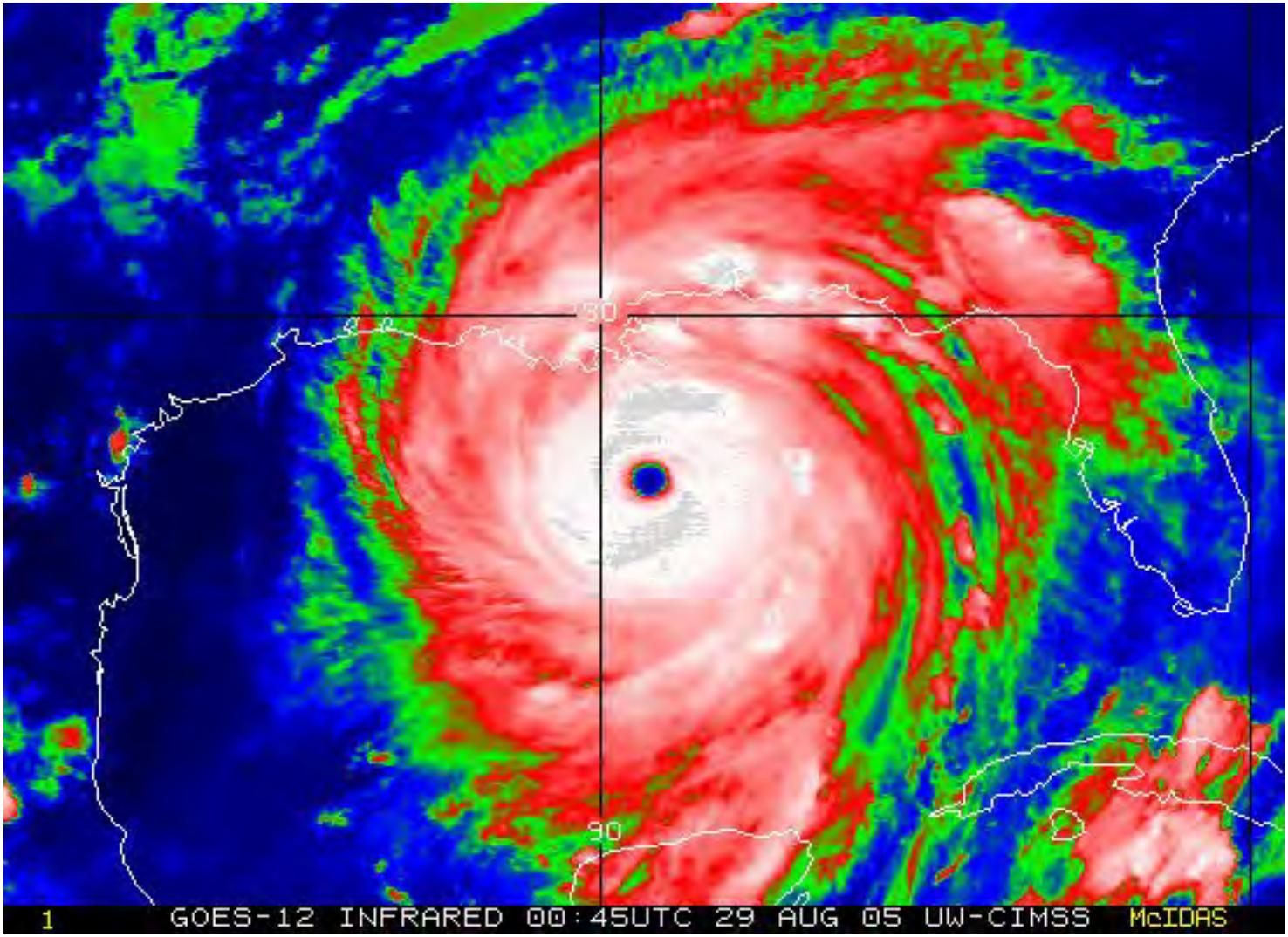

Measurement uncertainty in C/T age

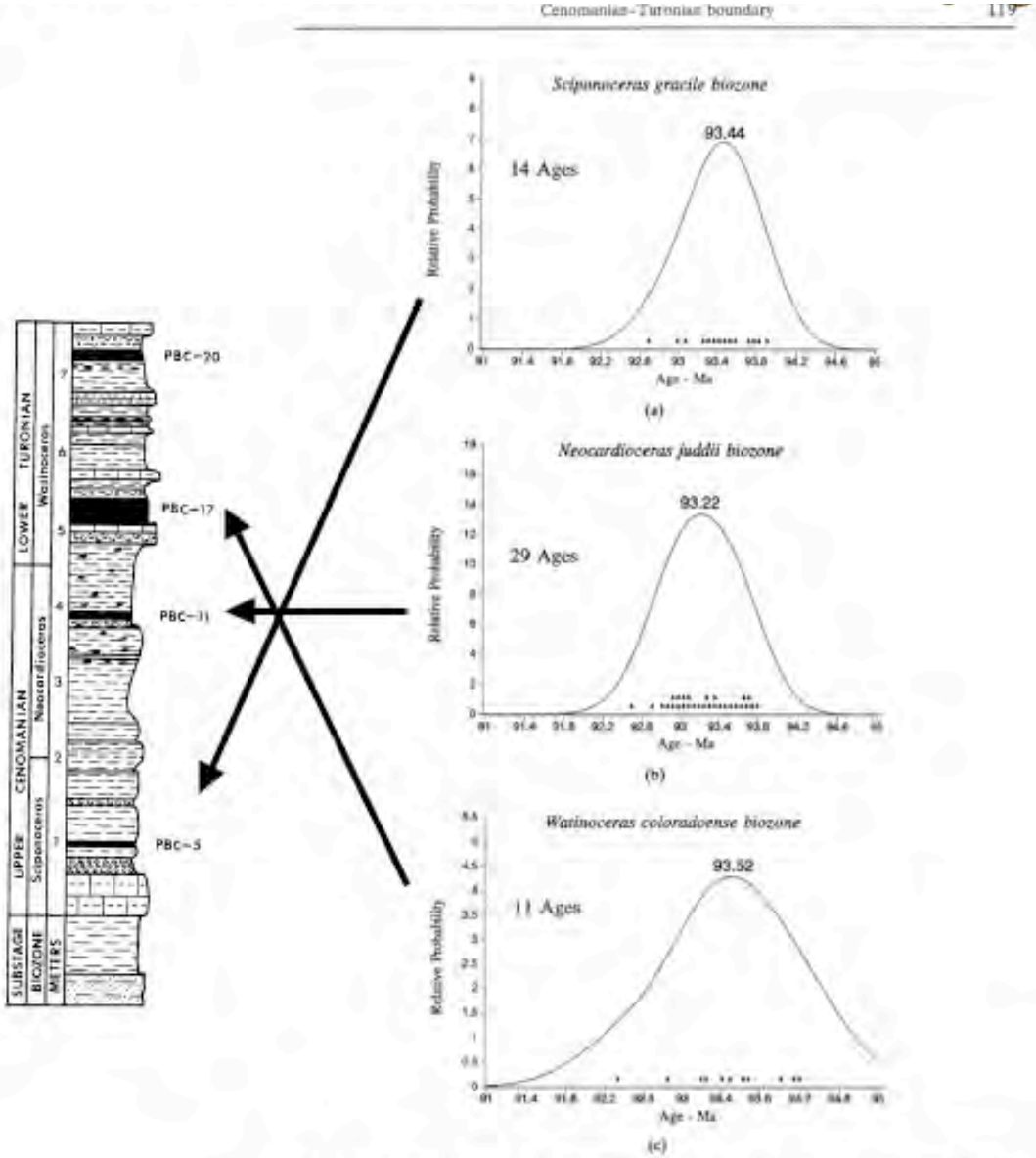

Figure 7. Single-crystal laser-fusion $^{40}Ar/^{39}Ar$ dating results represented as age-probability distributions for samples A, PBC-5, B, PBC-11, and C, PBC-17. Distributions are calculated by the methods described in Hurford *et al.* (1984) and Kowallis *et al.* (1986). Diamonds show the individual grain ages used in producing the plots. Numbers above the curves are the peak values or age modes.

Kowallis et al, 1995

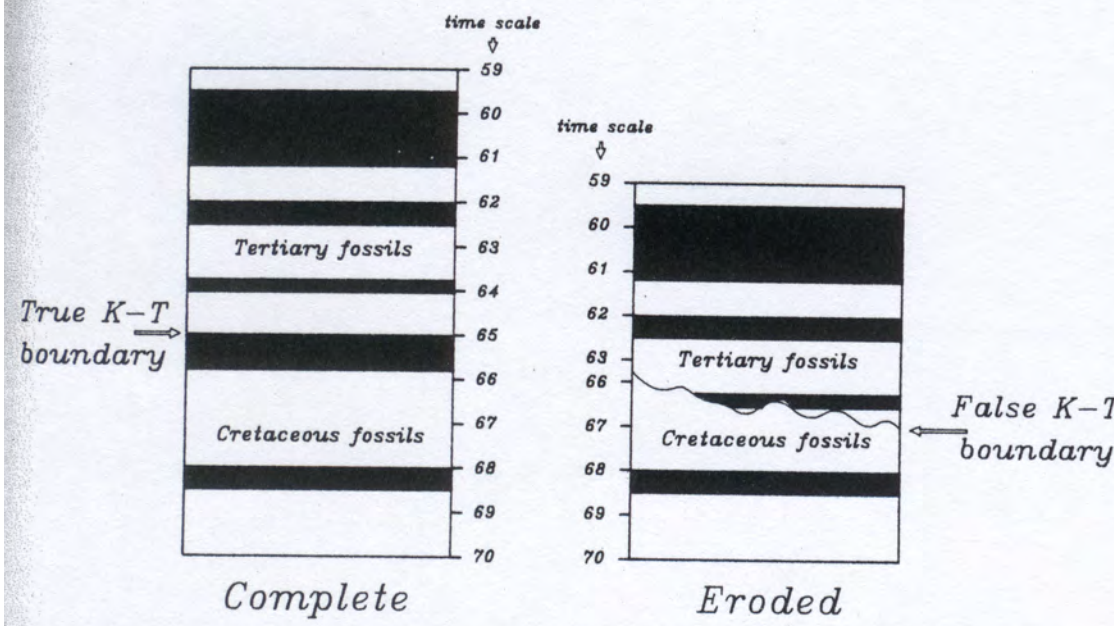

FIGURE 4-3. Two hypothetical rock sequences showing the effects of erosion on the position of the Cretaceous–Tertiary boundary. In the sequence on the right, several million years of record was lost after the end of Cretaceous time but before the start of Tertiary deposition. As a result, the first Tertiary formation rests on rocks deposited up to two million years before the end of Cretaceous time. The loss of this record causes uncertainty in times of extinction of Cretaceous lineages; a fossil may be present at a false K–T boundary yet not have survived up to the true time boundary.

INTERNATIONAL STRATIGRAPHIC CHART

International Commission on Stratigraphy

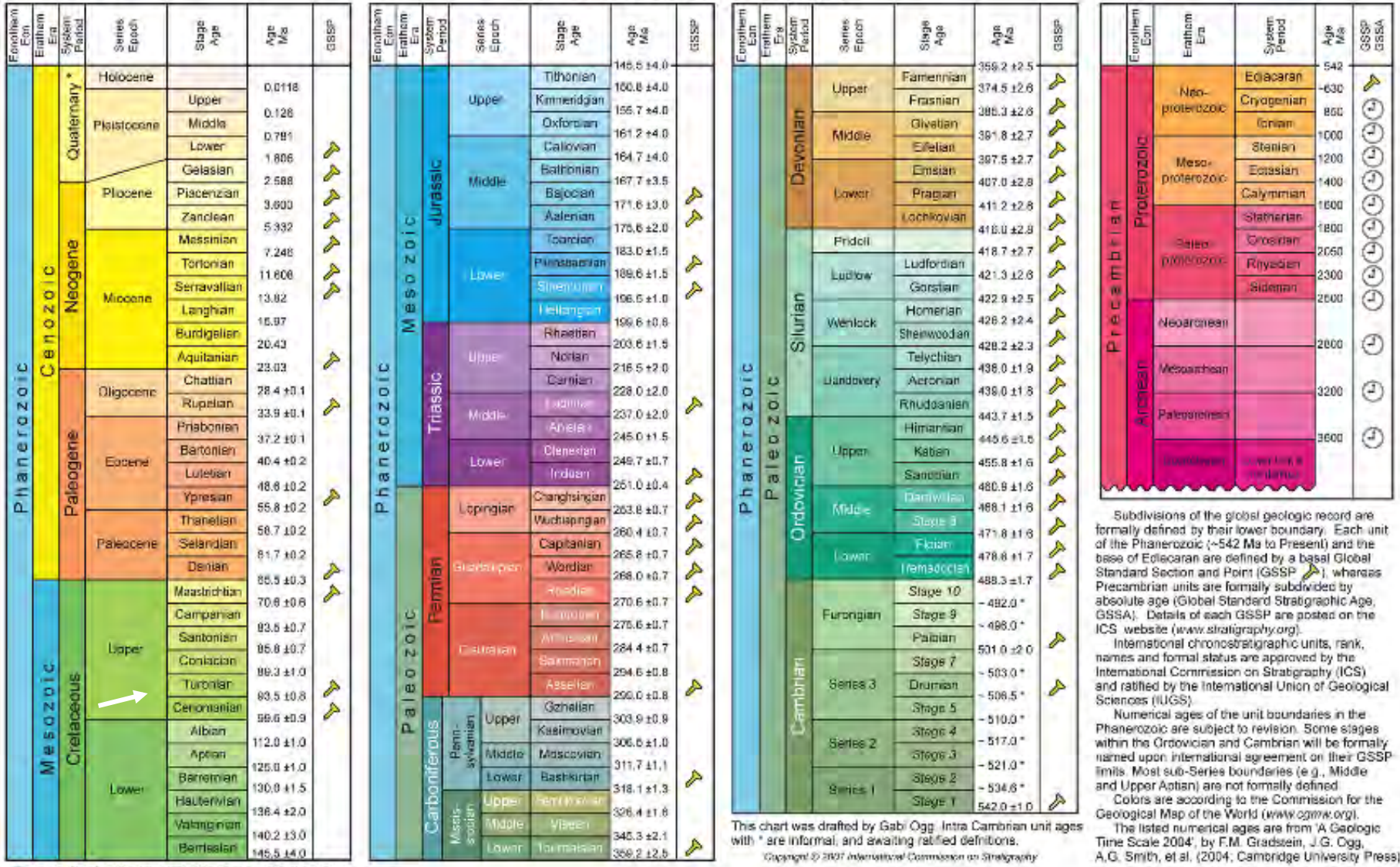

This chart was drafted by Gabi Ogg. Intra Cambrian unit ages with * are informal, and awaiting ratified definitions.

Subdivisions of the global geologic record are formally defined by their lower boundary. Each unit of the Phanerozoic (~542 Ma to Present) and the base of Ediacaran are defined by a basal Global Standard Section and Point (GSSP), whereas Precambrian units are formally subdivided by absolute age (Global Standard Stratigraphic Age, GSSA). Details of each GSSP are posted on the ICS website (*www.stratigraphy.org*).

International chronostratigraphic units, rank, names and formal status are approved by the International Commission on Stratigraphy (ICS) and ratified by the International Union of Geological Sciences (IUGS).

Numerical ages of the unit boundaries in the Phanerozoic are subject to revision. Some stages within the Ordovician and Cambrian will be formally named upon international agreement on their GSSP limits. Most sub-Series boundaries (e.g., Middle and Upper Aptian) are not formally defined.

Colors are according to the Commission for the Geological Map of the World (*www.cgmw.org*).

The listed numerical ages are from 'A Geologic Time Scale 2004', by F.M. Gradstein, J.G. Ogg, A.G. Smith, et al. (2004; Cambridge University Press).

Sumatra earthquake aftershock zone

December 2004

Mw 9.3

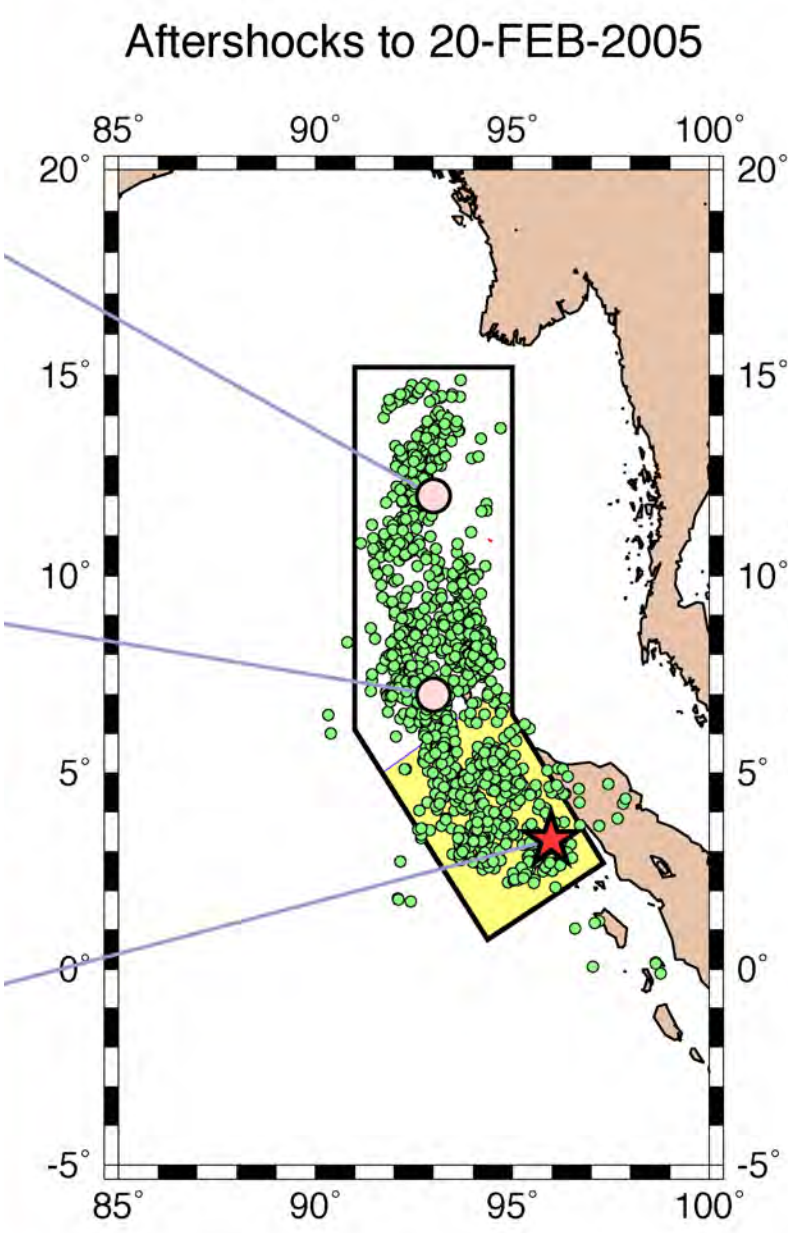

Number of Muslims in the world: significant digits

- 0.700 billion or more, Barnes & Noble Encyclopedia 1993
- 0.817 billion, The Universal Almanac (1996)
- 0.951 billion, The Cambridge Factfinder (1993)
- 1.100 billion, The World Almanac (1997)
- 1.200 billion, CAIR (Council on American-Islamic relations)

Total Number of Muslims on the Earth (1996)	1,482,596,925
Total Number of People on the Earth (1996)	5,771,939,007
Percentage of Muslims (1996)	26%
Islam annual growth rate (1994-1995) from U.N.	**6.40%**

LARGEST INTEGER FROM POWER OF 2

2**

```
2 4
3 8
4 16
5 32
6 64
7 128
8 256
9 512
10 1024
11 2048
12 4096
13 8192
14 16384
15 32768
16 65536
17 131072
18 262144
19 524288
20 1048576
21 2097152
22 4194304
23 8388608
24 16777216
25 33554432
26 67108864
27 134217728
28 268435456
29 536870912
30 1073741824
31 -2147483648
32 0
```

LINUX
WORKSTATION

FLOATING POINT PRECISION & RANGE

10** (10** +1.)- 10**

```
2  100.  1.
3  1000.  1.
4  10000.  1.
5  100000.  1.
6  1000000.  1.
7  10000000.  1.
8  100000000.  1.
9  1.E+09  1.
10  1.E+10  1.
11  9.9999998E+10  1.
12  9.99999996E+11  1.
13  9.99999983E+12  1.
14  1.E+14  1.
15  9.99999987E+14  1.
16  1.00000003E+16  1.
17  9.99999984E+16  1.
18  9.99999984E+17  1.
19  9.99999998E+18  1.
20  1.00000002E+20  0.
21  1.00000002E+21  0.
22  9.99999978E+21  0.
23  9.99999978E+22  0.
24  1.00000001E+24  0.
25  1.00000007E+25  0.
26  1.00000003E+26  0.
27  1.00000006E+27  0.
28  1.00000006E+28  0.
29  1.00000002E+29  0.
30  1.00000002E+30  0.
31  9.99999985E+30  0.
32  1.00000003E+32  0.
33  1.00000007E+33  0.
34  1.00000004E+34  0.
35  1.00000004E+35  0.
36  1.00000004E+36  0.
37  1.00000006E+37  0.
38  1.00000007E+38  0.
39  INF  NAN
```

ROUNDOFF
PRECISION
LOST

OVERFLOW

Figure A.8-4: Representation of a 32 bit floating point number.

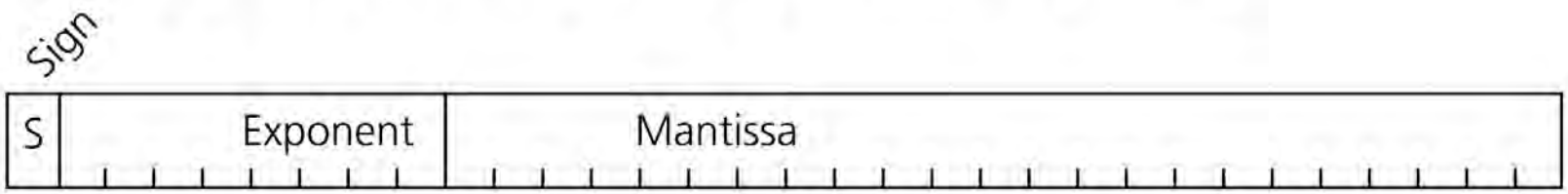

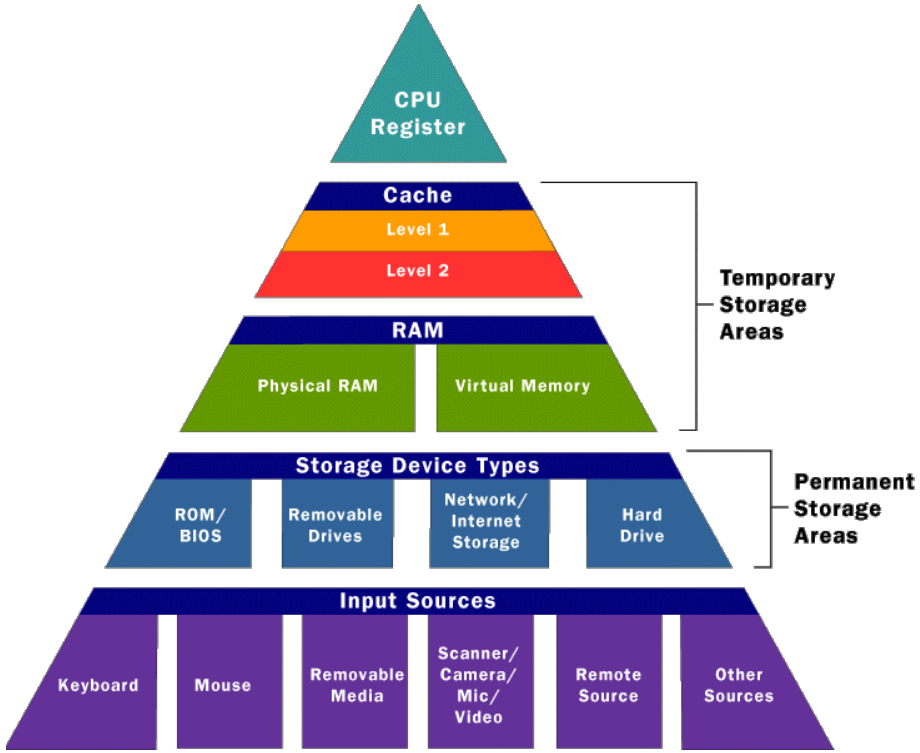

Precision & roundoff in Excel

EXCEL number	PRECISION number-1	n-(n-1)
1.00E+12	1.00E+12	1.00E+00
1.00E+14	1.00E+14	1.00E+00
1.00E+16	1.00E+16	0.00E+00
1.00E+18	1.00E+18	0.00E+00

EXCEL ROUNDOFF r=asin(acos(atan(tan(cos(sin(x))))))

	9.000000000	0.9000000000	0.0090000000
RAD	0.1570796326794900	0.015707963267949	0.000157079632679
SIN	0.1564344650402310	0.015707317311821	0.000157079632034
COS	0.9877890614843210	0.999876642627690	0.999999987662995
TAN	1.5163575525912100	1.556985242818470	1.557407682394260
ATAN	0.9877890614843210	0.999876642627690	0.999999987662995
ACOS	0.1564344650402310	0.015707317311823	0.000157079632305
ASIN	0.1570796326794900	0.015707963267952	0.000157079632951
DEGREES	9.0000000000000100	0.900000000000156	0.009000000015576
DIFF	-1E-14	-2E-13	-2E-11

error in 14th place

Explosion of Ariane 5

On June 4, 1996 an unmanned Ariane 5 rocket launched by the European Space Agency exploded 40 seconds after lift-off. The rocket was on its first voyage, after a decade of development costing $7 billion. The destroyed rocket and its cargo were valued at $500 million.

Explosion of Ariane 5

Ariane 5 rocket launched by the European Space Agency exploded 40 seconds after lift-off. The rocket was on its first voyage, after a decade of development costing $7 billion. The destroyed rocket and its cargo were valued at $500 million.

The cause of the failure was software error in the inertial reference system. A 64 bit floating point number relating to the horizontal velocity of the rocket with respect to the platform was converted to a 16 bit signed integer. The number was larger than 32,768, the largest integer storeable in a 16 bit signed integer, and thus the conversion failed.

Linear fit

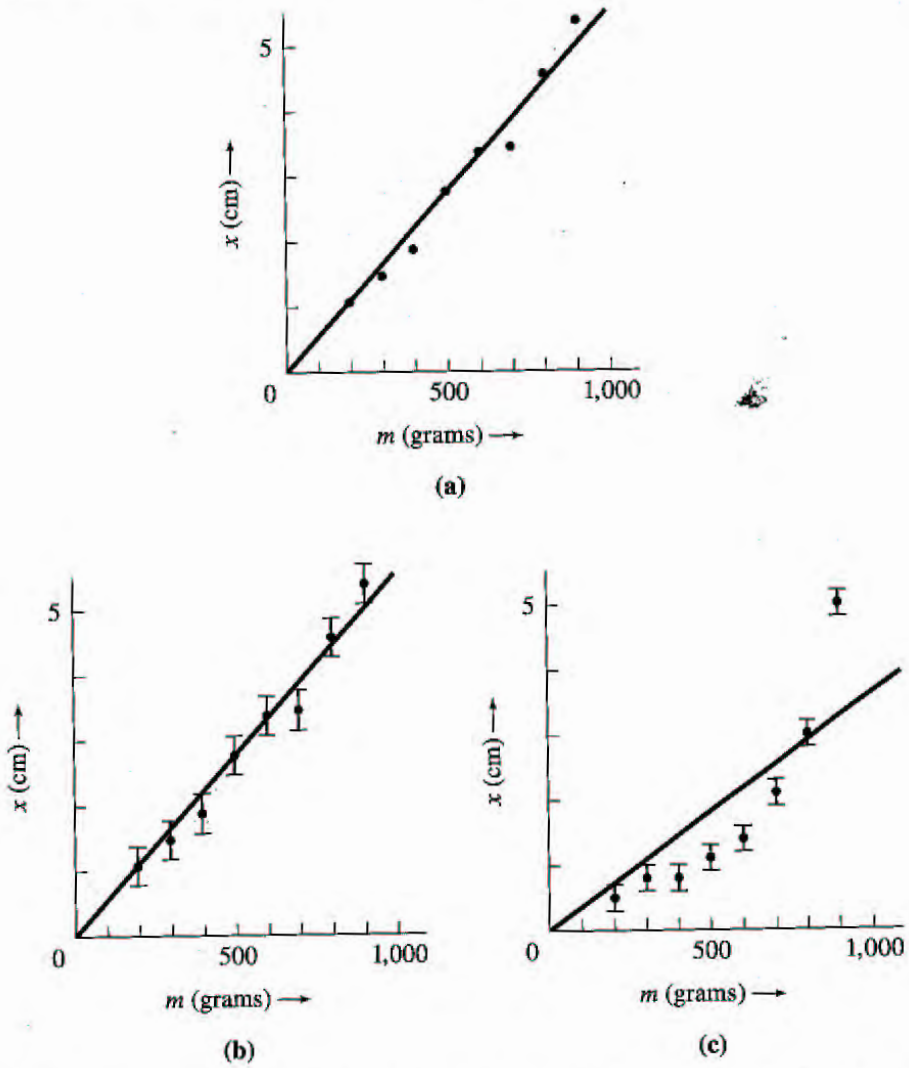

Figure 2.5. Three plots of extension x of a spring against the load m. **(a)** The data of Table 2.3 without error bars. **(b)** The same data with error bars to show the uncertainties in x. (The uncertainties in m are assumed to be negligible.) These data are consistent with the expected proportionality of x and m. **(c)** A different set of data, which are inconsistent with x being proportional to m.

Hotspot tracks

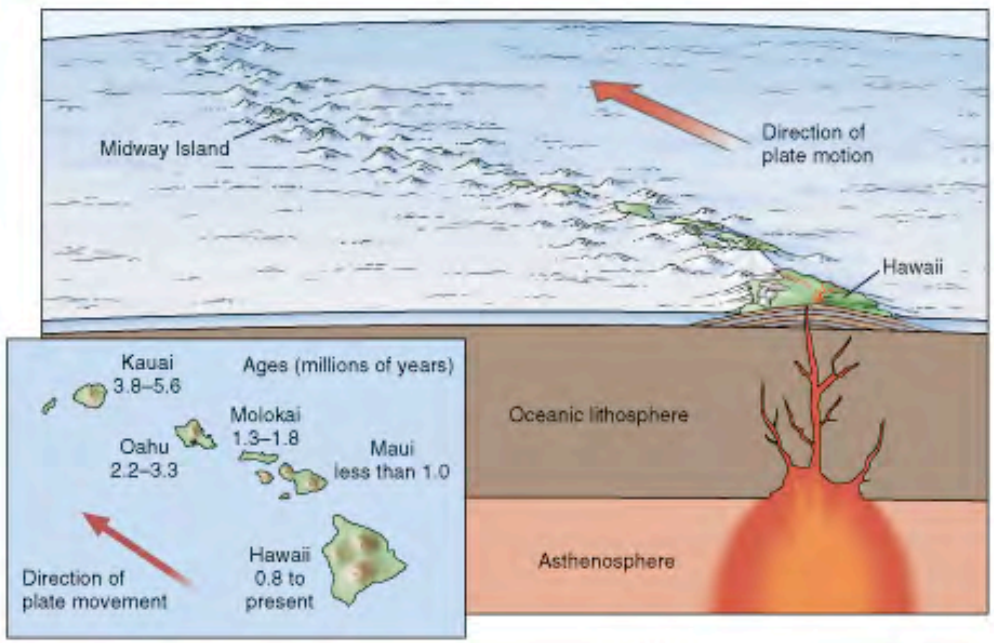

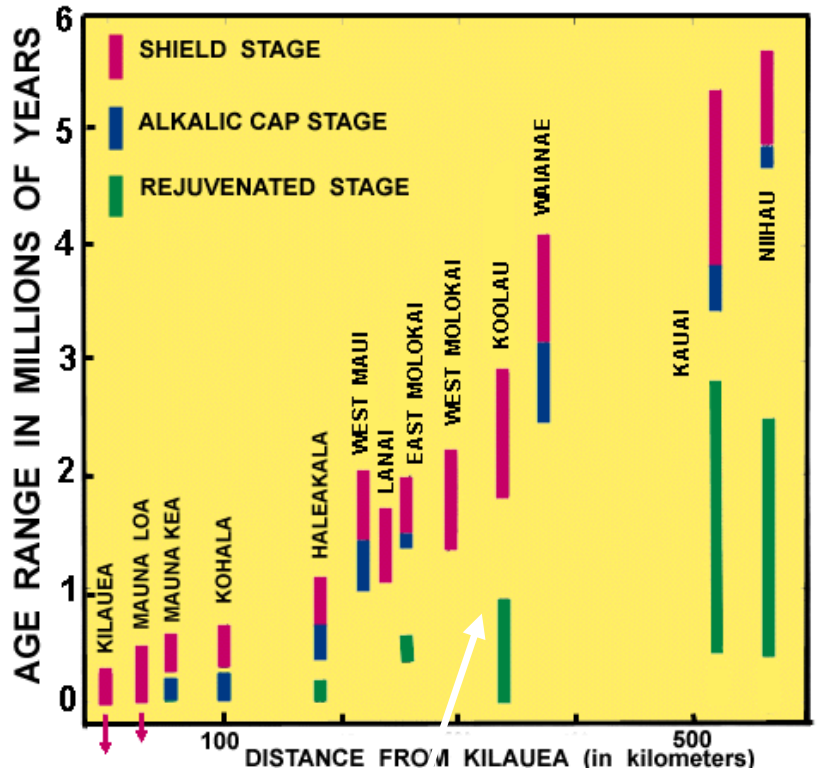

Diamond Head, Oahu
~200,000 yr

Line Islands: age progression?

Figure 1. Map shows location of Line Islands relative to some other island chains and location of fracture zones in the Pacific Ocean. Line shows trace of hypothetical hot spot on the Pacific plate [*Duncan and Clague*, 1985]. Red dots indicate location of presently active hot spots.

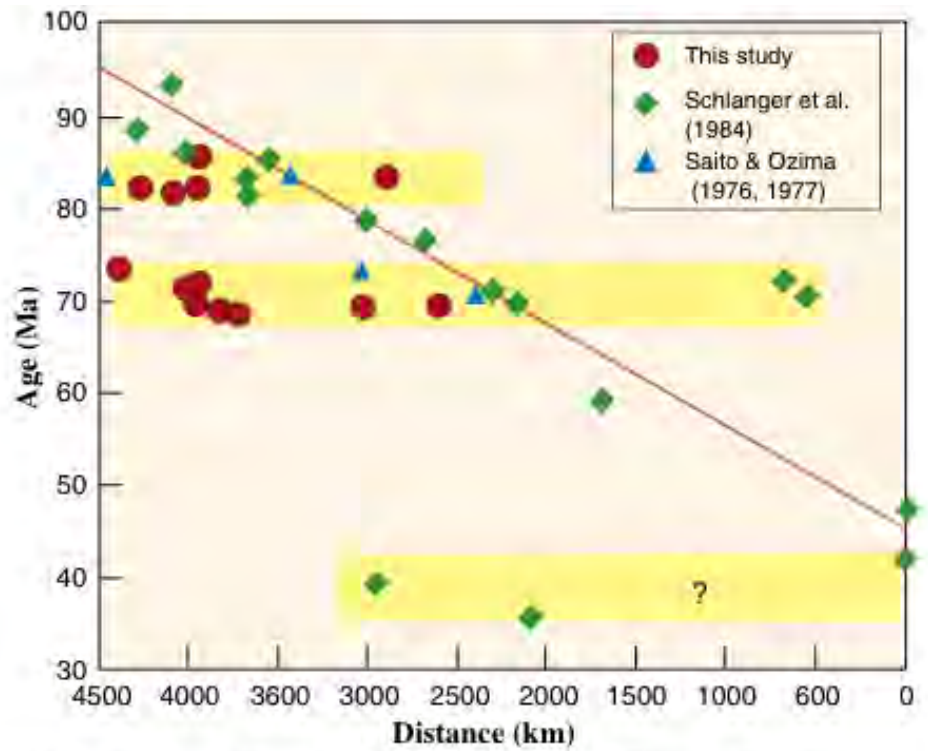

Figure 8. Radiometric ages of this study are shown, along with those of *Schlanger et al.* [1984] and of *Saito and Ozima* [1976, 1977], against distance from the Line-Tuamuto bend. Diagonal red line represents rate of volcanic propagation (9.6 ± 0.4 cm) proposed by *Schlanger et al.* [1984] as evidence for a hot spot trace. New ages indicate two major episodes of volcanism more than 10 million years apart. Ages of *Schlanger et al.* [1984] from the southern Line Islands suggest another episode of volcanism (~40 Ma) in this region.

Fitting a parabola

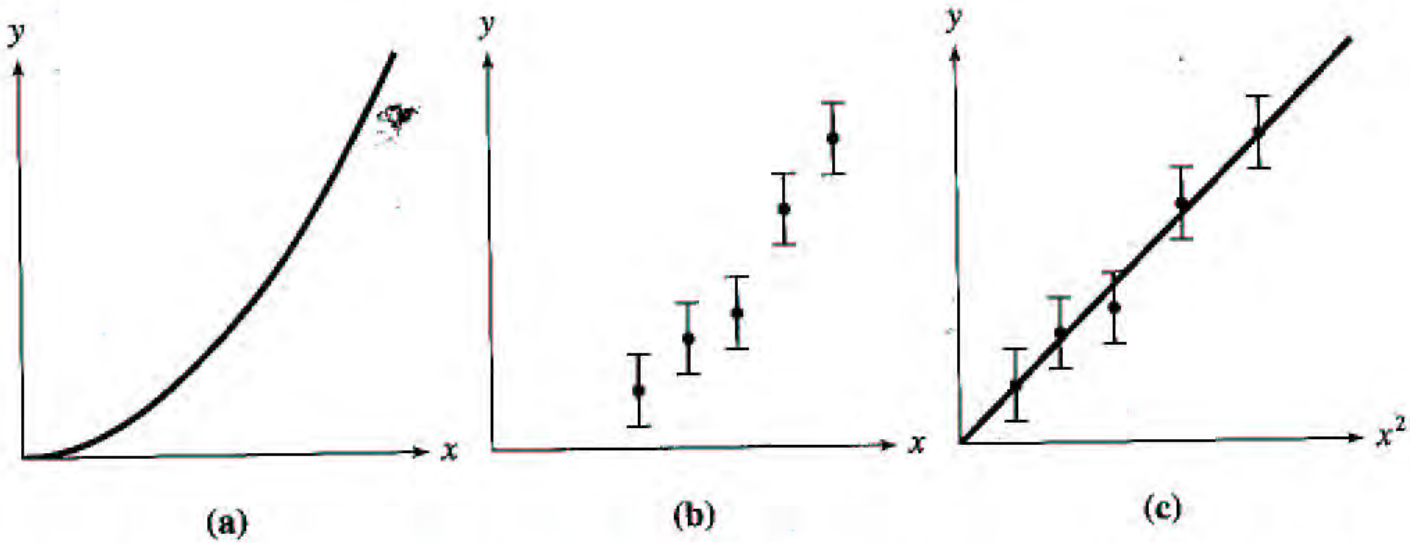

Figure 2.7. **(a)** If y is proportional to x^2, a graph of y against x should be a parabola with this general shape. **(b)** A plot of y against x for a set of measured values is hard to check visually for fit with a parabola. **(c)** On the other hand, a plot of y against x^2 should be a straight line through the origin, which is easy to check. (In the case shown, we see easily that the points *do* fit a straight line through the origin.)

Ocean depth versus square root of age

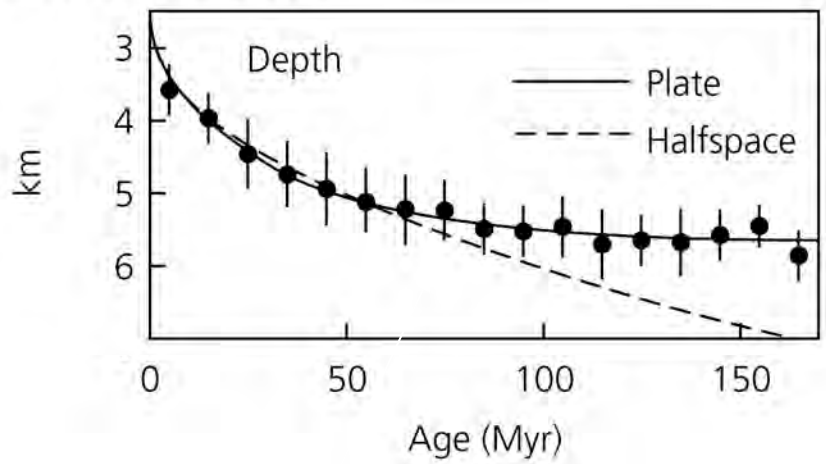

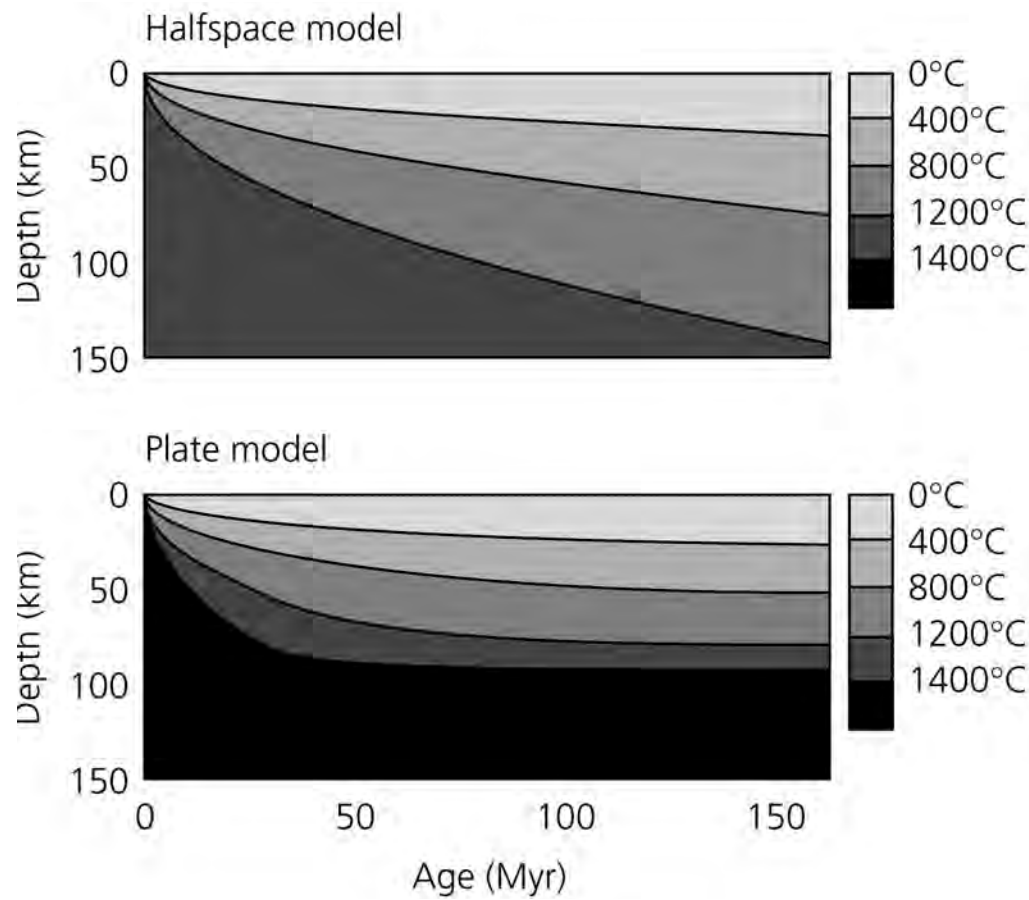

Uncertainties in both variables

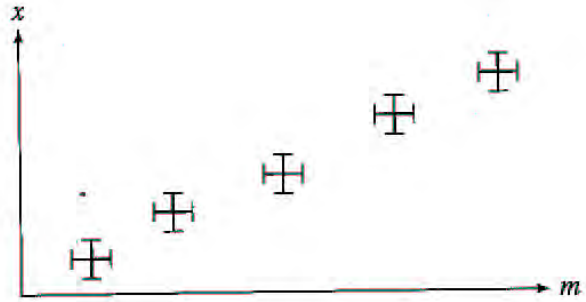

Figure 2.6. Measurements that have uncertainties in both variables can be shown by crosses made up of one error bar for each variable.

Figure 5.7-29: San Andreas shear strain rate as a function of time since the last earthquake.

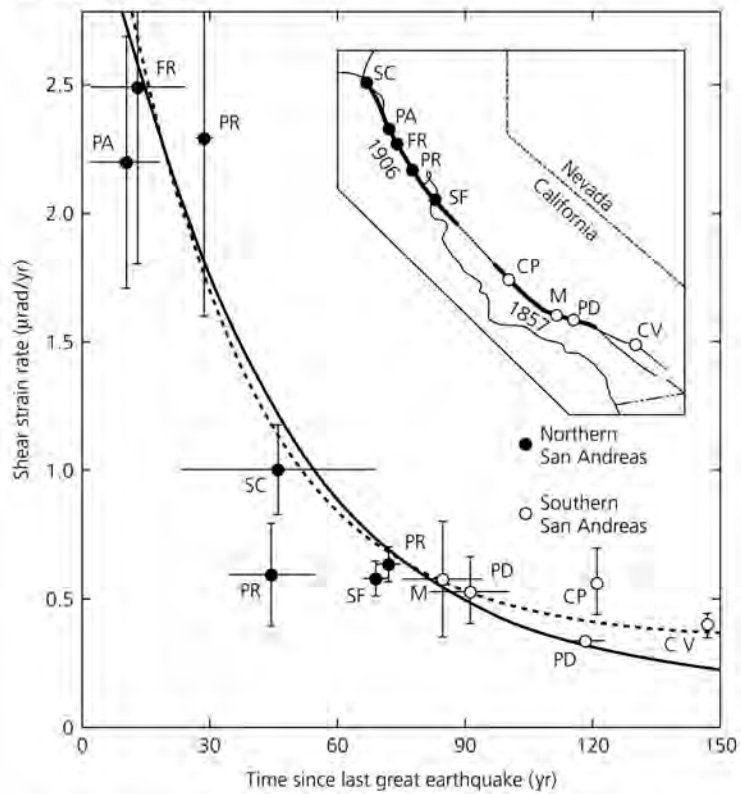

Finding mean & standard deviation with Excel

	A	B	C	D
1	TAYLOR T4.1		ADD 100	EXCEL
2			100	
3	71		71	
4	72		72	
5	72		72	
6	73		73	
7	71		71	
8	71.8	mean	76.5	AVERAGE(c2:c7)
9	0.8	sample sd	11.5	STDEV(C2:c7)
10	72	median	72	MEDIAN(c2:c7)
11				

San Andreas Fault near Palmdale, CA

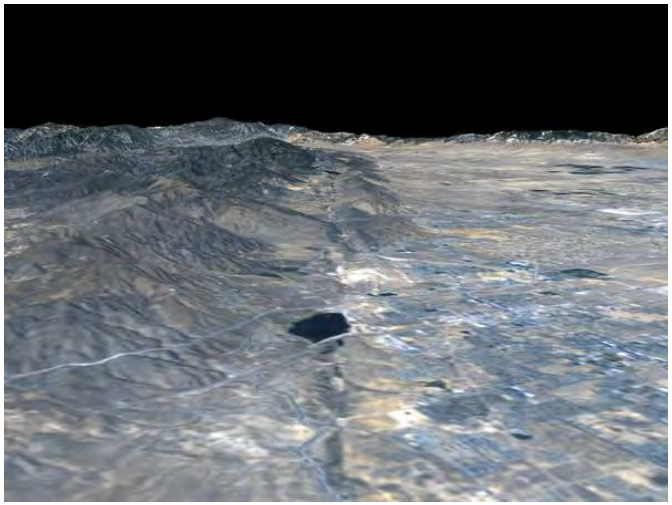

Mean & standard deviation of San Andreas Fault earthquake history

	A	B	C	D	E
1	Pallett Creek				EXCEL
2					
3	dates	intervals			
4	1857				
5	1812	45			
6	1480	332			
7	1346	134			
8	1100	246			
9	1048	52	mean	132	AVERAGE(B5:B13)
10	997	51	sample sd	105	STDEV(B5:B13)
11	797	200	median	63	MEDIAN(B5:B13)
12	734	63			
13	671	63			

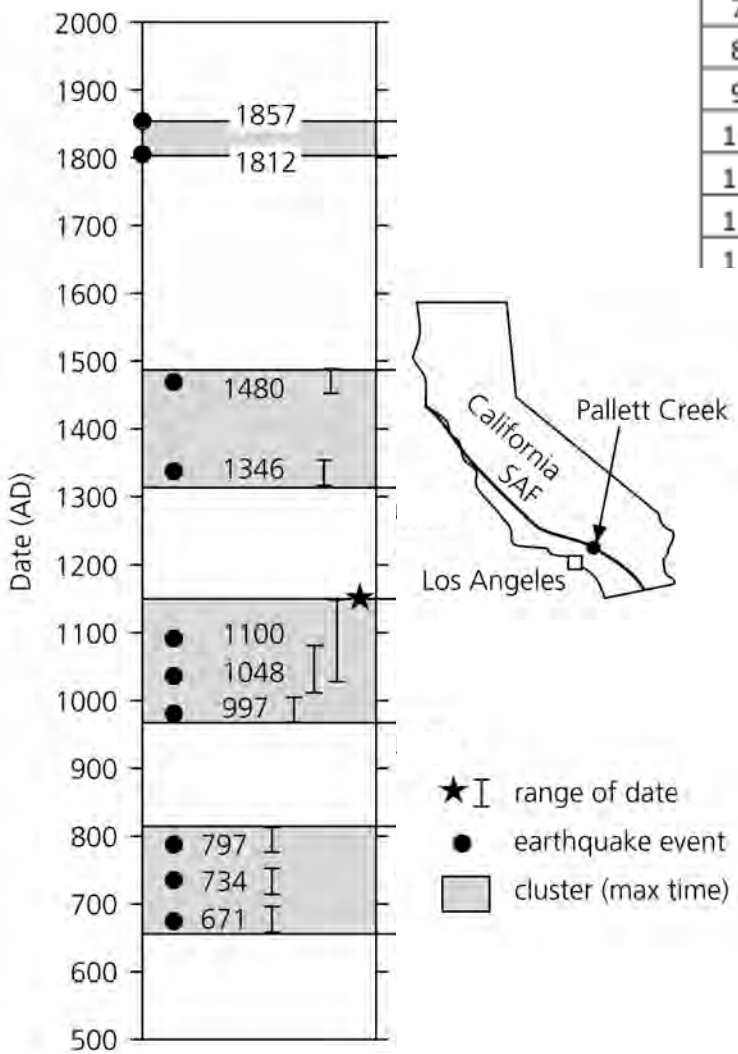

	Width	
Eyeball	Ruler	Tape
740	600	500
700	610	615
750	600	609
500	590	615
650	630	620
750	610	500
800	609	615
500	610	620
600	590	605
800	596	630
650	608	610
500	590	611
500	600	620
300	580	610
1500	750	500
average	612	592
stdev	40	48
median	600	611

Gaussian distribution

Figure 6.5-1: Gaussian distribution.

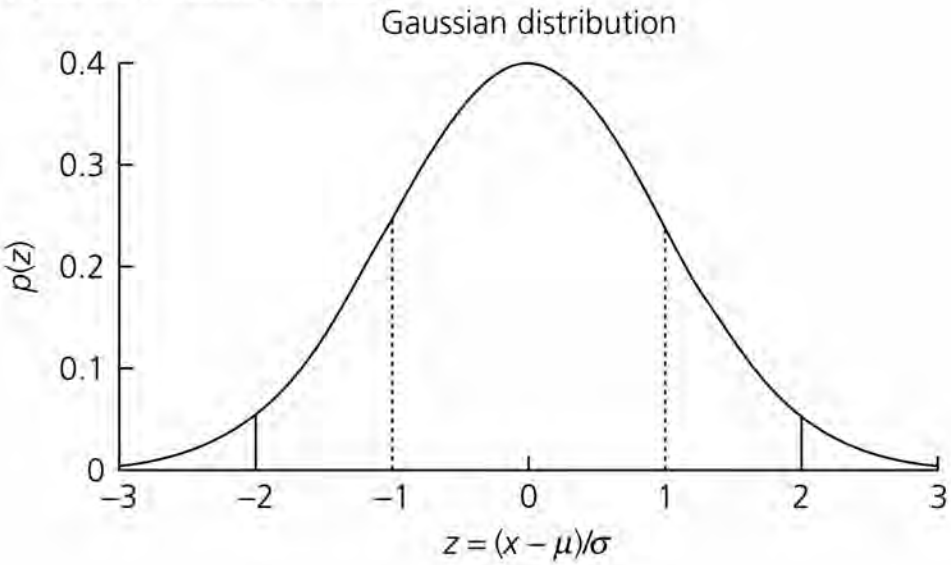

Figure 6.5-2: Results of drawing N samples from a Gaussian parent distribution.

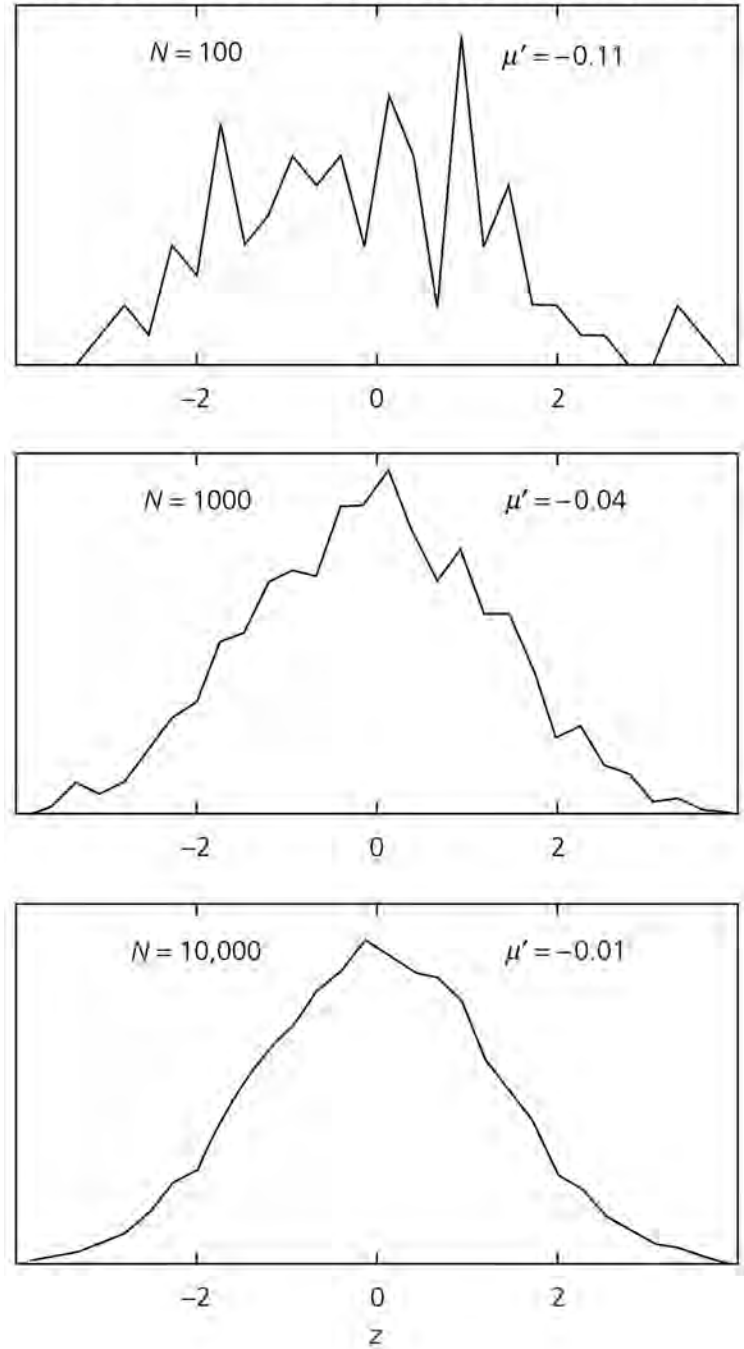

Mean 0
Standard deviation 1

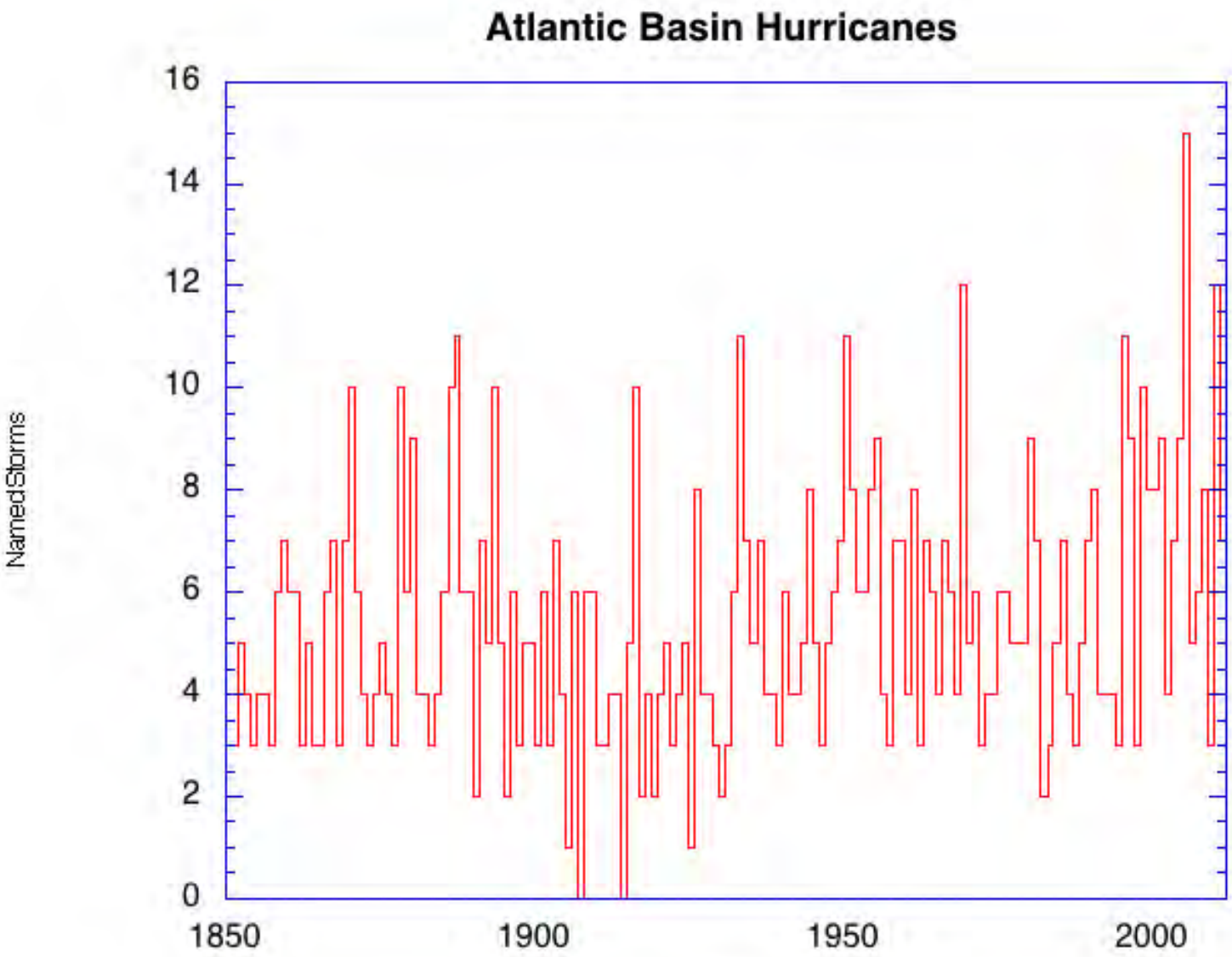

1968-2015 mean annual 6.2 standard deviation 2.9 $6.2^{1/2} = 2.5$

www.aoml.noaa.gov/hrd/tcfaq/E11.html

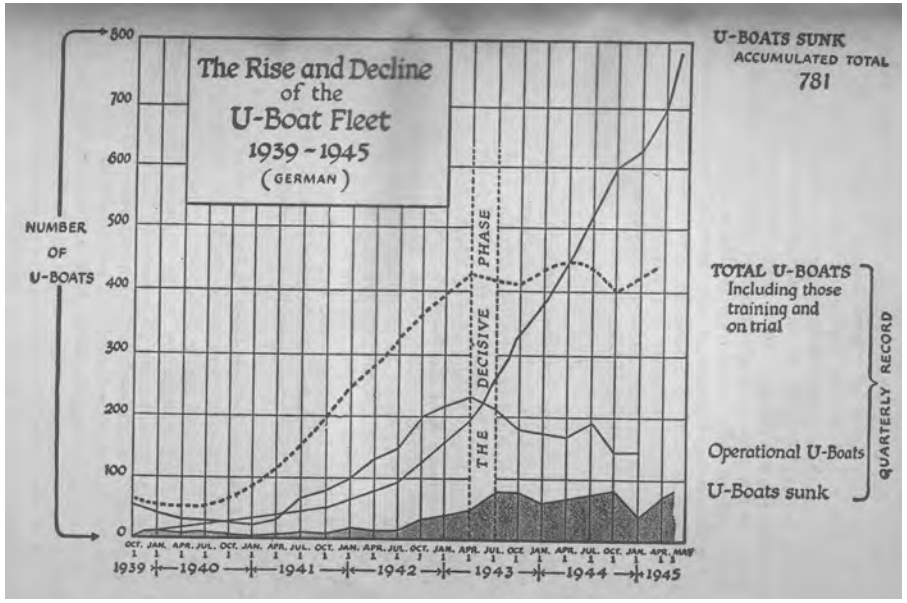

Trends in data

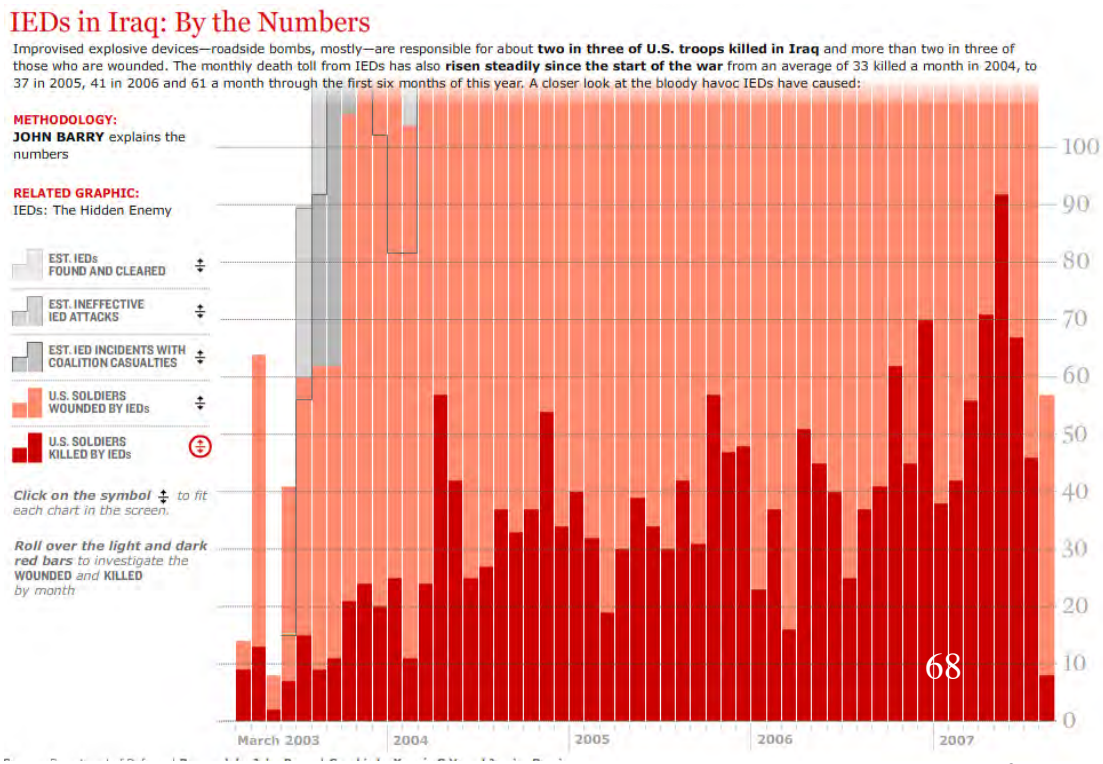

Graphical view of error propagation

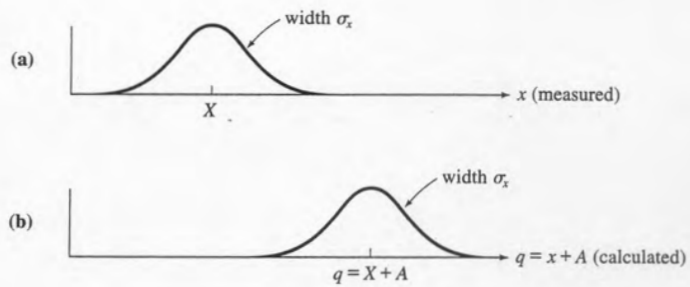

Figure 5.14. If the measured values of x are normally distributed with center $x = X$ and wid σ_x, the calculated values of $q = x + A$ (with A fixed and known) will be normally distributed with center $q = X + A$ and the same width σ_x.

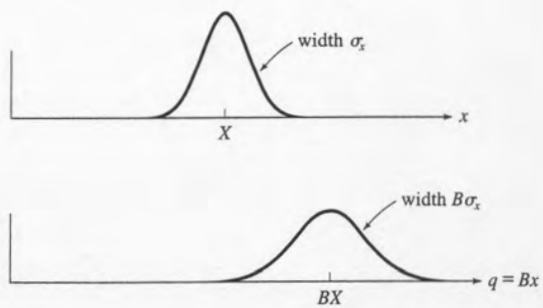

re 5.15. If the measured values of x are normally distributed with center $x = X$ and width hen the calculated values of $q = Bx$ (with B fixed and known) will be normally distributed center BX and width $B\sigma_x$.

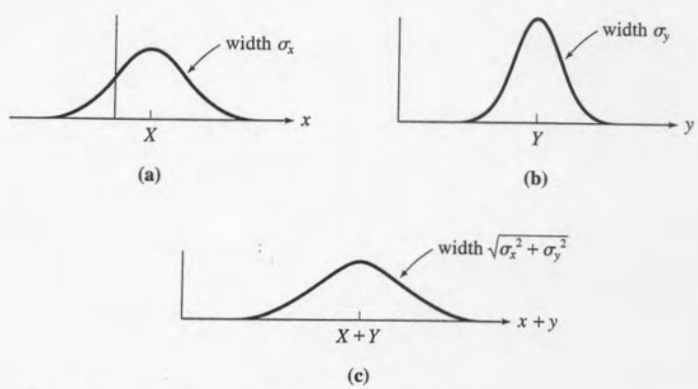

Figure 5.16. If the measurements of x and y are independent and normally distributed with ters X and Y and widths σ_x and σ_y, then the calculated values of $x+y$ are normally distribute with center $X + Y$ and width $\sqrt{\sigma_x^2 + \sigma_y^2}$.

MISSING CARBON SINK?

Atmospheric increase
=
Emissions from fossil fuels
+
Net emissions from changes in land use
-
Oceanic uptake
-
Missing carbon sink

3.2 (±0.2)
=
6.3 (±0.4)
+
2.2 (±0.8)
-
2.4 (±0.7)
-
2.9 (±1.1)

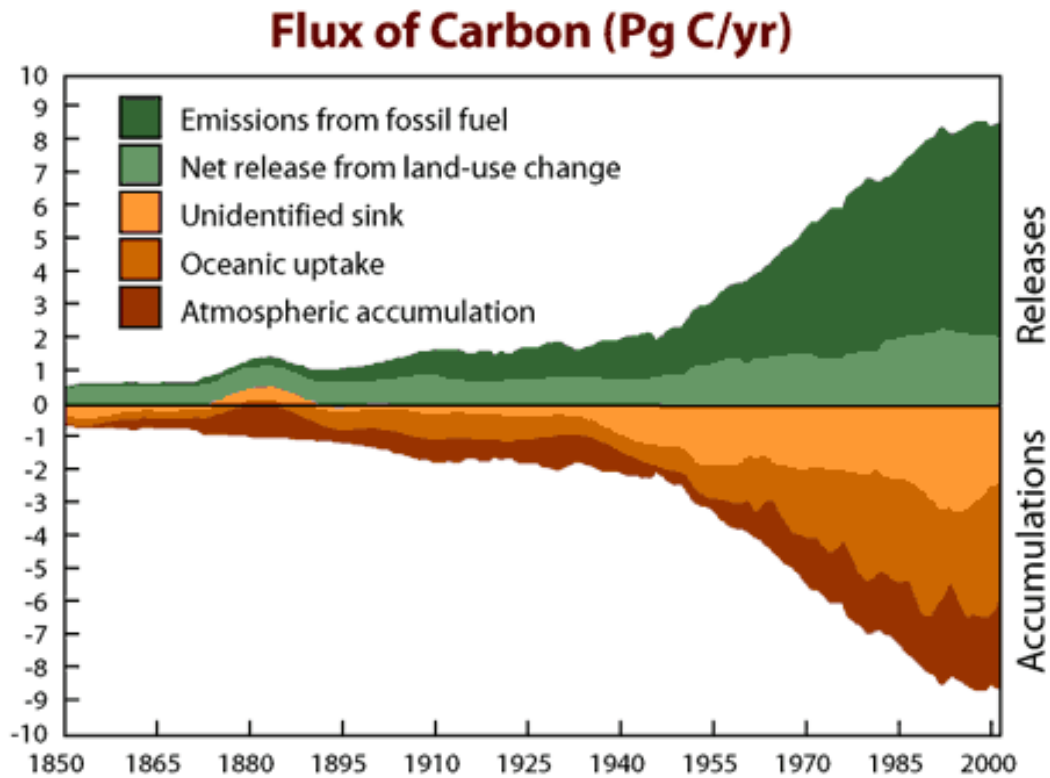

nature International weekly journal of science

NATURE | NEWS FEATURE

The hunt for the world's missing carbon

Researchers are racing to determine whether forests will continue to act as a brake on climate change by soaking up more carbon.

Gabriel Popkin

30 June 2015 | Corrected: 02 July 2015

The missing sink

In the 1990s, researchers stumbled across a mystery when they tried to track down all of the carbon humans were emitting by burning fossil fuels. Measurements showed that roughly three-quarters of the CO_2 was accumulating in the atmosphere and oceans. The remainder was presumably captured on land, but no one knew where it was going. The problem became known as the 'missing sink'.

The world's forests, which pull carbon out of the air through photosynthesis, were a possible hiding place. Today, they collectively hold around 650 billion tonnes of carbon, and it seemed plausible that they could be mopping up the missing carbon.

FIND FAULT & PLATE MOTIONS USING GPS GLOBAL POSITIONING SYSTEM
Find site position to few mm

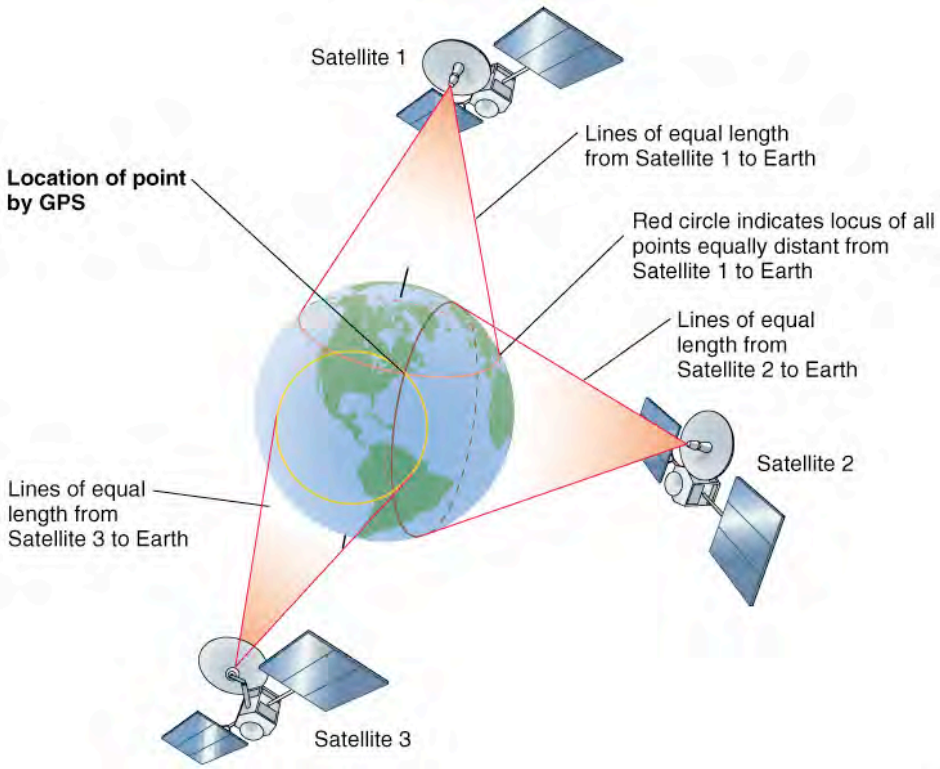

Change in position over time gives motion to precision of mm/yr

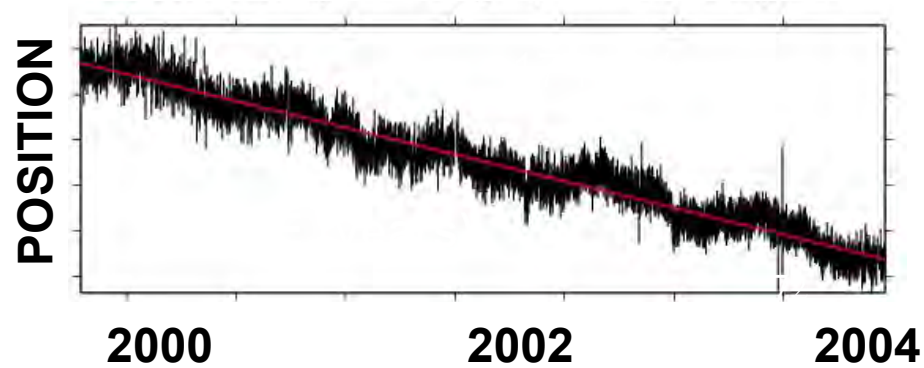

[redacted]

GPS velocity estimate uncertainty vs measurement timespan

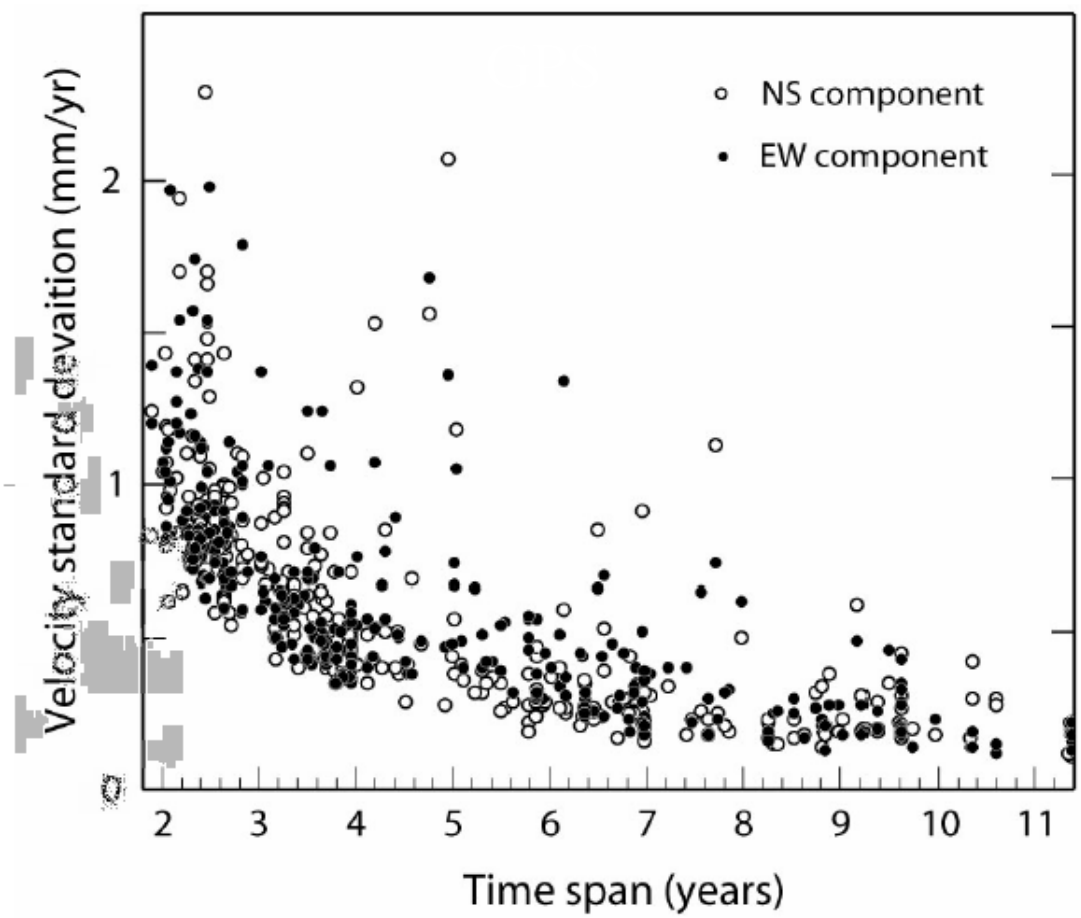

Figure 4. Velocity standard deviation as a function of measurement time span.

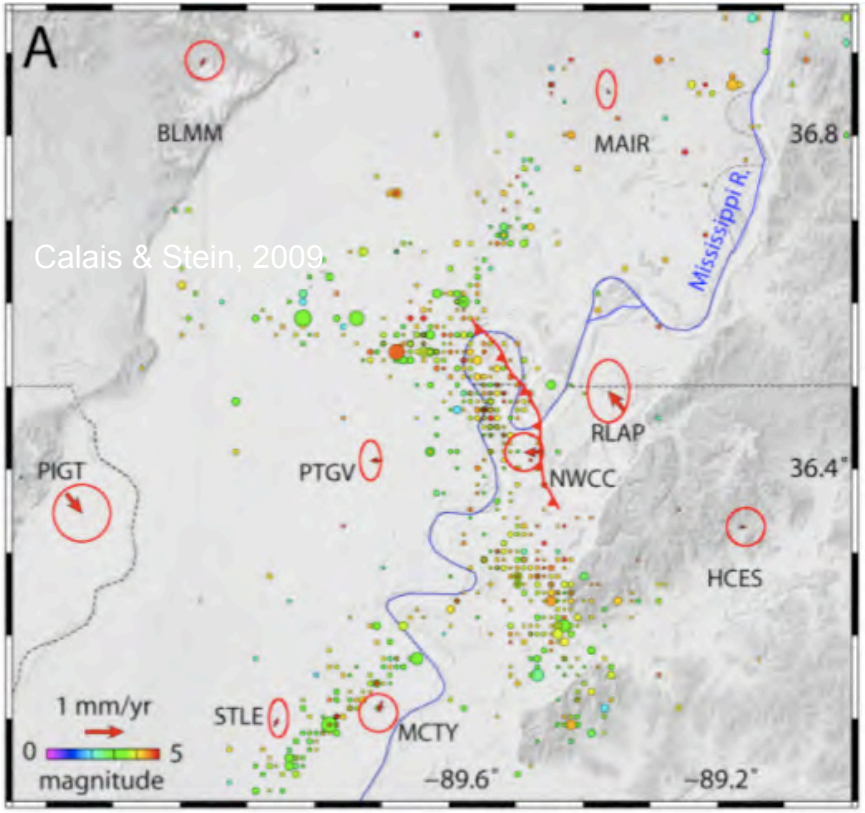

Calais & Stein, 2009

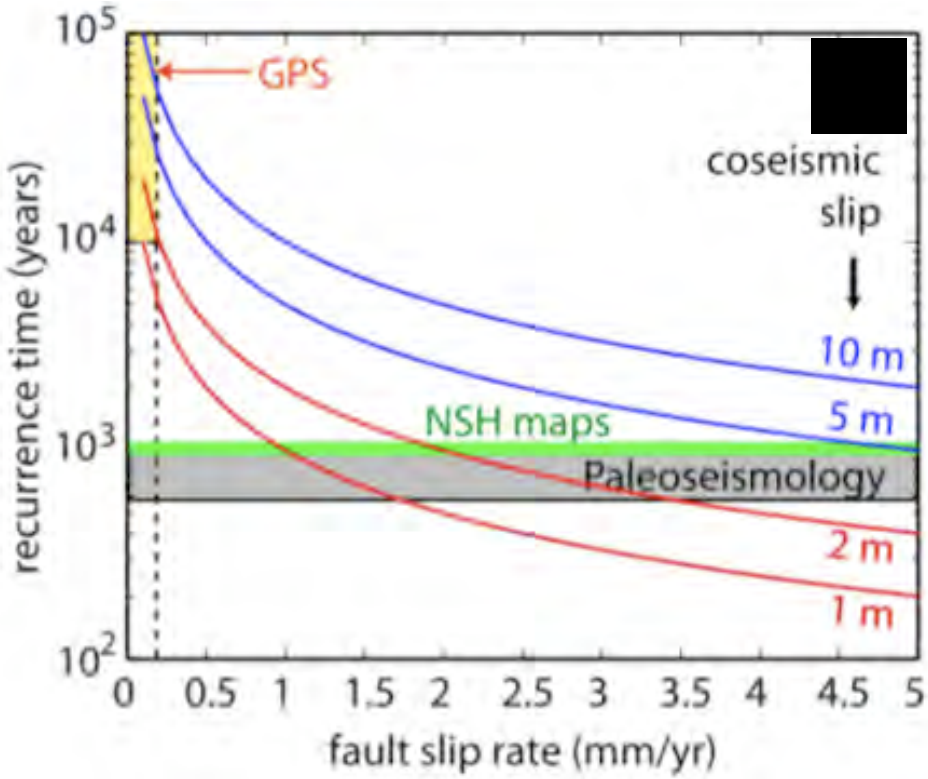

For steady motion, M 7 at least 10,000 years away: M 8 100,000

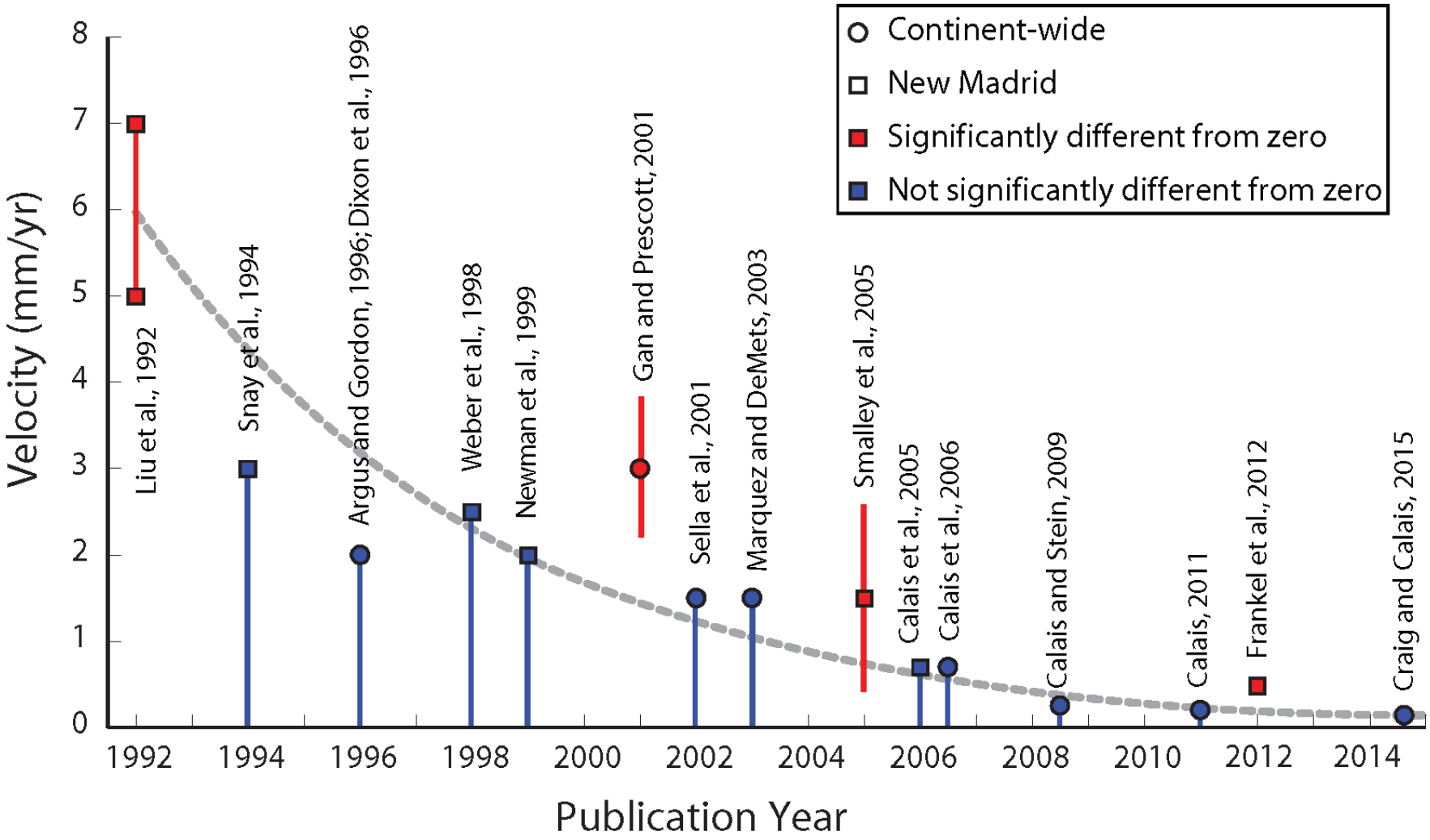
Continent-wide
New Madrid
Significantly different from zero
Not significantly different from zero
Velocity (mm/yr)
Publication Year
0
1
2
3
4
5
6
7
8
1992
1994
1996
1998
2000
2002
2004
2006
2008
2010
2012
2014
Liu et al., 1992
Snay et al., 1994
Argus and Gordon, 1996; Dixon et al., 1996
Weber et al., 1998
Newman et al., 1999
Gan and Prescott, 2001
Sella et al., 2001
Marquez and DeMets, 2003
Smalley et al., 2005
Calais et al., 2005
Calais et al., 2006
Calais and Stein, 2009
Calais, 2011
Frankel et al., 2012
Craig and Calais, 2015

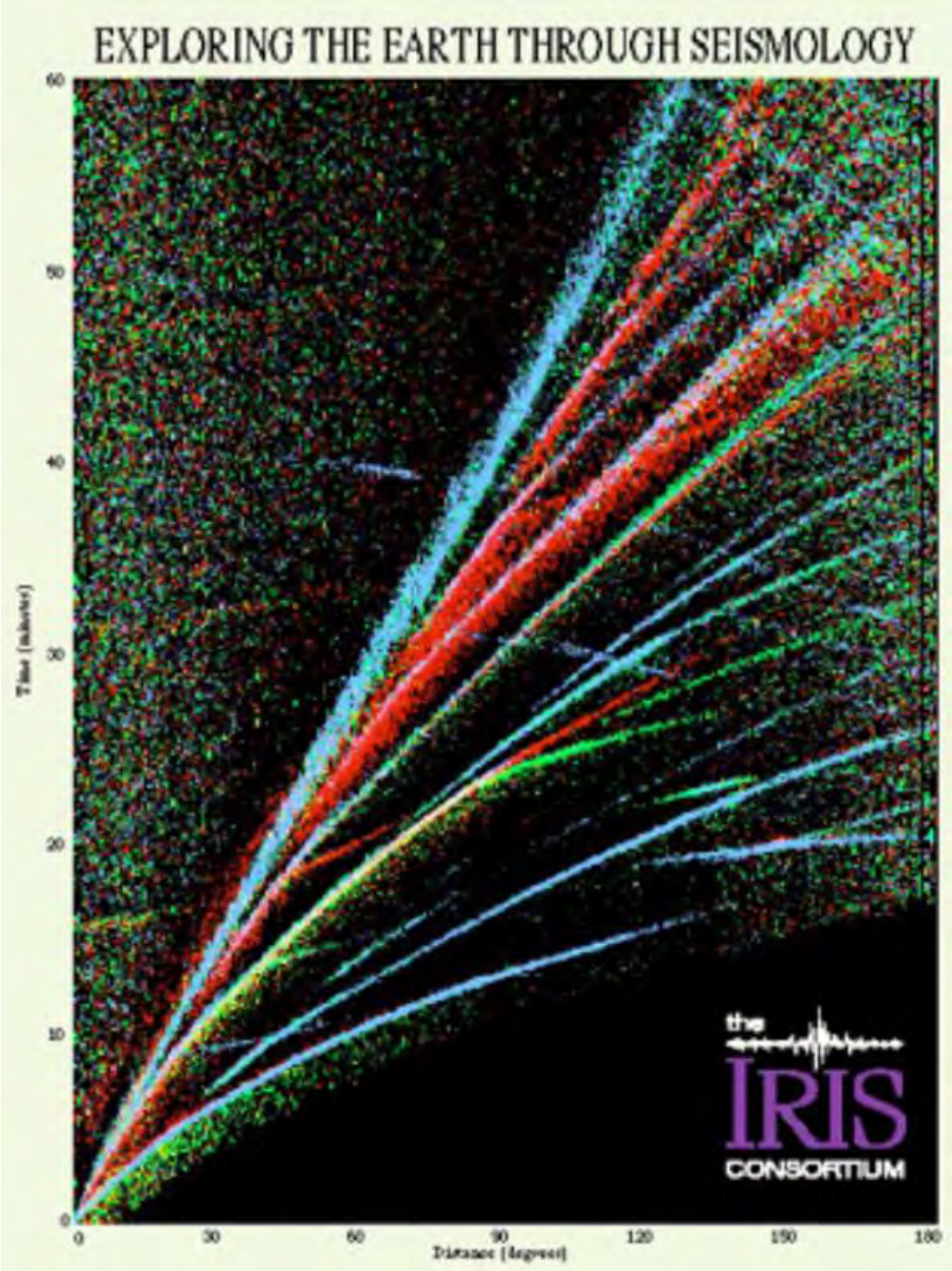
EXPLORING THE EARTH THROUGH SEISMOLOGY
Time (minutes)
Distance (degrees)
0
10
20
30
40
50
60
0
30
60
90
120
150
180
the
IRIS
CONSORTIUM

Gaussian distribution

Figure 6.5-1: Gaussian distribution.

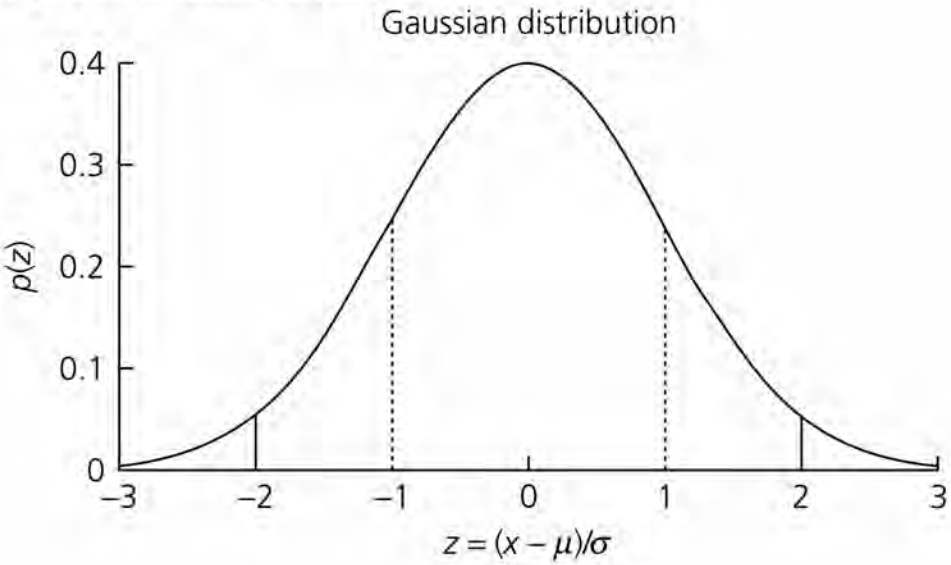

Figure 6.5-2: Results of drawing N samples from a Gaussian parent distribution.

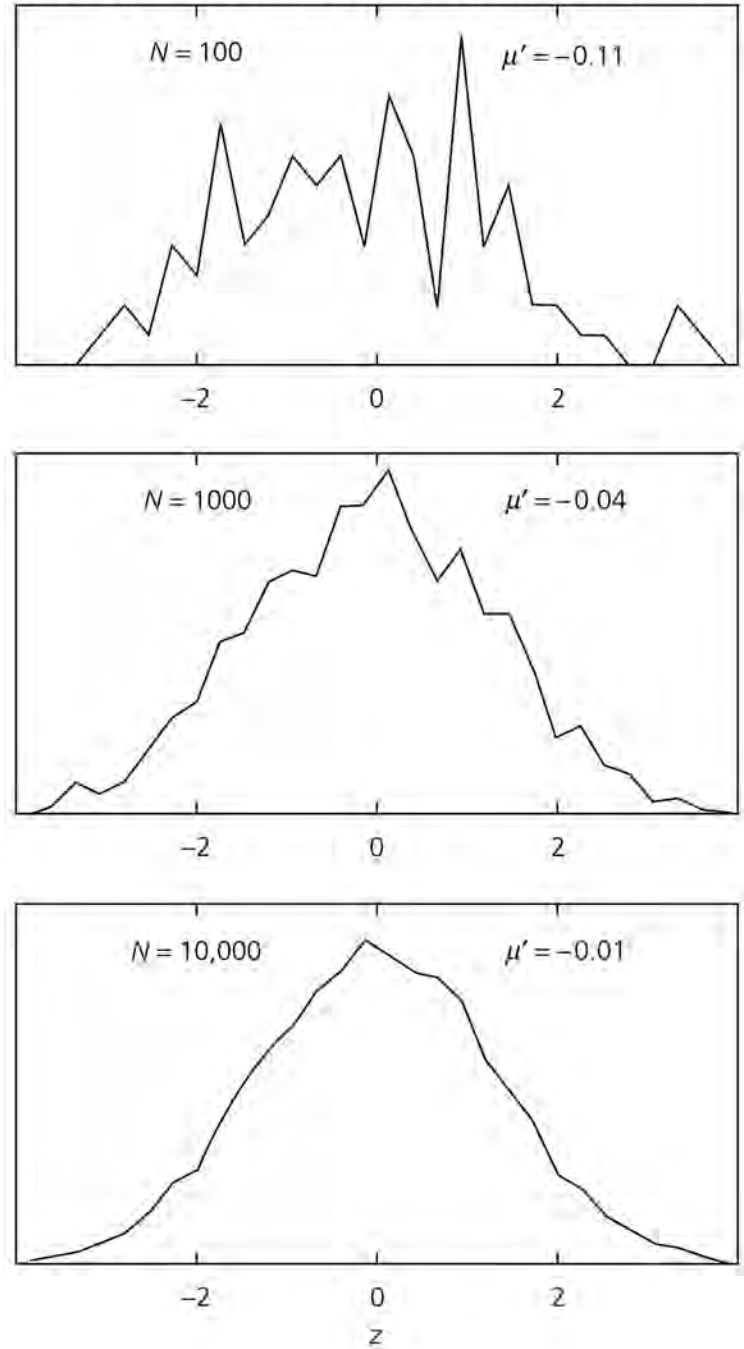

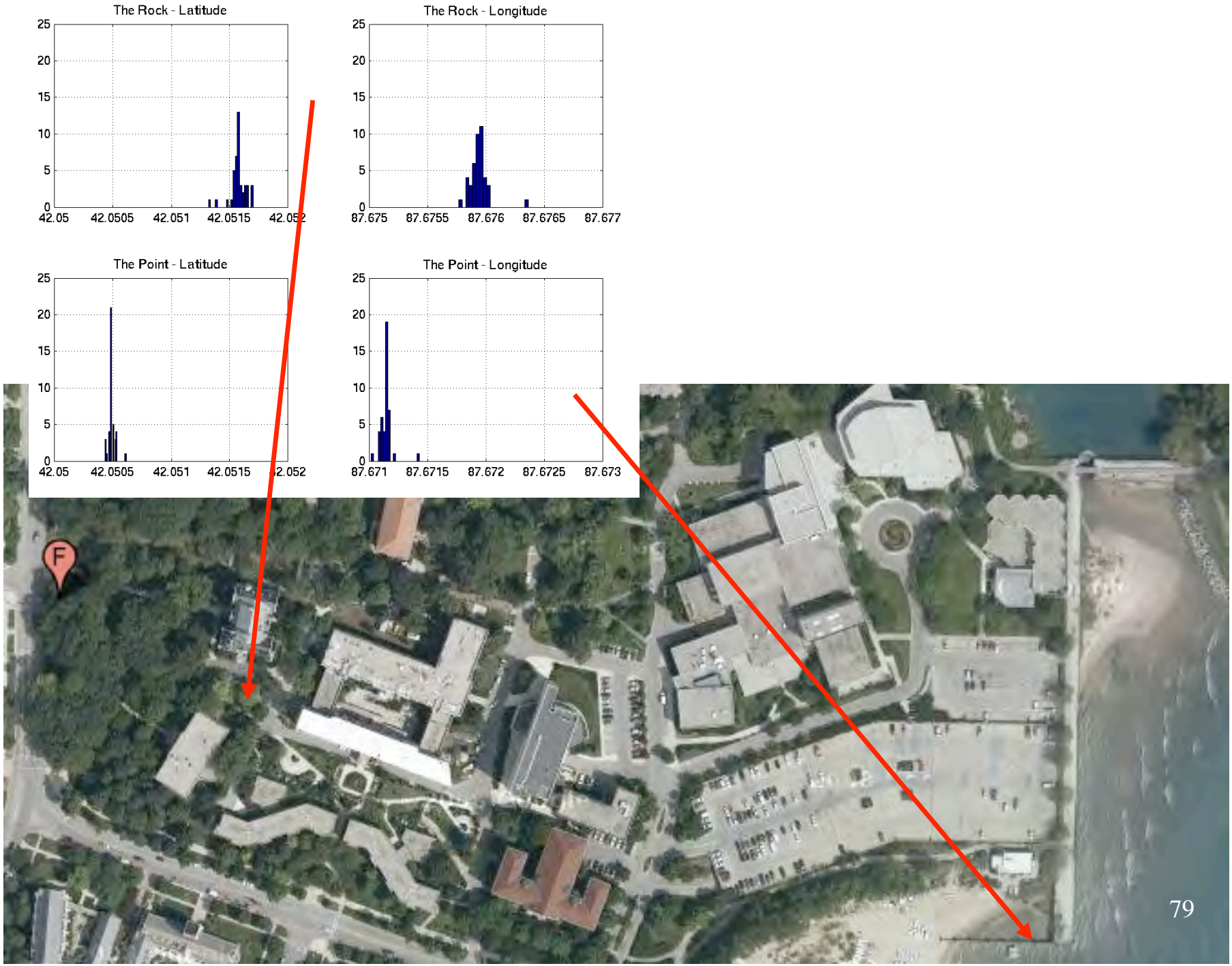
The Rock - Latitude
25
20
15
10
5
0
42.05
42.0505
42.051
42.0515
42.052
The Rock - Longitude
87.675
87.6755
87.676
87.6765
87.677
The Point - Latitude
The Point - Longitude
87.671
87.6715
87.672
87.6725
87.673
F
79

Taylor Appendix A

Table A. The percentage probability, $Prob(\text{within } t\sigma) = \int_{X-t\sigma}^{X+t\sigma} G_{X,\sigma}(x)\,dx$, as a function of t.

t	0.00	0.01	0.02	0.03	0.04	0.05	0.06	0.07	0.08	0.09
0.0	0.00	0.80	1.60	2.39	3.19	3.99	4.78	5.58	6.38	7.17
0.1	7.97	8.76	9.55	10.34	11.13	11.92	12.71	13.50	14.28	15.07
0.2	15.85	16.63	17.41	18.19	18.97	19.74	20.51	21.28	22.05	22.82
0.3	23.58	24.34	25.10	25.86	26.61	27.37	28.12	28.86	29.61	30.35
0.4	31.08	31.82	32.55	33.28	34.01	34.73	35.45	36.16	36.88	37.59
0.5	38.29	38.99	39.69	40.39	41.08	41.77	42.45	43.13	43.81	44.48
0.6	45.15	45.81	46.47	47.13	47.78	48.43	49.07	49.71	50.35	50.98
0.7	51.61	52.23	52.85	53.46	54.07	54.67	55.27	55.87	56.46	57.05
0.8	57.63	58.21	58.78	59.35	59.91	60.47	61.02	61.57	62.11	62.65
0.9	63.19	63.72	64.24	64.76	65.28	65.79	66.29	66.80	67.29	67.78
1.0	68.27	68.75	69.23	69.70	70.17	70.63	71.09	71.54	71.99	72.43
1.1	72.87	73.30	73.73	74.15	74.57	74.99	75.40	75.80	76.20	76.60
1.2	76.99	77.37	77.75	78.13	78.50	78.87	79.23	79.59	79.95	80.29
1.3	80.64	80.98	81.32	81.65	81.98	82.30	82.62	82.93	83.24	83.55
1.4	83.85	84.15	84.44	84.73	85.01	85.29	85.57	85.84	86.11	86.38
1.5	86.64	86.90	87.15	87.40	87.64	87.89	88.12	88.36	88.59	88.82
1.6	89.04	89.26	89.48	89.69	89.90	90.11	90.31	90.51	90.70	90.90
1.7	91.09	91.27	91.46	91.64	91.81	91.99	92.16	92.33	92.49	92.65
1.8	92.81	92.97	93.12	93.28	93.42	93.57	93.71	93.85	93.99	94.12
1.9	94.26	94.39	94.51	94.64	94.76	94.88	95.00	95.12	95.23	95.34
2.0	95.45	95.56	95.66	95.76	95.86	95.96	96.06	96.15	96.25	96.34
2.1	96.43	96.51	96.60	96.68	96.76	96.84	96.92	97.00	97.07	97.15
2.2	97.22	97.29	97.36	97.43	97.49	97.56	97.62	97.68	97.74	97.80
2.3	97.86	97.91	97.97	98.02	98.07	98.12	98.17	98.22	98.27	98.32
2.4	98.36	98.40	98.45	98.49	98.53	98.57	98.61	98.65	98.69	98.72
2.5	98.76	98.79	98.83	98.86	98.89	98.92	98.95	98.98	99.01	99.04
2.6	99.07	99.09	99.12	99.15	99.17	99.20	99.22	99.24	99.26	99.29
2.7	99.31	99.33	99.35	99.37	99.39	99.40	99.42	99.44	99.46	99.47
2.8	99.49	99.50	99.52	99.53	99.55	99.56	99.58	99.59	99.60	99.61
2.9	99.63	99.64	99.65	99.66	99.67	99.68	99.69	99.70	99.71	99.72
3.0	99.73									
3.5	99.95									
4.0	99.994									
4.5	99.9993									
5.0	99.99994									

Integral for Gaussian

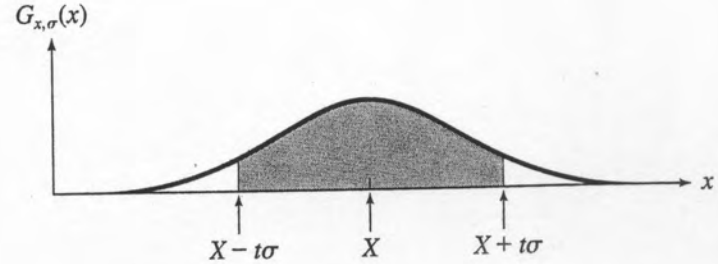

Figure 5.12. The shaded area between $X \pm t\sigma$ is the probability of a measurement within t standard deviations of X.

$$Prob(\text{within } t\sigma) = \frac{1}{\sqrt{2\pi}} \int_{-t}^{t} e^{-z^2/2}\, dz. \tag{5.35}$$

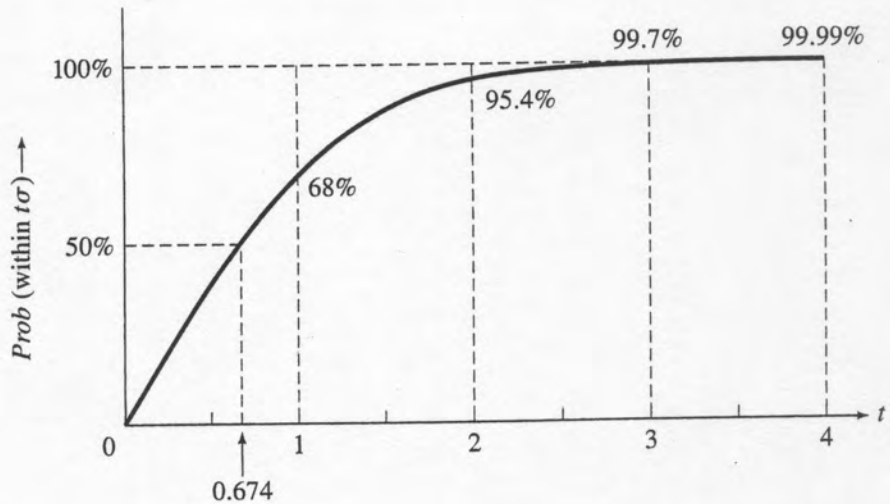

t	0	0.25	0.5	0.75	1.0	1.25	1.5	1.75	2.0	2.5	3.0	3.5	4.0
Prob (%)	0	20	38	55	68	79	87	92	95.4	98.8	99.7	99.95	99.99

Figure 5.13. The probability *Prob*(within $t\sigma$) that a measurement of x will fall within t standard deviations of the true value $x = X$. Two common names for this function are the *normal error integral* and the *error function,* erf(t).

Taylor Appendix B

Table B. The percentage probability, $Q(t) = \int_X^{X+t\sigma} G_{X,\sigma}(x)\,dx$, as a function of t.

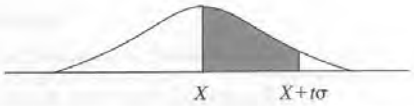

t	0.00	0.01	0.02	0.03	0.04	0.05	0.06	0.07	0.08	0.09
0.0	0.00	0.40	0.80	1.20	1.60	1.99	2.39	2.79	3.19	3.59
0.1	3.98	4.38	4.78	5.17	5.57	5.96	6.36	6.75	7.14	7.53
0.2	7.93	8.32	8.71	9.10	9.48	9.87	10.26	10.64	11.03	11.41
0.3	11.79	12.17	12.55	12.93	13.31	13.68	14.06	14.43	14.80	15.17
0.4	15.54	15.91	16.28	16.64	17.00	17.36	17.72	18.08	18.44	18.79
0.5	19.15	19.50	19.85	20.19	20.54	20.88	21.23	21.57	21.90	22.24
0.6	22.57	22.91	23.24	23.57	23.89	24.22	24.54	24.86	25.17	25.49
0.7	25.80	26.11	26.42	26.73	27.04	27.34	27.64	27.94	28.23	28.52
0.8	28.81	29.10	29.39	29.67	29.95	30.23	30.51	30.78	31.06	31.33
0.9	31.59	31.86	32.12	32.38	32.64	32.89	33.15	33.40	33.65	33.89
1.0	34.13	34.38	34.61	34.85	35.08	35.31	35.54	35.77	35.99	36.21
1.1	36.43	36.65	36.86	37.08	37.29	37.49	37.70	37.90	38.10	38.30
1.2	38.49	38.69	38.88	39.07	39.25	39.44	39.62	39.80	39.97	40.15
1.3	40.32	40.49	40.66	40.82	40.99	41.15	41.31	41.47	41.62	41.77
1.4	41.92	42.07	42.22	42.36	42.51	42.65	42.79	42.92	43.06	43.19
1.5	43.32	43.45	43.57	43.70	43.82	43.94	44.06	44.18	44.29	44.41
1.6	44.52	44.63	44.74	44.84	44.95	45.05	45.15	45.25	45.35	45.45
1.7	45.54	45.64	45.73	45.82	45.91	45.99	46.08	46.16	46.25	46.33
1.8	46.41	46.49	46.56	46.64	46.71	46.78	46.86	46.93	46.99	47.06
1.9	47.13	47.19	47.26	47.32	47.38	47.44	47.50	47.56	47.61	47.67
2.0	47.72	47.78	47.83	47.88	47.93	47.98	48.03	48.08	48.12	48.17
2.1	48.21	48.26	48.30	48.34	48.38	48.42	48.46	48.50	48.54	48.57
2.2	48.61	48.64	48.68	48.71	48.75	48.78	48.81	48.84	48.87	48.90
2.3	48.93	48.96	49.98	49.01	49.04	49.06	49.09	49.11	49.13	49.16
2.4	49.18	49.20	49.22	49.25	49.27	49.29	49.31	49.32	49.34	49.36
2.5	49.38	49.40	49.41	49.43	49.45	49.46	49.48	49.49	49.51	49.52
2.6	49.53	49.55	49.56	49.57	49.59	49.60	49.61	49.62	49.63	49.64
2.7	49.65	49.66	49.67	49.68	49.69	49.70	49.71	49.72	49.73	49.74
2.8	49.74	49.75	49.76	49.77	49.77	49.78	49.79	49.79	49.80	49.81
2.9	49.81	49.82	49.82	49.83	49.84	49.84	49.85	49.85	49.86	49.86
3.0	49.87									
3.5	49.98									
4.0	49.997									
4.5	49.9997									
5.0	49.99997									

EXCEL CDF & PDF for Gaussian

	A	B	C	D	E	F	G
1		GAUSSIAN					
2	CDF=	NORMSDIST(A6)			STEP		
3	PDF=	(B(7)-B(6))/E3			0.2		
4							
5	z	CDF	PDF				
6	-3	0.001	0				
7	-2.8	0.003	0.006				
8	-2.6	0.005	0.011				
9	-2.4	0.008	0.018				
10	-2.2	0.014	0.029				
11	-2	0.023	0.044				
12	-1.8	0.036	0.066				
13	-1.6	0.055	0.094				
14	-1.4	0.081	0.130				
15	-1.2	0.115	0.172				
16	-1	0.159	0.218				
17	-0.8	0.212	0.266				
18	-0.6	0.274	0.312				
19	-0.4	0.345	0.352				
20	-0.2	0.421	0.381				
21	4E-16	0.500	0.396				
22	0.2	0.579	0.396				
23	0.4	0.655	0.381				
24	0.6	0.726	0.352				
25	0.8	0.788	0.312				
26	1	0.841	0.266				
27	1.2	0.885	0.218				
28	1.4	0.919	0.172				
29	1.6	0.945	0.130				
30	1.8	0.964	0.094				
31	2	0.977	0.066				
32	2.2	0.986	0.044				
33	2.4	0.992	0.029				
34	2.6	0.995	0.018				
35	2.8	0.997	0.011				
36	3	0.999	0.006				

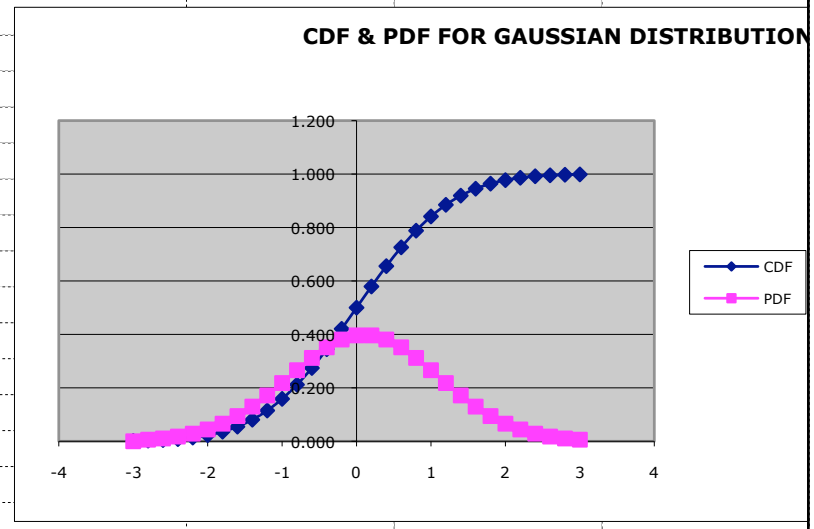

SMITHSONIAN INSTITUTION VOLCANIC

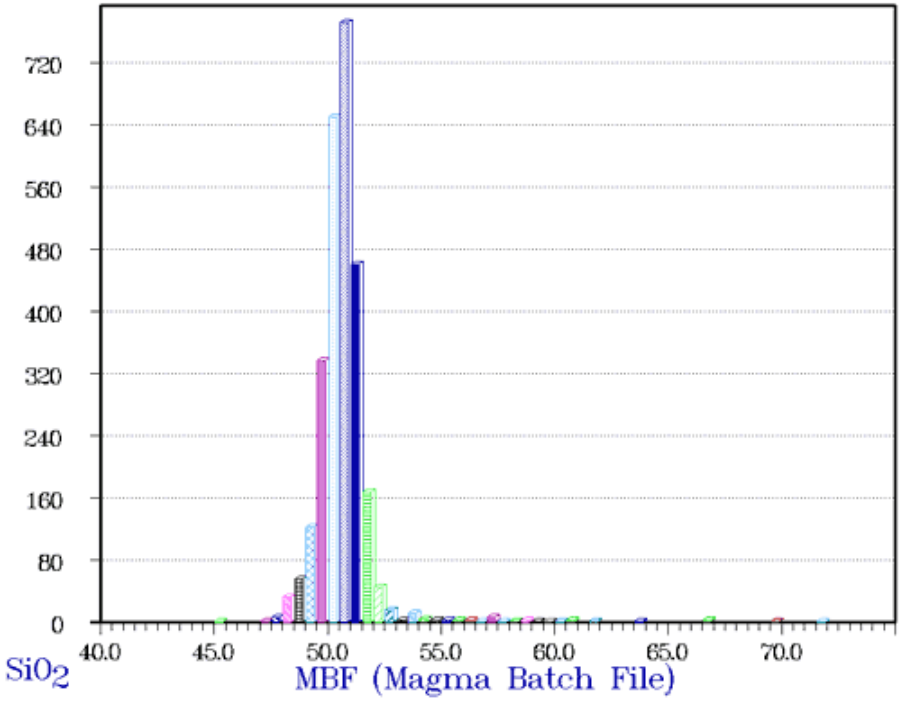

MAR BASALTS.

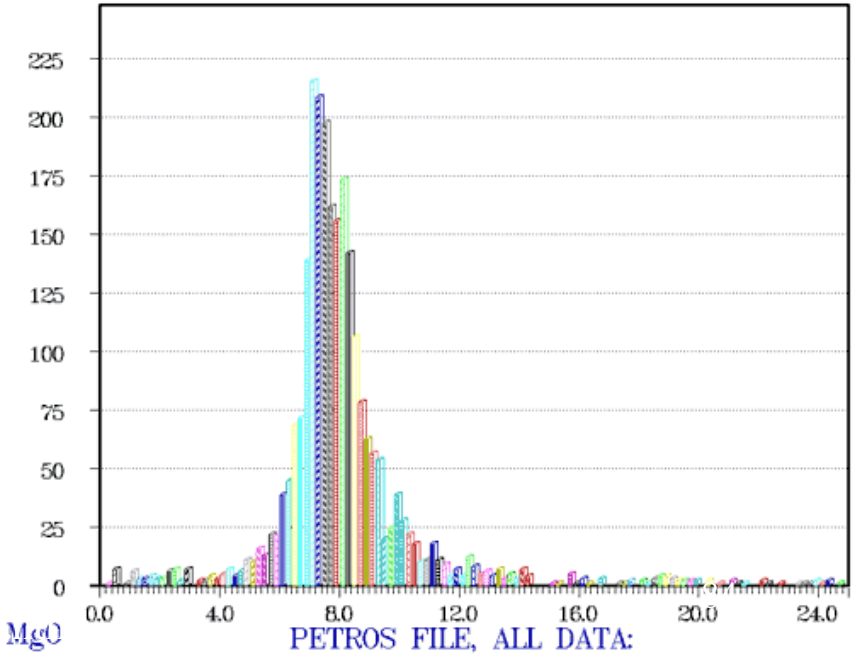

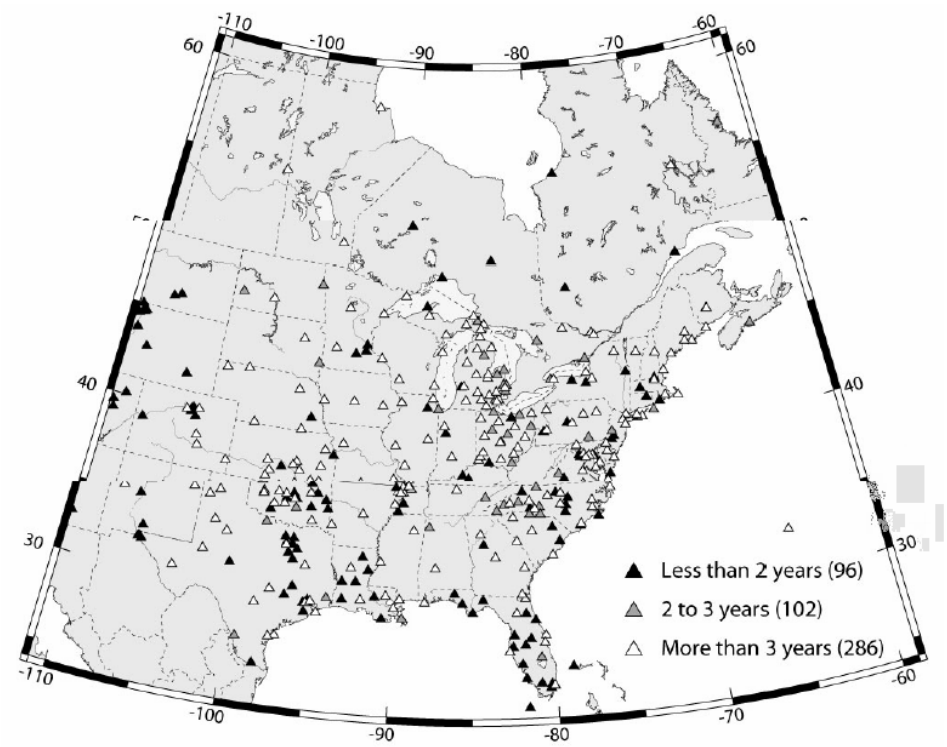

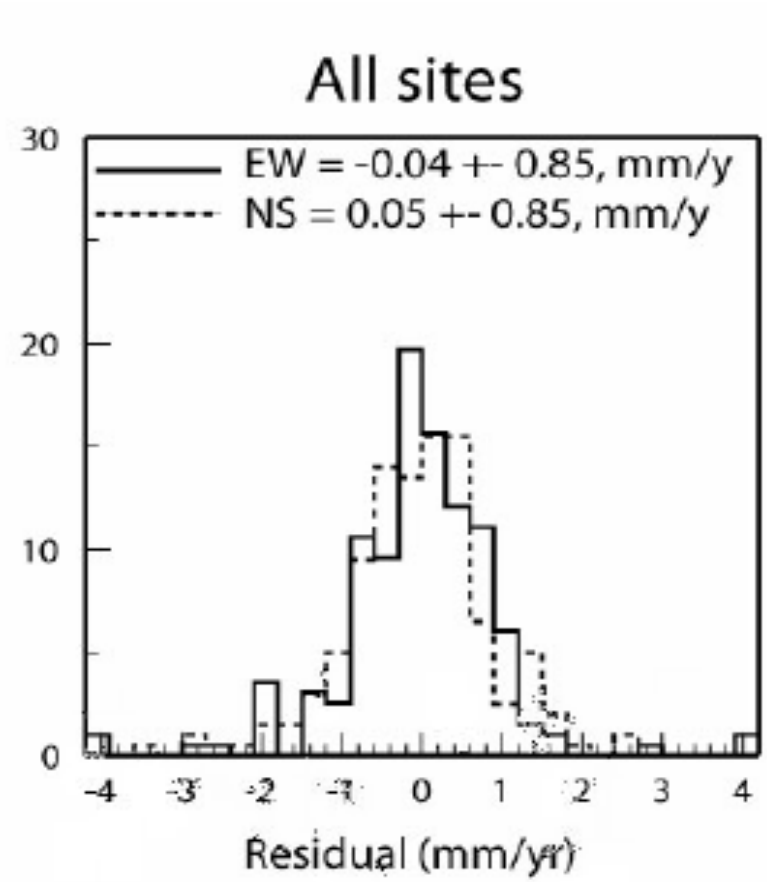

Figure 2. Map of continuous GPS stations used in this study. Symbol colors specify

Distribution of heights: men vs women

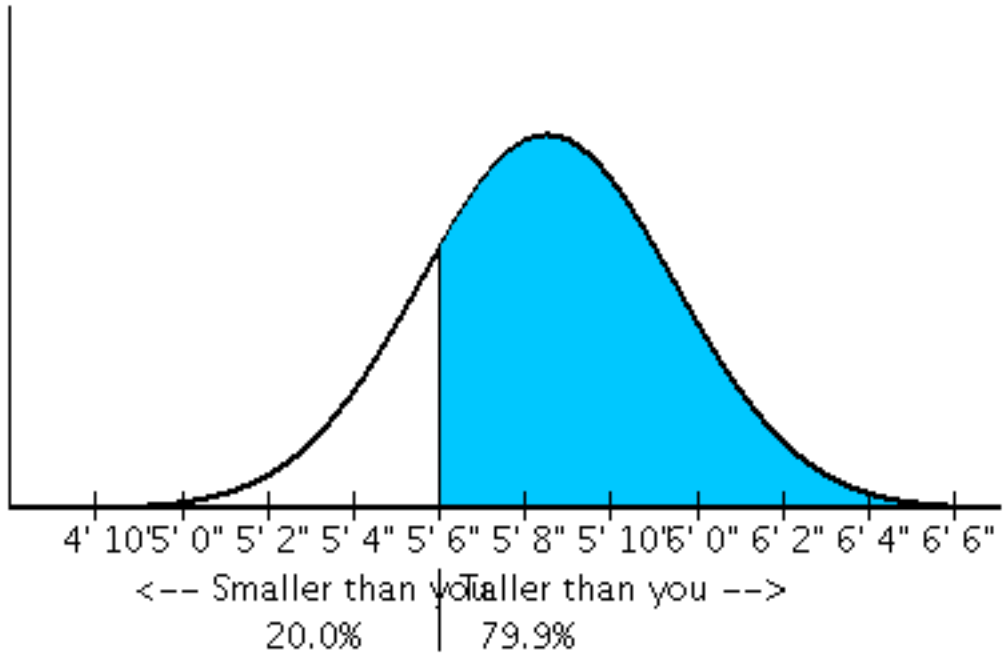

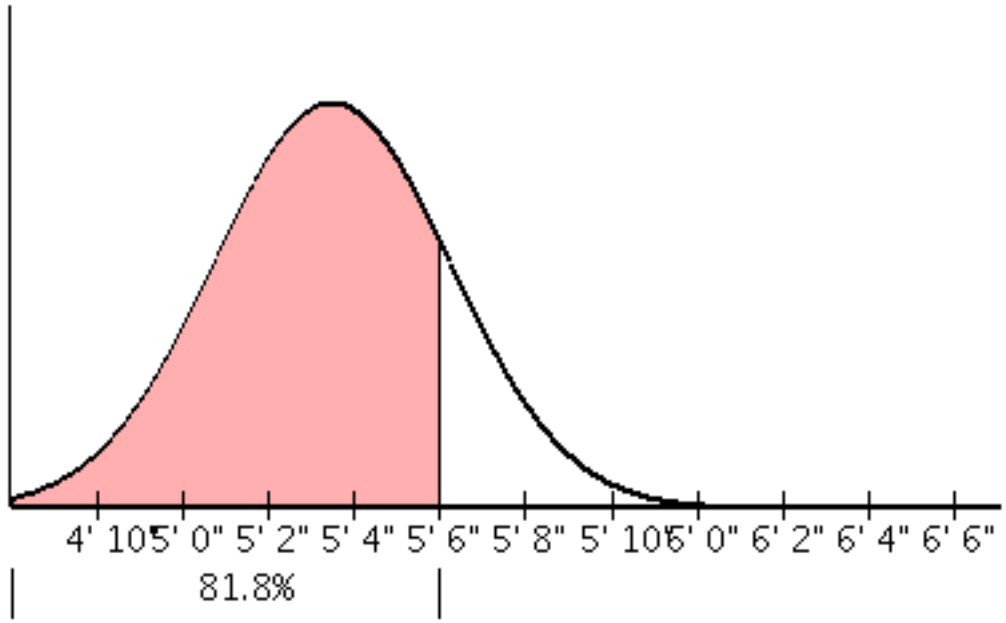

	A	B	C	D	E	F
1					CUMULATIVE DISTRIBUTION	
2					NORMDIST(x,mean,sdev)=prob	
3		x	mean	sdev	NORMDIST(B4,C4,D4,TRUE)	
4		66	65.5	2.5	0.58	
5						
6						
7					INVERSE OF CDF	
8					NORMINV(prob,mean,sdev)=x	
9		prob	mean	sdev	NORMINV(B10,C10,D10)	
10		0.58	65.5	2.5	66.0	
11						
12						
13					GET Z FROM X	
14					STANDARDIZE (x, mean,sdev)=z	
15		x	mean	sdev	STANDARDIZE(B16,C16,D16)	
16		66	65.5	2.5	0.20	
17						
18						
19					CDF FOR Z	
20					NORMSDIST(z)=prob	
21		z			NORMSDIST(B22)	
22		1			0.84	
23		-1			0.16	
24						
25						
26				z for given probability (inverse NORMSDIST)		
27					NORMSINV(prob)=z	
28		prob			NORMSINV(B28)	
29		0.25			-0.67	
30		0.75			0.67	

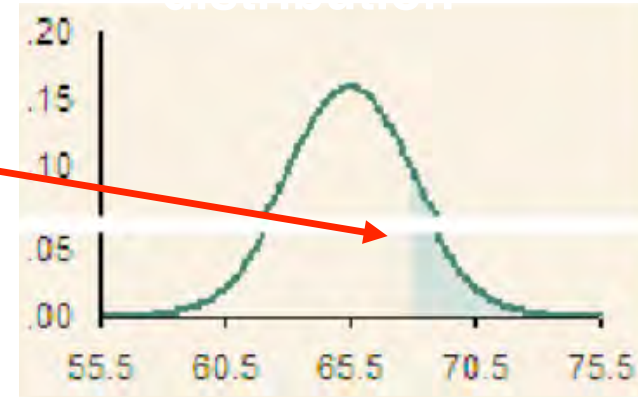

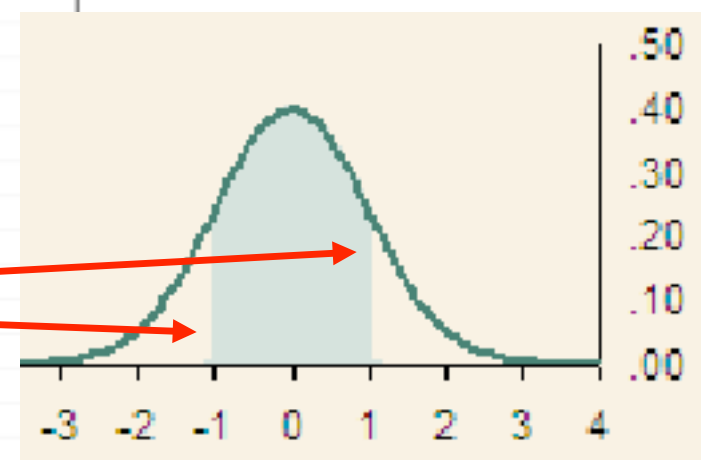

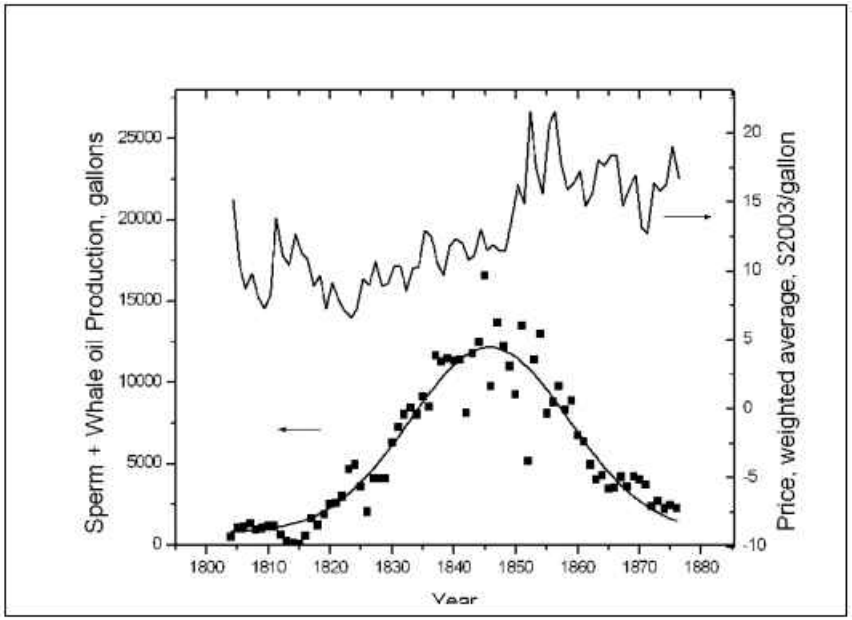

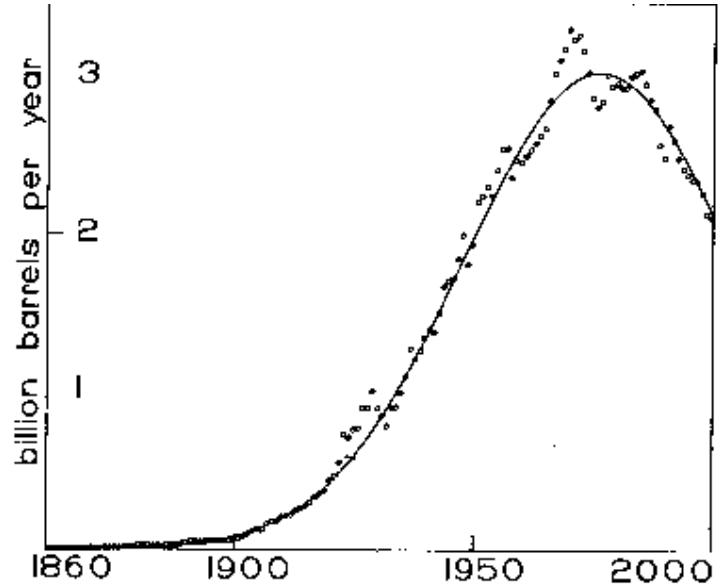

Annual production of U.S. crude oil (circles) with the best-fitting Gaussian curve superimposed as a solid line. Production from Alaska and from offshore oil fields is included.

Figure 3: U.K. Coal Production 1877-2000 and Hubbert Curve

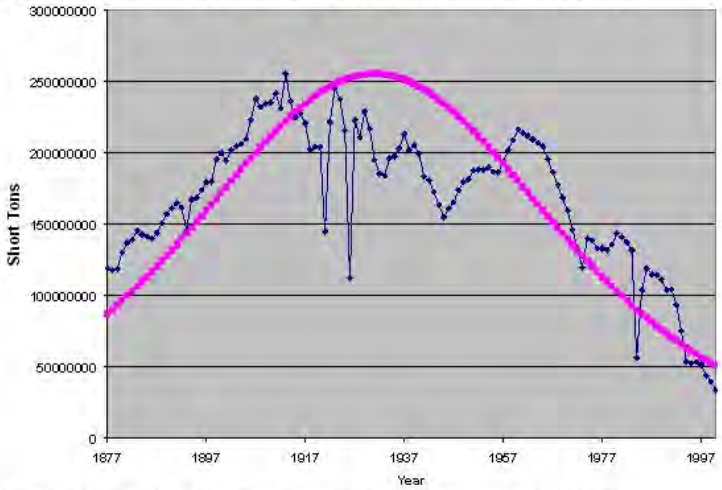

Source of Data: Durham Mining Museum, Coal Authority (U.K.), EIA

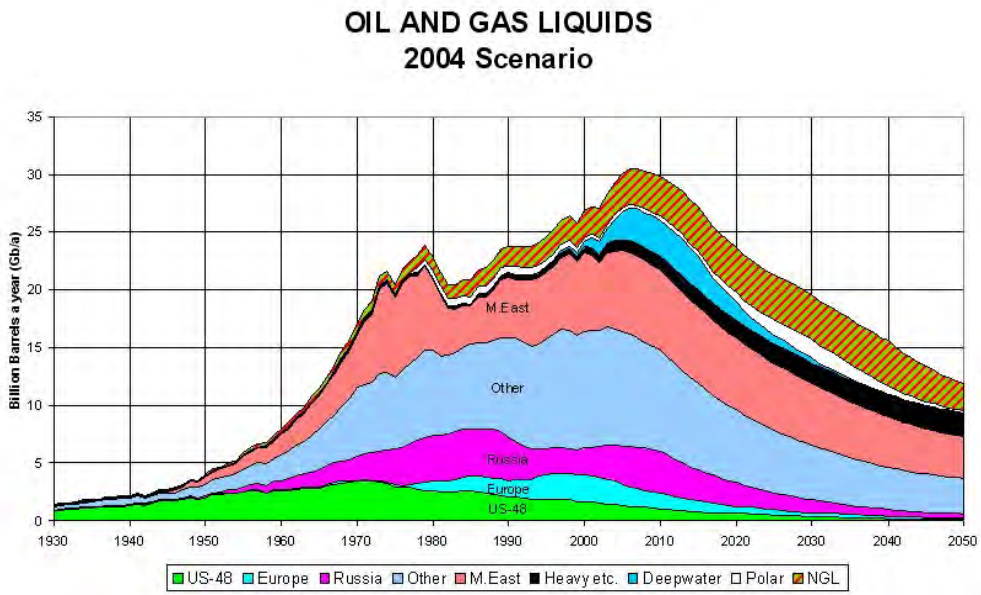

U.S. Field Production of Crude Oil

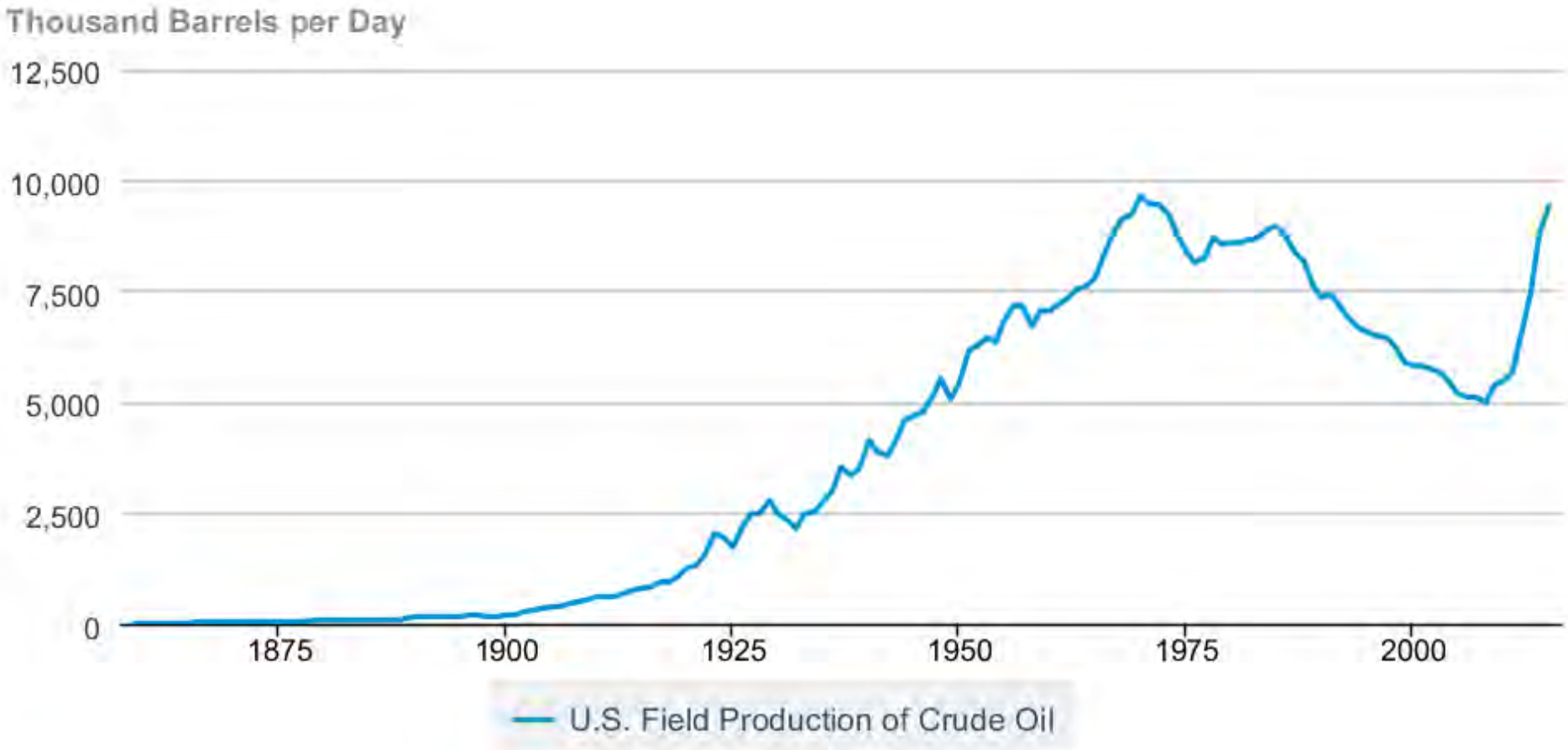

eia Source: U.S. Energy Information Administration

http://www.eia.gov/dnav/pet/hist/LeafHandler.ashx?n=PET&s=MCRFPUS2&f=A

[redacted]

Lognormal distributions in earth science

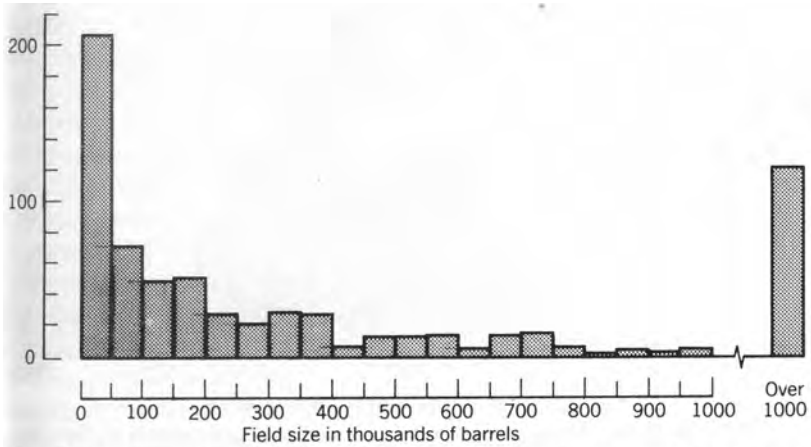

URE 2.34 Histogram of sizes of oil fields discovered in Denver Basin through

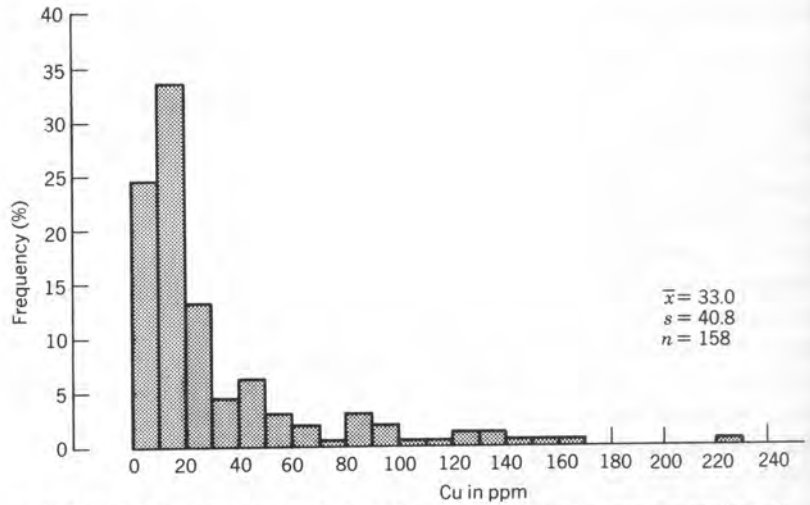

FIGURE 2.35 Histogram of copper content (in ppm) of stream sediments collected in Mt. Nansen area, Yukon. After Saager and Sinclair, 1974.

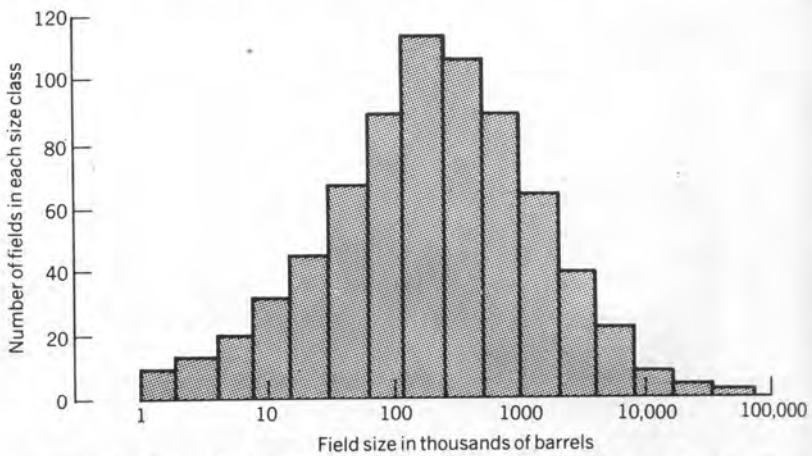

FIGURE 2.36 Histogram of sizes of oil fields discovered in Denver Basin through 1969, plotted on logarithmic scale. From Harbaugh, Doveton, and Davis (1977).

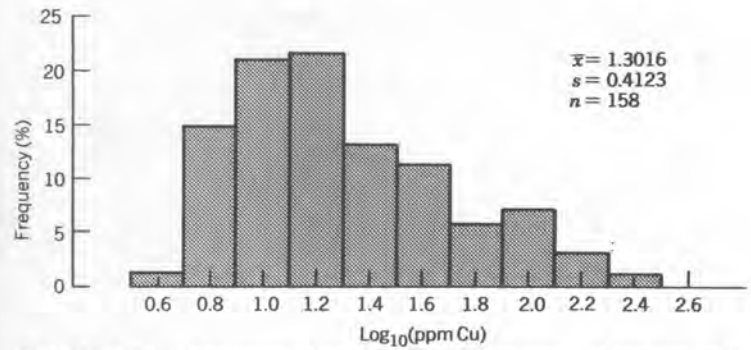

FIGURE 2.37 Histogram of copper content (in ppm) of stream sediments collected in Mt. Nansen area, Yukon, plotted on logarithmic scale. After Saager and Sinclair, 1974.

Davis, 1986

Properties of lognormal distributions

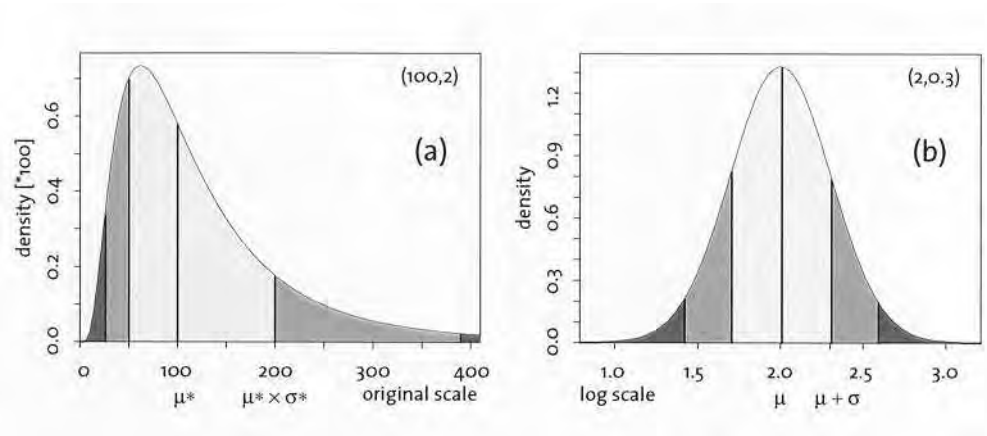

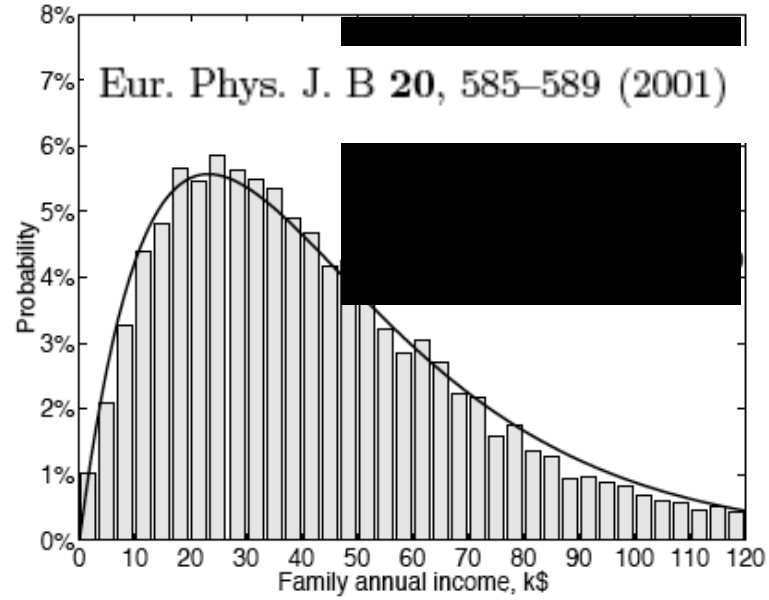

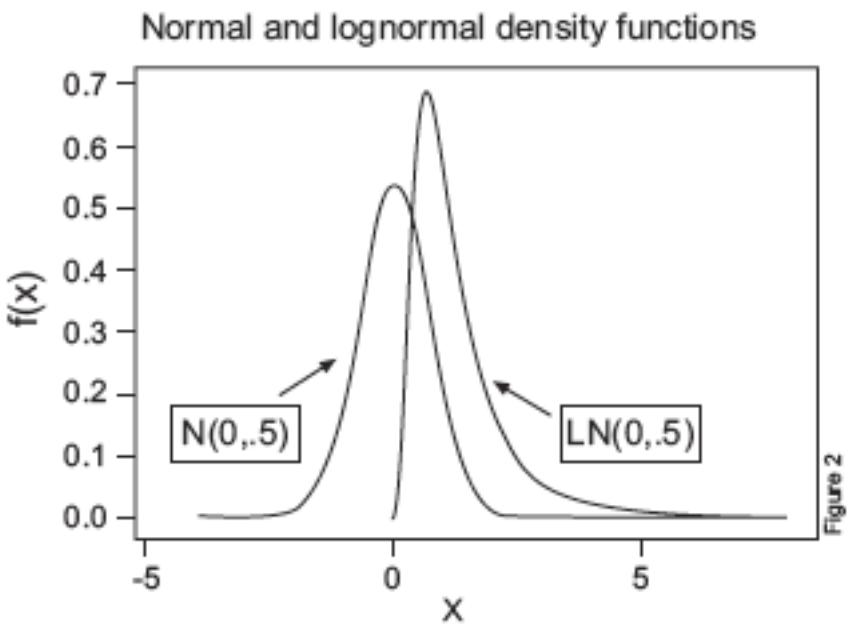

Figure 1 Graphs of normal N($\mu = 0$, $\sigma^2 = 0.5$) and lognormal LN($\mu = 0$, $\sigma^2 = 0.5$) density functions.

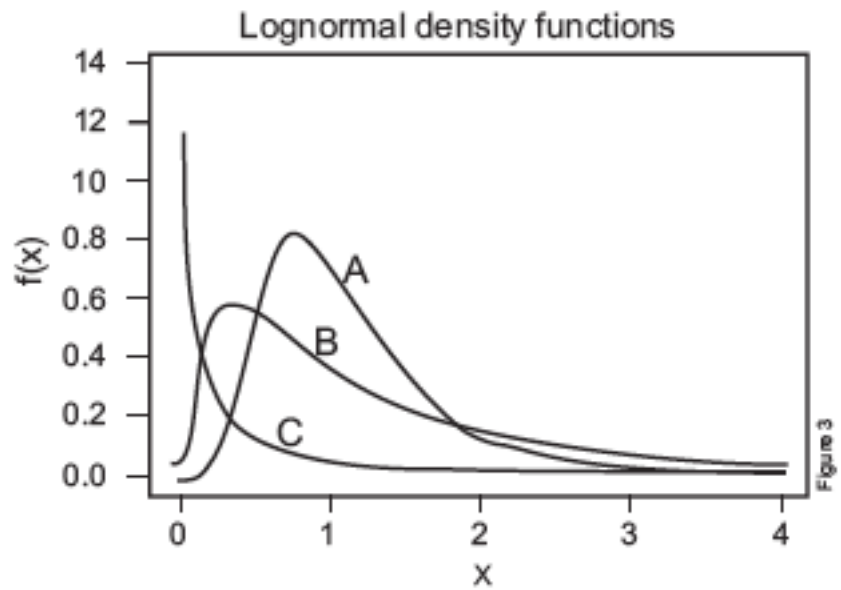

Figure 2 Graphs of A: LN($\mu = 0$, $\sigma^2 = 0.25$), B: LN($\mu = 0$, $\sigma^2 = 1.0$) and C: LN($\mu = 0$, $\sigma^2 = 25.0$) density functions.

Numerical demonstration of Central Limit Theorem

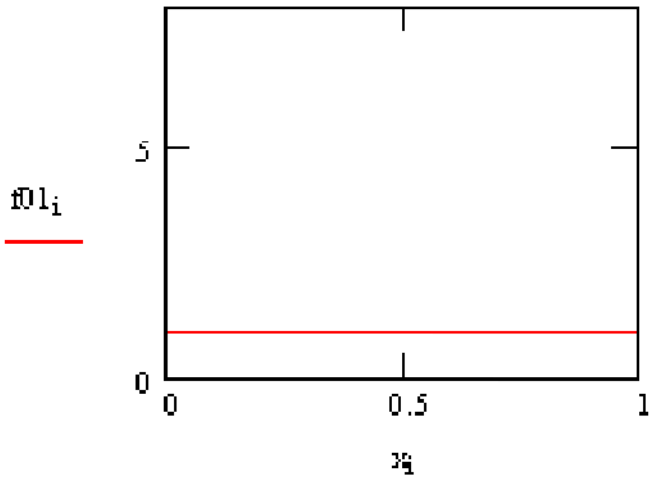

NonNormal Distribution of X

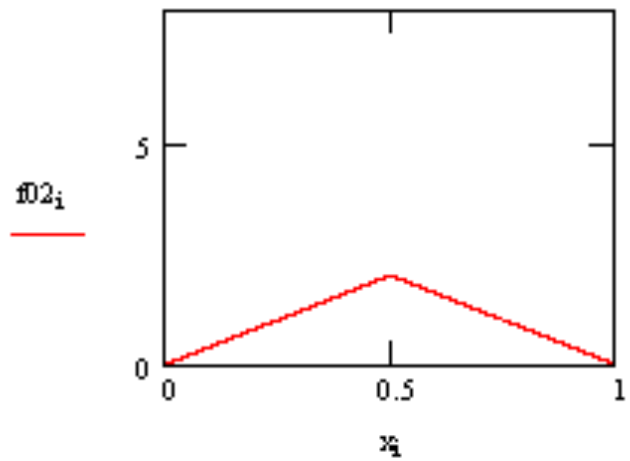

Distribution of Xbar when sample size is 2

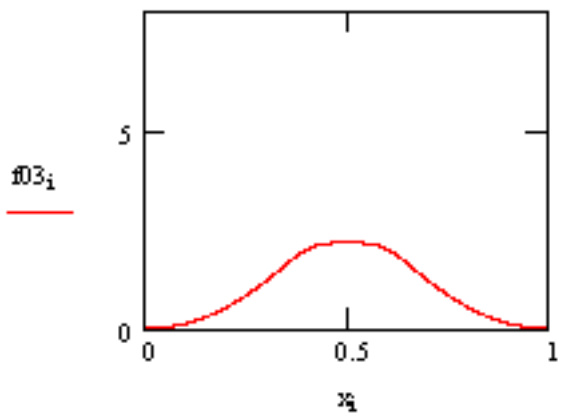

Distribution of Xbar when sample size is 3

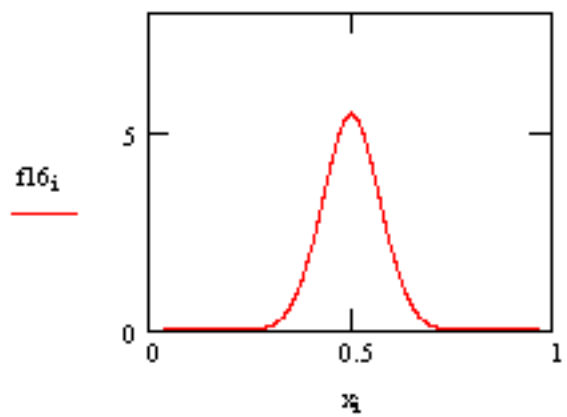

Distribution of Xbar when sample size is 16

www.statisticalengineering.com/central_limit_theorem.htm

Normal (additive) Lognormal (multiplicative)

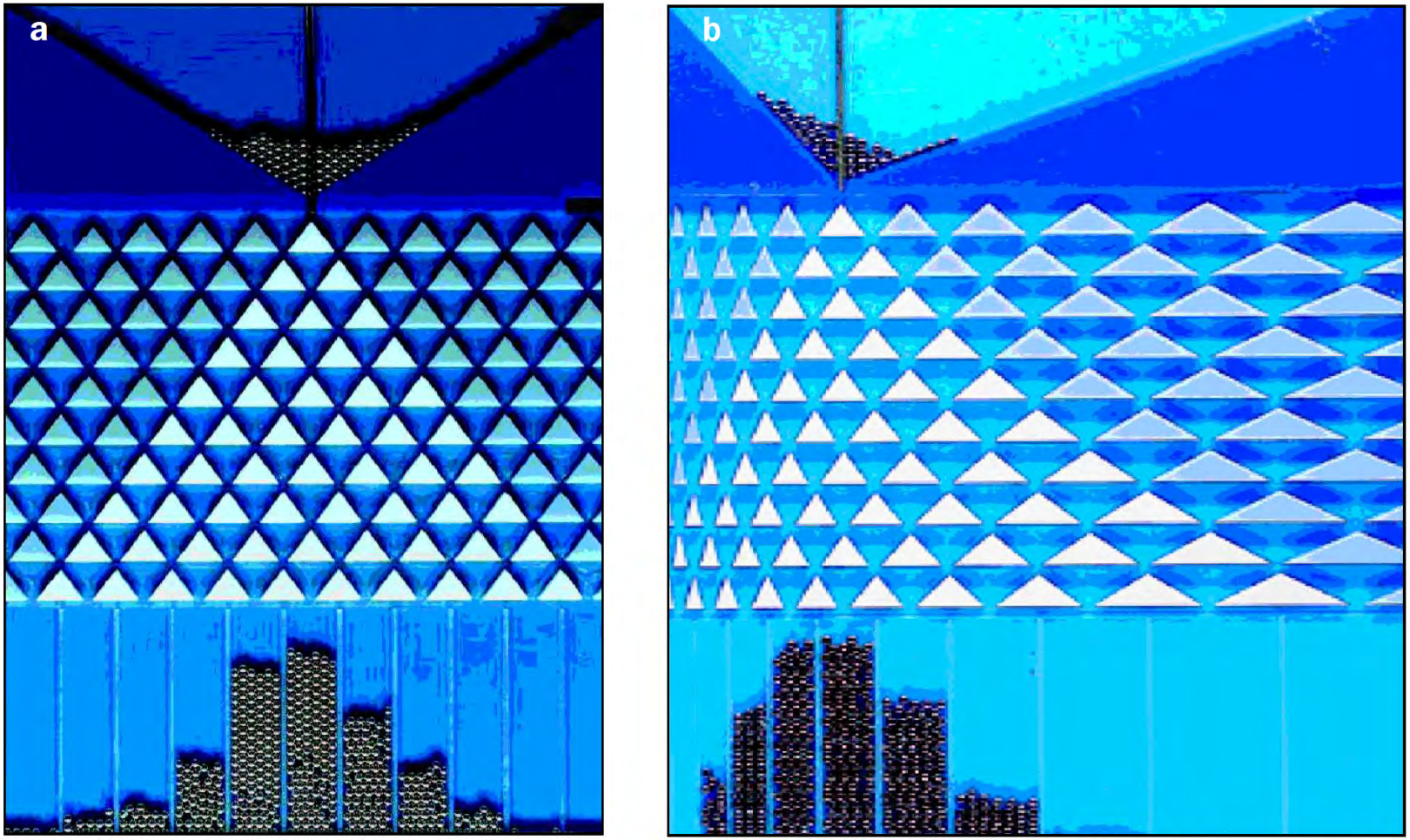

Figure 2. Physical models demonstrating the genesis of normal and log-normal distributions. Particles fall from a funnel onto tips of triangles, where they are deviated to the left or to the right with equal probability (0.5) and finally fall into receptacles. The medians of the distributions remain below the entry points of the particles. If the tip of a triangle is at distance x *from the left edge of the board, triangle tips to the right and to the left below it are placed at* $x + c$ *and* $x - c$ *for the normal distribution (panel a), and* $x \cdot c'$ *and* x / c' *for the log-normal (panel b, patent pending),* c *and* c' *being constants. The distributions are generated by many small random effects (according to the central limit theorem) that are additive for the normal distribution and multiplicative for the log-normal. We therefore suggest the alternative name multiplicative normal distribution for the latter.*

Limpert et al May 2001 / Vol. 51 No. 5 . BioScience 341

Power law distribution: WWW site usage

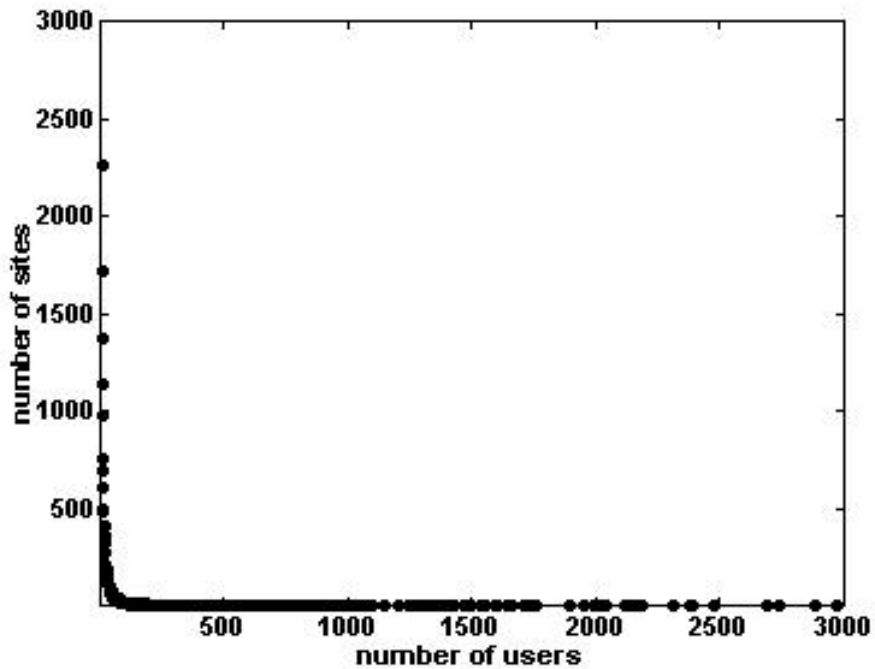

'ig. 1a Linear scale plot of the distribution of users among w

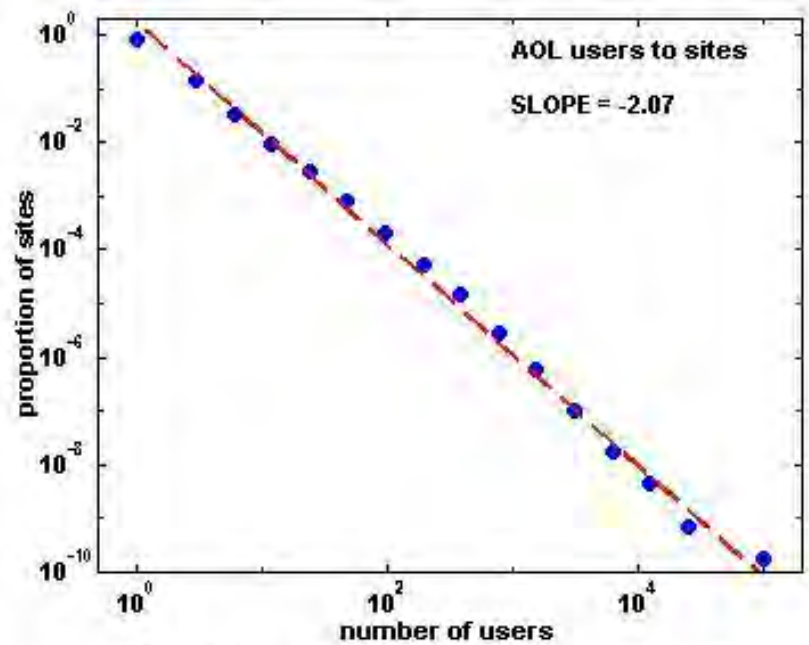

Fig. 2a Binned distribution of users to sites

Figure 4.7-1: Frequency-magnitude plot for earthquakes during 1968-1997.

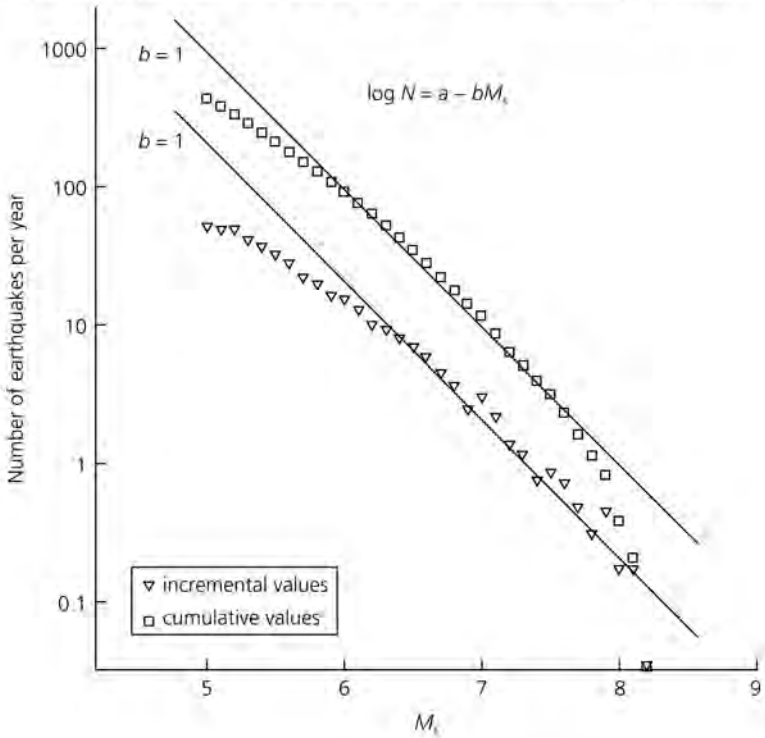

Figure 4.7-2: Frequency-moment plot for earthquakes during 1976-1998.

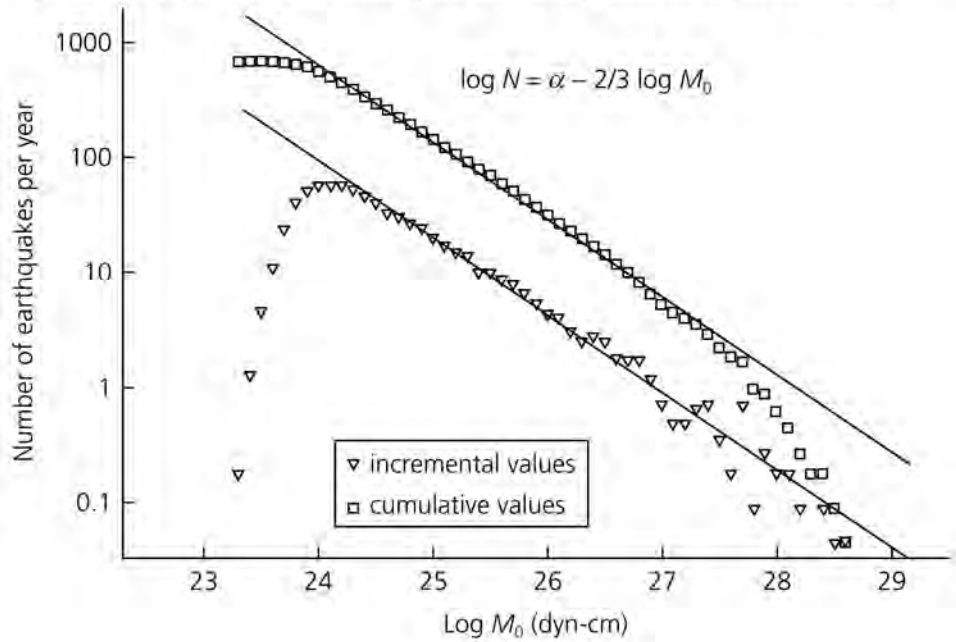

Earthquake b values

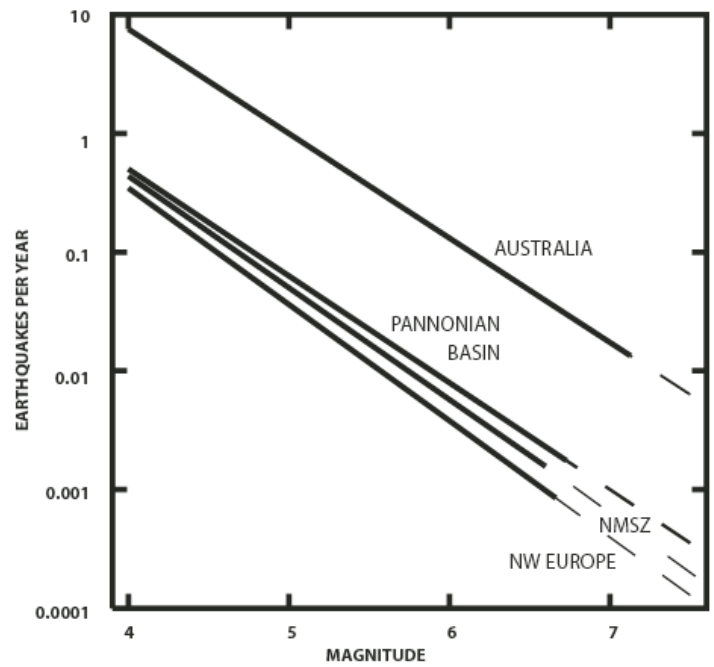

Mo has units of dyn-cm or Nt-m

(Nt-m = 10^7 dyn-cm)

SEISMIC MOMENT Mo = fault area * slip * rigidity (dyn-cm)

MOMENT MAGNITUDE Mw = log Mo /1.5 - 10.73

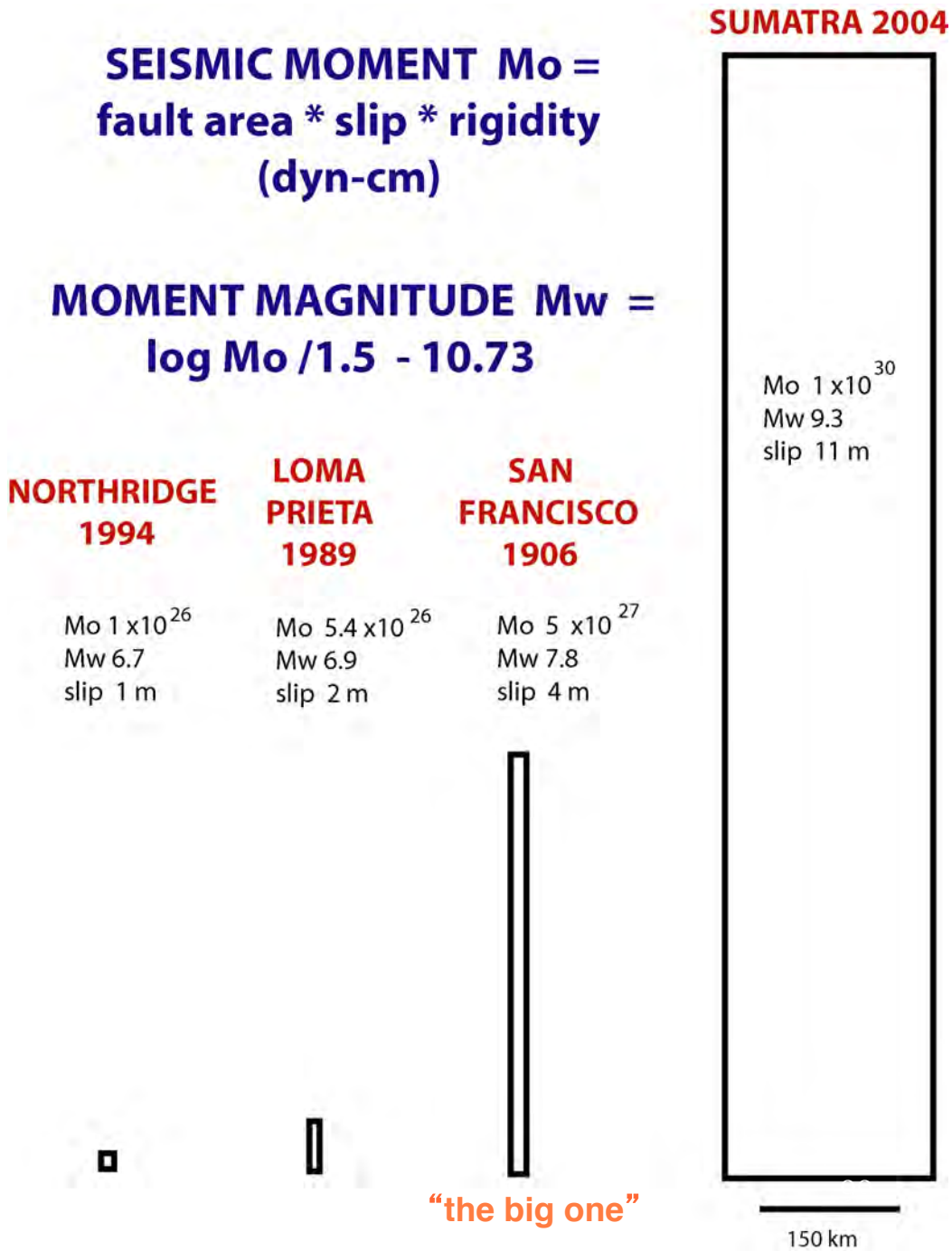

THE GREAT NEW MADRID "MEDIA QUAKE" OF 1990
NEW MADRID, MISSOURI

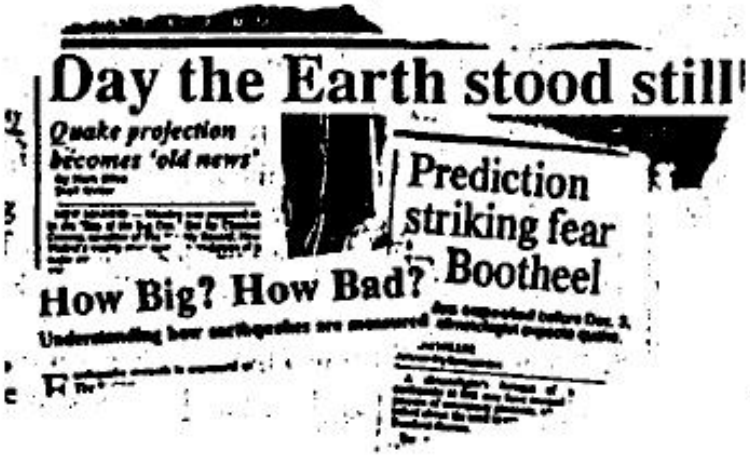

Day the Earth stood still

Quake projection becomes 'old news'

Prediction striking fear Bootheel

How Big? How Bad?

Understanding how earthquakes are measured

Power law distribution

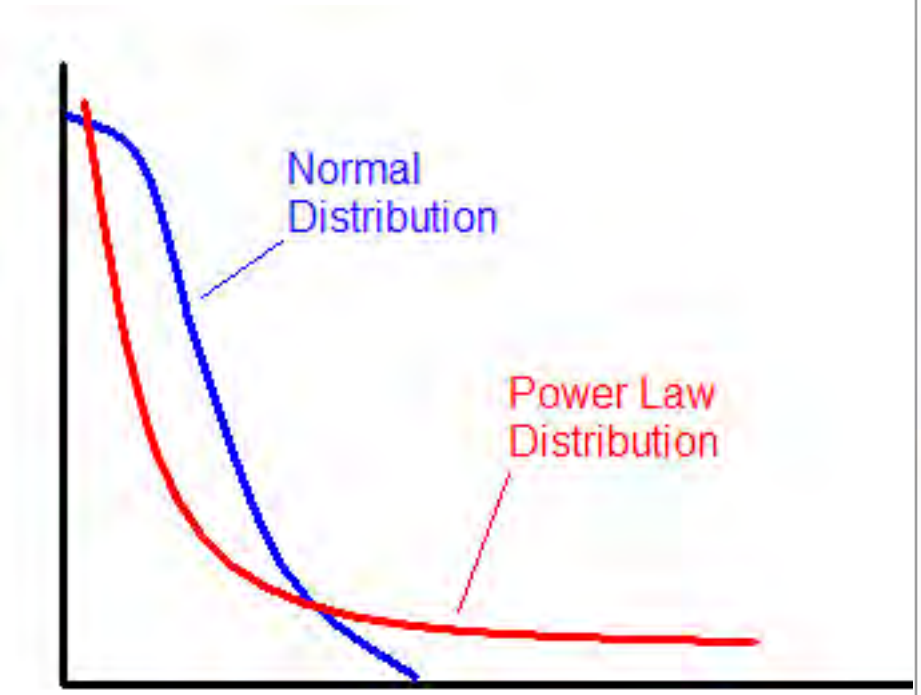

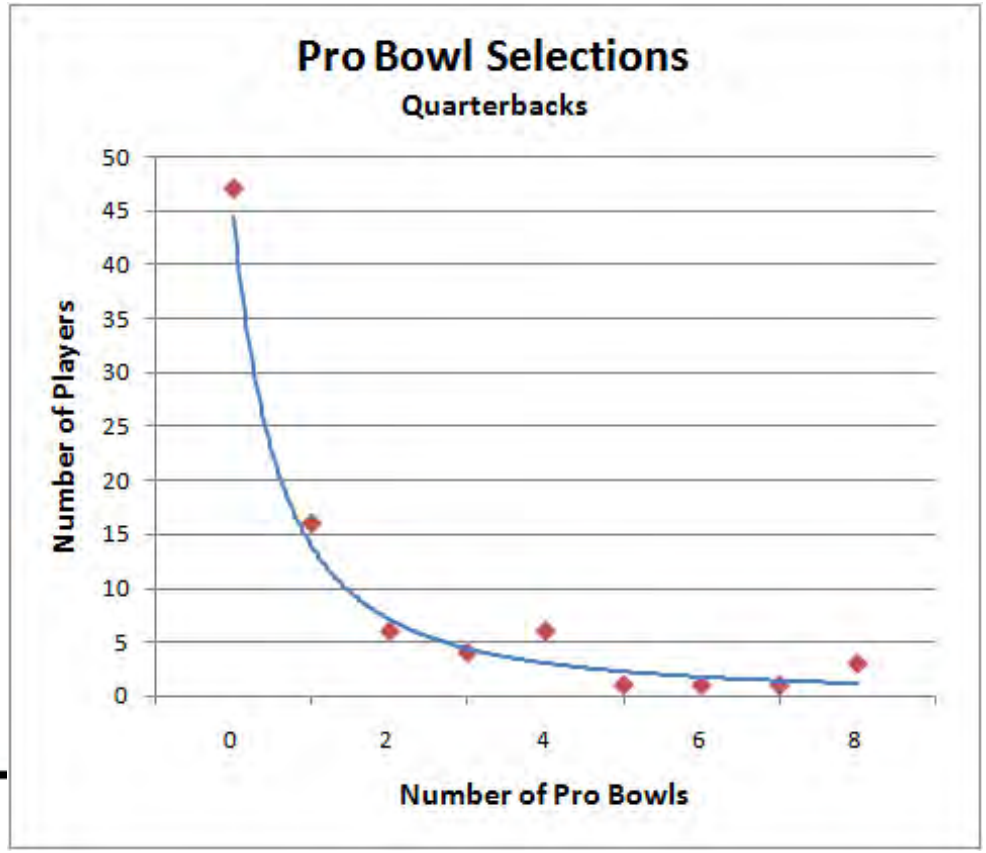

80/20 concept

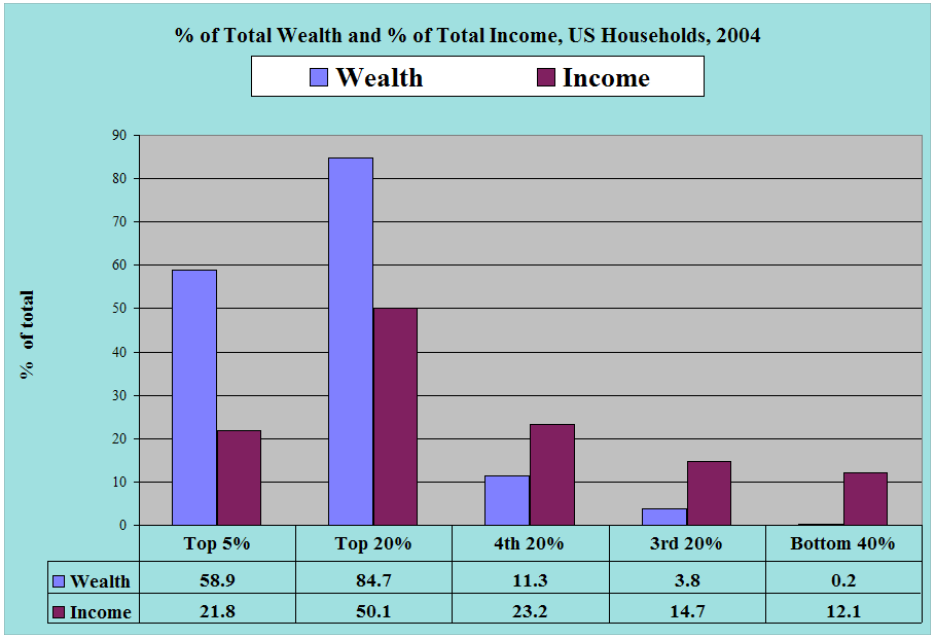

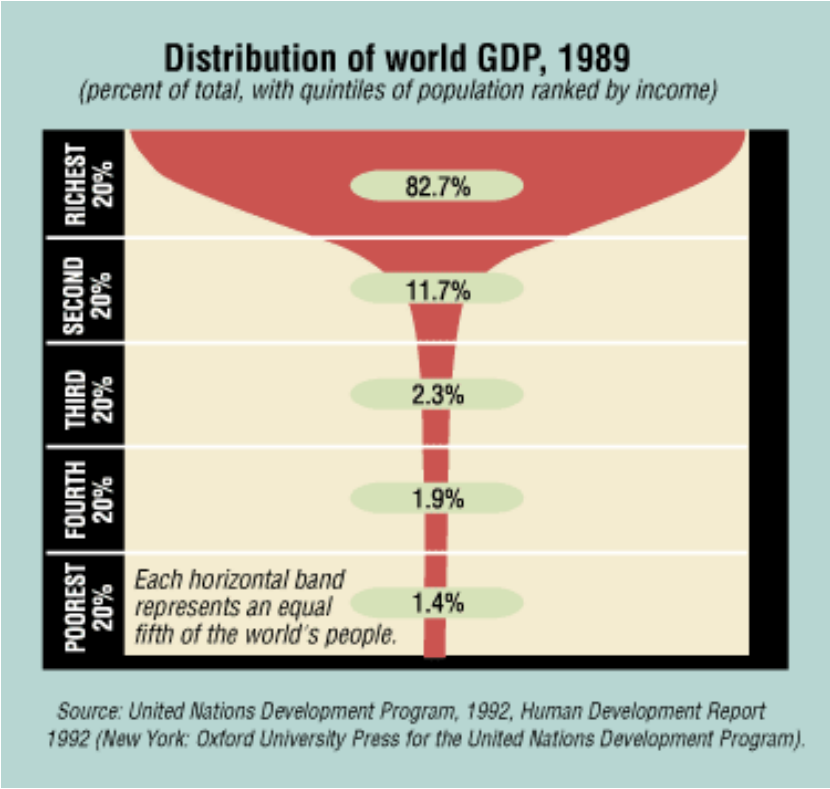

http://www.faculty.fairfield.edu/faculty/hodgson/courses

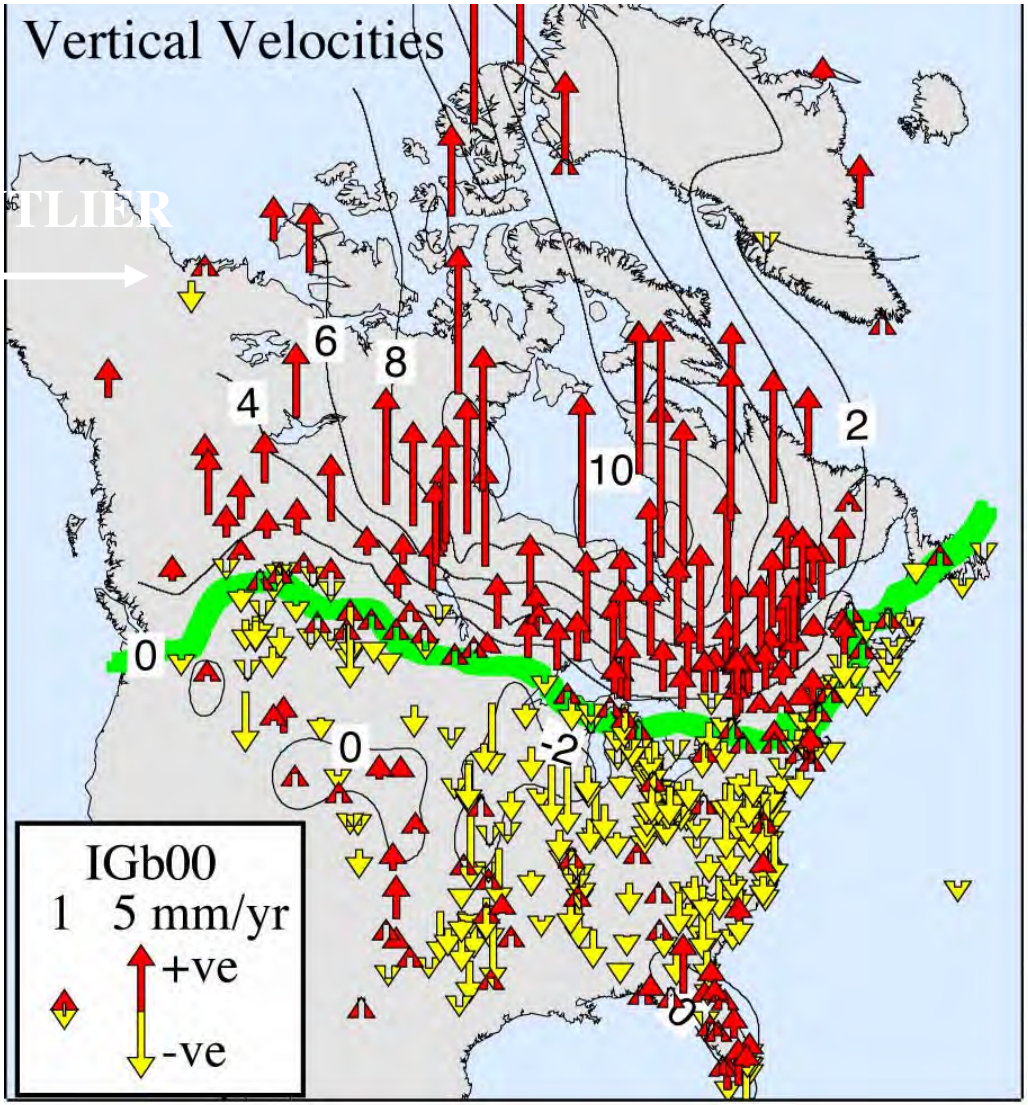
Vertical Velocities
TLIER
6
8
4
2
10
0
0
-2
IGb00
1 5 mm/yr
+ve
-ve

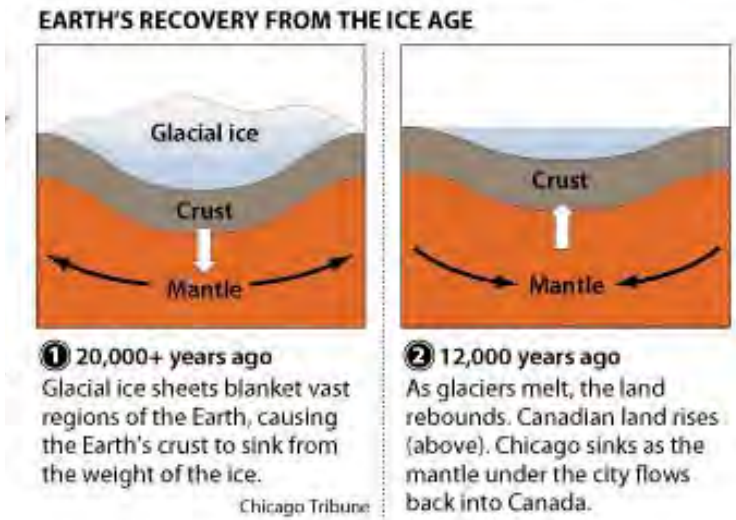
EARTH'S RECOVERY FROM THE ICE AGE
Glacial ice
Crust
Mantle
Crust
Mantle
1 20,000+ years ago
Glacial ice sheets blanket vast regions of the Earth, causing the Earth's crust to sink from the weight of the ice.
Chicago Tribune
2 12,000 years ago
As glaciers melt, the land rebounds. Canadian land rises (above). Chicago sinks as the mantle under the city flows back into Canada.


Rising
Sinking
Chicago
HINGE
Regions to the south are generally sinking, regions to the north are generally rising.

PARKFIELD, CALIFORNIA SEGMENT OF SAN ANDREAS

M 5-6 earthquakes about every 22 years: 1857, 1881, 1901, 1922, 1934, and 1966

In 1985, expected next in 1988; U.S. Geological Survey predicted 95% confidence by 1993

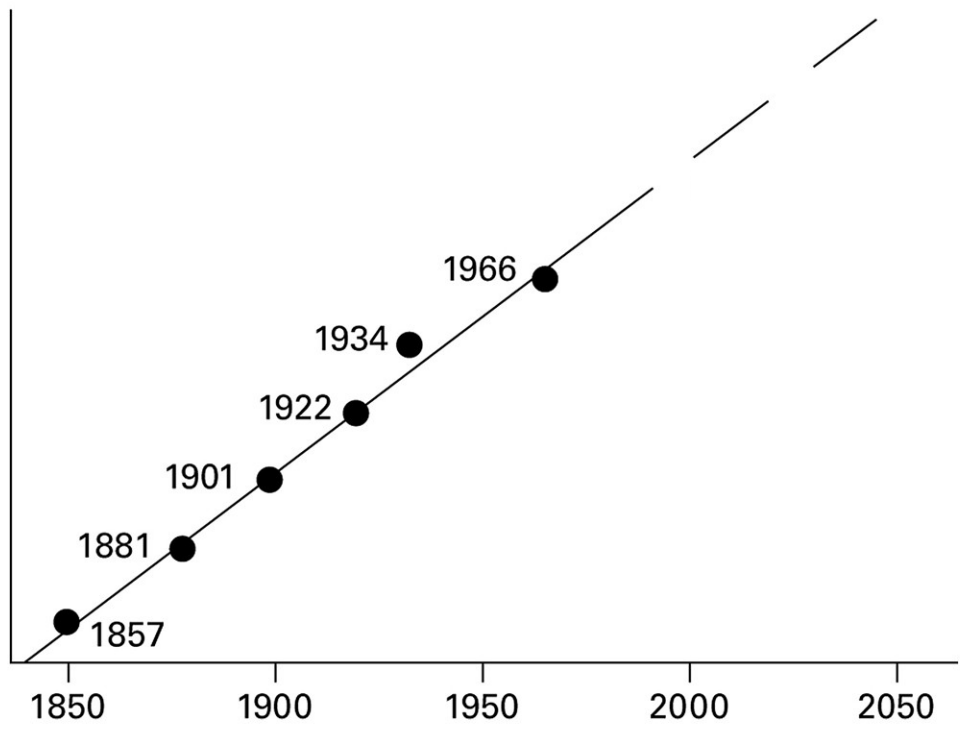

PARKFIELD, CALIFORNIA SEGMENT OF SAN ANDREAS

M 5-6 earthquakes about every 22 years: 1857, 1881, 1901, 1922, 1934, and 1966

In 1985, expected next in 1988; U.S. Geological Survey predicted 95% confidence by 1993

Occurred in 2004 (16 years late)

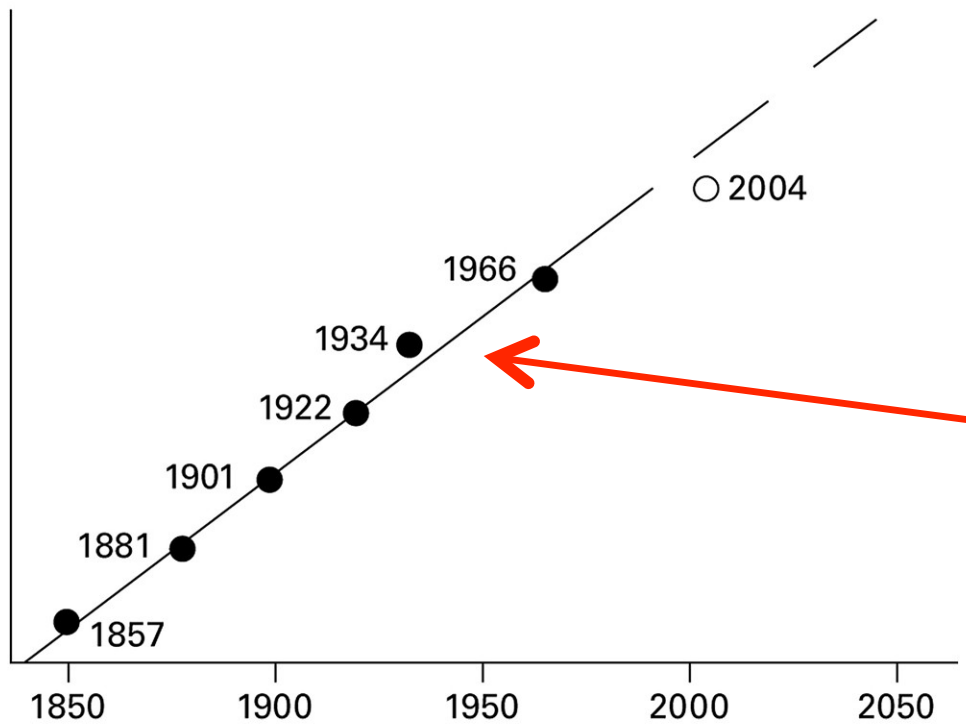

Discounting misfit of 1934 quake predicted higher confidence

Global Heat Flow Map *(Degree 12 Spherical Harmonic)*

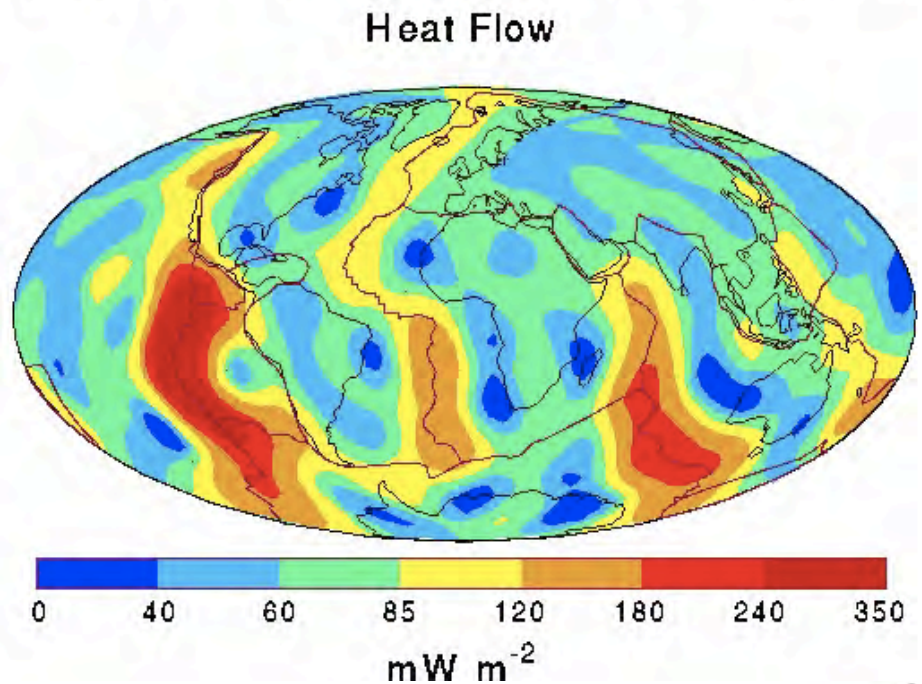

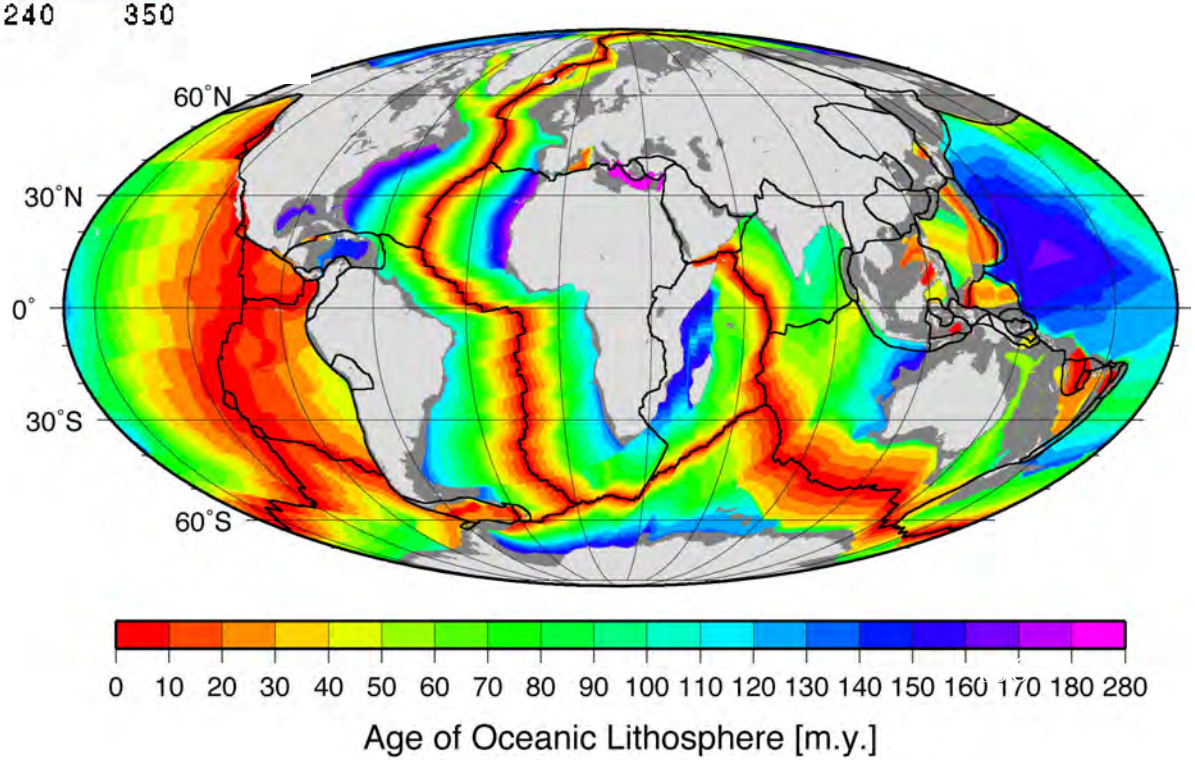

Weighted average for CO_2 flux

Table 1. Tentative Budget of Air-Water CO_2 Fluxes in the Coastal, Open and Global Oceans

	Surface (10^6 km^2)	Air-Water CO_2 Flux: mol C m^{-2} yr^{-1}		Air-Water CO_2 Flux: Pg C yr^{-1}
60°–90° (high latitude)				
Open	30.77	−0.61[f]		−0.22
Marginal seas	7.08[a]	−1.94[g]	−1.21	−0.10
Estuaries	0.11[b]	46.00[h]		
Sub-total	37.96	−0.72		−0.33
30°–60° (temperate)				
Open	122.44	−1.40[f]		−2.06
Marginal seas	14.49[a]	−1.84[i]		
Coastal upwelling	0.24[a]	0.11[j]	−0.73	−0.13
Estuaries	0.27[b]	46.00[h]		
Marsh waters	0.14[c]	21.40[k]		
Sub-total	137.58	−1.33		−2.19
0°–30° (subtropical and tropical)				
Open	182.77	0.32[f]		0.71
Marginal seas	1.46[a]	1.84[l]		
Coastal upwelling	1.25[a]	0.11[j]		
Coral reefs	0.28[d]	1.51[m]	4.19	0.18
Mangrove waters	0.15[e]	18.66[n]		
Estuaries	0.56[b]	16.83[o]		
Sub-total	186.44	0.40		0.90
Total				
Open ocean	336.0	−0.39		−1.57
Coastal ocean	26.0[a]	−0.15		−0.05
Global ocean	362.0	−0.37		−1.61

Regression using Excel

	A	B	C	D	E	F	G
1		x	y				
2		65	-20		LINEST		
3		75	17		y=A+Bx		
4		85	42		taylor 191		
5		95	94				
6		105	127				
7							
8		B	A				
9		3.71	-263.35		3.71	-263.35	
10	sig B	0.21	18.2	sig A	0.21126603	18.2044637	
11	r**2	0.99	6.7	sig y	0.99036552	6.68081831	
12	F	308.4	3.0	df			
13		13764.1	133.9		LINEST(C2:C6,B2:b6,TRUE,TRUE)		
14							
15							
16							
17		ctr shift enter		need array output		into 2 column, 5 row	

Constant volume of gas
T temperature (y)
P pressure (x)
T=A+BP

At P=0, get absolute zero =A

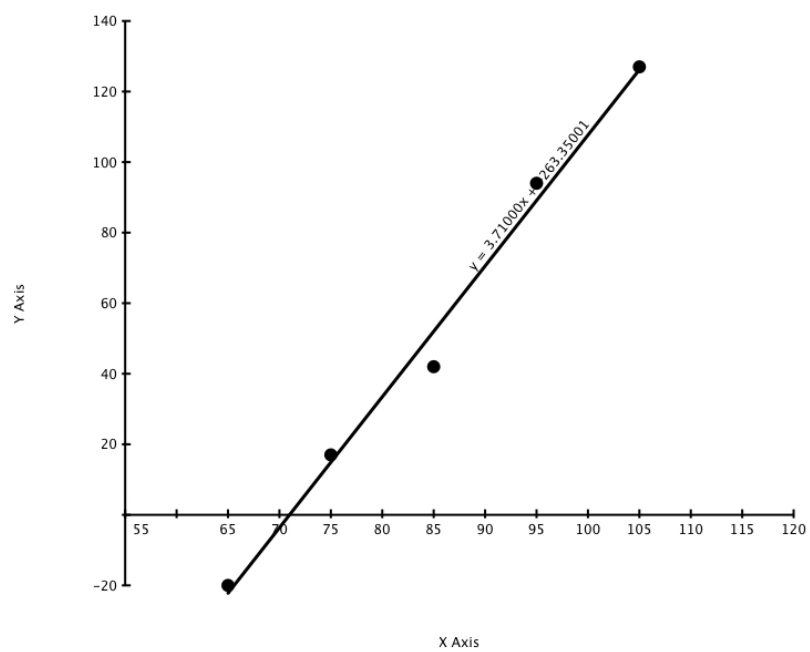

Regression in radiometric dating

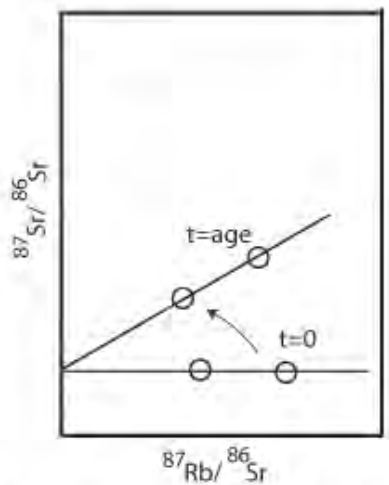

Figure 5.5.5: Evolution of rubidium-strontium ratios for two minerals in the rock formed at the same time. The ratios define a line with slope $(e^{\lambda t} - 1)$, so the slope gives the age.

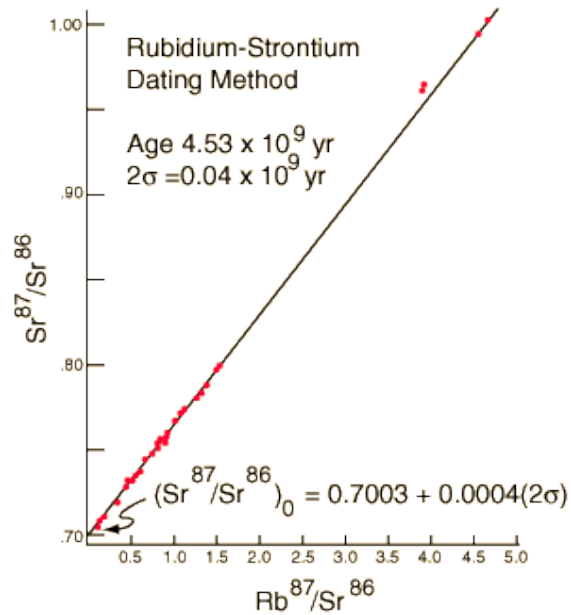

G. W. Wetherill, Ann. Rev. Nucl. Sci. 25, 283 (1975)

Figure 5.5.6: Rubidium-strontium data for meteorites formed early in the solar system's history (Wetherill, 1975).

Regression for GPS site velocity

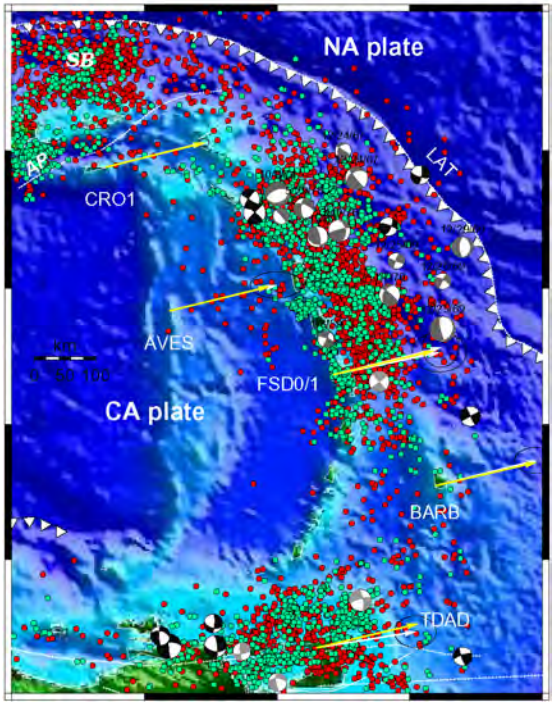

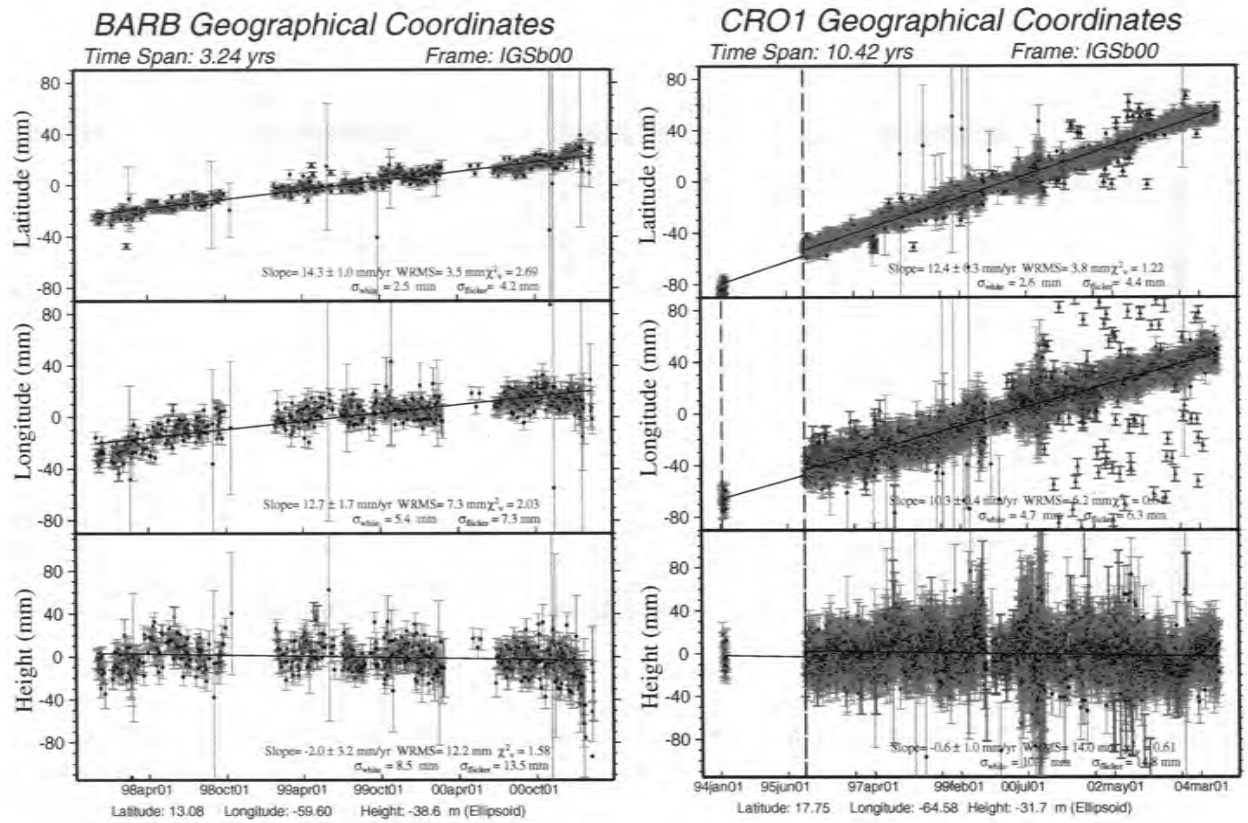

Figure 2.8: Estimated velocities for continuous sites BARB and CRO1.

Stein et al., 1986 Lopez et al., 2006

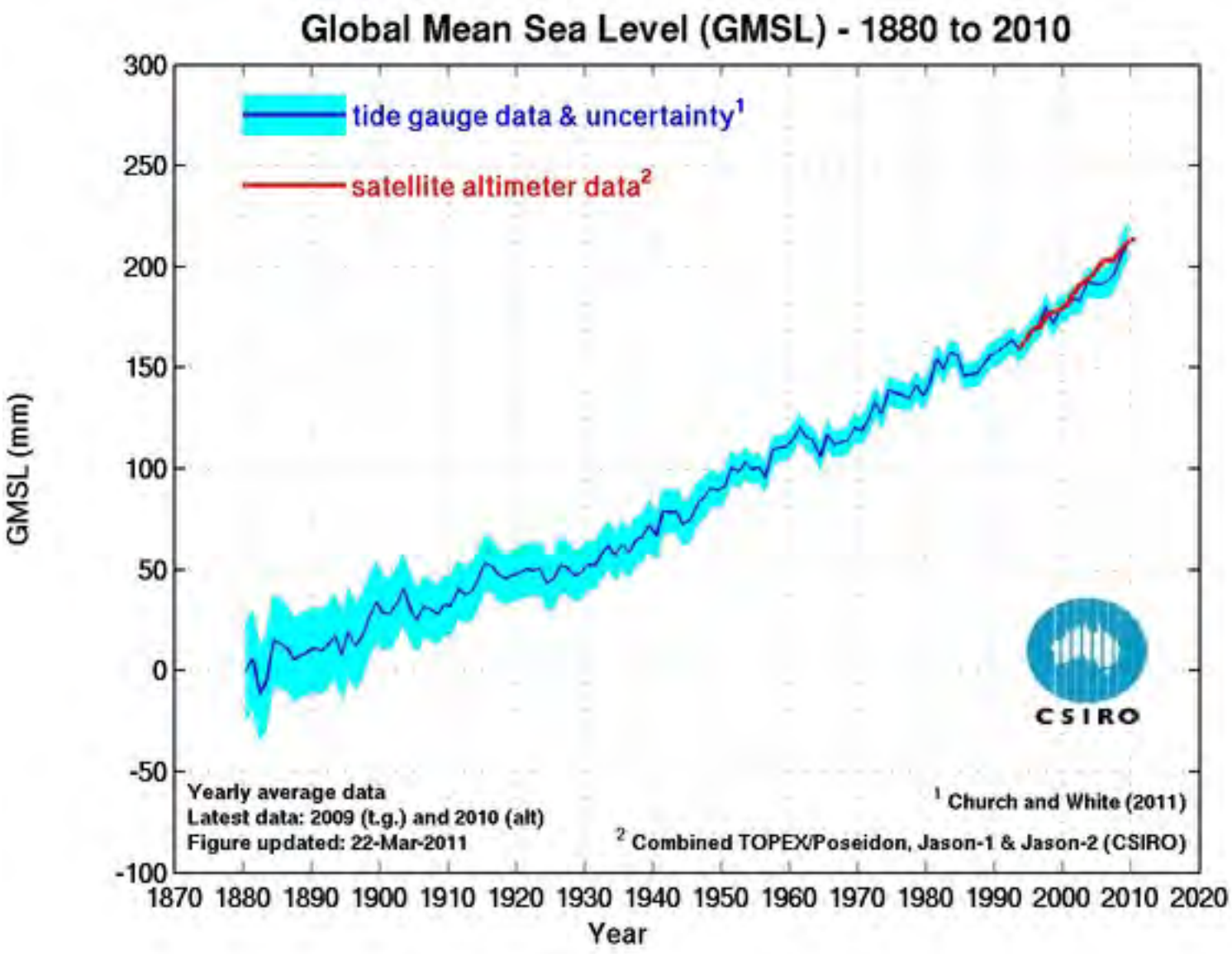

http://www.cmar.csiro.au/sealevel/

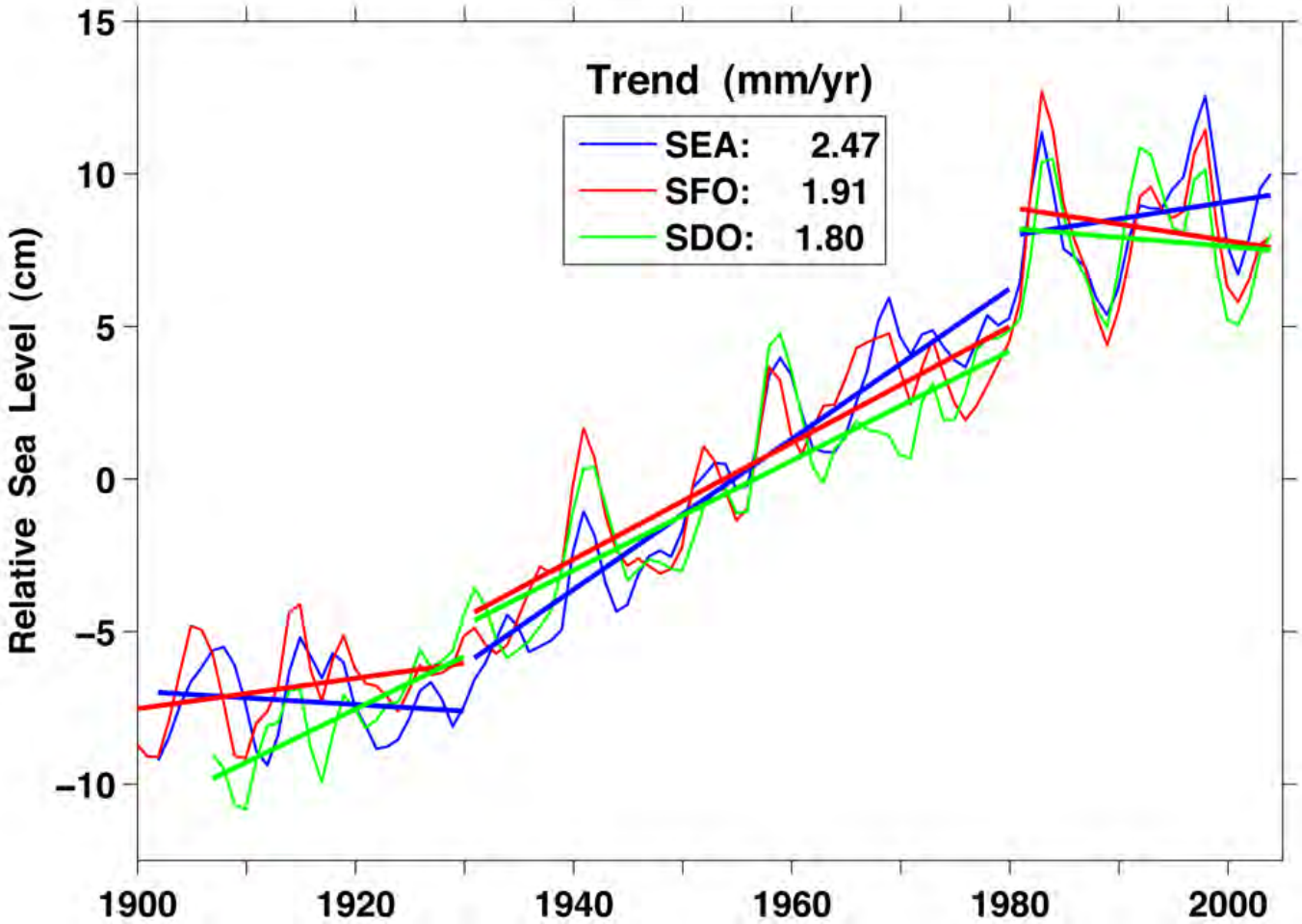

Tide gauge data at Seattle, San Francisco and San Diego show sea level along the Pacific coast rising at about the global rate from 1930 to about 1980, but scant rise or even a lowering of sea level over the past three decades that is consistent with altimetry. Large interannual fluctuations in the trends are associated with El Niño.

RUTGERS-HARVARD TEAM: SEA LEVELS RISING MORE RAPIDLY THAN PREVIOUSLY THOUGHT

JANUARY 21, 2015

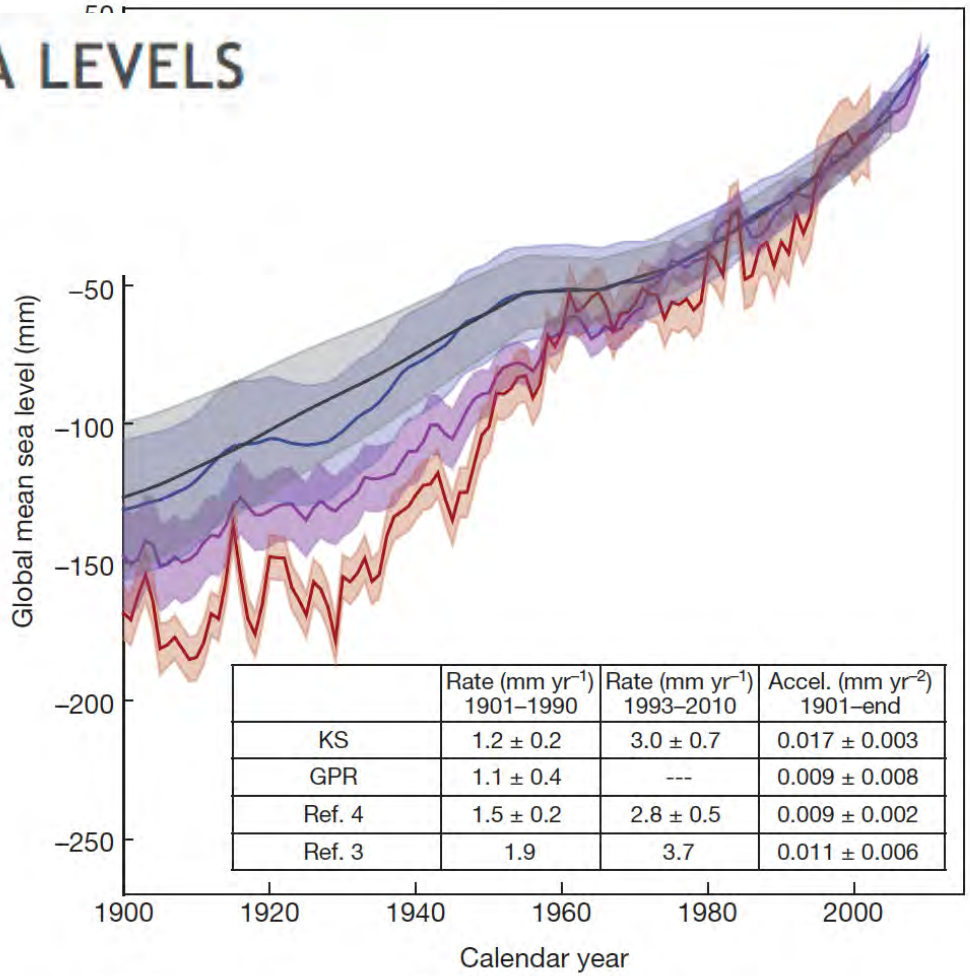

	Rate (mm yr^{-1}) 1901–1990	Rate (mm yr^{-1}) 1993–2010	Accel. (mm yr^{-2}) 1901–end
KS	1.2 ± 0.2	3.0 ± 0.7	0.017 ± 0.003
GPR	1.1 ± 0.4	---	0.009 ± 0.008
Ref. 4	1.5 ± 0.2	2.8 ± 0.5	0.009 ± 0.002
Ref. 3	1.9	3.7	0.011 ± 0.006

Figure 2 | Time series of GMSL for the period 1900–2010. Shown are estimates of GMSL based on KS (blue line), GPR (black line), Church and White[4] (magenta line) and Jevrejeva *et al.*[3] (red line). Shaded regions show $\pm 1\sigma$ pointwise uncertainty. Inset, trends for 1901–90 and 1993–2010, and accelerations, all with 90% CI. Confidence intervals for Church and White[4] are from refs 7 and 23. Confidence intervals were not available for Jevrejeva *et al.*[3]; data in this reference ends in 2002, so the rate quoted here for 1993–2010 is actually for 1993–2002. Since the GPR methodology outputs decadal sea level, no trend is estimated for 1993–2010. Accelerations are consistently estimated from the KS, GPR, and GMSL time series in refs 3 and 4 (see Methods) from 1901 to the end of each reconstruction.

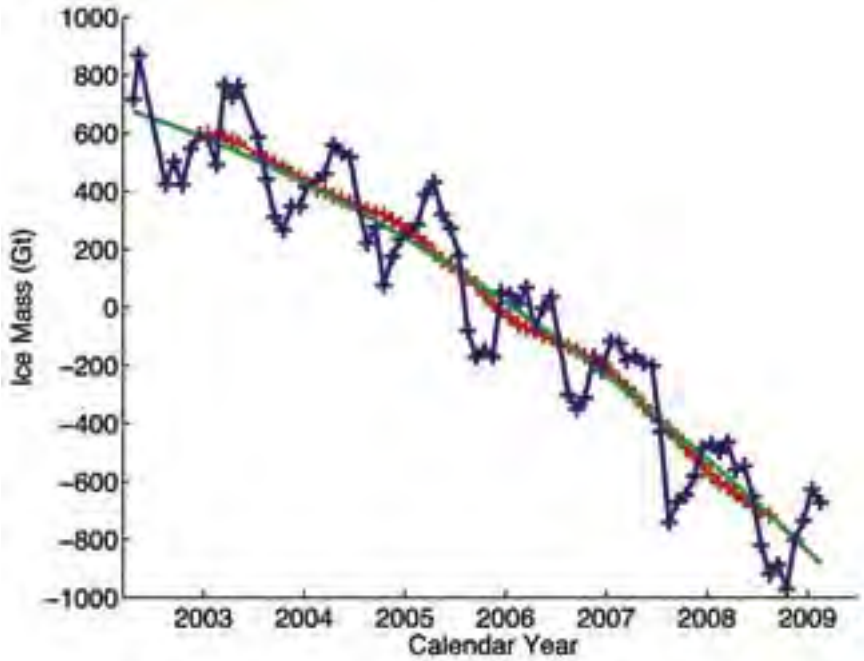

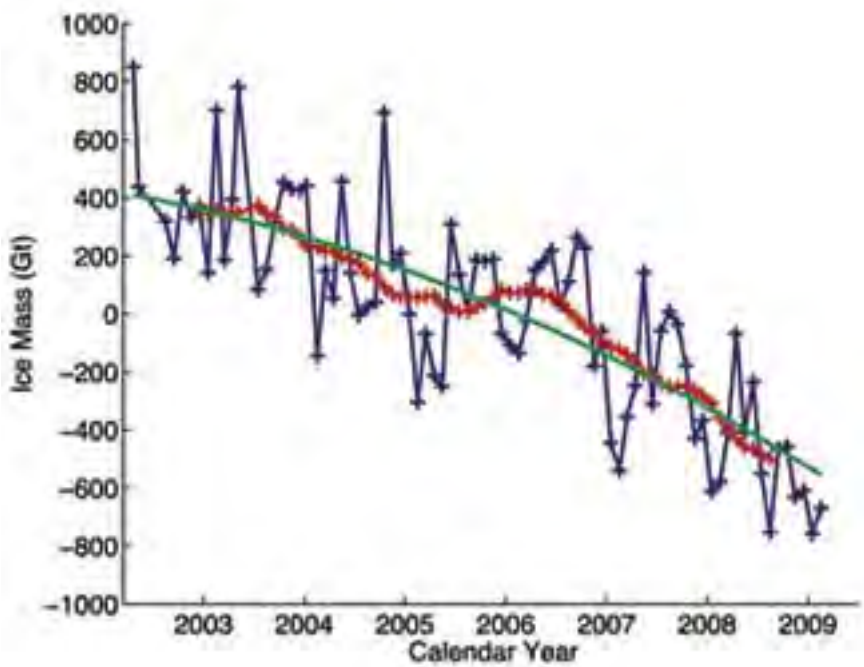

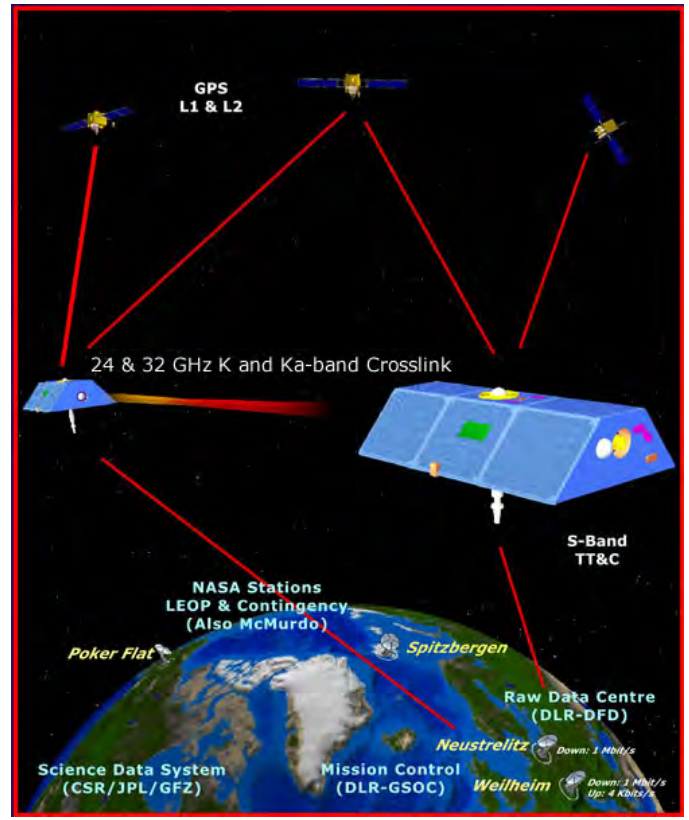

These graphs show how the rates of ice mass loss on the Greenland Ice Sheet (top) and the Antarctic Ice Sheet (bottom) have been increasing rapidly. Rates of ice loss are shown in gigatons per year. Data are from the Gravity Recovery and Climate Experiment (GRACE). (Courtesy I. Velicogna, *Geophysical Research Letters*)

http://earthdata.nasa.gov/featured-stories/featured-research/un-ice-age

Regression for hotspot track

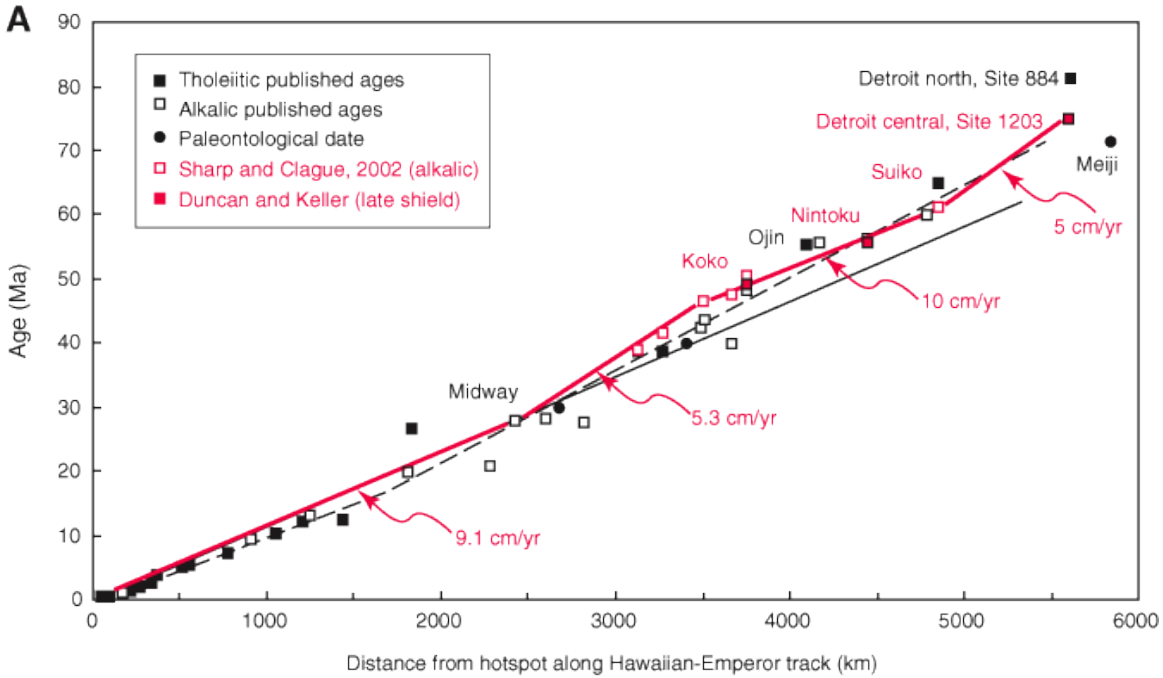

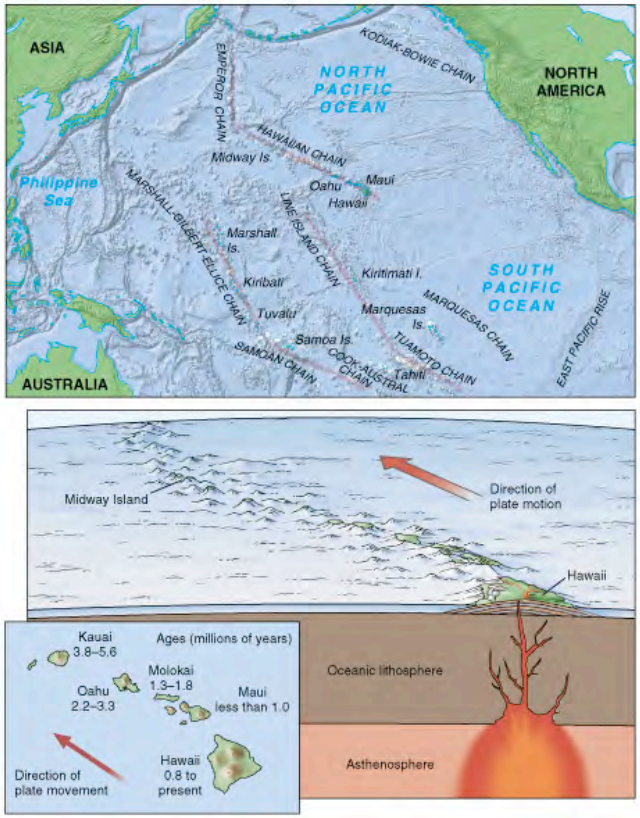

Sumatra 2004 earthquake

Measure Q from the decay of an oscillation.

Take the natural logarithm of

$$A(t) = A_0 e^{-\omega_0 t/2Q}$$

to get

$$\ln A(t) = \ln A_0 - \omega_0 t/2Q$$

so Q can be found from the slope of the logarithmic decay.

Regression for attenuation measurement

Figure 3.7-11: Wave amplitude for a damped harmonic oscillator.

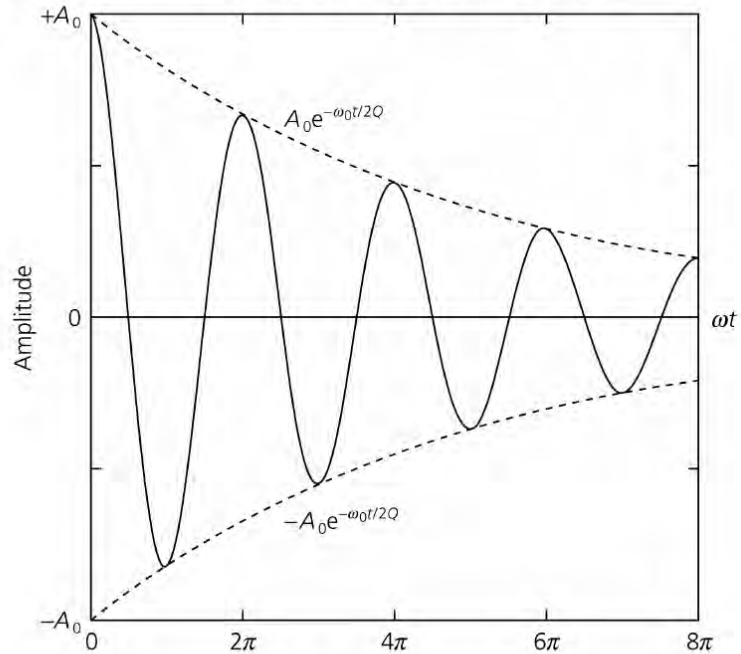

MAJO -- Matsushiro, Japan

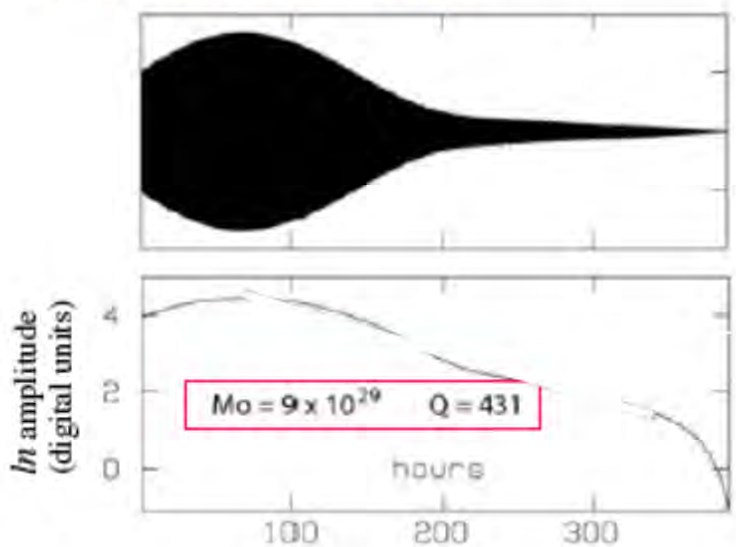

Least square line fit to log of data

Numerical fit: finding parameters that give lowest misfit

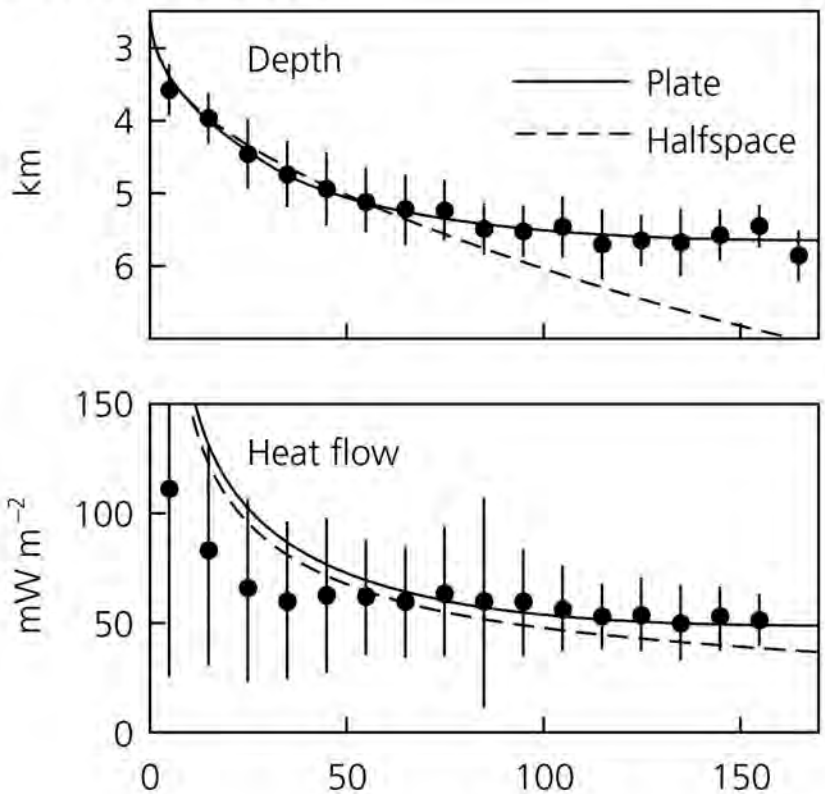

The corresponding heat flow is

$$q(x) = k\left(\frac{\partial T}{\partial z}\right)_{z=0} = q_s\left[1 + 2\sum_{n=1}^{\infty} \exp(-\beta_n x/a)\right]$$

where $q_s = kT_m/a$ is the asymptotic heat flow for old lithosphere, in which the thermal gradient is linear. The ocean depth varies with distance as

$$d(x) = d_r + d_s\left[1 - \frac{8}{\pi^2}\sum_{j=1}^{\infty} j^{-2} \exp(-\beta_j x/a)\right]$$

$$d_s = \frac{\alpha \rho_m T_m a}{2(\rho_m - \rho_w)}$$

Stein & Wysession 2003

Figure 5.3-8: Best fit model of plate thickness and basal temperature.

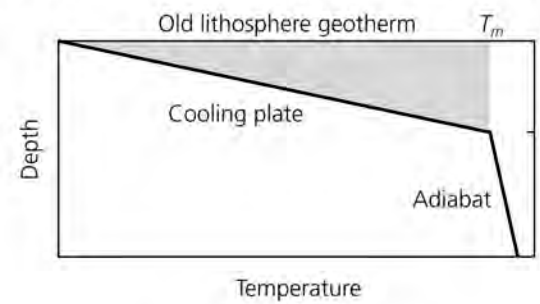

a

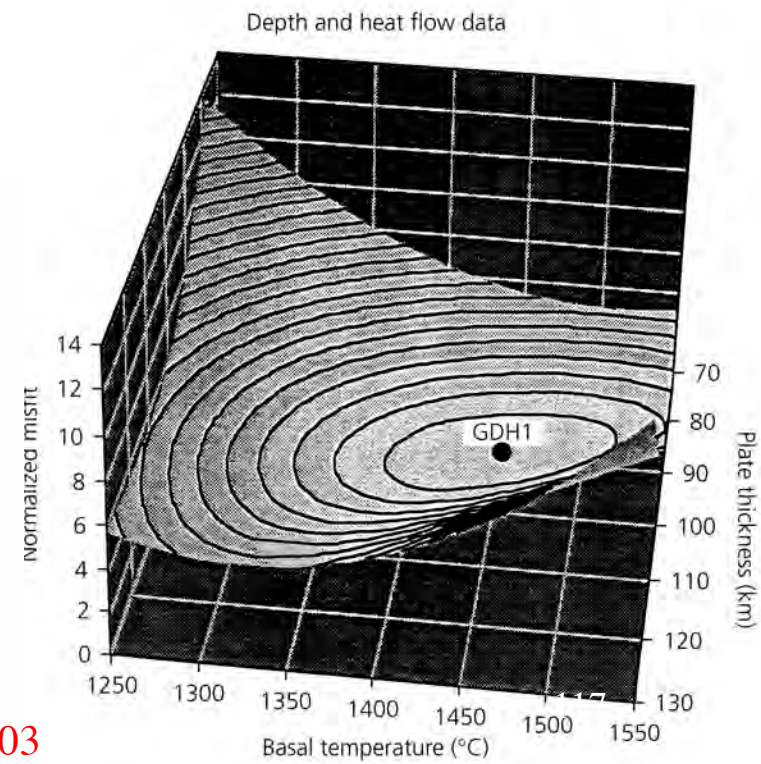

Going to College Is a Mistake for Many

31 19

By RICHARD VEDDER, Director of Center for College Affordabili and Productivity

November 17, 2011

Media debate

because "People that go to college are different kind of people ... (more) disciplined ... smarter. They did better in high school. They would have made more money even if they never went to college."

The alternative is argued based on these data shown. What's your assessment? How would you test these alternative hypotheses?

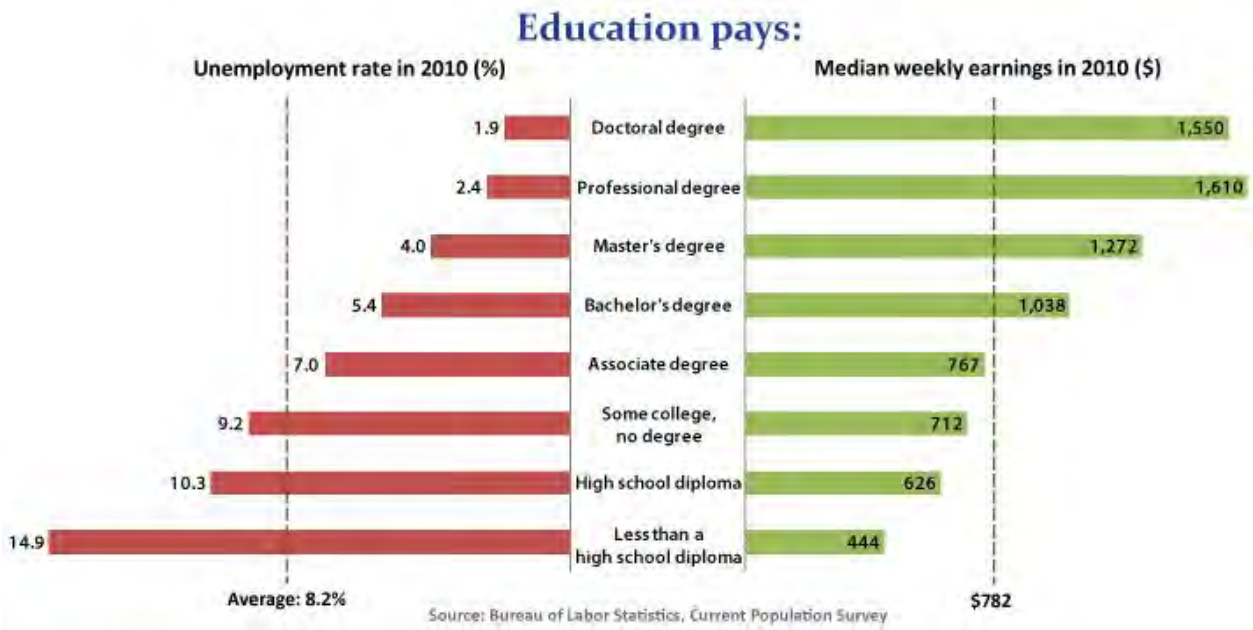

http://http://www.bls.gov/emp/ep_chart_001.htm

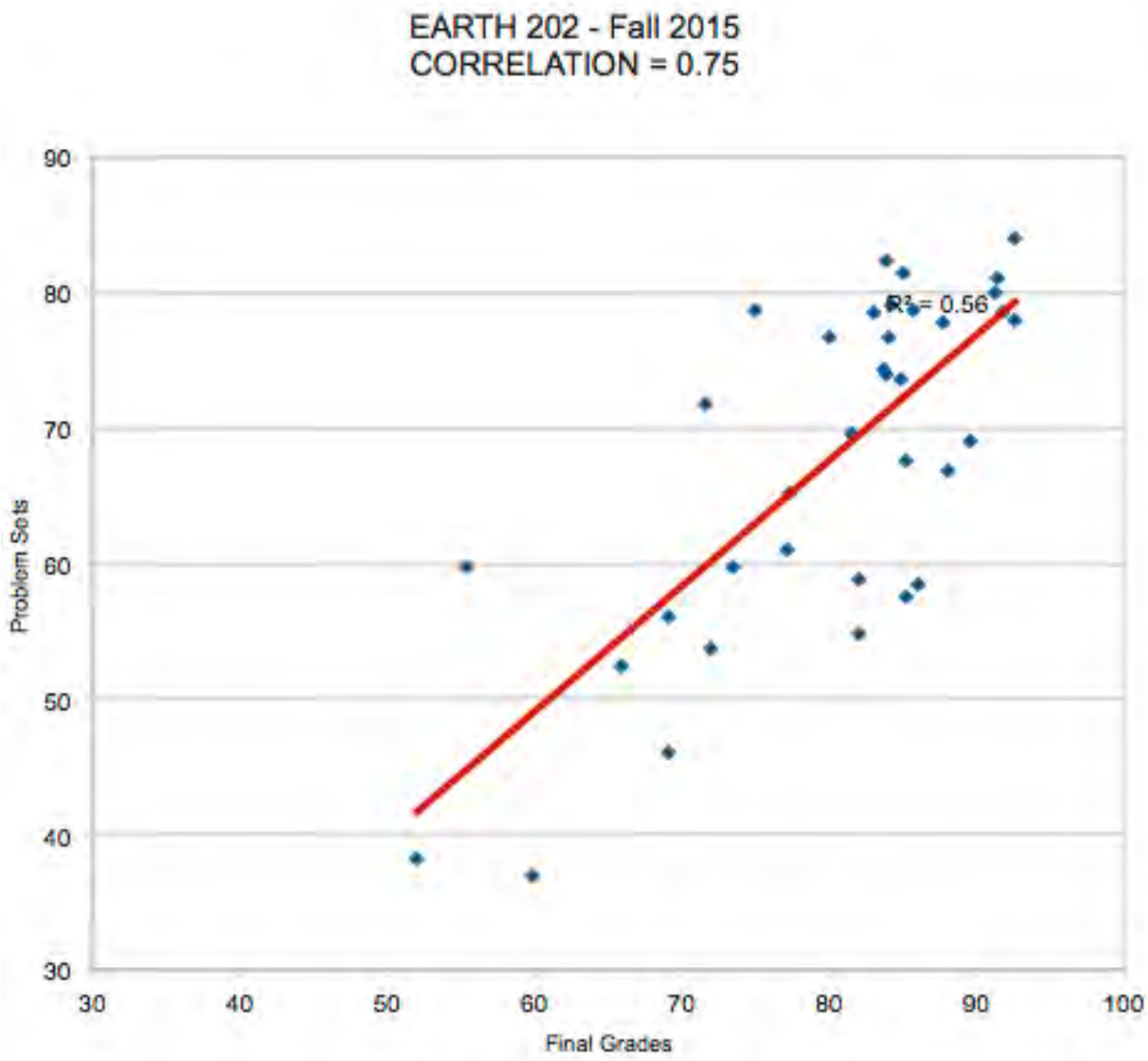
EARTH 202 - Fall 2015
CORRELATION = 0.75
R² = 0.56
Problem Sets
Final Grades
90
80
70
60
50
40
30
30
40
50
60
70
80
90
100

Linear correlation

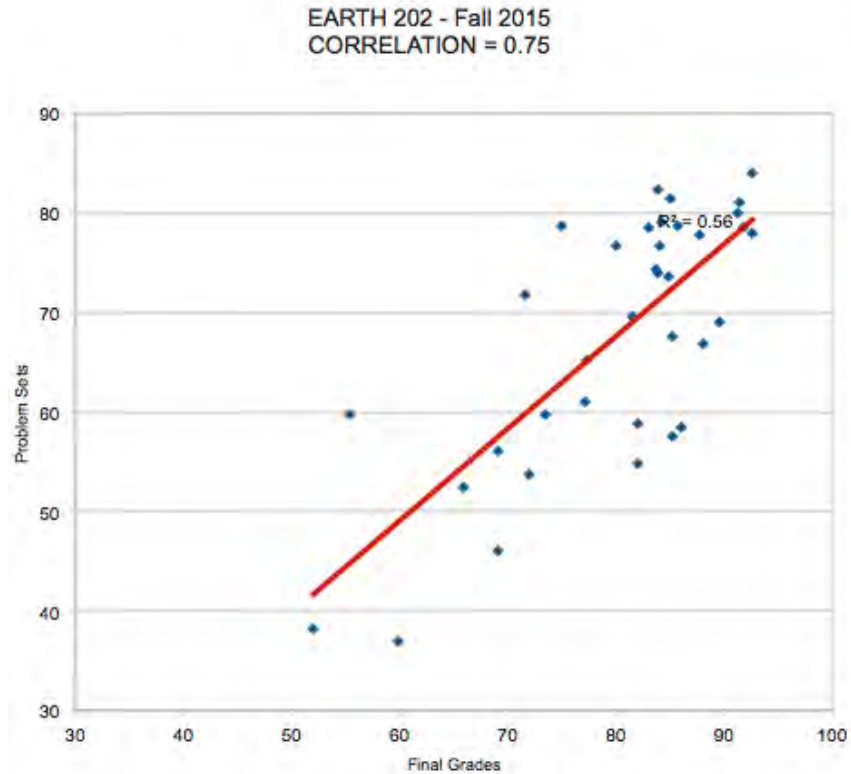

Table 9.4. The probability $Prob_N(|r| \geqslant r_o)$ that N measurements of two uncorrelated variables x and y would produce a correlation coefficient with $|r| \geqslant r_o$. Values given are percentage probabilities, and blanks indicate values less than 0.05%.

	r_o										
N	0	0.1	0.2	0.3	0.4	0.5	0.6	0.7	0.8	0.9	1
3	100	94	87	81	74	67	59	51	41	29	0
6	100	85	70	56	43	31	21	12	6	1	0
10	100	78	58	40	25	14	7	2	0.5		0
20	100	67	40	20	8	2	0.5	0.1			0
50	100	49	16	3	0.4						0

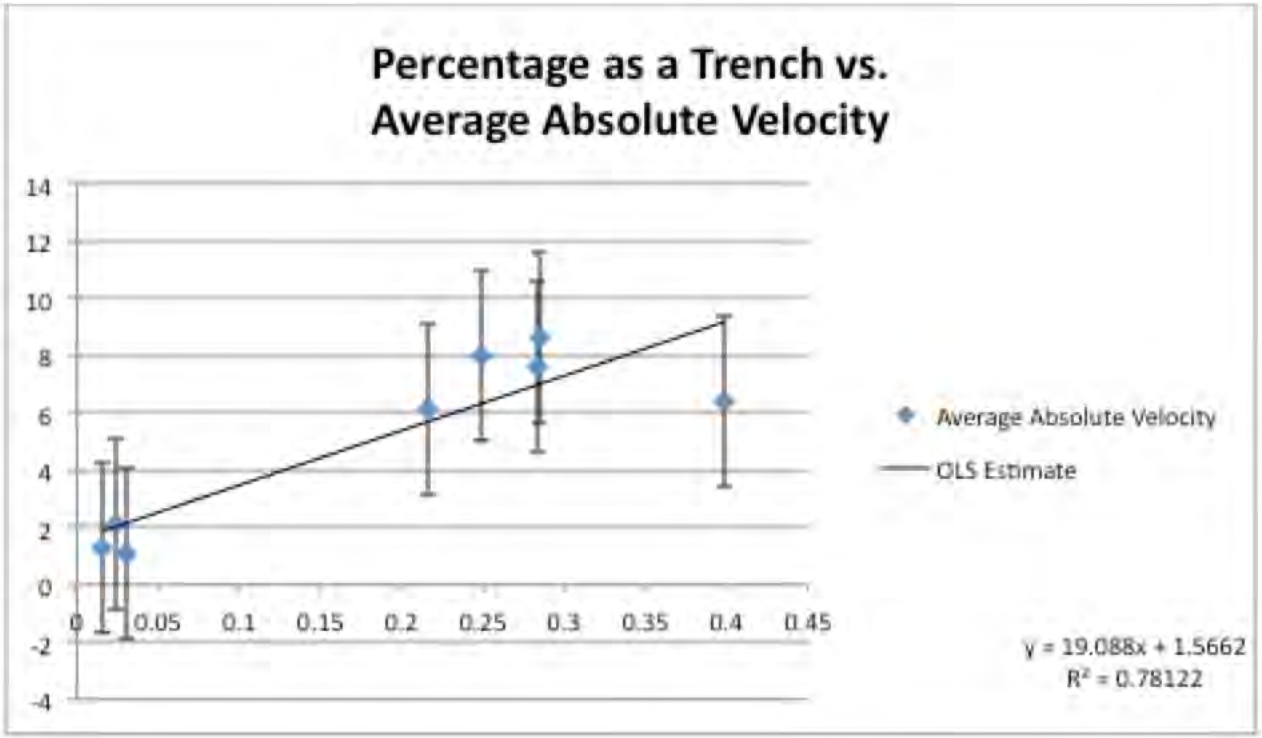

$r^2 = 0.78 \qquad r = 0.883$

For N=8 $P(|r| > 0.8) = 0.4\%$

Very unlikely to occur by chance

Result is highly significant

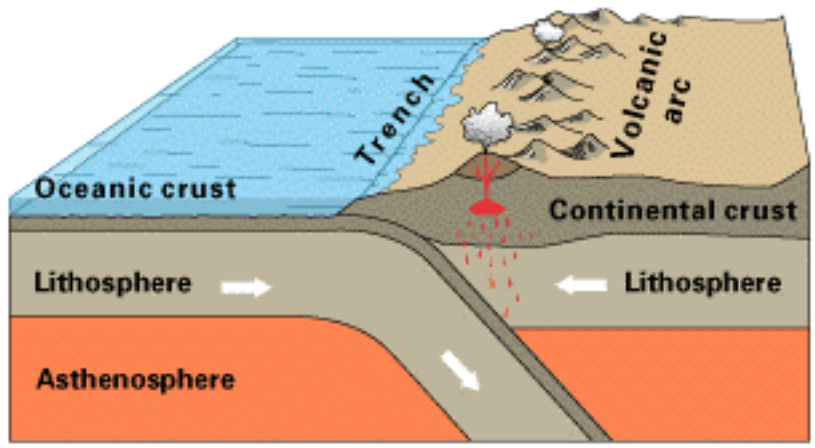

Oceanic-continental convergence

Fig. 1

IS FACEBOOK DRIVING THE GREEK DEBT CRISIS?

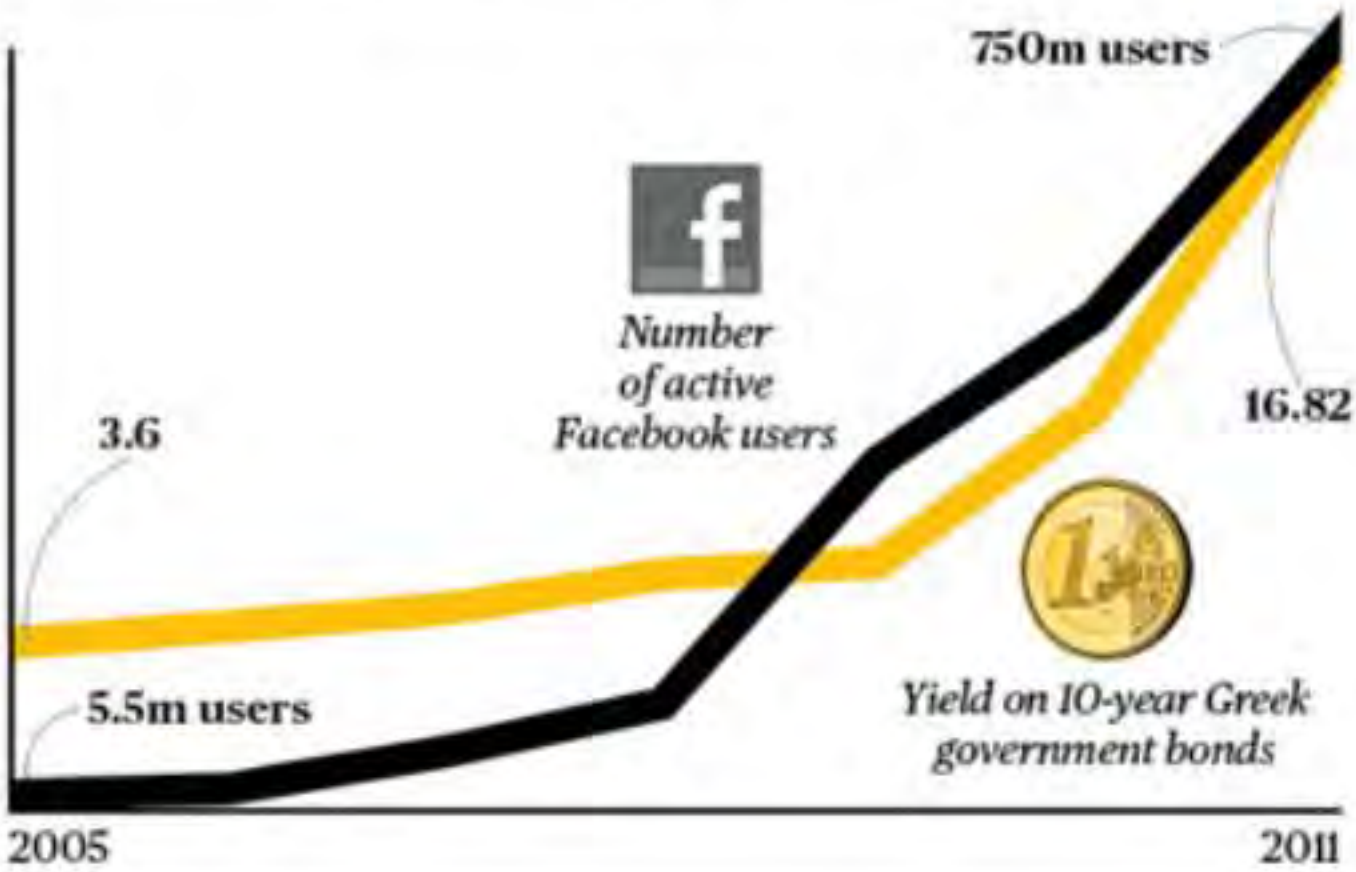

It's easy to find spurious correlations

Total number of bachelor's degrees granted by discipline, 1985 to 2000

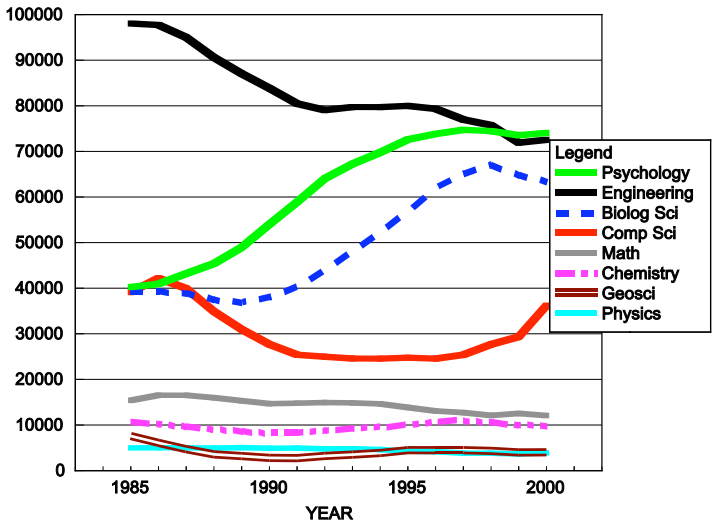

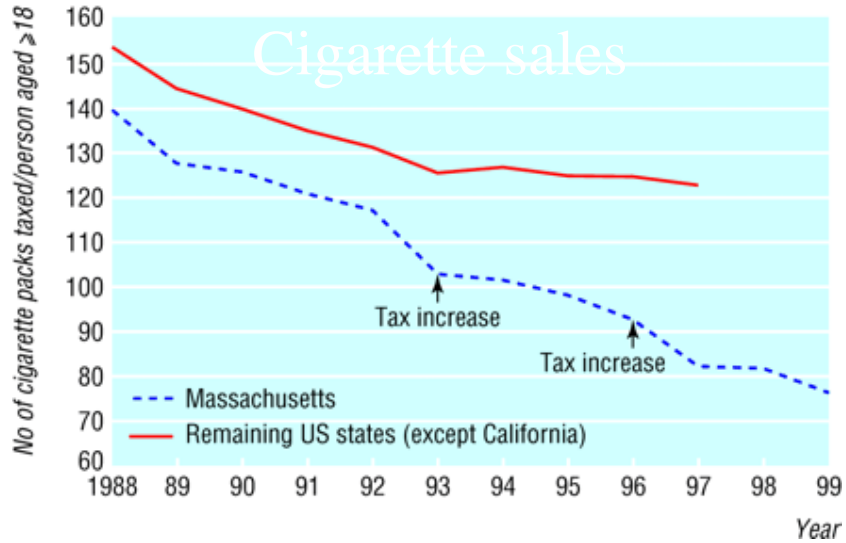

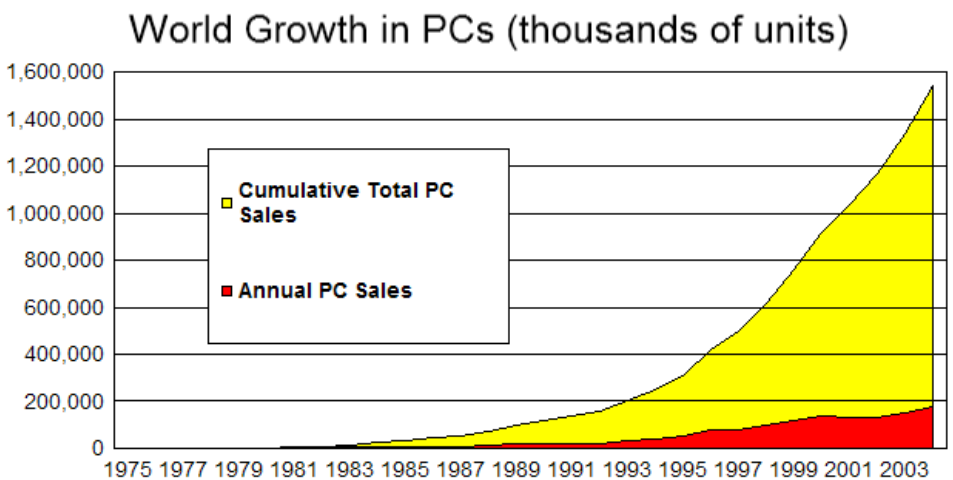

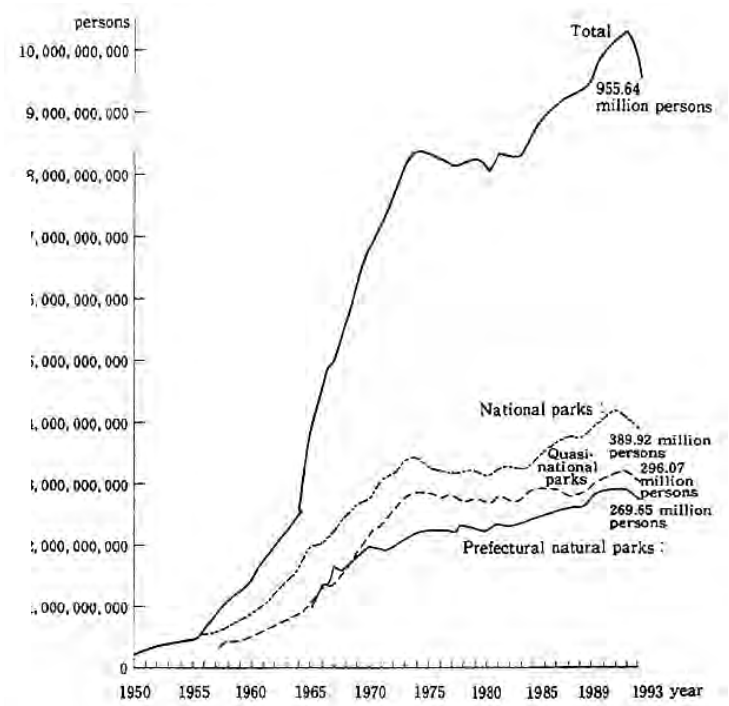

http://tylervigen.com/spurious-correlations

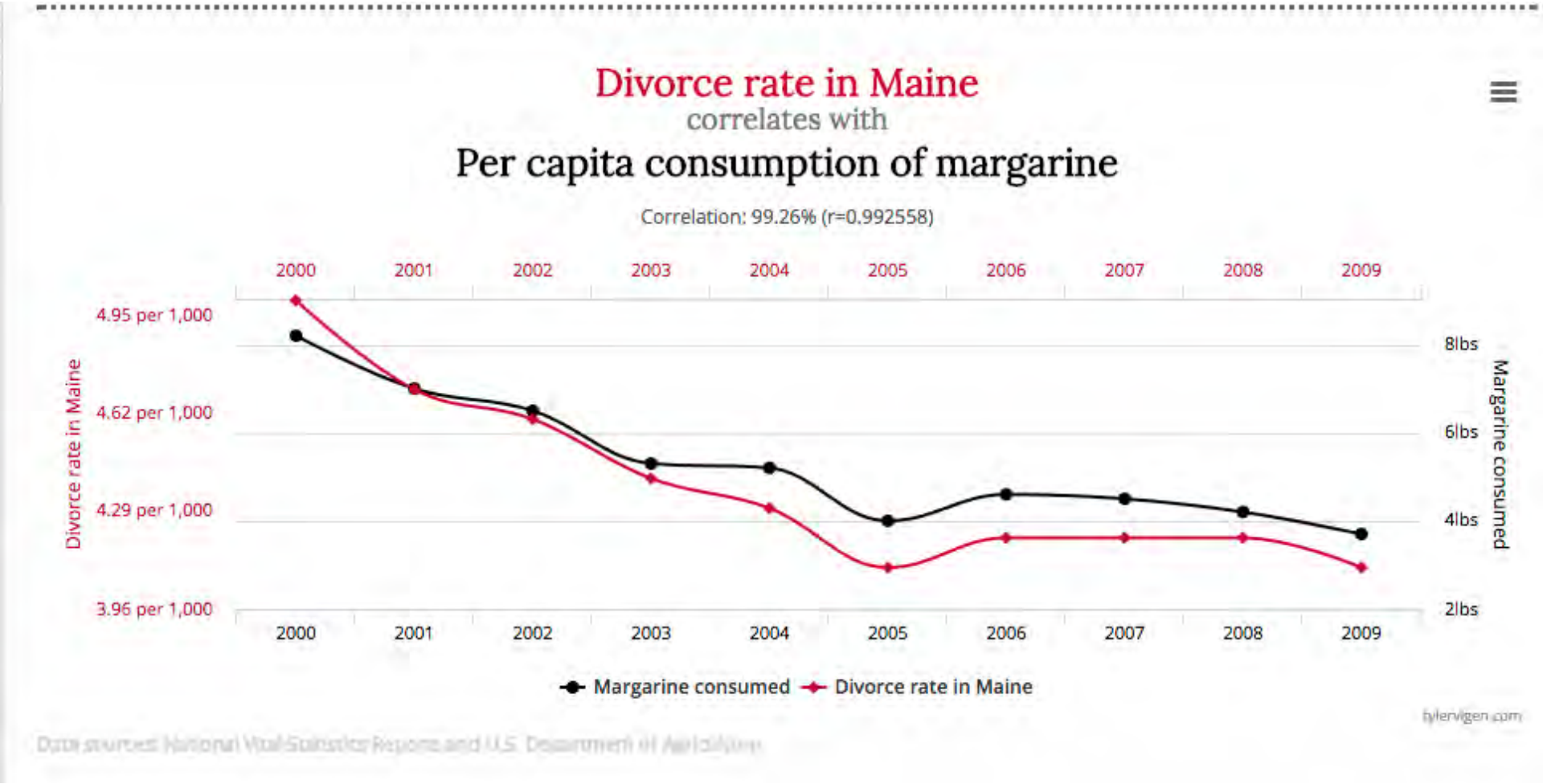

Data with same statistics can be very different

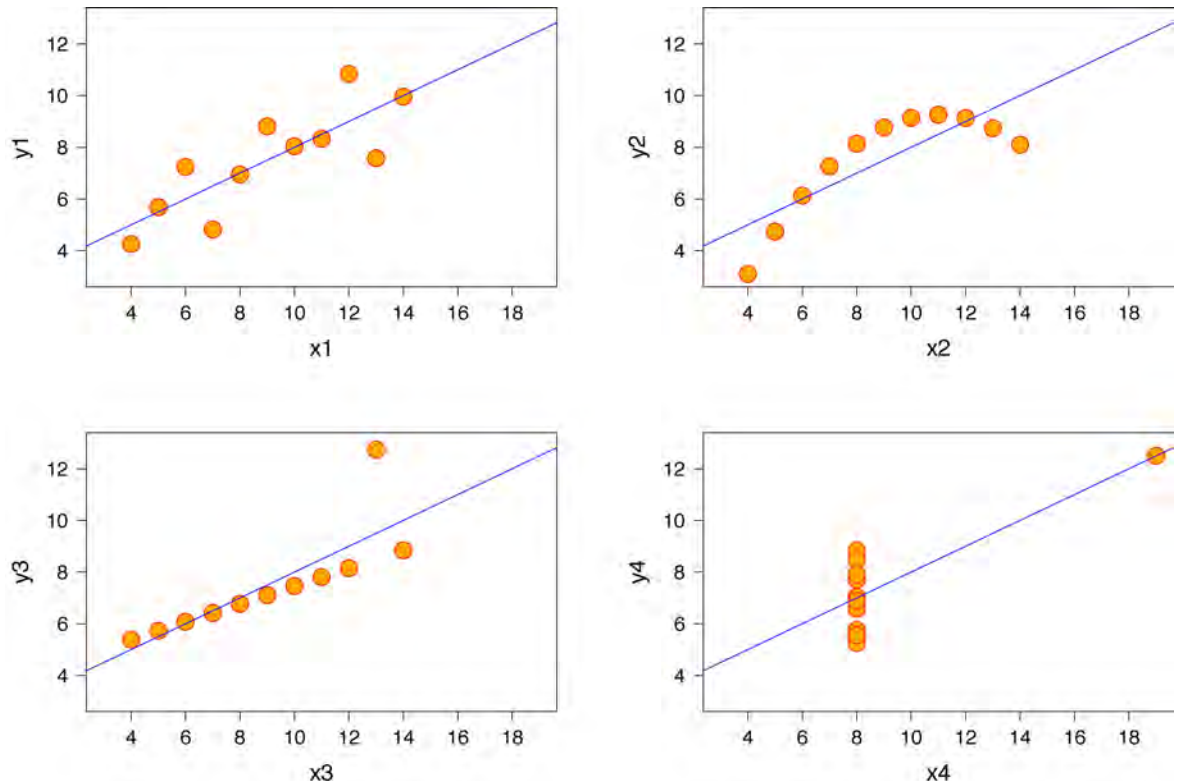

Each dataset has the following identical set of summary statistics:

N	11
Mean of x's	9.0
Mean of y's	7.5
Equation of regression line	y = 3 + 0.5x
sum of squares (X - Xbar)	110.0
correlation coefficient	0.82
r^2	0.67

Anscombe, Amer. Statistician, 1973

Linear correlation shown by r

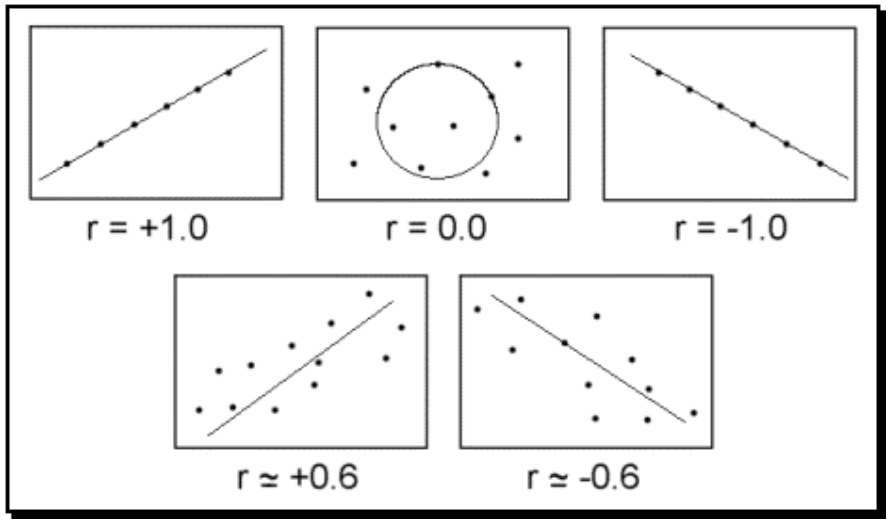

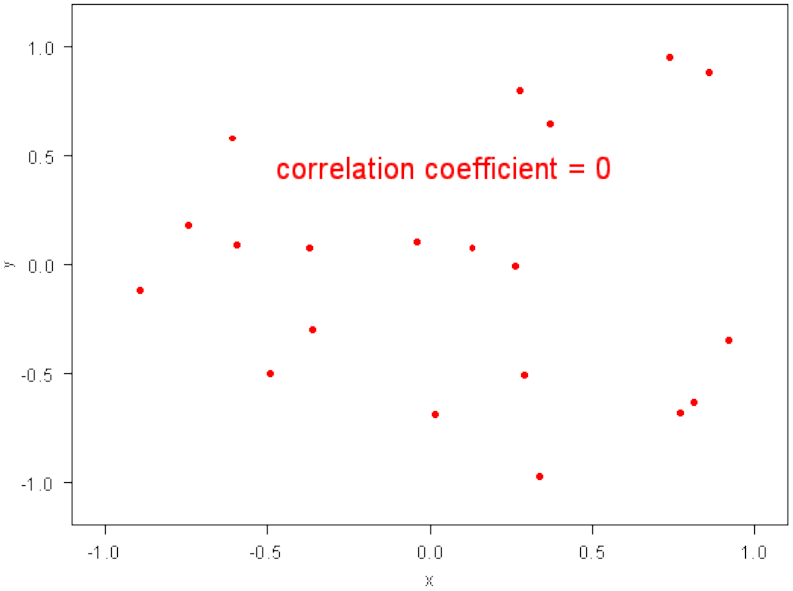

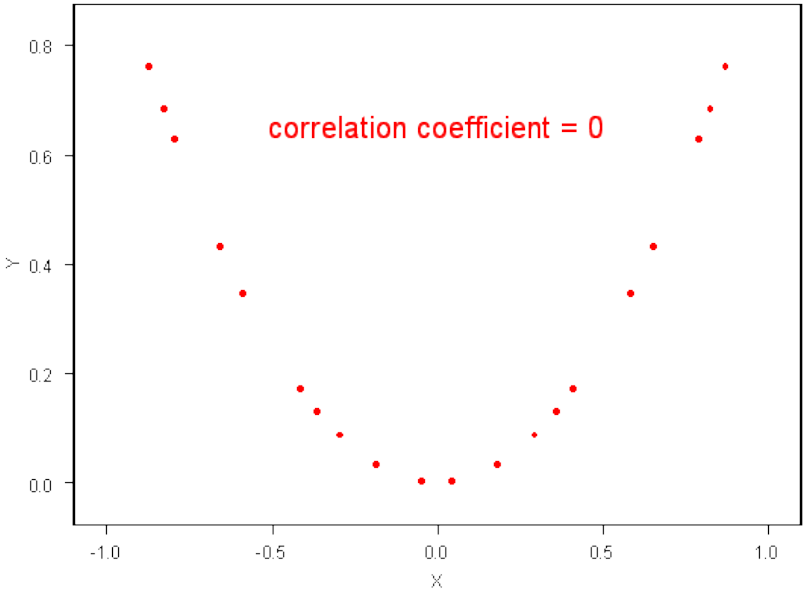

Berkeley sex bias case

[ed

One of the best known real life examples of Simpson's paradox occurred when the University of California, Berkeley was sued for bias against women applying to graduate school. The admission figures for fall 1973 showed that men applying were more likely than women to be admitted, and the difference was so large that it was unlikely to be due to chance.[15][3]

	Applicants	**% admitted**
Men	8442	**44%**
Women	4321	35%

However when examining the individual departments, it was found that no department was significantly biased against women; in fact, most departments had a small bias against men.

Major	**Men**		**Women**	
	Applicants	% admitted	Applicants	% admitted
A	825	62%	108	**82%**
B	560	63%	25	**68%**
C	325	**37%**	593	34%
D	417	33%	375	**35%**
E	191	**28%**	393	24%
F	272	6%	341	**7%**

Berkeley sex bias case

[ed

One of the best known real life examples of Simpson's paradox occurred when the University of California, Berkeley was sued for bias against women applying to graduate school. The admission figures for fall 1973 showed that men applying were more likely than women to be admitted, and the difference was so large that it was unlikely to be due to chance.[15][3]

	Applicants	**% admitted**
Men	8442	**44%**
Women	4321	35%

However when examining the individual departments, it was found that no department was significantly biased against women; in fact, most departments had a small bias against men.

Major	**Men**		**Women**	
	Applicants	% admitted	Applicants	% admitted
A	825	62%	108	**82%**
B	560	63%	25	**68%**
C	325	**37%**	593	34%
D	417	33%	375	**35%**
E	191	**28%**	393	24%
F	272	6%	341	**7%**

The explanation turned out to be that women tended to apply to departments with low rates of admission, while men tended to apply to departments with high rates of admission. The conditions under which department-specific frequency data constitue a proper defense against charges of discrimination are formulated in Pearl (2000).

Figure 5.4-12: Plate velocity as a function of the amount of subducting lithosphere.

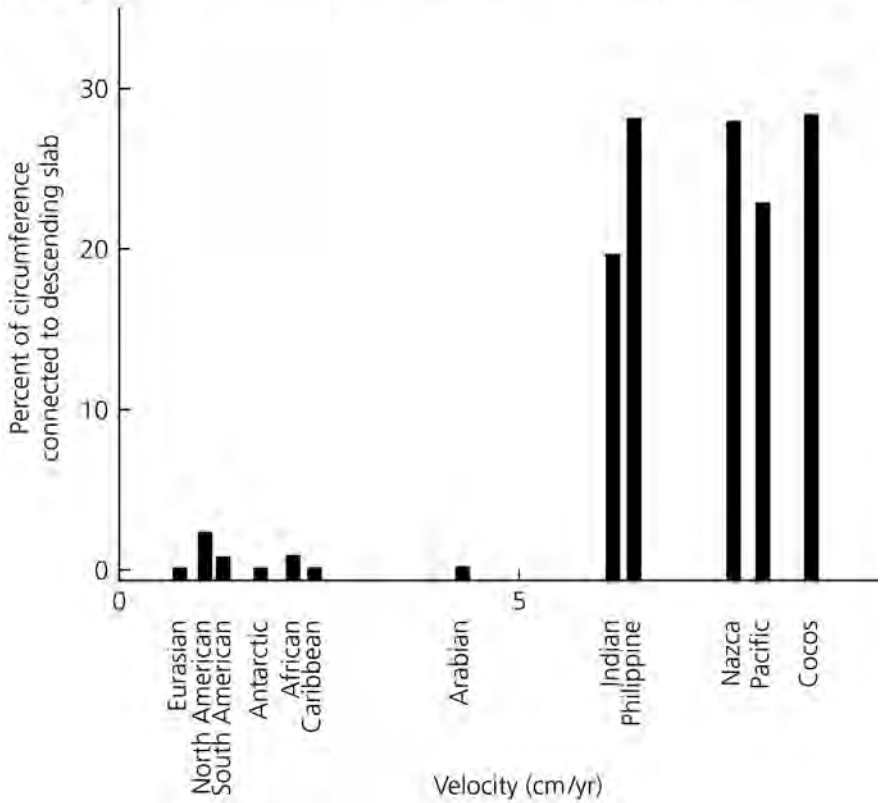

In earth science, data often show complicated relations

Figure 5.4-4: Maximum earthquake depth as a function of thermal parameter.

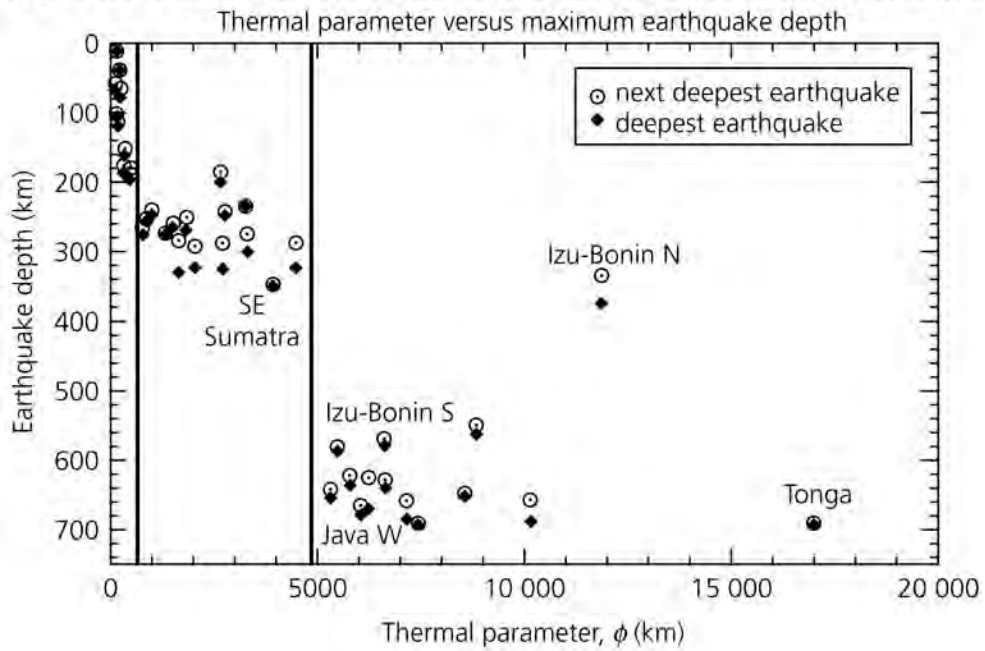

I JUST GAVE YOU 5 HUGE STOCK-WINNERS

Now, Get Ready to DOUBLE Your Money – AGAIN!

Here's what I've told you in just the last 14 months:

- I said buy True North Energy at $2.25 - it quickly ran to $6.02
- I said buy Liberty Star Uranium at $0.60 - it quickly ran to $1.27
- I said buy Homeland Precious Metals at $0.55 - it quickly ran to $0.95
- I said buy Yellowcake Mining at $2.50 - it quickly ran to $3.65
- I said buy Strategic Resources a $0.65 - it quickly ran to $1.15

Now I am giving you yet another opportunity for rapid-fire gains with my Urgent-Buy on Aurelio Resources up to $2.00 per share.

Act quickly... and you'll own Aurelio Resources (AULO) cheaper than everyone else. If you hesitate - even briefly - expect to pay above $4!

New Orleans flood 2005

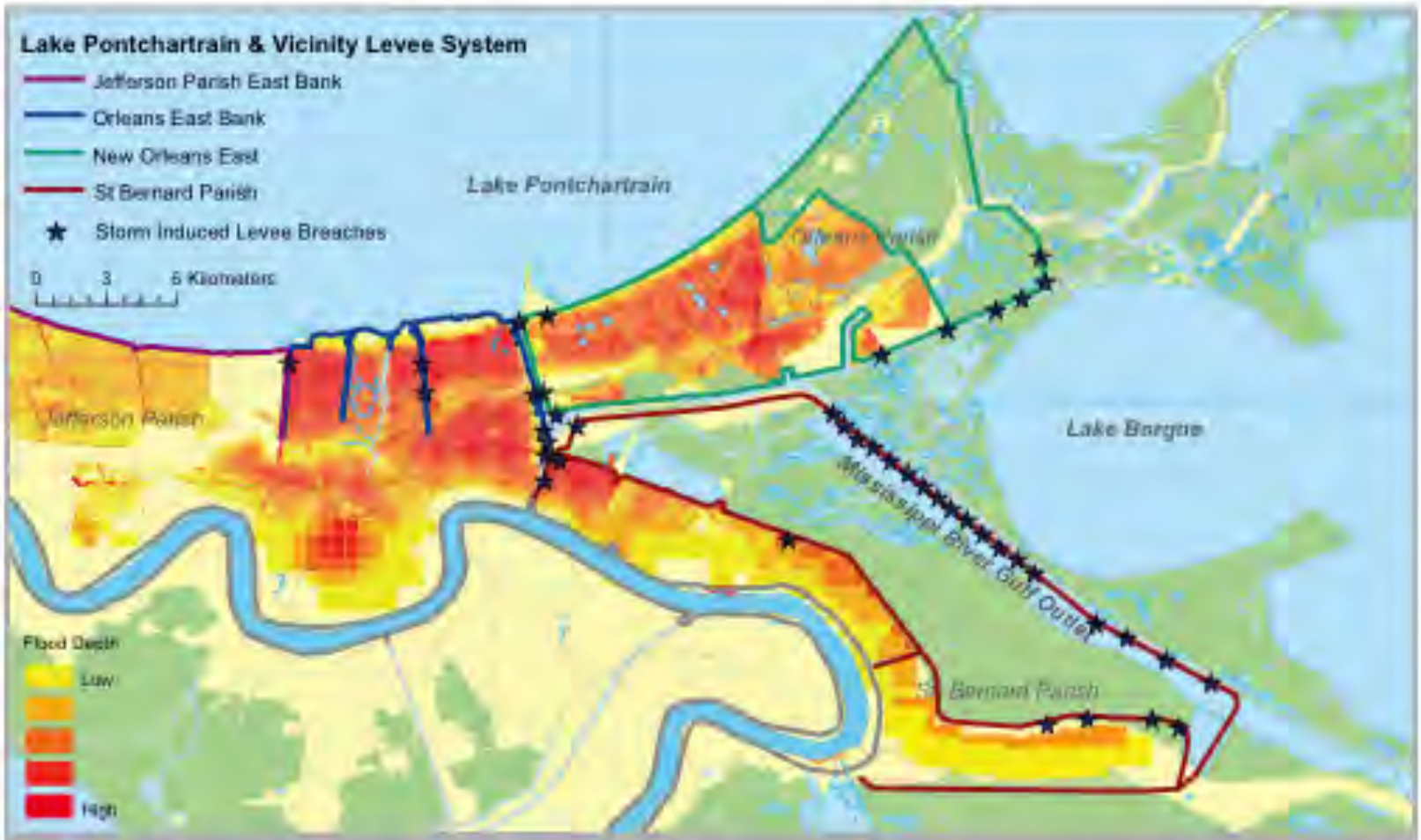

The impact of Hurricane Katrina: maximum flood depths in protected regions of New Orleans and its vicinity developed by RMS and flood loss hotspots documented in the Independent Levee Investigation Team Report (ILIT, 2006)

Hurricane hazard & risk

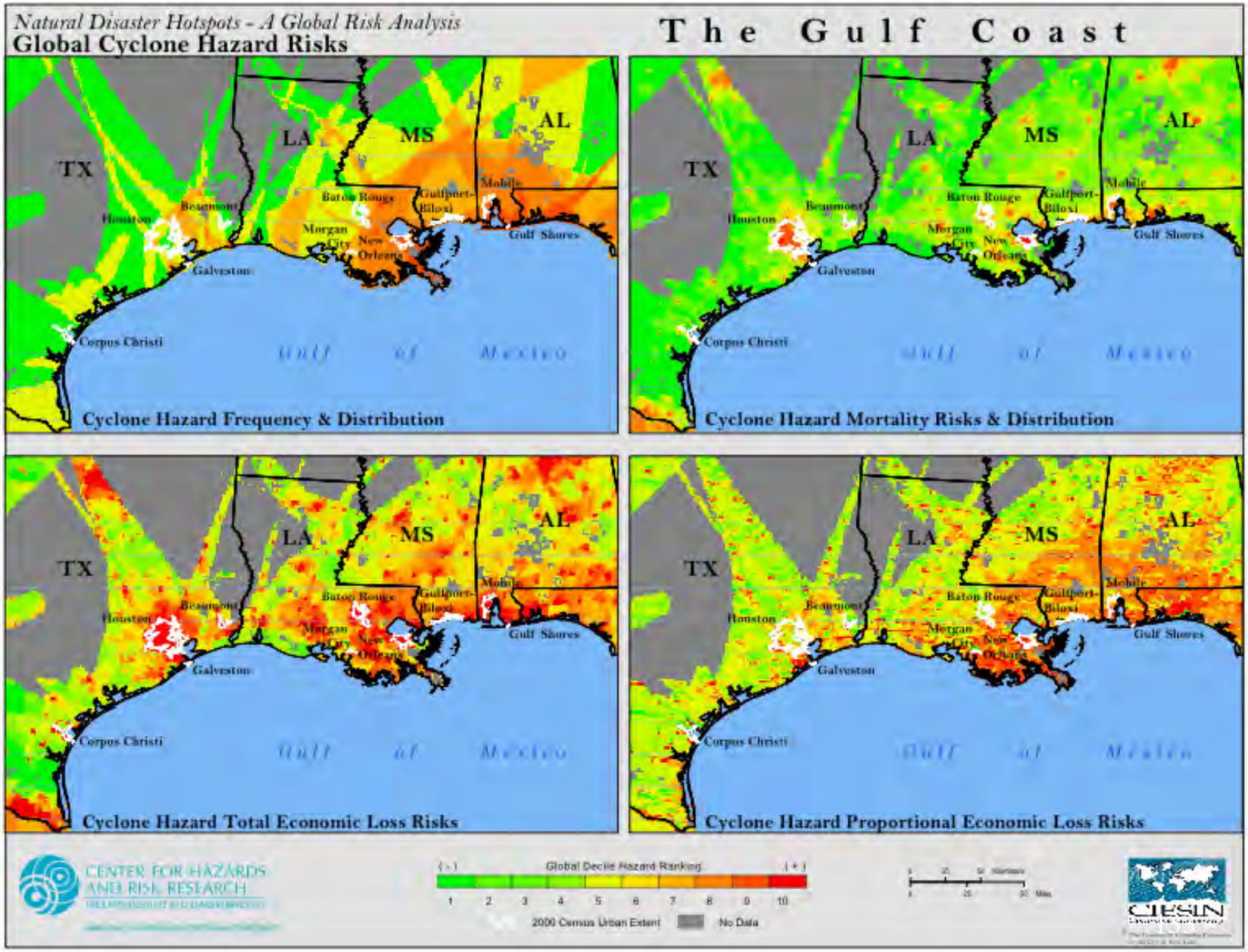

Mt Rainier volcanic hazard

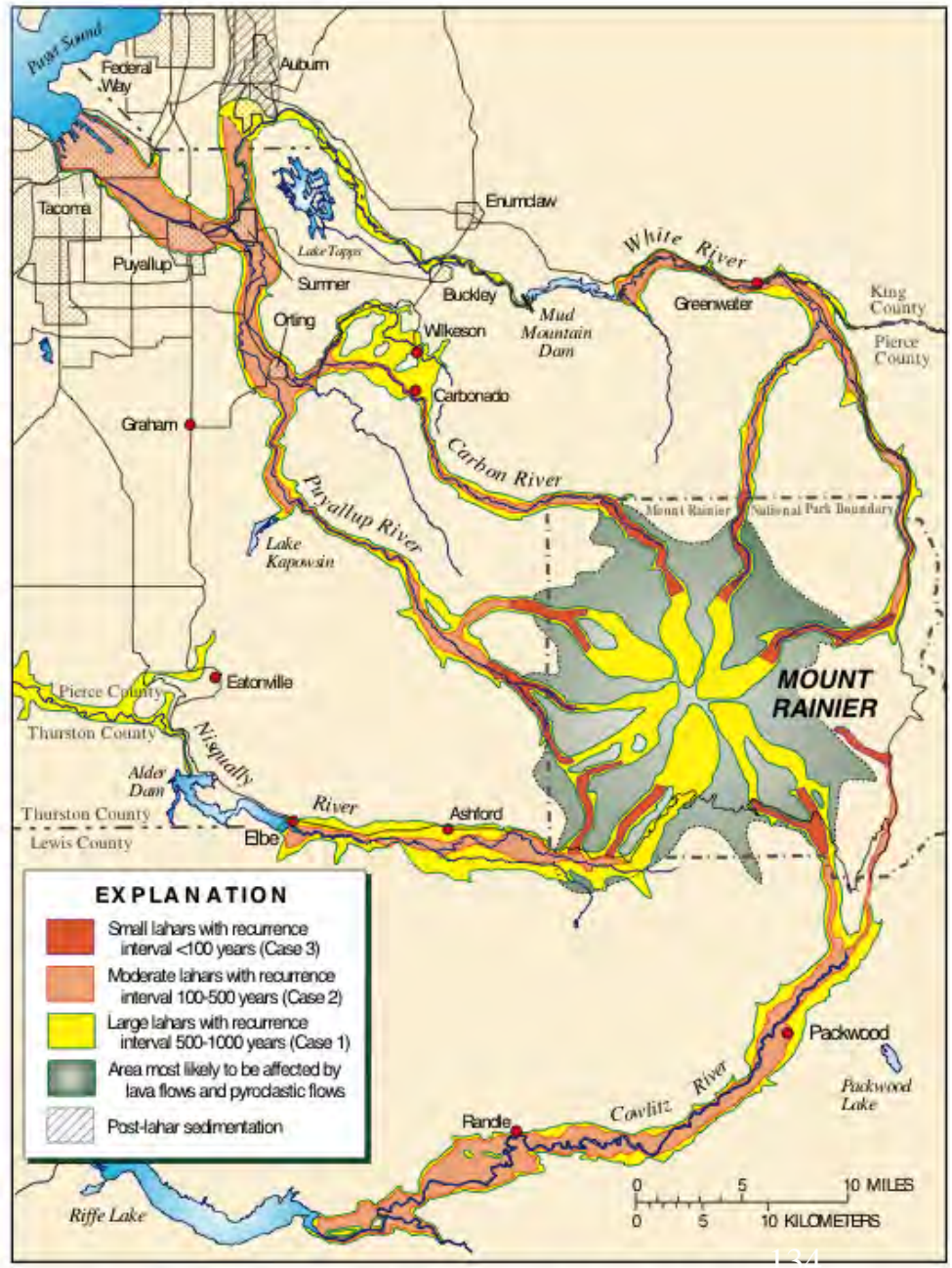

FIGURE 3.—Hazard zones for lahars, lava flows, and pyroclastic flows from Mount Rainier (Hoblitt and others, 1998; US Geological Survey Open-File Report 98–428).

Monserrat volcano probability tree

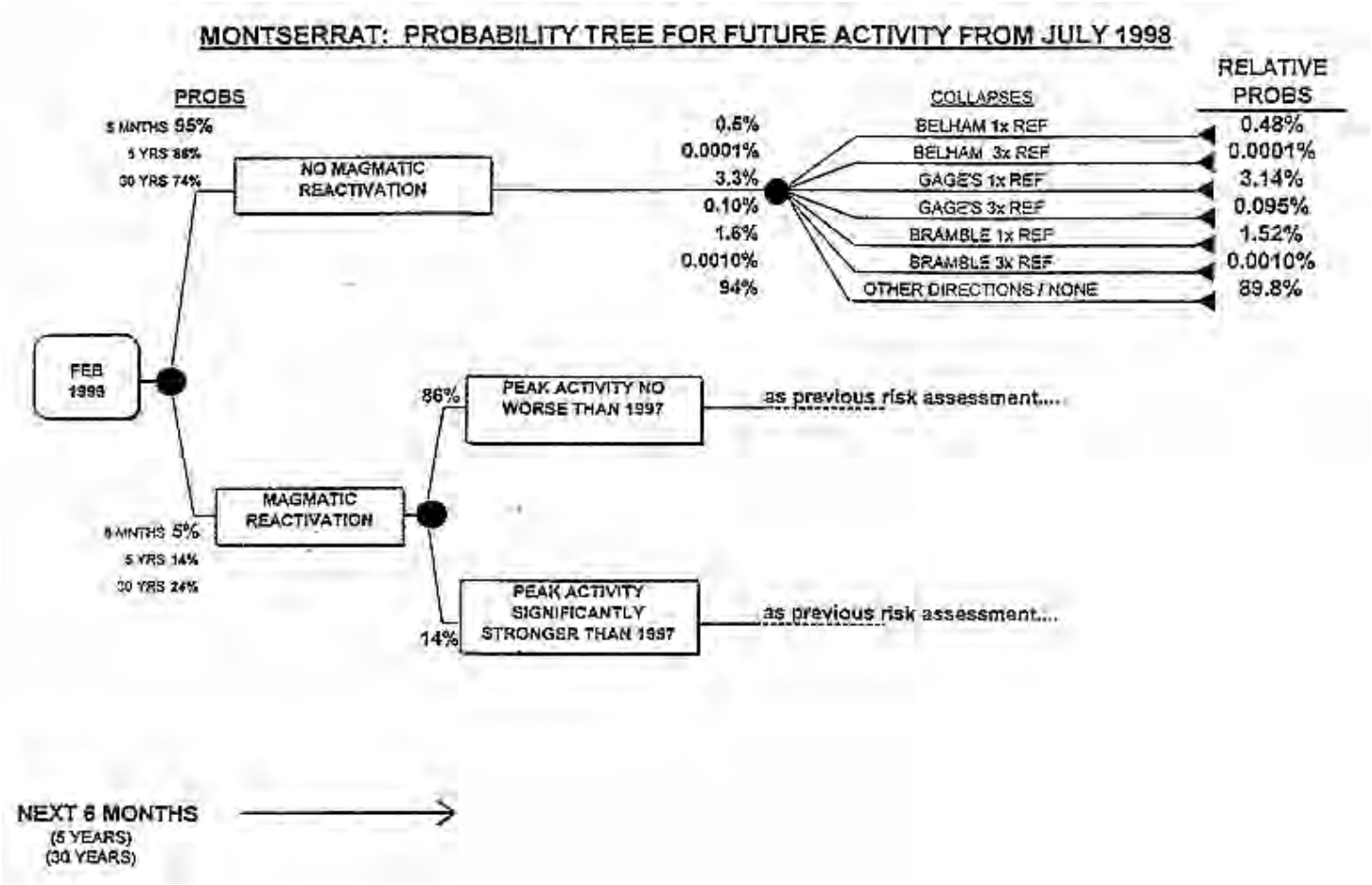

Nonlinearity from growth of small perturbations

2x**2 -1		difference
0.750	0.749	0.00
0.125	0.122	0.00
-0.969	-0.970	0.00
0.877	0.883	-0.01
0.538	0.558	-0.02
-0.421	-0.377	-0.04
-0.646	-0.716	0.07
-0.166	0.026	-0.19
-0.945	-0.999	0.05
0.785	0.994	-0.21
0.233	0.978	-0.75
-0.892	0.912	-1.80
0.590	0.665	-0.07
-0.303	-0.116	-0.19
-0.817	-0.973	0.16
0.334	0.895	-0.56
-0.777	0.601	-1.38
0.208	-0.278	0.49
-0.914	-0.845	-0.07
0.670	0.430	0.24
-0.103	-0.631	0.53
-0.979	-0.204	-0.77
0.916	-0.916	1.83
0.678	0.680	0.00
-0.080	-0.075	0.00
-0.987	-0.989	0.00
0.949	0.955	-0.01
0.800	0.823	-0.02
0.281	0.354	-0.07
-0.842	-0.749	-0.09
0.419	0.122	0.30
-0.649	-0.970	0.32
-0.157	0.882	-1.04
-0.951	0.555	-1.51
0.808	-0.383	1.19
0.304	-0.706	1.01
-0.815	-0.002	-0.81
0.329	-1.000	1.33
-0.784	1.000	-1.78

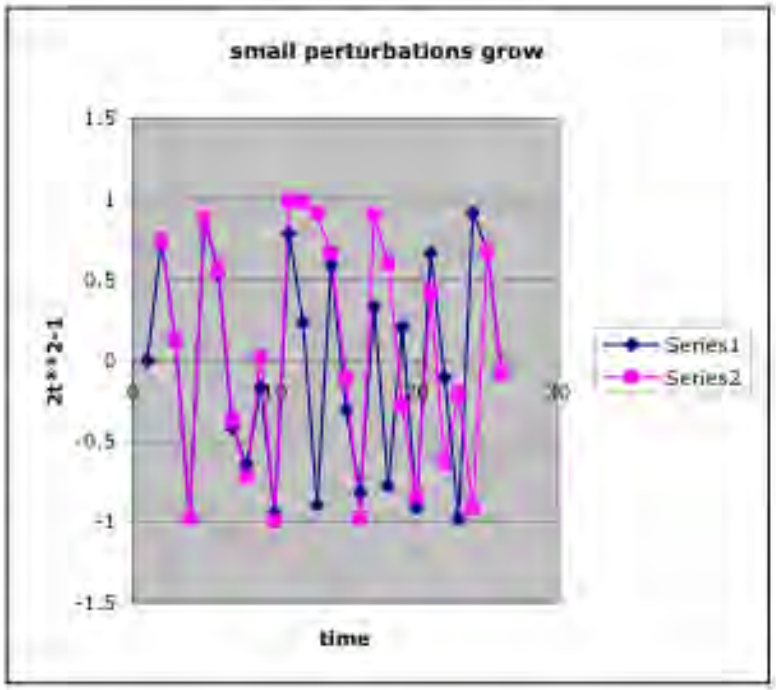

Coin tossing

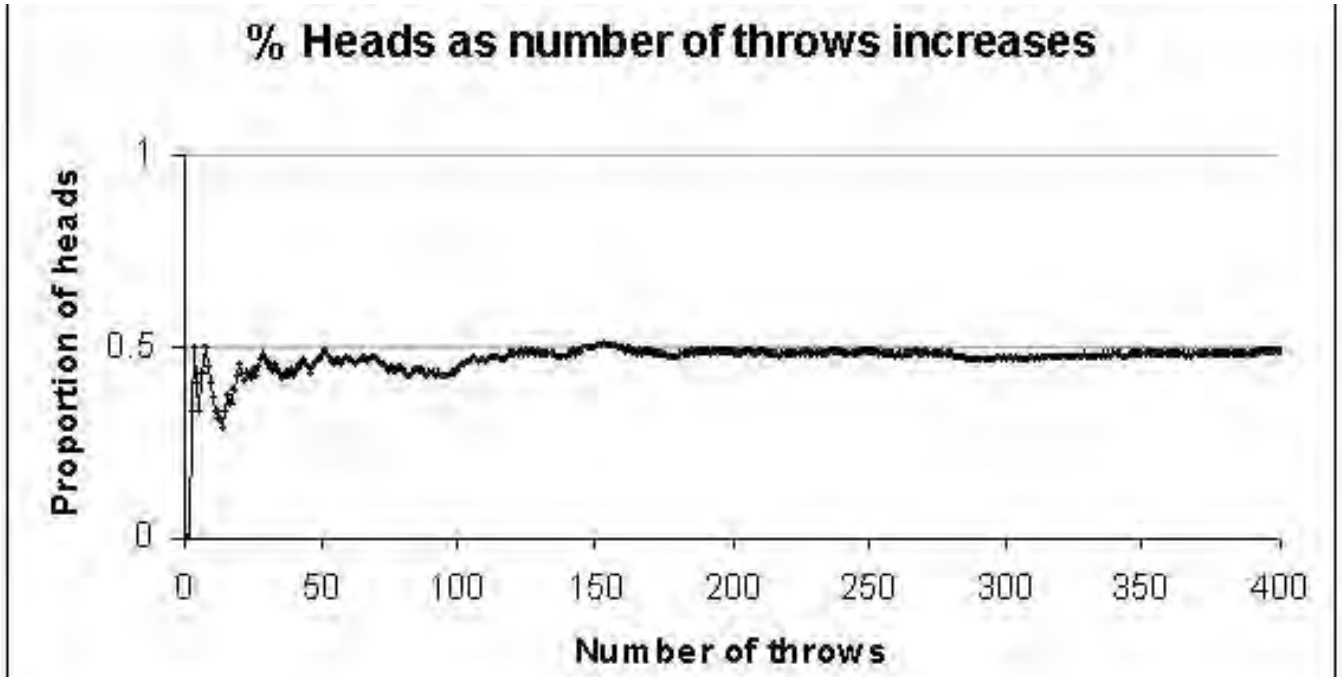

POSSIBLE RESULTS IN A COIN-TOSSING EXPERIMENT

No. of Tosses	*No. of Heads*	*No. of Tails*	*Ratio of Heads to Total Tosses*	*Absolute[5] Excess of Heads over Tails*
100	54	46	0.540	8
500	254	246	0.508	8
1000	501	499	0.510	2
5000	2516	2484	0.503	32
10,000	4979	5021	0.498	42

Long record needed to see real earthquake hazard

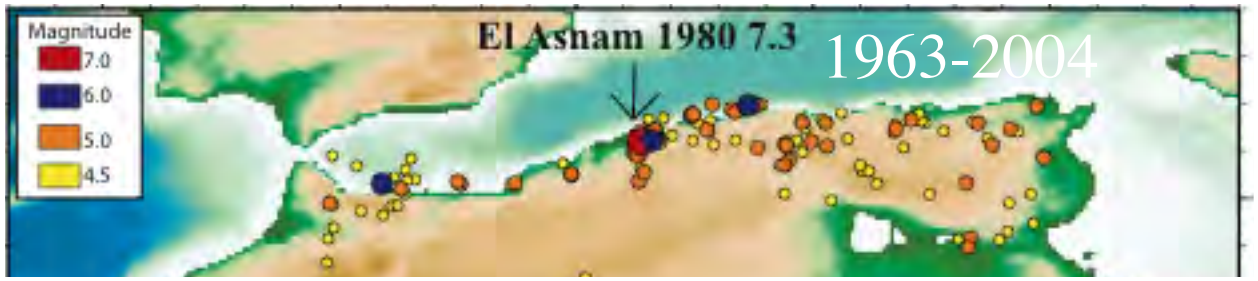

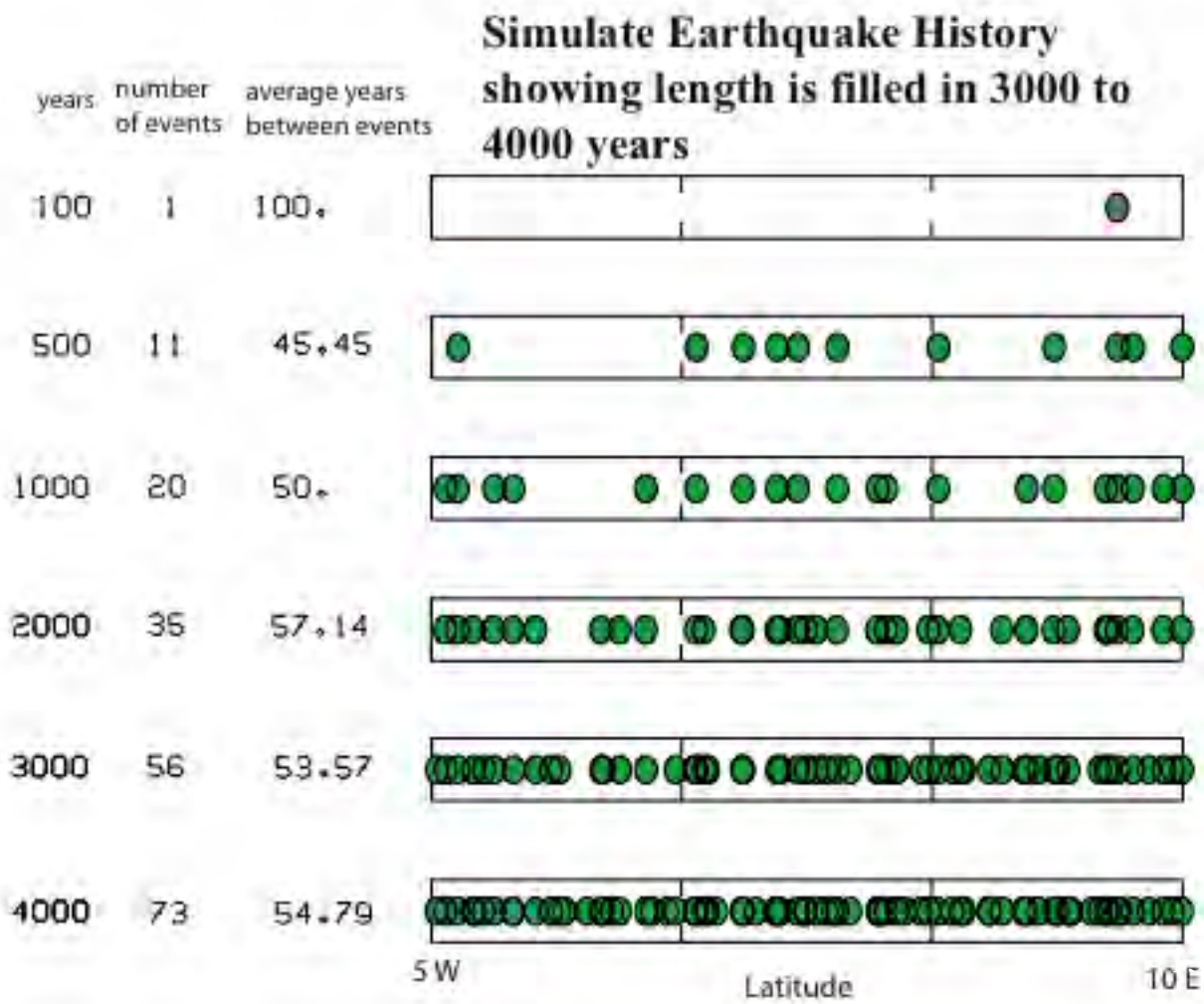

Swafford & Stein, 2007

Historical hurricane recurrence

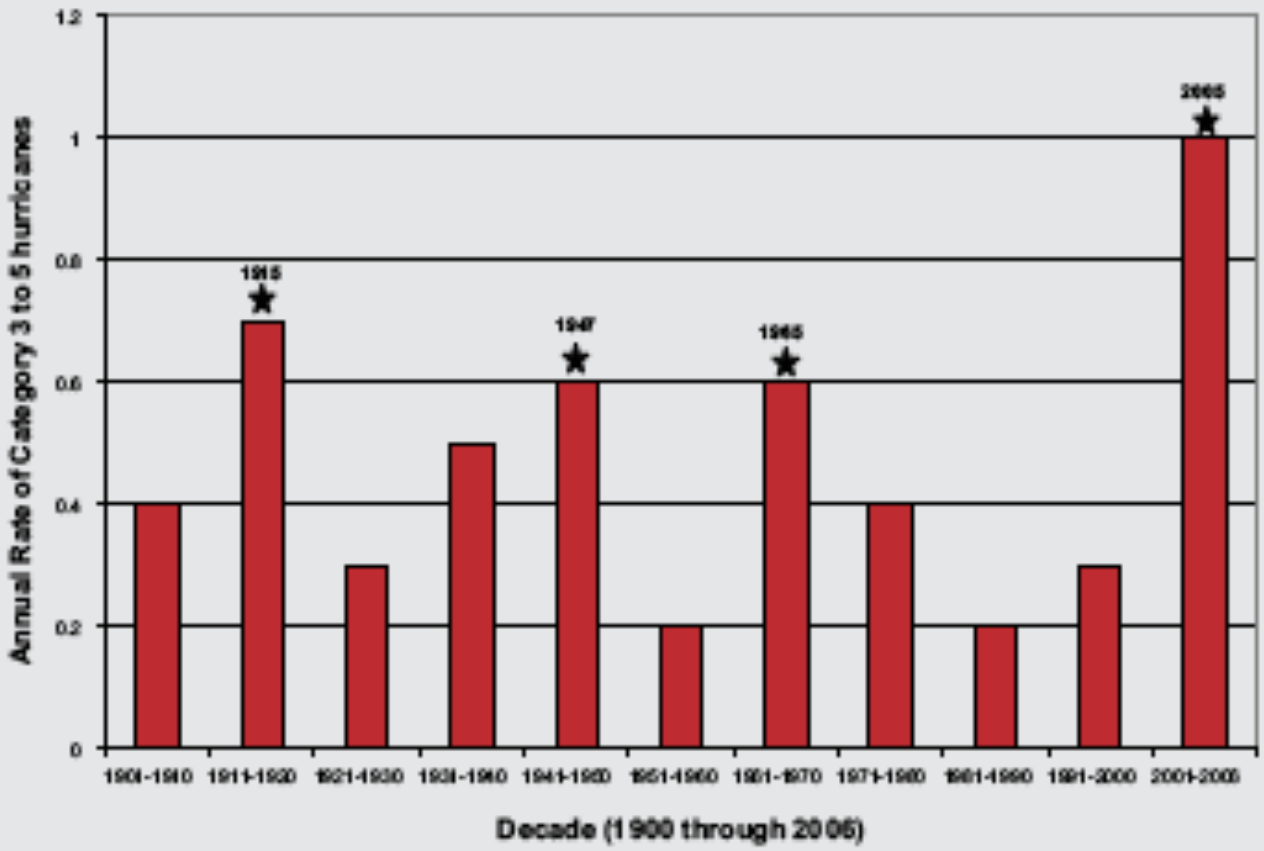

Decadal variations in annual rates of category 3 to 5 landfalling hurricanes along the Gulf Coast (from the southern tip of Florida to the Texas-Mexico border)

Geological Hurricane recurrence

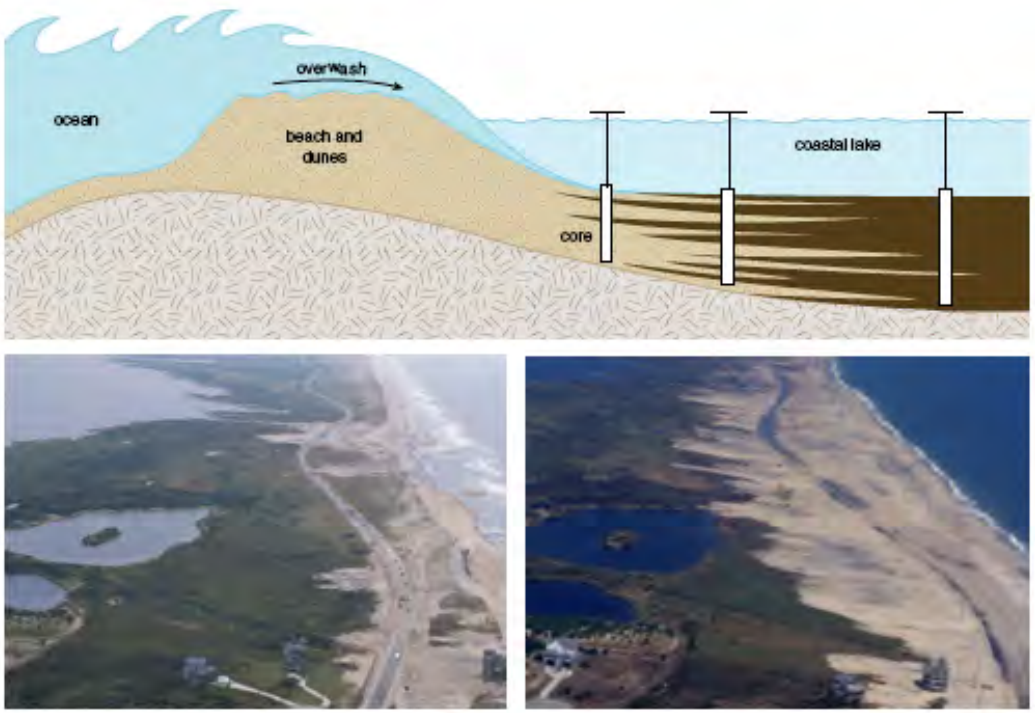

Figure 3. The author and his students have obtained sediment cores from different positions in various coastal lakes. The sand layers in these sediments constitute a record of ancient hurricane strikes, because the accompanying storm surges wash sand from the nearby beach into the lake *(diagram)*. This process was evident near Rodanthe, North Carolina, after Hurricane Isabelle struck in late September 2003 *(photographs)*. Before the storm *(left)*, beach sand was largely confined to the region between the ocean and the highway, whereas afterward sand is seen having been washed inland far enough to reach a small lake *(right)*. (Photographs courtesy of the U.S. Geological Survey.)

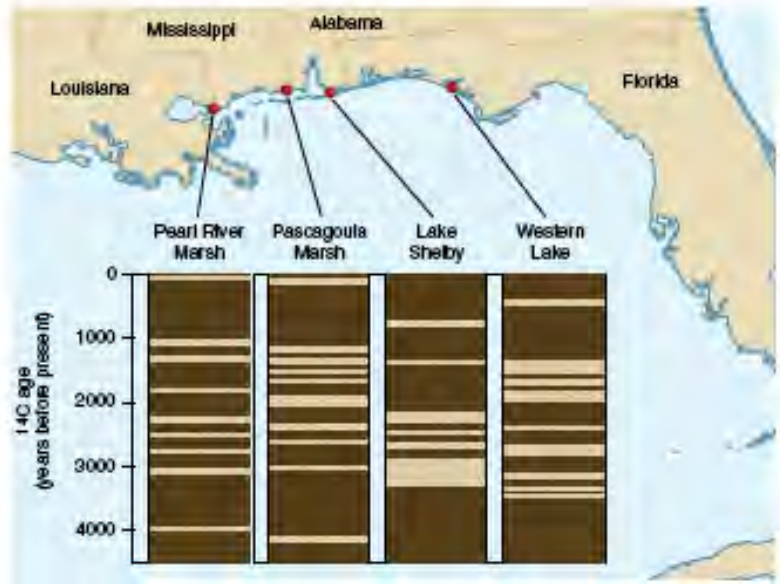

Figure 5. Sedimentary records from four coastal lakes show a distinct variation in hurricane activity in the Gulf region during the past few millennia. Whereas the interval between about 3,800 and 1,000 years ago was marked by frequent catastrophic hurricanes (typically one at each site every 200 years), the periods before and after were relatively quiet (with hurricanes striking any one locale just once every 1,000 years on average).

New Orleans flood risk modeling

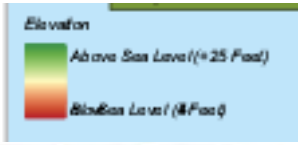

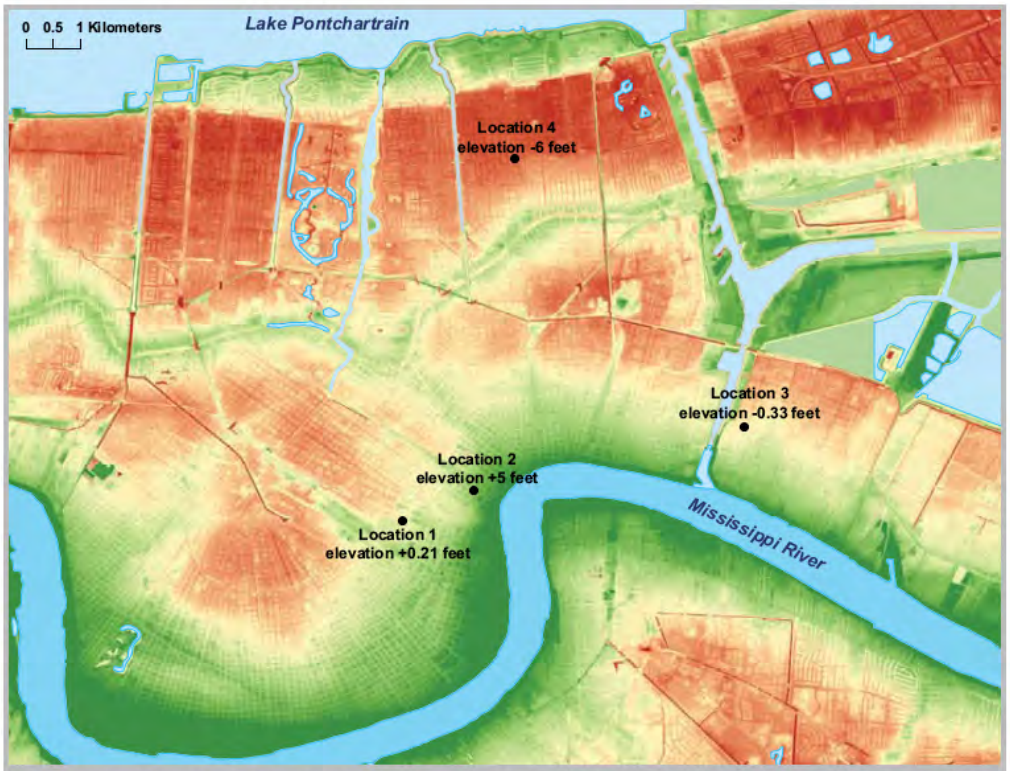

Locations within New Orleans chosen for further study: the Superdome (Location 1), the French Quarter (Location 2), the Lower Ninth Ward (Location 3), and the Gentilly Area (Location 4)

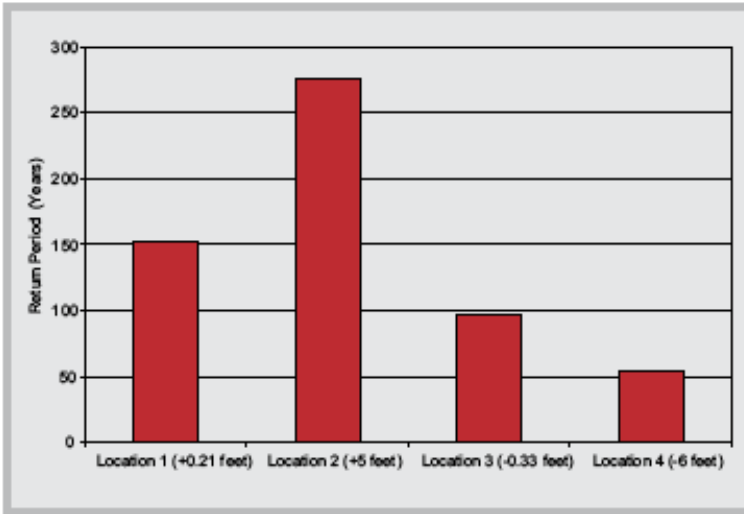

Baseline risk assessment results, showing return period of first flooding for four locations in New Orleans assuming medium term hurricane activity (2007-2011) and current level of flood defenses

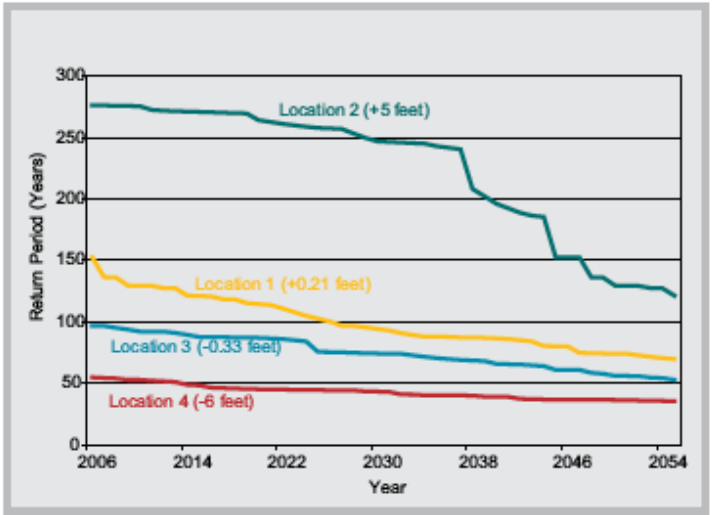

Sensitivity analysis of future flood risk, showing changes in return period of first flooding over time at four locations in New Orleans, assuming medium term hurricane activity (2007-2011), current level of flood defenses, and an average subsidence rate of 0.4 in per year (10 mm per year)

New Orleans: effects of flood protection, development, & subsidence

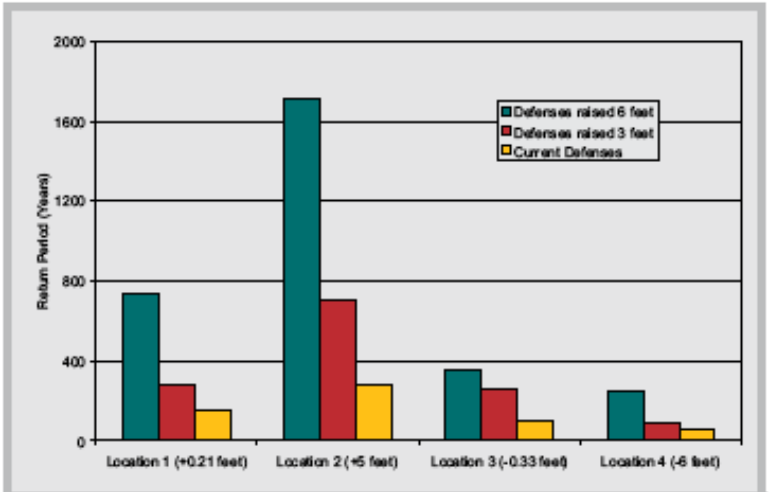

Sensitivity analysis of flood risk, showing return period of first flooding for four locations in New Orleans assuming medium term hurricane activity (2007-2011) with current flood defenses and raises in flood defenses of 3 ft (0.9 m) and 6 ft (1.8 m)

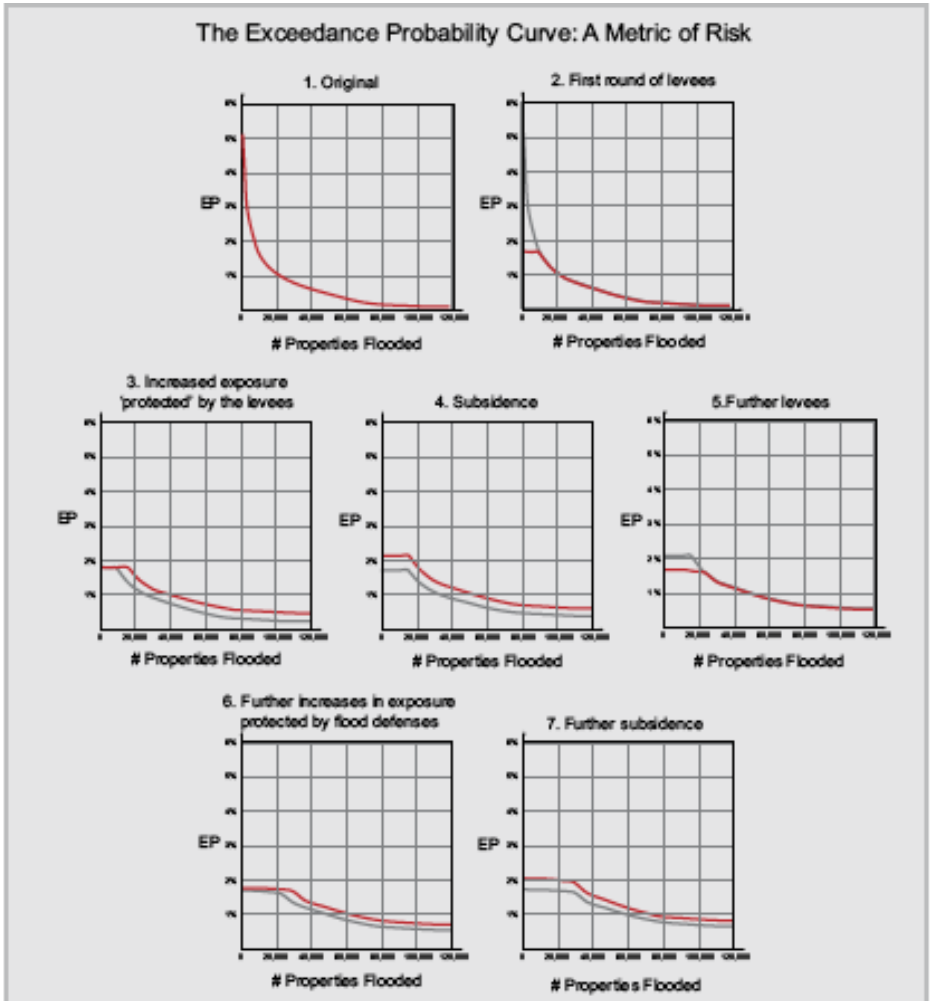

The annual exceedance probability (EP) curve specifies the probability that a certain level of loss will be exceeded in a year. (For more information on EP curves and catastrophe modeling, see Grossi and Kunreuther, 2005). Using an EP curve, the flood risk for New Orleans can be illustrated over time showing the pattern of flood loss. First, (1) the original EP curve without any flood defenses; then (2) a truncated EP curve indicating protection against the most frequent storm surge events after the first round of levees; (3) an extended EP curve indicating increases in loss due to increased exposure protected by flood defenses; (4) a raised EP curve indicating increases in risk due to subsidence over time; (5) a second truncated EP curve indicating increased protection with a second round of levees; (6) a second extended EP curve indicating increases in loss due to increased exposure protected by flood defenses; and (7) a second raised EP curve indicating increases in risk due to further subsidence over time. In this example it can be seen that the 1% annual probability of exceedance (i.e., 1 in 100, or 100-year return period) of 20,000 properties flooded has increased fourfold over the pattern of the two cycles of levee building, new development, and further subsidence. Meanwhile the floodplain has been continuously protected against all floods with a 2% annual exceedance probability (i.e., 1 in 50, or return period of 50 years).

Random walk

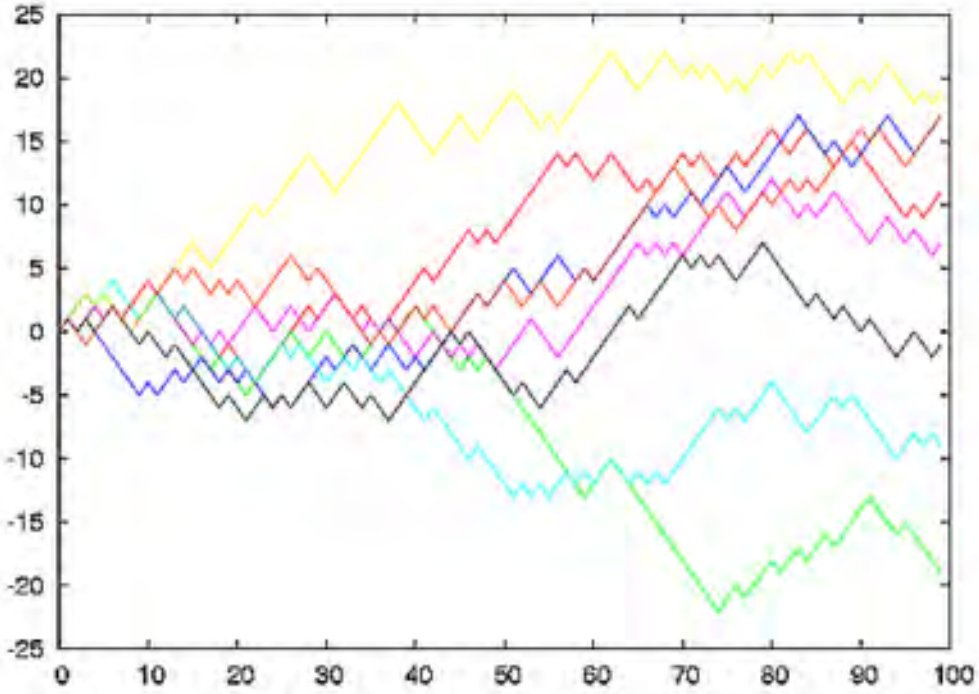
25
20
15
10
5
0
-5
-10
-15
-20
-25
0
10
20
30
40
50
60
70
80
90
100

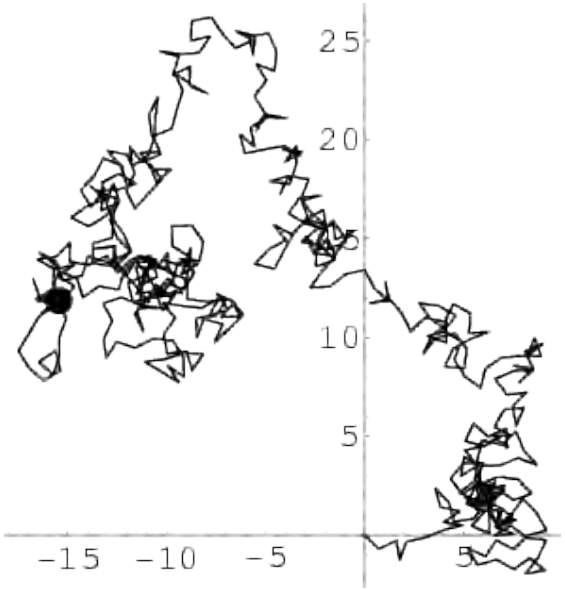
25
20
10
5
-15
-10
-5
5

Stock market variability: short & long term

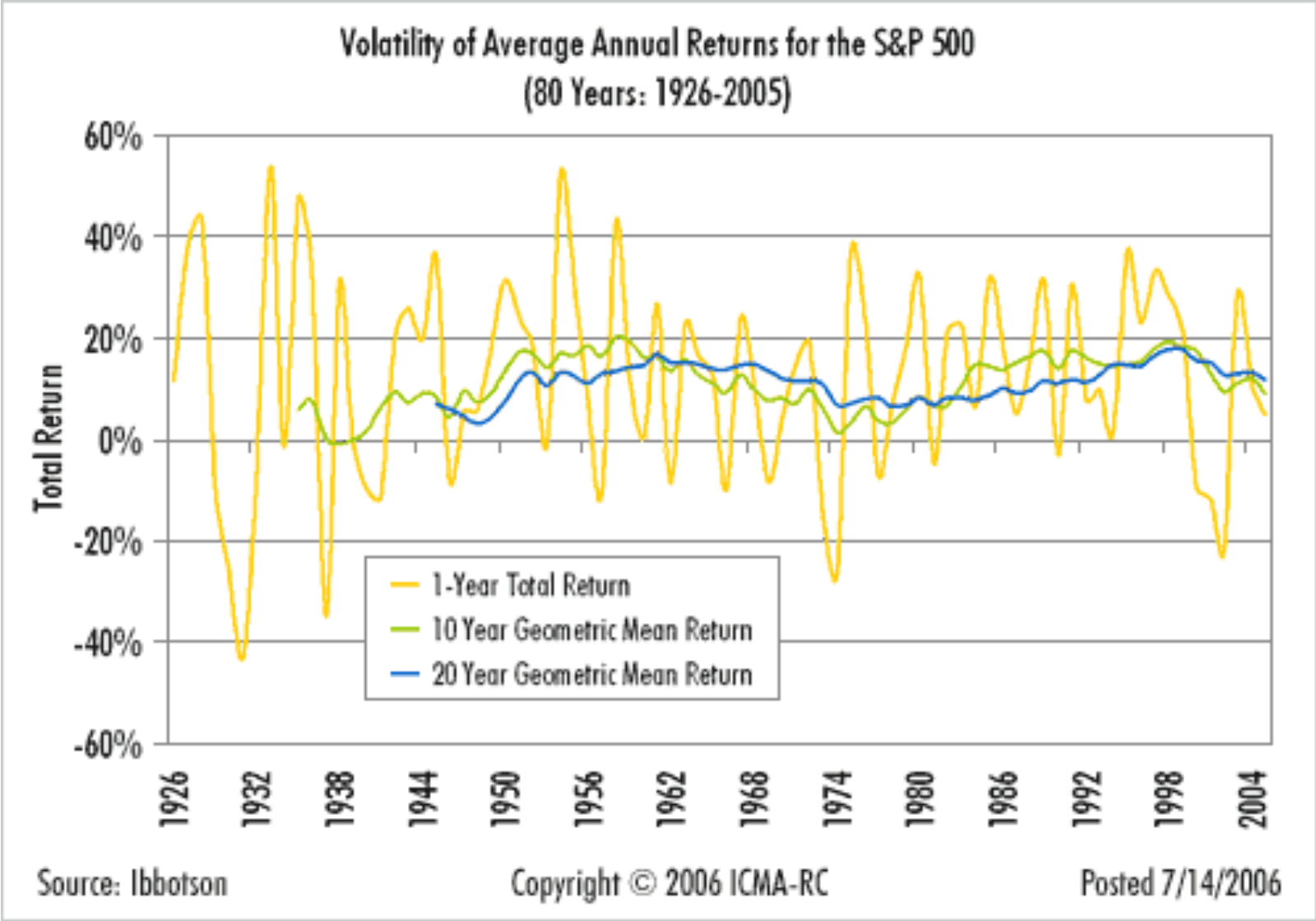

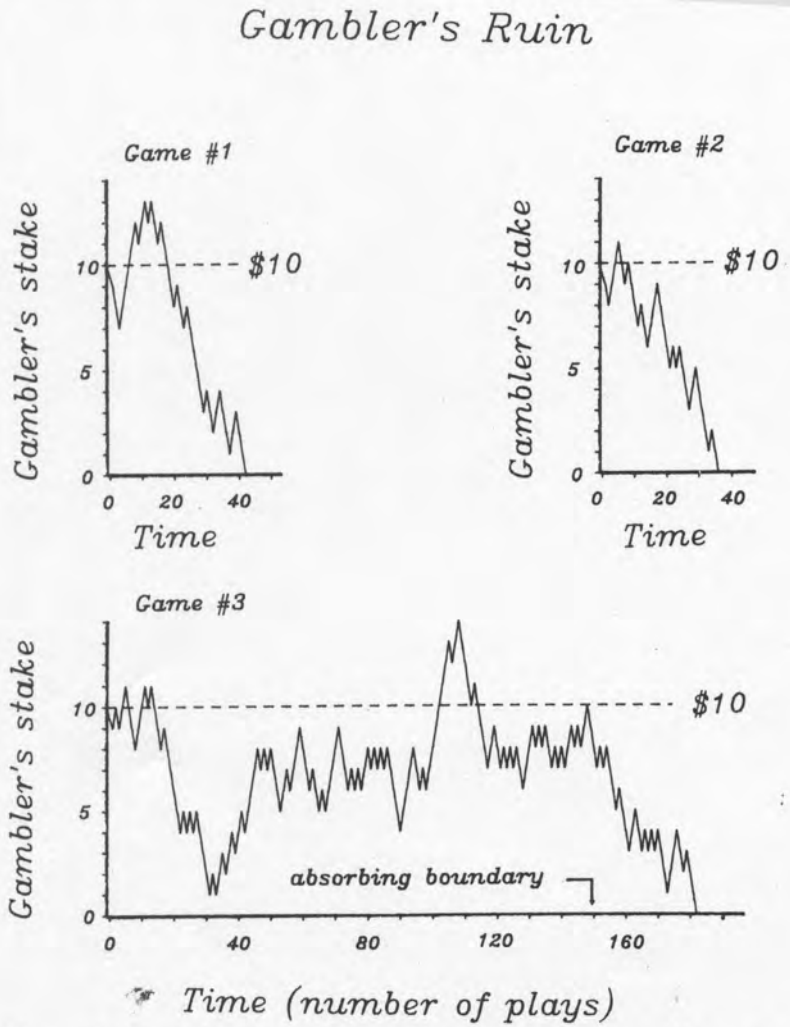

FIGURE 3-1. Simulated gambling results in an even-odds game (fifty-fifty chance of winning on each play). The gambler's initial stake is $10, and each bet is $1. Thus, the stake fluctuates up and down randomly, in steps of $1. Gambler's Ruin occurs when the absorbing boundary—zero—is reached. Each game is like the fate of a genus that starts with ten species. The number of species goes up when a species branches to form another species and goes down when a species goes extinct.

Gambler's Ruin [redacted]

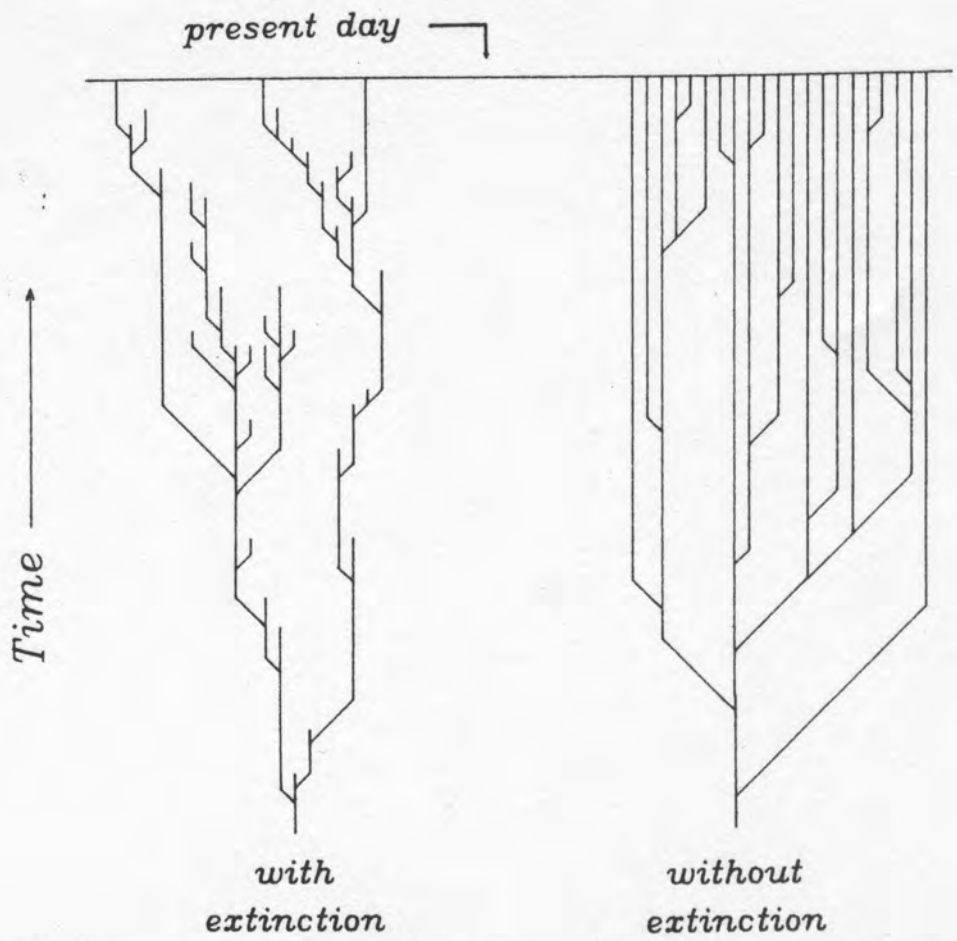

FIGURE 1-3. Hypothetical evolutionary trees showing the effect of species extinction on biodiversity. The tree on the left reflects the actual history of life, with many species formed by lineage branching but most going extinct. Only three species survive to the present day. The tree on the right is what evolution would look like if species never went extinct: the number of coexisting species (biodiversity) would increase until saturation was reached.

Evolution with vs without extinctions

Eruptive history of Vesuvius

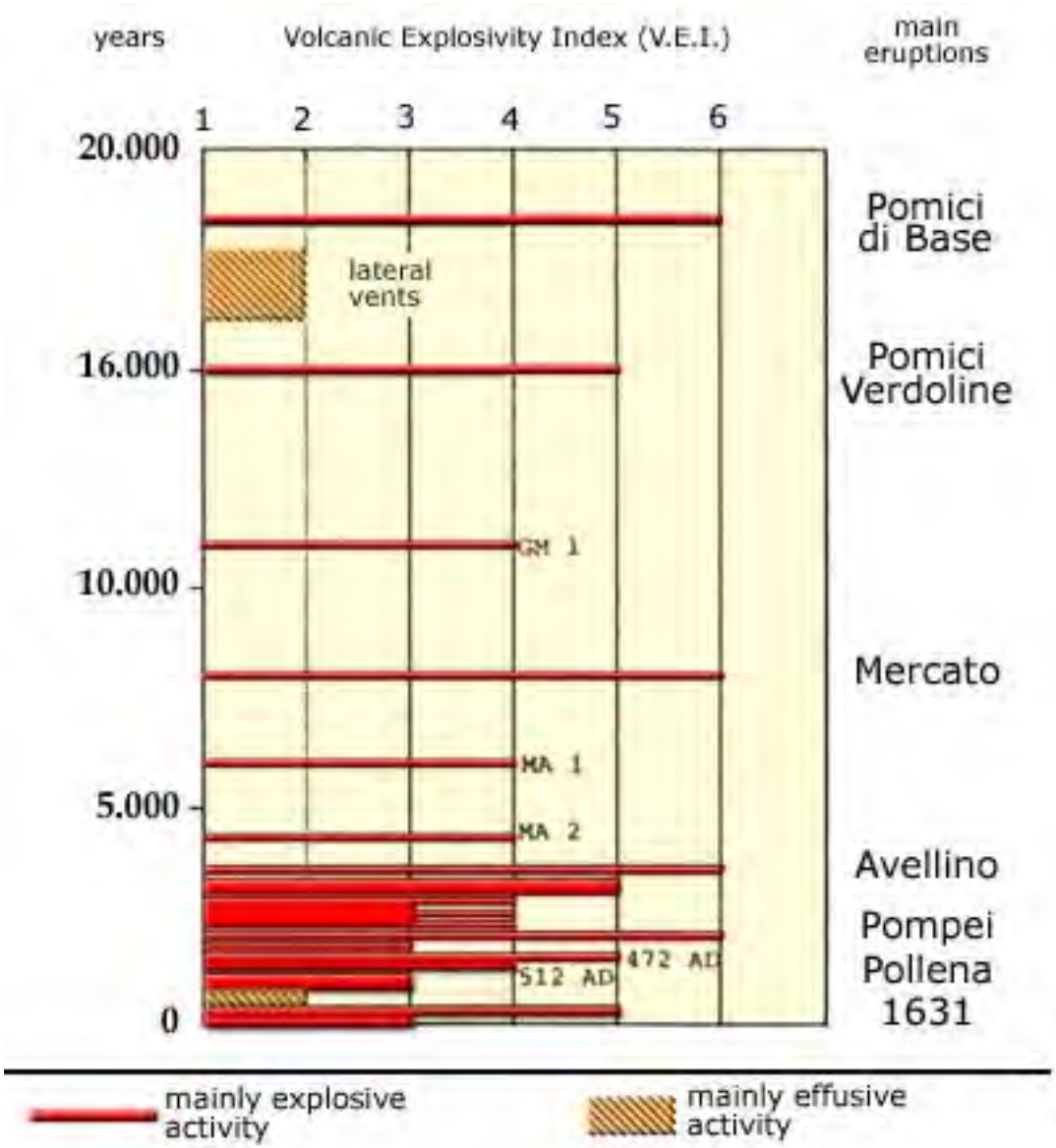

Gaussian approximation to binomial distribution

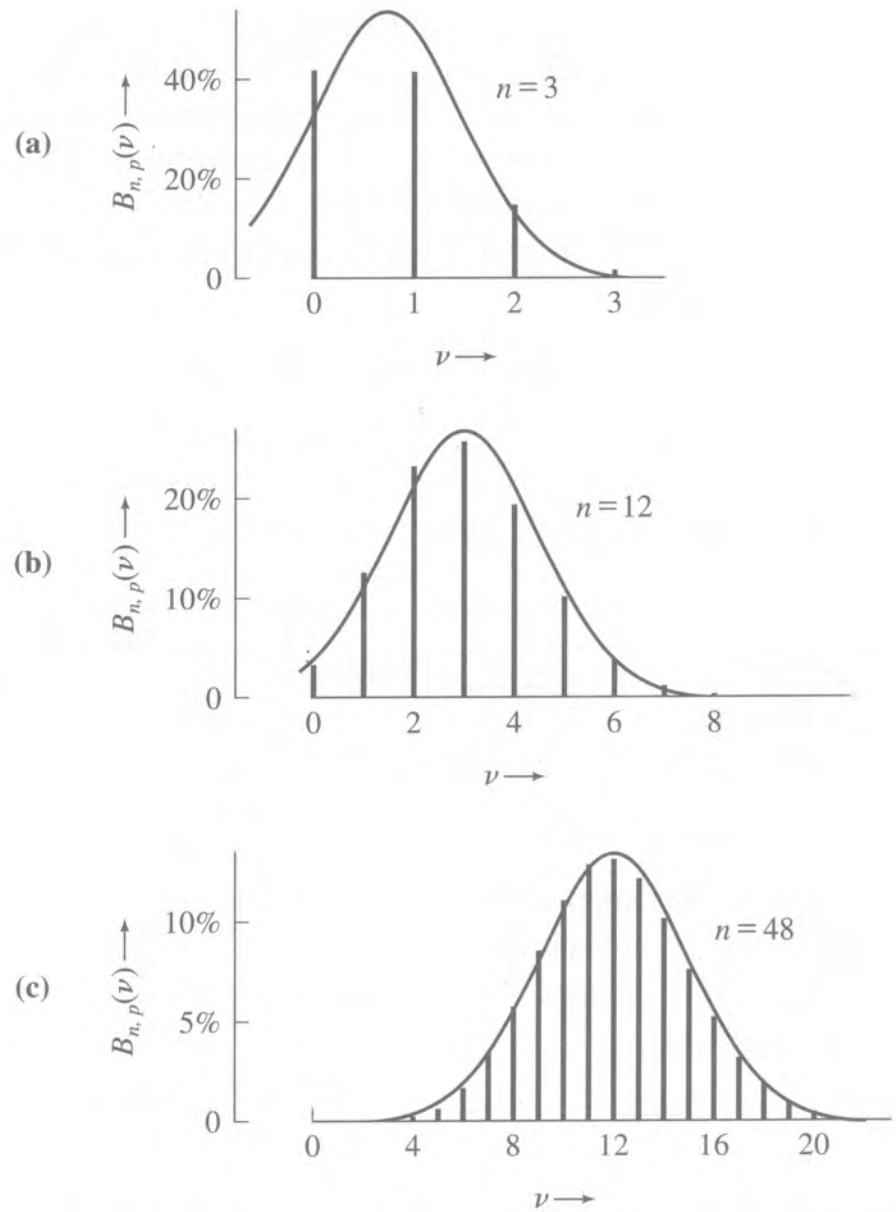

Figure 10.3. The binomial distributions for $p = 1/4$ and $n = 3$, 12, and 48. The continuous curve superimposed on each picture is the Gauss function with the same mean and same standard deviation.

Poisson distribution

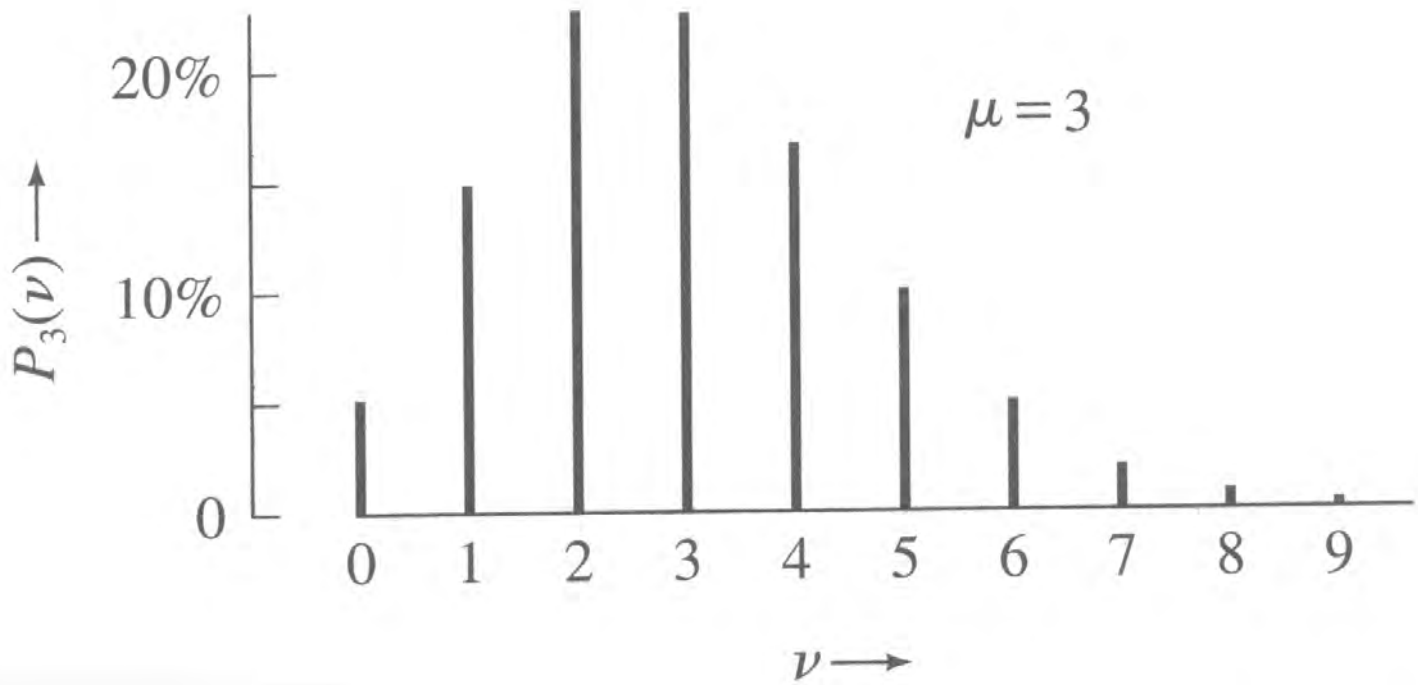

Earthquake probability models

Figure 4.7-9: Earthquake probability estimate for the Pallett Creek segment of the San Andreas fault.

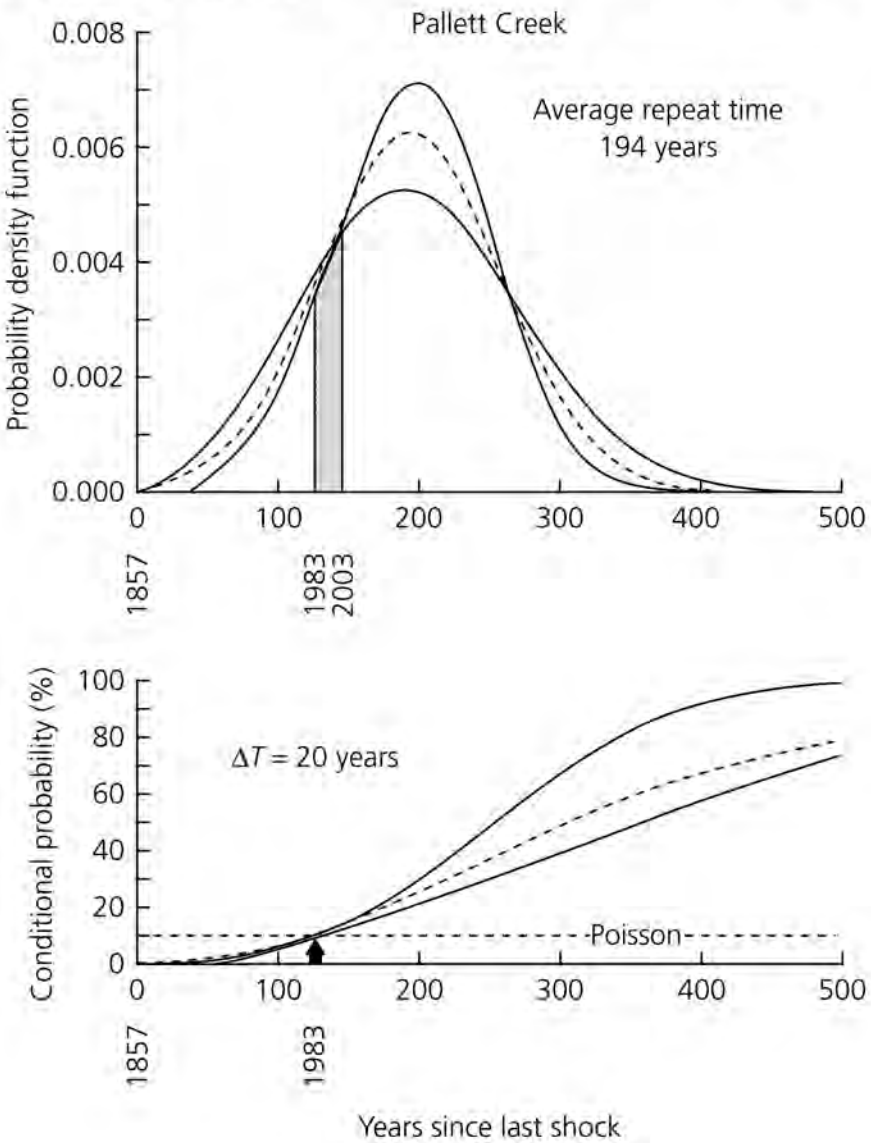

Figure 4.7-10: Synthetic earthquake histories for Poisson and Gaussian models.

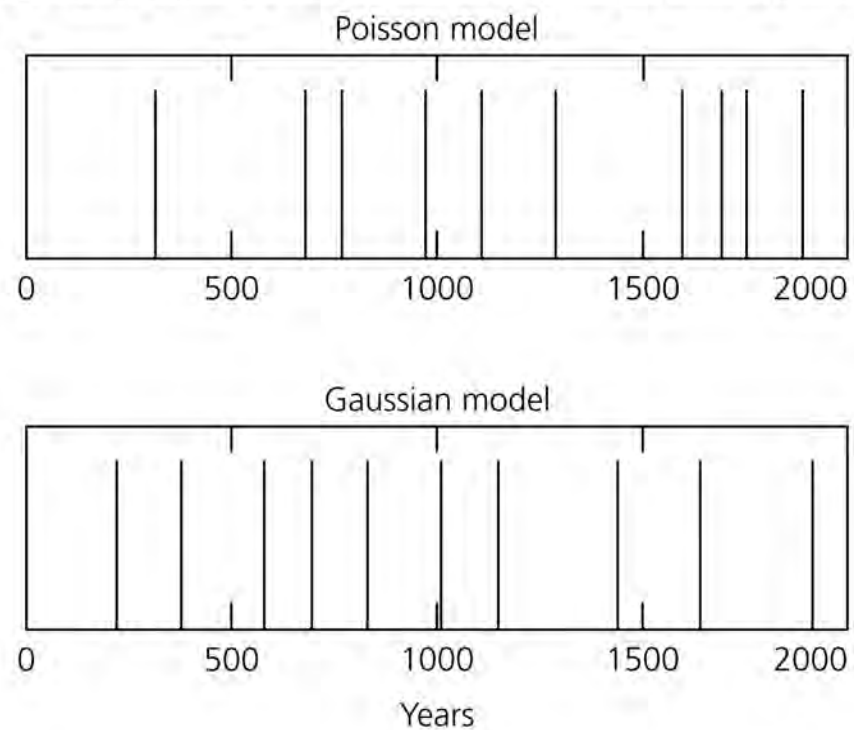

Reduced Chi square table

Table 12.6. The percentage probability $Prob_d(\tilde{\chi}^2 \geqslant \tilde{\chi}_o^2)$ of obtaining a value of $\tilde{\chi}^2$ greater than or equal to any particular value $\tilde{\chi}_o^2$, assuming the measurements concerned are governed by the expected distribution. Blanks indicate probabilities less than 0.05%. For a more complete table, see Appendix D.

ν	$\tilde{\chi}_o^2$ χ^2_ν												
d	0	0.25	0.5	0.75	1.0	1.25	1.5	1.75	2	3	4	5	6
1	100	62	48	39	32	26	22	19	16	8	5	3	1
2	100	78	61	47	37	29	22	17	14	5	2	0.7	0.2
3	100	86	68	52	39	29	21	15	11	3	0.7	0.2	—
5	100	94	78	59	42	28	19	12	8	1	0.1	—	—
10	100	99	89	68	44	25	13	6	3	0.1	—	—	—
15	100	100	94	73	45	23	10	4	1	—	—	—	—

CDF for chi-squared

Figure 7.5-1: Cumulative probability distribution.

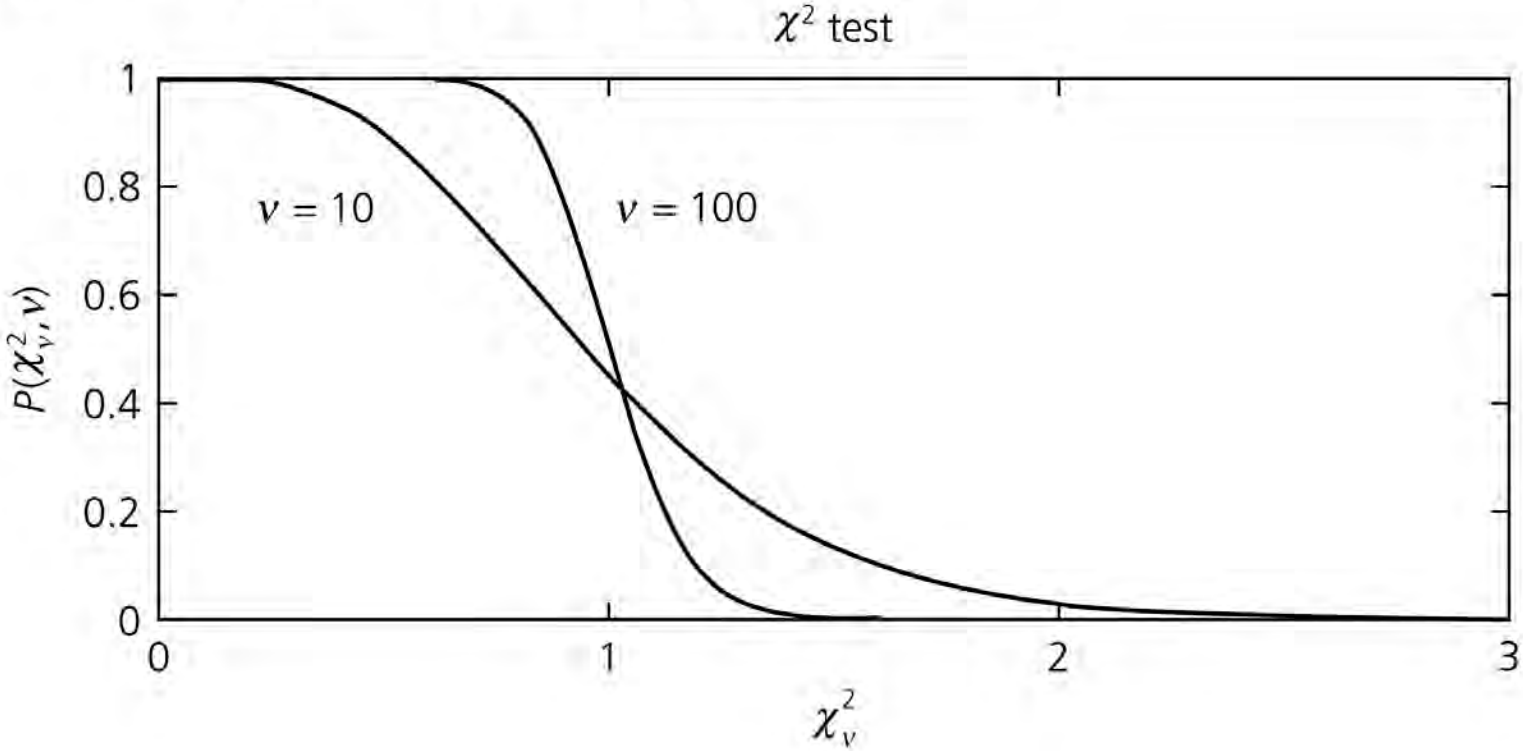

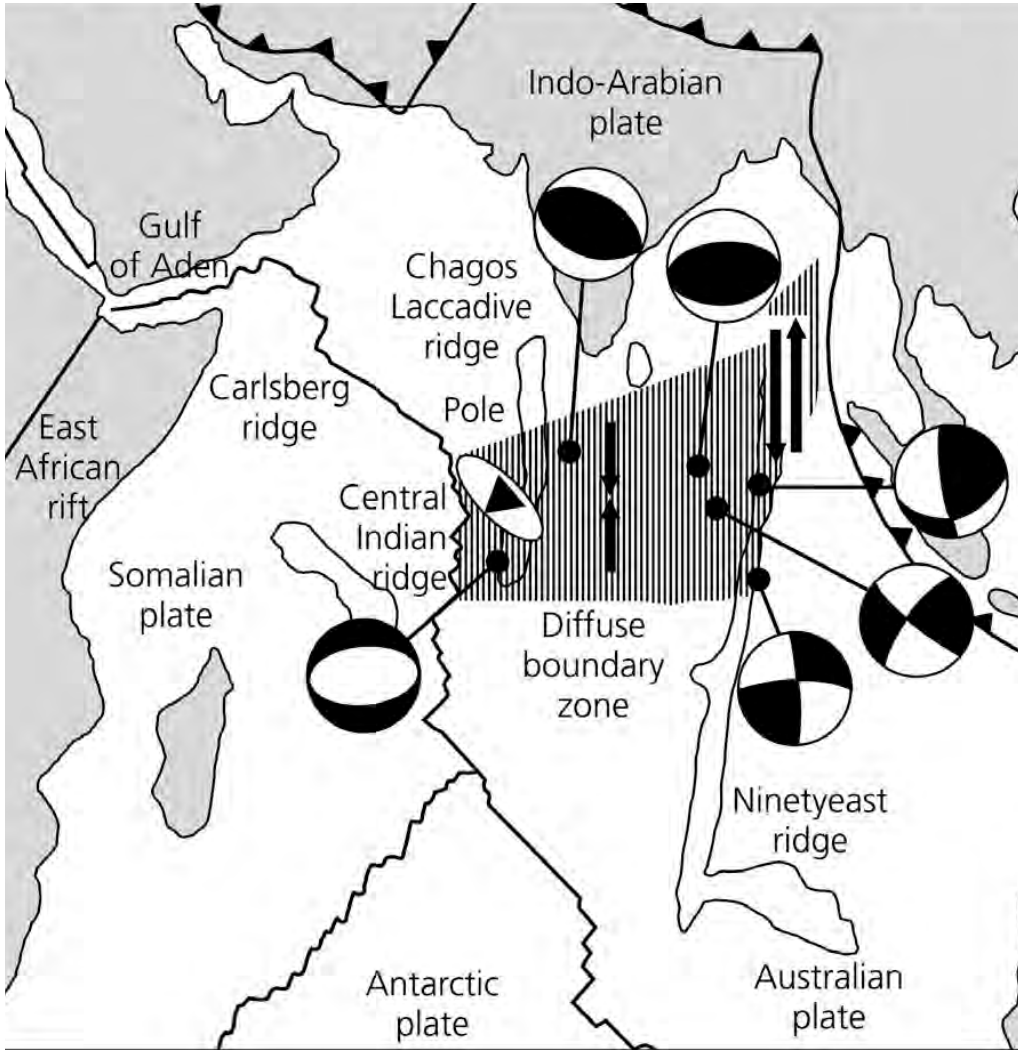
Indo-Arabian plate
Gulf of Aden
Chagos Laccadive ridge
Carlsberg ridge
East African rift
Pole
Central Indian ridge
Somalian plate
Diffuse boundary zone
Ninetyeast ridge
Antarctic plate
Australian plate

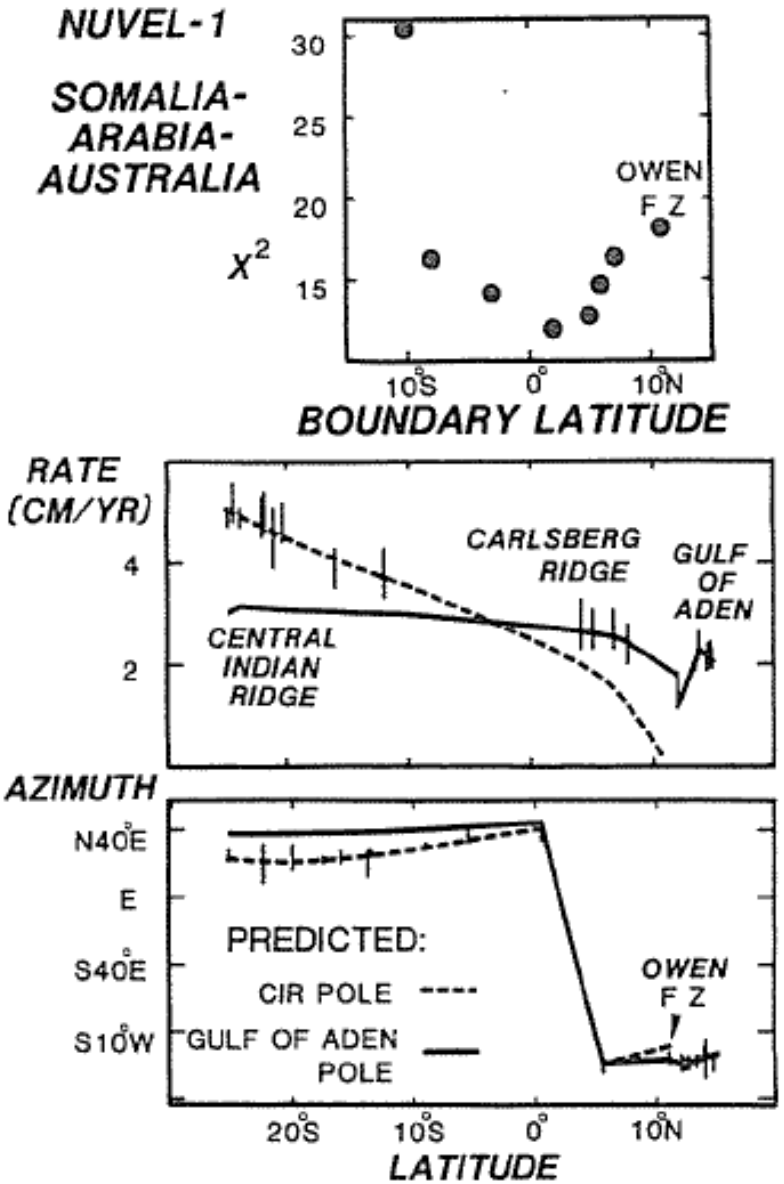
NUVEL-1
SOMALIA-ARABIA-AUSTRALIA
X^2
30
25
20
15
OWEN F Z
10°S
0°
10°N
BOUNDARY LATITUDE
RATE (CM/YR)
4
2
CARLSBERG RIDGE
GULF OF ADEN
CENTRAL INDIAN RIDGE
AZIMUTH
N40°E
E
S40°E
S10°W
PREDICTED:
CIR POLE
GULF OF ADEN POLE
OWEN F Z
20°S
10°S
0°
10°N
LATITUDE

F test

Because more plates can describe motions in an area better because the model has more parameters, test whether the improved fit (reduction in χ^2_ν) is more than expected purely by chance due to the additional parameters.

An *F-ratio* test shows whether the fit to n GPS data of a model with $p+1$ plates is significantly better than that of one with p plates. The p plate model has $3p$ parameters ($n-3p$ degrees of freedom) whereas the $p+1$ plate model has $3p+3$ parameters ($n-3p-3$ degrees of freedom). We form

$$F = \frac{[\chi^2(p \text{ plates}) - \chi^2(p+1 \text{ plates})] \,/\, 3}{\chi^2(p+1 \text{ plates}) \,/\, (n-3p-3)}$$

and examine the probability of observing an F value greater than for a random sample.

Values for F test, $\nu_1 = 3$

ν_2	$F_{0.05}$	$F_{0.01}$
10	3.71	6.55
20	3.1	4.94
25	2.99	4.68
30	2.92	4.51
40	2.84	4.31
60	2.76	4.13
120	2.68	3.95
∞	2.60	3.78

For example, if P_F is 0.01, there is only a 1% chance that the improved fit of the model is due purely to chance, so the additional plate seems distinct. Conversely, if the improved fit is likely simply from the additional parameters, the data do not strongly indicate an additional plate. However, the plate may be there - *just not resolvable with these data*.

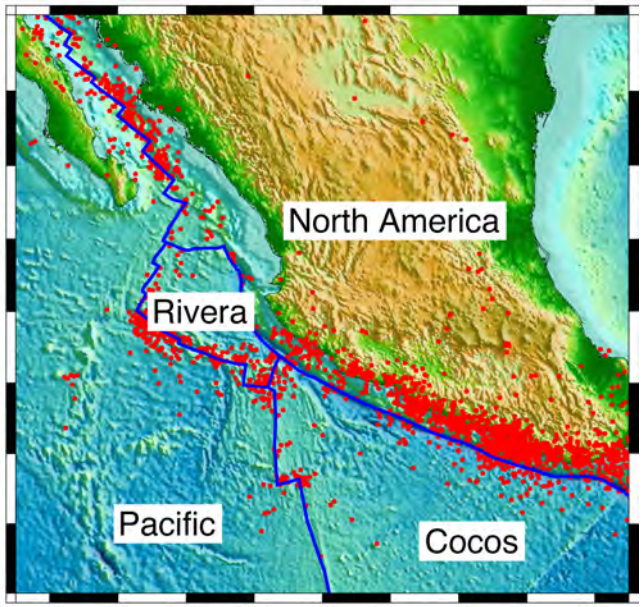

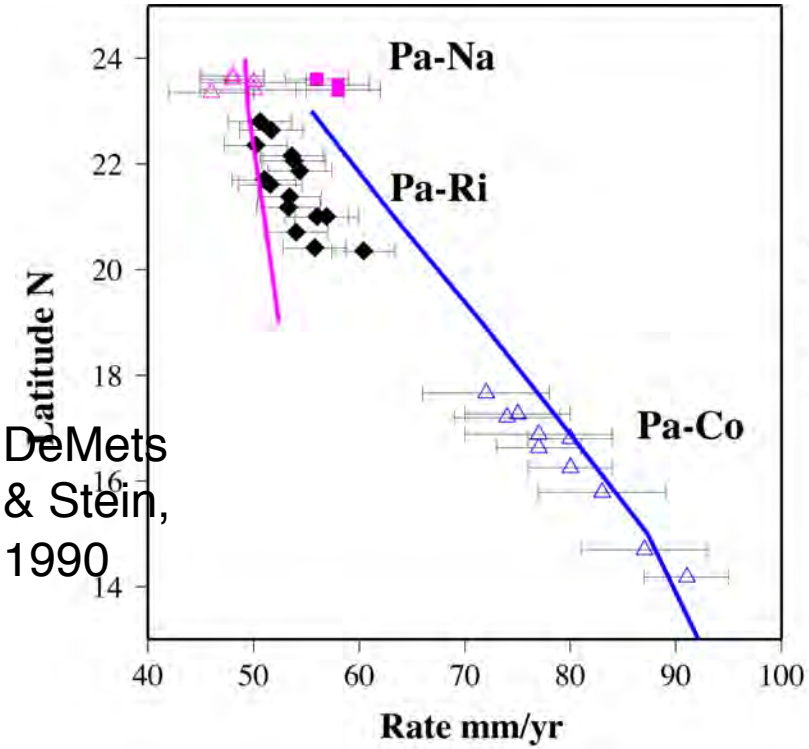

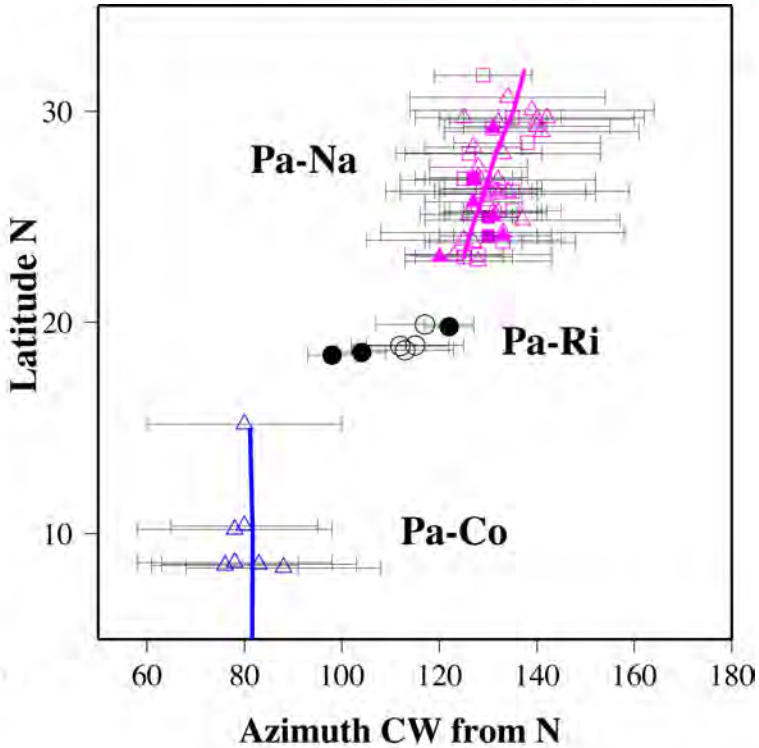

DeMets & Stein, 1990

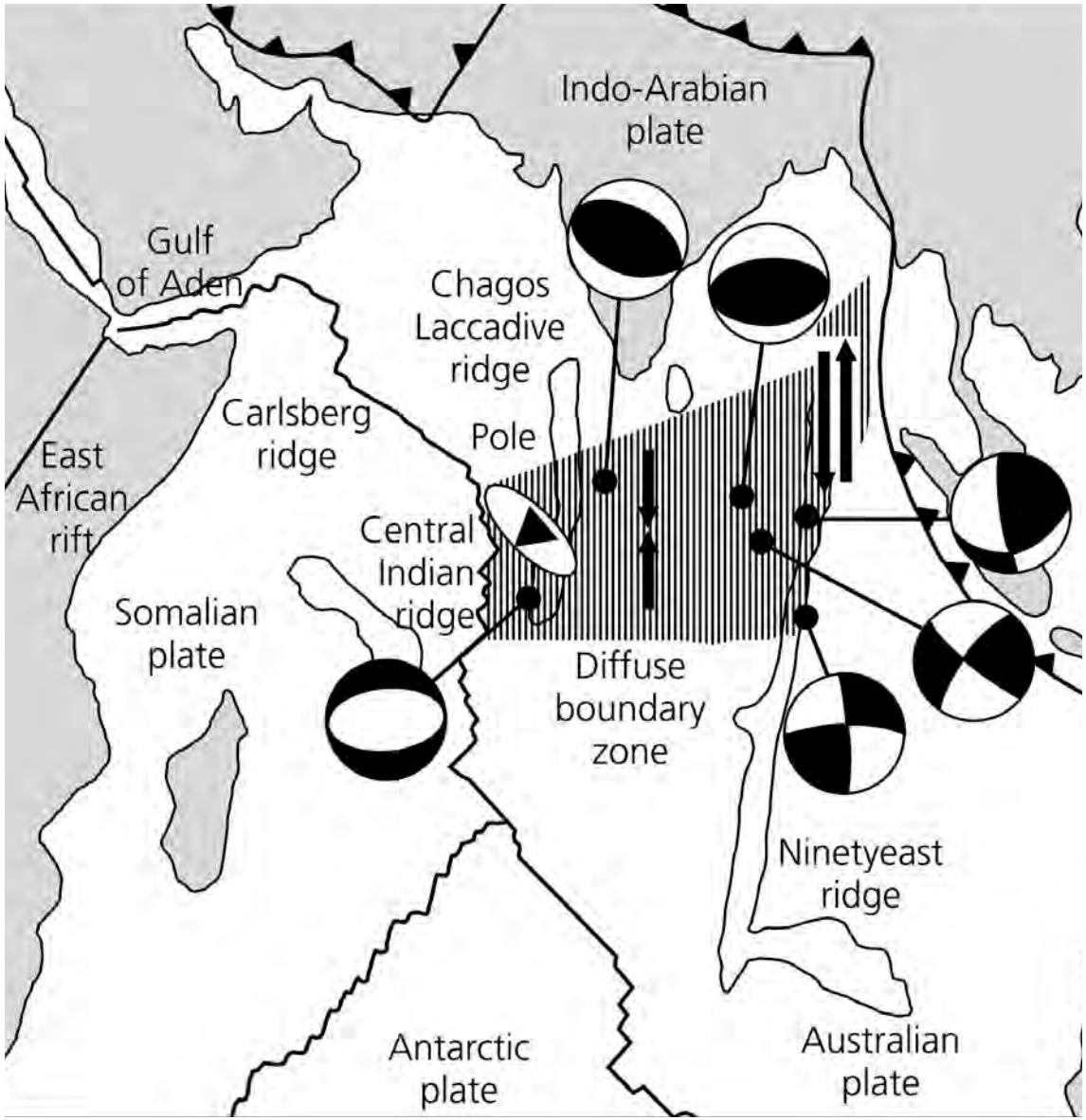

Wiens et al., 1985